Vol. 287, No. 1–2, March 10, 1994 ISSN 0003-2670

ANALYTICA CHIMICA ACTA

An international journal devoted to all branches of analytical chemistry

ELSEVIER

ANALYTICA CHIMICA ACTA

Scope. *Analytica Chimica Acta* publishes original papers, rapid publication letters and reviews dealing with every aspect of modern analytical chemistry. Reviews are normally written by invitation of the editors, who welcome suggestions for subjects. Letters can be published within **four months** of submission. For information on the Letters section, see inside back cover.

Submission of Papers

Americas

Prof. Harry L. Pardue
Department of Chemistry
1393 BRWN Bldg, Purdue University
West Lafayette, IN 47907-1393
USA

Tel:(+1-317) 494 5320
Fax:(+1-317) 496 1200

Computer Techniques

Prof. J.T. Clerc
Universität Bern
Pharmazeutisches Institut
Baltzerstrasse 5, CH-3012 Bern
Switzerland

Tel:(+41-31) 6314191
Fax:(+41-31) 6314198

Prof. Sarah C. Rutan
Department of Chemistry
Virginia Commonwealth University
P.O. Box 2006
Richmond, VA 23284-2006
USA
Tel:(+1-804) 367 1298
Fax:(+1-804) 367 7517

Other Papers

Prof. Alan Townshend
Department of Chemistry
The University
Hull HU6 7RX
Great Britain

Tel:(+44-482) 465027
Fax:(+44-482) 466410

Prof. Willem E. van der Linden
Laboratory for Chemical Analysis
Department of Chemical Technology
Twente University of Technology
P.O. Box 217, 7500 AE Enschede
The Netherlands
Tel:(+31-53) 892629
Fax:(+31-53) 356024

Prof. Paul Worsfold
Dept. of Environmental Sciences
University of Plymouth
Plymouth PL4 8AA
Great Britain

Tel:(+44-752) 233006
Fax:(+44-752) 233009

Submission of an article is understood to imply that the article is original and unpublished and is not being considered for publication elsewhere. *Anal. Chim. Acta* accepts papers in English only. There are no page charges. Manuscripts should conform in layout and style to the papers published in this issue. See inside back cover for "Information for Authors".

Publication. *Analytica Chimica Acta* appears in 16 volumes in 1994 (Vols. 281-296). *Vibrational Spectroscopy* appears in 2 volumes in 1994 (Vols. 6 and 7). Subscriptions are accepted on a prepaid basis only, unless different terms have been previously agreed upon. It is possible to order a combined subscription (*Anal. Chim. Acta* **and** *Vib. Spectrosc.*).
Our p.p.h. (postage, packing and handling) charge includes surface delivery of all issues, except to subscribers in the U.S.A., Canada, Australia, New Zealand, China, India, Israel, South Africa, Malaysia, Thailand, Singapore, South Korea, Taiwan, Pakistan, Hong Kong, Brazil, Argentina and Mexico, who receive all issues by air delivery (S.A.L.-Surface Air Lifted) at no extra cost. For Japan, air delivery requires 25% additional charge of the normal postage and handling charge; for all other countries airmail and S.A.L. charges are available upon request.

Subscription orders. Subscription prices are available upon request from the publisher. Subscription orders can be entered only by calendar year and should be sent to: Elsevier Science B.V., Journals Department, P.O. Box 211, 1000 AE Amsterdam, The Netherlands. Tel: (+31-20) 5803 642, Telex: 18582, Telefax: (+31-20) 5803598, to which requests for sample copies can also be sent. Claims for issues not received should be made within six months of publication of the issues. If not they cannot be honoured free of charge. Readers in the U.S.A. and Canada can contact the following address: Elsevier Science Inc., Journal Information Center, 655 Avenue of the Americas, New York, NY 10010, U.S.A. Tel: (+1-212) 6333750, Telefax: (+1-212) 6333990, for further information, or a free sample copy of this or any other Elsevier Science journal.
Advertisements. Advertisement rates are available from the publisher on request.

US mailing notice - Analytica Chimica Acta (ISSN 0003-2670) is published 3 times a month (total 48 issues) by Elsevier Science B.V. (Molenwerf 1, Postbus 211, 1000 AE Amsterdam). Annual subscription price in the USA US$ 3035.75 (valid in North, Central and South America), including air speed delivery. Second class postage paid at Jamaica, NY 11431. *USA Postmasters*: Send address changes to Anal. Chim. Acta, Publications Expediting, Inc., 200 Meacham Av., Elmont, NY 11003. Airfreight and mailing in the USA by Publication Expediting.

ANALYTICA CHIMICA ACTA

An international journal devoted to all branches of analytical chemistry

(Full texts are incorporated in CJELSEVIER, a file in the Chemical Journals Online database available on STN International; Abstracted, indexed in: Aluminum Abstracts; Anal. Abstr.; Biol. Abstr.; BIOSIS; Chem. Abstr.; Curr. Contents Phys. Chem. Earth Sci.; Engineered Materials Abstracts; Excerpta Medica; Index Med.; Life Sci.; Mass Spectrom. Bull.; Material Business Alerts; Metals Abstracts; Sci. Citation Index)

VOL. 287 NO. 1–2 CONTENTS MARCH 10, 1994

(Continued overleaf)

Contents (continued)

ANALYTICA CHIMICA ACTA
VOL. 287 (1994)

ANALYTICA CHIMICA ACTA

An international journal devoted to all branches of analytical chemistry
Revue internationale consacrée à tous les domaines de la chimie analytique
Internationale Zeitschrift für alle Gebiete der analytischen Chemie

Anal. Chim. Acta, Vol. 287 (1994)

ELSEVIER, Amsterdam–London–New York–Tokyo

0003-2670/94/$07.00

ELSEVIER

Analytica Chimica Acta 287 (1994) 1–6

ANALYTICA CHIMICA ACTA

ACKNOWLEDGEMENTS TO REFEREES

Scientific reviewers provide an invaluable service to authors and editors alike by offering objective criticisms that help authors to improve their manuscripts and editors to make proper decisions. Accordingly, we thank the following persons for their generous and expert assistance during the past year.

Harry L. Pardue
Alan Townshend
J.T. Clerc
Willem E. van der Linden
Paul J. Worsfold

Abbott, R.W., Welwyn, UK
Achterberg, E., Liverpool, UK
Adams, F., Wilrijk, Belgium
Affolter, Ch., Bern, Switzerland
Agarwal, V., New Haven, CT, USA
Agterdenbos, J., Nieuwegein, Netherlands
Aizawa, M., Yokohama, Japan
Al-Tamrah, S.A., Riyadh, Saudi Arabia
Al-Warthan, A.A., Riyadh, Saudi Arabia
Albin, M., Forest City, CA, USA
Anderson, H.A., Aberdeen, UK
Anderson, R.F., Palisades, USA
Ando, T., Shiga, Japan
Arnold, M., Iowa City, IA, USA

Baeyens, W.R.G., Ghent, Belgium
Bagnat, R., Milan, Italy
Baldwin, R., Louisville, KY, USA
Balk, L.J., Wuppertal, Germany
Barceló, D., Barcelona, Spain
Barnes, R.M., Amherst, MA, USA
Barnett, N.W., Geelong, Australia
Bartick, E., Quantico, VA, USA
Bartroli, J., Barcelona, Spain
Bauer, H.E., Stuttgart, Germany
Baxter, D.C., Umeå, Sweden
Bayona, J.M., Barcelona, Spain
Bender, H., Leuven, Belgium
Benoit, D., St. Germain en Laye, France
Benson, R., Caulfield East, Australia
Beran, P., Prague, Czech Republic
Bermejo-Barrera, M.P., Santiago de Compostella, Spain
Beugeling, T., Enschede, Netherlands
Bezegh, A., Budapest, Hungary
Blanco Gonzalez, E., Oviedo, Spain
Blount, A., Newark, NJ, USA
Blundell, N., Plymouth, UK
Bodenhausen, G., Geneva, Switzerland
Bond, A.M., Bundoora, Australia
Borén, H., Linköping, Sweden
Bos, A., Enschede, Netherlands
Bos, M., Enschede, Netherlands
Bosch, E., Barcelona, Spain
Bourquin, Bern, Switzerland
Brajter-Toth, A., Gainesville, FL, USA
Branica, M., Zagreb, Croatia
Brereton, R.G., Bristol, UK
Bright, F., Buffalo, NY, USA
Brinkman, U.A.Th., Amsterdam, Netherlands
Brown, A., Plymouth, UK
Brown, R., Norcross, GA, USA
Brown, S.D., Newark, DE, USA
Bruland, K.W., Santa Cruz, CA, USA
Brzozka, Z., Warsaw, Poland
Buch-Rasmussen, T., Hillerød, Denmark
Bucknall, S., Weybrigde, UK
Buckner, S., Tucson, AZ, USA
Buffle, J., Genèva, Switzerland
Burguera, J.L., Merida, Venezuela
Burguera, M., Merida, Venezuela
Burns, D.T., Belfast, UK
Buydens, L.M.C., Nijmegen, Netherlands
Byrne, R.H., St. Petersburg, FL, USA

0003-2670/94/$07.00
SSDI 0003-2670(94)00011-A

Calokerinos, A.C., Athens, Greece
Cámara, C., Madrid, Spain
Campbell, M., Ghent, Belgium
Cano Pavon, J.M., Malaga, Spain
Cardwell, T.J., Bundoora, Australia
Carlsen, M., Lyngby, Denmark
Carr, P., Minneapolis, MN, USA
Caruso, J.A., Cincinnati, OH, USA
Casey, H., Wareham, UK
Cerda, V., Palma de Mallorca, Spain
Ceulemans, M., Antwerp, Belgium
Chen, E., West Lafayette, IN, USA
Cheng, Y.-F., Edmonton, Canada
Chiavarini, S., Rome, Italy
Chipperfield, J.R., Hull, UK
Choppin, G.R., Tallahassee, FL, USA
Christie, I., Salford, UK
Christie, O.H.J., Stavanger, Norway
Churacek, J., Pardubice, Czech Republic
Clark, B.J., Bradford, UK
Cleven, R.F.M.J., Bilthoven, Netherlands
Clinch, J.R., Rotherham, UK
Cofino, W., Amsterdam, Netherlands
Cornelis, R., Ghent, Belgium
Coulet, P.R., Lyon, France
Covington, A.K., Newcastle-upon-Tyne, UK
Crabbe, N., Huddersfield, UK
Craig, P.J., Leicester, UK
Cresser, M., Aberdeen, UK
Crouch, S.R., East Lansing, MI, USA

Dachs, J., Barcelona, Spain
Dams, R., Ghent, Belgium
Daniels, R.S., Wolfville, Canada
Danielson, N., Oxford, OH, USA
Danielsson, L.G., Stockholm, Sweden
Danzer, K., Jena, Germany
Darks, J., Barcelona, Spain
Das, H.A., Petten, Netherlands
Dasgupta, P.K., Lubbock, TX, USA
Davison, W., Lancaster, UK
De Boevere, C., Ghent, Belgium
De Brabander, H., Ghent, Belgium
De Corte, F., Ghent, Belgium
De Haan, J., Eindhoven, Netherlands
De la Calle, B., Madrid, Spain
De Loos-Vollebregt, M.T.C., Delft, Netherlands
De Maine, P.A.D., Auburn, AL, USA
De Mora, S.J., Auckland, New Zealand
De Ruig, W.G., Wageningen, Netherlands
De Schrijver, G., Ghent, Belgium
De Spiegeleer, B., Puurs, Belgium
Dean, J.R., Newcastle-upon-Tyne, UK
Delves, T., Southampton, UK
Demas, J., Charlottesville, VA, USA
Deming, S., Houston, TX, USA
Devi, S., Baroda, India
Di Corcia, A., Rome, Italy
Diaz, M., Oviedo, Spain
Dirkx, W., Antwerp, Belgium
Diserens, J.-M., Lausanne, Switzerland
Donard, O.F.X., Bordeaux, France
Donat, J.R., Norfolk, VA, USA
Doornbos, D.A., Groningen, Netherlands
Dorsey, J., Cincinnati, OH, USA
Drabaek, I., Søborg, Denmark
Dursch, I., Freising, Germany
Dyrssen, D., Göteborg, Sweden

Ebdon, L.C., Plymouth, UK
Eckert, J.M., Sydney, Australia
Eckharri, I., Zaragoza, Spain
Elton, N.J., Cornwall, UK
English, A.D., Wilmington, DE, USA
Ertl, G., Berlin, Germany
Esteban, M., Barcelona, Spain
Evans, O., Cincinnati, OH, USA
Everaerts, F.M., Eindhoven, Netherlands
Everett, G.L., Royston, UK
Ewing, D., Hull, UK

Fain, S., Ashland, OR, USA
Fehér, Z., Budapest, Hungary
Fell, A.F., Bradford, UK
Fernando, Q., Tucson, AZ, USA
Fielden, P., Manchester, UK
Fisher, A., Plymouth, UK
Fogg, A.G., Loughborough, UK
Forina, M., Genova, Italy
Foulkes, M., Plymouth, UK
Fraissard, J., Paris, France
Franks, J., Wilton, UK
Freiser, B., West Lafayette, IN, USA
Frenzel, W., Berlin, Germany
Furton, K., Miami, FL, USA

Gachanja, A.J., Plymouth, UK
Gamble, D.S., Ottawa, Canada
Gammelgaard, B., Copenhagen, Denmark
Gardner, M., Marlow, UK
Garten, R.P.H., Dortmund, Germany
Gelan, J., Diepenbeek, Belgium
Gibson, T.D., Leeds, UK
Giger, W., Dübendorf, Switzerland
Gijbels, R., Wilrijk, Belgium
Gillespie, A.M., Detroit, MI, USA
Głab, S., Warsaw, Poland
Gleason, K., Cambridge, MA, USA
Goodall, D.M., York, UK
Gooijer, C., Amsterdam, Netherlands
Gorton, L., Lund, Sweden
Grabke, N.J., Düsseldorf, Germany
Grallath, G., Dortmund, Germany
Grasserbauer, M., Vienna, Austria

Green, J.D., Hull, UK
Greenway, G.M., Hull, UK
Griffiths, P., Moscow, ID, USA
Groeneveld, E.R., Lisse, Netherlands
Grunze, M., Heidelberg, Germany
Gubitz, G., Graz, Austria
Guilbault, G.G., New Orleans, LA, USA
Guy, R.D., Halifax, Canada

Haase, N.U., Göttingen, Germany
Haddad, P.R., Hobart, Australia
Haggart, R., Cambridge, UK
Halls, D.J., Glasgow, UK
Hantsche, H., Berlin, Germany
Hara, H., Shiga, Japan
Hargis, L., New Orleans, LA, USA
Harrington, P., Athens, OH, USA
Harris, R.K., Durham, UK
Hart, J.P., Bristol, UK
Harvey, B.R., Lowestoft, UK
Haswell, S.J., Hull, UK
Haworth, D.T., Milwaukee, WI, USA
Heitzman, R., Newbury, UK
Helmlin, H.-J., Bern, Switzerland
Hemmila, I., Turku, Finland
Hendra, P., Southampton, UK
Henze, G., Trier, Germany
Heumann, K.G., Regensburg, Germany
Hieftje, G., Bloomington, IN, USA
Hill, S., Plymouth, UK
Hilton, J., Ambleside, UK
Hinze, W.L., Winston-Salem, NC, USA
Hippe, Z.-S., Rzeszow, Poland
Holcombe, J., Austin, TX, USA
Holler, J., Lexington, KY, USA
Hopke, P.K., Potsdam, NY, USA
Horstman, H.J., Wageningen, Netherlands
Horvai, G., Budapest, Hungary
Houk, R.S., Ames, IA, USA
Howard, A.G., Southampton, UK
Howell, J., Kalamazoo, MI, USA
Huber, C., Milwaukee, WI, USA
Hulanicki, A., Warsaw, Poland
Hummel, R.E., Gainesville, FL, USA
Hungerford, J.M., Bothwell, WA, USA
Hurley, P.W., Cambridge, UK
Hurtubise, R.J., Laramie, WY, USA

Imai, K., Tokyo, Japan
Imasaka, T., Fukuoka, Japan
Ingle, J.D., Corvallis, OR, USA
Ingman, F., Stockhom, Sweden
Issopoulos, P.B., Ioannina, Greece
Ivaska, A., Turku, Finland

Jackwerth, E., Bochum, Germany
Jagner, D., Göteborg, Sweden
Jakubowski, N., Dortmund, Germany
Jenkins, R., Swarthmore, PA, USA
Jerome, S., Teddington, UK
Johansson, G., Lund, Sweden
Johnson, D.C., Ames, IA, USA
Jones, P., Plymouth, UK
Jordan, J., Cincinnati, OH, USA
Jurs, P.C., University Park, PA, USA

Kaiser, M., Newark, DE, USA
Karcher, R., Detroit, MI, USA
Karjalainen, E., Helsinki, Finland
Karlberg, B., Sollentuna, Sweden
Karube, I., Tokyo, Japan
Kateman, G., Nijmegen, Netherlands
Kathir, P., London, UK
Katsu, T., Okayama, Japan
Kauffmann, J.M., Brussels, Belgium
Keim, E.G., Enschede, Netherlands
Keller, H., Basle, Switzerland
Kellner, R., Vienna, Austria
Keto, R., Rockville, MD, USA
Klinowski, J., Cambridge, UK
Kobos, R., Wilmington, DE, USA
Koeltzow, D., Kansas, MO, USA
Koenig, J.L., Cleveland, OH, USA
Kok, W.Th., Amsterdam, Netherlands
Kokot, S., Brisbane, Australia
Kolev, S.D., Sofia, Bulgaria
Kooyman, R.P.H., Enschede, Netherlands
Kotrly, S., Pardubice, Czech Republic
Kragten, J., Amsterdam, Netherlands
Kramer, J.R., Hamilton, Canada
Krivan, V., Ulm, Germany
Krull, U.J., Mississauga, Canada
Kubic, T., Northport, NY, USA
Kuhr, W.G., Riverside, CA, USA
Kulys, J., Hillerod, Denmark
Kurusu, K., Yokohama, Japan
Kuwana, T., Lawrence, KA, USA
Kvalheim, O.V., Bergen, Norway
Kwakman, P.J.M., Amsterdam, Netherlands

Lancaster, J.S., Hull, UK
Langford, C., Quebec, Canada
Lanza, P., Bologna, Italy
Larsen, K., Chicago, IL, USA
Laude Jun, D.A., Austin, TX, USA
Lauer, H.H., Emmen, Netherlands
Le Gressus, C., Bruyeres-Le-Chalet, France
Leidner, R., West Lafayette, IN, USA
Leonards, P., Amsterdam, Netherlands
Leroy, M., Strasbourg, France
Leussing, D., Columbus, OH, USA
Lewenstam, A., Turku, Finland
Li, Y.Q., Xiamen, China
Liebich, H.M., Tübingen, Germany

Lingeman, H., Amsterdam, Netherlands
Littlejohn, D., Glasgow, UK
Lochmüller, C.H., Durham, NC, USA
Logan, B., Seattle, WA, USA
Lohninger, J., Wien, Austria
Low, G.K.-C., Menai, Australia
Lubert, K.-H., Leipzig, Germany
Lukaszewski, Z., Poznan, Poland
Luque de Castro, M.D., Córdoba, Spain
Luther III, G.W., Lewes, DE, USA
Lytle, F.E., West Lafayette, IN, USA

Macca, C., Padova, Italy
Macdonald, A.M.G., Birmingham, UK
Maciel, G., Fort Collins, USA
Mackey, D., Hobart, Australia
MacLaurin, P., Huddersfield, UK
Macrae, R., Hull, UK
Maghuin-Rogister, G., Liège, Belgium
Maier, E.A., Brussels, Belgium
Malinska, J., Poznan, Poland
Malinski, T., Rochester, MI, USA
Mall, W., Vernon Hills, IL, USA
Mangani, P., Urbino, Italy
Marcott, C., Cincinnati, OH, USA
Mark, H.B., Cincinnati, OH, USA
Marko-Varga, G., Lund, Sweden
Martell, A.E., College Station, TX, USA
Martin, F., Bordeaux, France
Martinez Calatayud, J., Valencia, Spain
Massart, L.D., Brussels, Belgium
Mathiasson, B., Lund, Sweden
Mathis, G., Bagnols sur Ceze, France
McCombes, P., Chester, UK
McCord, B., Quantico, VA, USA
McDowall, R.D., Beckenham, UK
McGorrin, R.J., Glenview, IL, USA
McKelvie, I., Caulfield East, Australia
McLeod, C.W., Sheffield, UK
Meier, P., Schaffhausen, Switzerland
Mellon, F.A., Norwich, UK
Meloun, M., Pardubice, Czech Republic
Mentasti, E., Turin, Italy
Mermet, J.M., Lyon, France
Merrick, M., South Carolina West, VA, USA
Meyer, H.H.D., Freising-Weihenstephan, Germany
Michotte, Y., Brussels, Belgium
Miles, W.J., Denver, CO, USA
Miller, J.N., Loughborough, UK
Miller, R.M., Port Sunlight, UK
Minkkinen, P., Lappeenranta, Finland
Moffett, J., Woods Hole, MA, USA
Morabito, R., Rome, Italy
Morgan, L., Hightstown, NJ, USA
Morley, N., Southampton, UK
Morosini, M., Ulm, Germany
Morris, M.D., Ann Arbor, MI, USA
Morrison, G., Göteborg, Sweden
Mosk, J., Amsterdam, Netherlands
Motomizu, S., Okayama, Japan
Mottola, H.A., Stillwater, OK, USA
Müller, H., Merseburg, Germany
Munk, M.E., Tempe, AZ, USA
Munoz de la Pena, A., Badajoz, Spain

Naes, T., As, Norway
Nagels, L., Antwerp, Belgium
Narayanaswamy, R., Manchester, UK
Neidhart, B., Marburg, Germany
Nielsen, J., Lyngby, Denmark
Nieman, T.A., Urbana, IL, USA
Niessner, R., Münich, Germany
Nimmo, M., Plymouth, UK
Nomura, T., Matsumoto, Japan
Nusko, R., Regensburg, Germany

Ogasaware, F., East Lansing, MI, USA
Ohkura, Y., Fukuoka, Japan
Ohta, K., Mie, Japan
Okada, T., Ibaraki, Japan
Okamoto, Y., New York, NY, USA
Otto, M., Freiberg, Germany
Owen, T., Waldbron, Germany

Pacakova, V., Prague, Czech Republic
Palecek, E., Brno, Czech Republic
Palys, M., Warsaw, Poland
Pardue, J., Chestervield, VA, USA
Parry, S.J., Ascot, UK
Parthasarathy, N., Geneva, Switzerland
Pemberton, J.E., Tucson, AZ, USA
Pérez-Bendito, D., Córdoba, Spain
Pfendt, L.B., Belgrade, Yugoslavia
Pietrzyk, D., Iowa city, IA, USA
Pingarron, J.M., Madrid, Spain
Pitts, L., Plymouth, UK
Plavsic, M., Zagreb, Croatia
Pletcher, D., Southampton, UK
Poole, C.F., Detroit, MI, USA
Poppe, H., Amsterdam, Netherlands
Pramauro, E., Turin, Italy
Presley, L., Washington, DC, USA
Pretsch, E., Zürich, Switzerland
Price, D., Plymouth, UK
Przemeck, E., Göttingen, Germany
Pulfer, J.D., USA

Quevauviller, P.R., Brussels, Belgium

Rajakovic, L., Belgrade, Yugoslavia
Rapsomanikis, S., Mainz, Germany
Regnier, F., West Lafayette, IN, USA
Reich, G., Vienna, Austria
Ren, K., Poznan, Poland

Riby, P., London, UK
Rivas, C., Madrid, Spain
Robien, W., Vienna, Austria
Rocks, B., Brighton, UK
Rommers, P., Eindhoven, Netherlands
Rossi, D., Columbus, OH, USA
Rossi, T.M., Spring House, PA, USA
Rowland, S., Plymouth, UK
Rüedi, P., Zürich, Switzerland
Russell, M., Poole, UK
Rüttimann, G.T., Bern, Switzerland

Sahuquillo, A., Barcelona, Spain
Saito, T., Kanagawa, Japan
Sakai, Y., Tokyo, Japan
Salinas, F., Badajoz, Spain
Sanz Medel, A., Oviedo, Spain
Sarzanini, C., Turin, Italy
Sato, H., Yokohama, Japan
Sauer, M.J., Weybridge, UK
Scheller, F., Berlin, Germany
Scheper, Th., Hannover, Germany
Schmid, R.D., Braunschweig, Germany
Schoenmakers, P., Amsterdam, Netherlands
Schügerl, K., Hannover, Germany
Schulman, S.G., Gainesville, FL, USA
Schulz, W., Wilmington, DE, USA
Schuster, M., Garching, Germany
Schwedt, G., Clausthal-Zellerfeld, Germany
Schweitzer, G., Knoxville, TN, USA
Seibt, E.W., Karlsruhe, Germany
Seitz, R., Durham, NH, USA
Senesi, N., Bari, Italy
Shpigun, L.K., Moscow, Russia
Sluyters-Rehbach, M., Utrecht, Netherlands
Smit, H.C., Amsterdam, Netherlands
Smith, D.K., University Park, PA, USA
Smith, R.M., Loughborough, UK
Smyth, M.R., Dublin, Ireland
Smyth, W.F., Coleraine, UK
Snook, R.D., Manchester, UK
Somberg, Karlsruhe, Germany
Sommer, L., Brno, Czech Republic
Sparkes, S., Plymouth, UK
Stäb, J., Amsterdam, Netherlands
Statham, P.J., Southampton, UK
Stocklein, W., Braunschweig, Germany
Stoeppler, M., Jülich, Germany
Stoney, D., Chicago, IL, USA
Störi, H., Vienna, Austria
Stulik, K., Prague, Czech Republic
Sturgeon, R.E., Ottawa, Canada
Suzuki, T., Yamaguta, Japan
Szepesi, G., Budapest, Hungary

Tabata, M., Saga, Japan
Tempelman, J., Delft, Netherlands
Terada, K., Ishikawa, Japan
Tercier, M.-L., Geneva, Switzerland
Thomas, J.D.R., Cardiff, UK
Thompson, K.C., Sheffield, UK
Thornton, J., Berkeley, CA, USA
Timerbaev, A.R., Linz, Austria
Tipping, E., Ambleside, UK
Tomaino, G., Easton, PA, USA
Tosi, G., Modena, Italy
Town, R., Geneva, Switzerland
Trojanowicz, M., Warsaw, Poland
Turner, D.R., Gothenburg, Sweden
Turner, A.P.F., Cranfield, UK
Tycko, R., Murray Hill, USA
Tyson, J.F., Amhurst, MA, USA

Uden, P., Amherst, MA, USA
Uhegbu, C., Youngstown, OH, USA
Umetani, S., Kyoto, Japan
Umezawa, Y., Tokyo, Japan

Vadgama, P., Salford, UK
Valcárcel, M., Córdoba, Spain
Van Bennekom, Utrecht, Netherlands
Vandeginste, B.G.M., Vlaardingen, Netherlands
Van den Berg, C.M.G., Liverpool, UK
Van den Berg, J.H.M., Weesp, Netherlands
Van den Hoop, M., Netherlands
Van der Schoot, B.H., Neuchatel, Switzerland
Van der Wal, P.D., Neuchatel, Switzerland
Van der Wal, S., Geleen, Netherlands
Van de Waterbeemd, H., Basel, Switzerland
Van Dyke, D.A., King of Prussia, PA, USA
Van Espen, P., Wilrijk, Belgium
Van Grieken, R.E., Wilrijk, Belgium
Van Leeuwen, H.P., Wageningen, Netherlands
Van Lento, F., Cleveland, OH, USA
Vanoosthuyze, K., Ghent, Belgium
Van Raaphorst, C. Petten, Netherlands
Van Staden, J.F., Pretoria, South Africa
Van Straten, A.J., Rotterdam, Netherlands
Van Veen, E.H., Delft, Netherlands
Van Zoonen, P., Bilthoven, Netherlands
Veeman, W.S., Dortmund, Germany
Viefhaus, H., Düsseldorf, Germany
Vigh, G., College Station, TX, USA
Viré, J.C., Brussels, Belgium
Volke, J., Prague, Czech Republic
Vytras, K., Pardubice, Czech Republic

Wada, H., Nagoya, Japan
Wade, A., Vancouver, Canada
Waldock, M., Burnham-on-Crouch, UK
Wallace, G.G. Wollongong, Australia
Wang, J., Las Cruces, NM, USA
Warner, I.M., Atlanta, GA, USA

Weeks, I., Cardiff, UK
Wegscheider, W., Graz, Austria
Wehry, E.L., Knoxville, TN, USA
Weijland, J.W., Enschede, Netherlands
Wells, D.E., Aberdeen, UK
Welz, B., Uberlingen, Germany
Werner, H.W., Waalre, Netherlands
West, N.W., Sheffield, UK
Whiteside, I., Middlesbrough, UK
Wigfield, D.C., Ottawa, Canada
Wilkins, C., Riverside, CA, USA
Winefordner, J.D., Gainesville, FL, USA
Wolfbeis, O.S., Graz, Austria
Wolff, G., Liverpool, UK
Woo, J., Syracuse, NY, USA
Wurster, R., Stuttgart, Germany

Yacynych, A., New Brunswick, NJ, USA
Yasuda, Y., Gifu, Japan
Yeung, E., Ames, IA, USA

Zadjura, R., Bridgewater, NJ, USA
Zagatto, E.A.G., Sao Paulo, Brasil
Zelic, M., Zagreb, Croatia
Zirino, A., San Diego, CA, USA
Zuberbühler, A.D., Basel, Switzerland
Zupan, J., Ljubljana, Slovenia
Zwanziger, H., Merseburg, Germany

Analytica Chimica Acta, 287 (1994) 7–15
Elsevier Science B.V., Amsterdam

Determination of atrazine, deethylatrazine and deisopropylatrazine in water and sediment by isotope dilution gas chromatography–mass spectrometry

D.A. Cassada and R.F. Spalding

Water Sciences Laboratory, Water Center, Institute of Agriculture and Natural Resources, 103 Natural Resources Hall, University of Nebraska, Lincoln, NE 68583-0844 (USA)

Z. Cai and M.L. Gross

Midwest Center for Mass Spectrometry, University of Nebraska, Lincoln, NE 68588-0304 (USA)

(Received 25th July 1993; revised manuscript received 4th October 1993)

Abstract

Methods for the trace analyses of atrazine, deethylatrazine (DEA), and deisopropylatrazine (DIA) in water and sediment have been developed by using stable-isotope dilution with gas chromatography–mass spectrometry detection. Water samples are spiked with known amounts of $^{13}C_3$-atrazine, $^{13}C_3$-DEA and $^{13}C_3$-DIA and submitted to solid-phase extraction with C_{18} bonded silica. Pesticides are eluted from the solid phase with ethyl acetate. Sediment samples are spiked and equilibrated with a known amount of each labeled standard before supercritical fluid extraction (SFE) using a 4% (v/v) methanol–CO_2 mobile phase at 43°C and 10 MPa with off-line collection in methanol. A gas chromatograph coupled with a quadrupole mass spectrometer operated in the selected ion monitoring (SIM) mode was used to analyze the concentrated sample extracts. When compared to conventional liquid–liquid extraction methods, these methods decrease extraction time, labor, and solvent volume required. Quantification of the triazines by using isotope dilution compensates for differences in physical recovery for atrazine and its metabolites, especially when large (> 100 ml) water volumes are extracted. Method detection limits for atrazine, DEA and DIA are 0.02, 0.02 and 0.10 $\mu g\ l^{-1}$, respectively, in water. In sediment, the method detection limits are 0.10, 0.20 and 0.50 ng g^{-1} for atrazine, DEA and DIA, respectively. More than 4000 water and 800 sediment samples have been analyzed by these methods for more than two years. The average accuracy (bias) for atrazine-fortified water samples is +6.4% ($n = 200$) and the precision from duplicate analyses is ±6.0%. Precision of the SFE method for atrazine is ±11% at the 2 ng g^{-1} level whereas accuracy is −3.2% ($n = 8$) for recovery of $^{13}C_3$-atrazine standard at the 5 ng g^{-1} level.

Keywords: Gas chromatography–mass spectrometry; Atrazine; Deethylatrazine; Deisopropylatrazine; Sediments; Waters

The increased demand for analytical accuracy in environmental samples has enhanced the importance of the use of isotope dilution procedures involving isotopically-labeled standards and mass spectrometers [1]. In these procedures, the isotopically-labeled compounds are added to the sample prior to analysis and compensate for analyte losses and provide both chromatographic (retention time) and mass standards. Among the

Correspondence to: R.F. Spalding, Water Sciences Laboratory, Water Center, Institute of Agriculture and Natural Resources, 103 Natural Resources Hall, University of Nebraska, Lincoln, NE 68583-0844 (USA).

SSDI 0003-2670(93)E0578-U

current analytical methods for atrazine (2-chloro-4-ethylamino-6-isopropylamino-1,3,5-triazine) in water, the use of $^{2}H_5$-atrazine as an internal standard has been developed for procedures involving liquid–liquid extraction with methylene chloride [2] and solid phase extraction with C_{18} bonded silica [3,4]. $^{13}C_3$-Atrazine has been shown to be an ideal internal standard for sub-ng l^{-1} level analyses of ground water samples by using high resolution mass spectrometry [5]. The use of $^{13}C_3$-deethylatrazine (DEA) (2-chloro-4-amino-6-isopropylamino-1,3,5-triazine) and $^{13}C_3$-deisopropylatrazine (DIA) (2-chloro-4-amino-6-ethylamino-1,3,5-triazine) as internal standards for the atrazine metabolites, however, has not yet been reported.

Solid phase extraction (SPE) has become widely accepted in recent years as concerns increase about the environmental impact of organic solvents used in conventional liquid–liquid extractions. Solid phases that are commonly used to extract pesticides include C_{18} bonded silica [3,4,6–8] and graphitized carbon black (Carbopack B) [9]. While C_{18} bonded silica has been used successfully for extracting atrazine, breakthrough [7] and recovery [8] studies for DEA and DIA indicate that these polar analytes can be prematurely lost in aqueous elution from the C_{18} cartridge. For these less retained compounds, the isotope dilution technique is especially appropriate, as it significantly enhances method accuracy as long as some labeled standard is recovered [2–5].

Atrazine extraction from sediment has been accomplished with a variety of methods that involve the use of organic solvents. Although extractions with methanol–water [3,10], acetone–hexane via a sonic probe [2], and methanol via a Soxhlet procedure [11,12] have been successfully used, sample throughput times are lengthy and disposal of waste organic solvents generated in these processes is costly. Supercritical fluid extraction (SFE) is an extraction alternative that decreases the time of analysis and virtually eliminates the need for organic solvents in sediment analyses [13]. In addition, supercritical CO_2 eliminates the need to concentrate the extract by solvent evaporation. SFE has been used to extract atrazine from sediment by using either CO_2 [14] or methanol [15] with recoveries $> 80\%$ for samples whose concentrations were above 50 ng g^{-1}. More sensitive SFE methods are required, however, to detect atrazine in the intermediate vadose zone, between the root zone and the water table, since concentrations generally approach 0.1 ng g^{-1} [16].

In this paper, solid-phase extraction for water and supercritical fluid extraction for sediment is coupled with isotope dilution GC–MS to analyze atrazine, DEA and DIA at trace concentrations.

EXPERIMENTAL

Apparatus

A Hewlett-Packard (HP) 5890 Series II gas chromatograph interfaced with a HP 5970 MSD quadrupole mass spectrometer was used for all sample analyses. The MSD was operated in the selected ion monitoring (SIM) mode for the ions listed in Table 1. Sample extracts and calibration standards were injected onto a GC column by a HP 7673A autosampler, and chromatograms were recorded by using an HP 59940A MS Chemsta-

TABLE 1

Quantitation, confirming and isotope reference ions used for DIA, DEA and atrazine (dwell time for all ions: 70 ms)

Analyte	Quantitation ion (m/z)	Confirming ion 1 (m/z)	Confirming ion 2 (m/z)	^{13}C Reference ion (m/z)	^{13}C Reference standard
DIA	173.0	158.0	145.0	176.0	$^{13}C_3$-DIA
DEA	172.0	187.0	145.0	175.0	$^{13}C_3$-DEA
Atrazine	200.0	215.0	173.0	203.0	$^{13}C_3$-Atrazine

tion software (HP-UX series) operated by a HP9000/340 computer. Separation was accomplished with a fused silica capillary column (DB-1, 30 m × 0.25 mm i.d., 0.25 μm film thickness, J&W Scientific) under the following conditions: splitless injection (1.0 μl) at 80°C, held for 0.75 min then a temperature gradient was programmed at 40°C min^{-1} to 140°C, then 4°C min^{-1} to 211°C, and then 39°C min^{-1} to 250°C and then held for 10 min. Injector and transfer line temperatures were both 280°C, and the split/splitless purge valve was opened 0.75 min after injection. Head pressure of the carrier gas (He, Chromatographic grade, Air Products) was 52 kPa (7.5 p.s.i.).

GC–high resolution MS analyses were performed on a Carlo-Erba GC/Kratos MS-50 double focusing mass spectrometer system at the Midwest Center for Mass Spectrometry. Sample extract (1 μl) was injected into a DB-1 fused silica capillary GC column (30 m × 0.25 mm i.d., J&W Scientific) with on-column injection at 50°C, held for 1 min then a temperature gradient was programmed at 15°C min^{-1} to 250°C. The column effluent was passed directly into the source via an interface operated at 250°C. The GC carrier gas was helium with a head pressure of 150 kPa (21 p.s.i.). The mass spectrometer was operated in the electron impact ionization (EI) mode at 70 eV, source temperature 250°C and resolution 8000–10000 (10% valley definition). Data acquisition and processing for the mass spectrometer were controlled by a Kratos MACH-3 computer system. A selected ion monitoring group in the mass profile mode was designed for the qualitative and quantitative analyses [5].

Extraction of water samples was performed with a six station vacuum manifold (Fig. 1). A precombusted glass fiber filter (Type A/E, 1.0 μm, Gelman Sciences) was used to remove suspended particles prior to the water entering the SPE cartridge.

Supercritical fluid extraction was performed on a SFE/50 extraction system (Suprex) equipped with a 250-ml syringe pump and a solvent modifier valve with a 10-ml loop. The extraction vessel (50 ml, Suprex) was connected to the SFE/50 using double slip-free connectors (10 cm × 0.50 mm i.d., Keystone Scientific). Mobile phase was

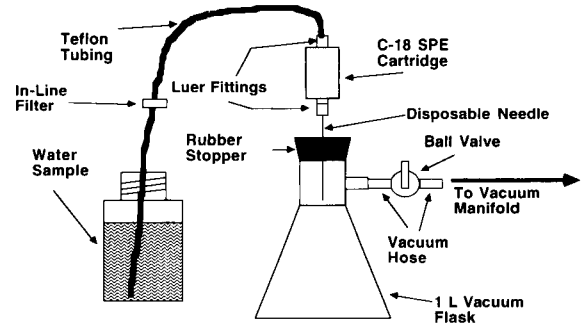

Fig. 1. Solid phase extraction (SPE) station used in the extraction of water samples. The station shown is one of six on the vacuum manifold.

4% (v/v) methanol–CO_2 at 43°C and 10 MPa (100 atm). The extract was collected off-line using a stainless steel restrictor [0.25 mm (0.010 in.) i.d., Supelco] into 2 ml of methanol.

Reagents and standards

Reference standards of atrazine, DEA and DIA (all Riedel de Haen Pestanal grade) were obtained from Crescent Chemical. Reference standards of $^{13}C_3$-atrazine, $^{13}C_3$-DEA, $^{13}C_3$-DIA and $^{2}H_{10}$-phenanthrene were obtained from Merck Sharp & Dohme/Isotopes (Division of Merck Frosst Canada). These standards were verified by ^{1}H and ^{13}C nuclear magnetic resonance spectroscopy (NMR) at Merck Isotopes and by high resolution mass spectrometry (HRMS) at the Midwest Center for Mass Spectrometry at the University of Nebraska. Methanol and ethyl acetate (both Optima grade) were obtained from Fisher Scientific. Sodium sulfate (anhydrous, certified ACS grade) was obtained from Fisher Scientific and purified by Soxhlet extraction with reagent grade methylene chloride for 10 h. Sodium bicarbonate (certified ACS grade) and silica sand were obtained from Fisher Scientific.

Stock solutions of both native and labeled standards were prepared in individual 4-ml amber silanized vials (Alltech) by dissolving approximately 20 mg of each standard in methanol (4 ml). Six calibration solutions were prepared by diluting analyte stock solutions in ethyl acetate, in which the concentrations of atrazine and DEA ranged from 0 to 35 ng μl^{-1} and the DIA con-

centration from 0 to 70 ng μl^{-1}. The concentrations of $^{13}C_3$-atrazine, $^{13}C_3$-DEA, $^{13}C_3$-DIA and $^2H_{10}$-phenanthrene were kept constant at 30 ng μl^{-1} for all calibration solutions. The spiking solutions of analytes and internal standards were each prepared by dilution of stock standards with methanol to obtain concentrations of 10 and 50 ng μl^{-1}, respectively. All solutions were stored at −10°C until needed.

Accuracy and precision

Fortified matrix samples (known additions) were used to determine the accuracy of the water method. A known amount of each analyte ($Am._{Spiked}$) was added to a predetermined sample matrix ($Am._{Matrix}$). These spiked samples were then extracted and analyzed. The result ($Am._{Measured}$) obtained from the analysis was compared to the spiked amount to obtain the accuracy (bias) for each determination (Eqn. 1).

$$\text{Bias} = 100 \times \frac{(Am._{Measured} - Am._{Matrix}) - Am._{Spiked}}{Am._{Spiked}} \quad (1)$$

The average bias for each analyte was then calculated from the bias values and is reported in a subsequent section. The relative standard deviation (s_{rel}) for each average is also given as an indication of the precision of the bias measurement at a confidence level of 1σ. For the sediment method, the bias was measured from the measured amount of $^{13}C_3$-atrazine relative to the response standard ($^2H_{10}$-phenanthrene), which gave an indication of extraction completeness.

The precision of the water method was determined from the relative percent difference (RPD) in the concentrations ($Conc._{Dup_x}$) obtained from the analysis of duplicate (split) samples (Eqn. 2).

$$\text{RPD} = 100 \times \left| \frac{[Conc._{Dup_1}] - [Conc._{Dup_2}]}{\left(\frac{[Conc._{Dup_1}] + [Conc._{Dup_2}]}{2} \right)} \right| \quad (2)$$

The s_{rel} of the RPD is given along with the number of duplicate pairs analyzed for each analyte. For the sediment method, the precision was determined by repeated extraction of an unsaturated zone sediment sample which contained low concentrations (< 5 ng g^{-1}) of the analytes. The average, s_{rel}, and number of determinations are also given.

Extraction procedure, water

Ground and surface water samples (800 ml) were collected in preweighed, combusted amber bottles, transported to the analytical laboratory in ice-filled coolers, and stored at 4°C. Fortified water samples were prepared by adding the analyte spiking solution into organic-free water to give concentrations in the range of 0.50 to 3.00 $\mu g\ l^{-1}$. Fortified matrix samples were prepared by standard addition of the analyte solution into a duplicated sample. Laboratory blanks, field blanks, and equipment blanks were prepared by using organic-free water. C_{18} SPE cartridges Sep-Pak Plus, $+C_{18}$ Environmental, Waters Chromatography (Division of Millipore) were prewashed with successive 5-ml applications of ethyl acetate, methanol and organic-free water.

After a water sample was weighed, the internal standards were added to the sample to produce $^{13}C_3$-atrazine, $^{13}C_3$-DEA and $^{13}C_3$-DIA concentrations between 4 and 5 $\mu g\ l^{-1}$. The sample was vigorously hand-shaken for 30 s and vacuum-siphoned through a SPE cartridge at a flow rate of 10–15 ml min^{-1}. After the sample had been extracted, the cartridge was allowed to aspirate for another 3–5 min to remove water residues.

The cartridge was eluted with 2 ml of ethyl acetate by using a solid phase extraction manifold (Supelco). The eluate was collected in a small test tube (10 × 75 mm), and the residual water layer was removed with a pipet and discarded. Miscible water was removed from the eluted ethyl acetate by adding anhydrous sodium sulfate. A response standard (4 μg of $^2H_{10}$-phenanthrene) was added to the extract, and after thorough mixing via a hand vortex mixer for 15 s, the extract was transferred by pipet to another small test tube. The extract was concentrated to 50 μl under a stream of dry nitrogen, pipetted to a 100-μl gas chromatograph vial, and crimp-sealed with a polytrifluoroethylene (PTFE) lined silicone cap.

Extraction procedure, sediment

Unconsolidated sediment cores were collected with a hollow-stem auger equipped with a split tube core barrel in acrylic liners (0.76 m × 6.4 cm o.d.), frozen in dry ice-filled coolers, and transported to the laboratory. After thawing, a 100-g sediment sample was cored from the interior of the sediment core, wrapped in aluminum foil, and refrozen until analysis. A sediment sample from Shelton, Nebraska containing a measurable atrazine concentration was periodically used to check extraction conditions. Silica sand was used as a matrix for method blanks.

The frozen sediment sample was manually pulverized while being thawed, and 20 g was placed in a precombusted glass container. Internal standards ($^{13}C_3$-atrazine, $^{13}C_3$-DEA and $^{13}C_3$-DIA) were added to the sediment at 5 ng g^{-1} levels along with 15 ml of methanol. The sample was hand-swirled for 15 s and the methanol was allowed to evaporate overnight in a fume hood. To increase permeability, the sediment was then combined with a mixture of 10 g of silica sand and 10 g of anhydrous sodium sulfate and transferred to an extraction vessel that contained 10 g of PTFE boiling chips. Methanol (2 ml) was then added to the vessel to prevent any water present in the sample from freezing and clogging the restrictor during the initial stages of the extraction. The vessel was sealed and the SFE/50 syringe pump was filled to 125 ml with 5 ml of methanol in approximately 120 ml of liquid CO_2 to produce a 4% (v/v) mobile phase. A 15-ml vial containing 1–2 ml methanol was placed at the end of the restrictor tube. A leak check was performed, and the system was equilibrated at 10 MPa (100 atm) and 43°C for 20 min. The analytes were collected in the 15-ml vial by bubbling the escaping CO_2 through the methanol at approximately 6 ml min^{-1}. The methanol was then evaporated under a stream of room air to approximately 1 ml and 1 drop of an aqueous solution of saturated sodium bicarbonate was added to neutralize the mixture. 2 ml of ethyl acetate was then added to the vial, the mixture vortexed, and transferred to a small test tube (10 × 75 mm). The mixture was allowed to separate, and the aqueous layer was removed with a pipet. Drying and concentrating the mixture followed the previously described protocol.

RESULTS AND DISCUSSION

Chromatography

Under the gas chromatographic conditions described above, the retention times of atrazine, DEA and DIA were 13.61, 11.66 and 11.34 min, respectively. Computed relative retention times (compared to atrazine) for DEA and DIA were 0.86 and 0.83, respectively, which were identical to those obtained by Ripley and Braun [17] using an equivalent SE-30 column. The separation between each analyte and its labeled standard was less than 0.6 s (0.01 min), and retention time reproducibility between gas chromatographic runs was better than ±0.2%. Total analysis time was 31.0 min to allow for elution of components with higher boiling points.

Mass spectrometry and calibration

On the basis of full scan (m/z 50–400) mass spectra of atrazine, its metabolites, and the corresponding labeled standards (Fig. 2), the base peak ion for each analyte was selected as its quantification ion. The next two most abundant ions in the mass spectrum served as confirmation ions. For the labeled standards, the reference ion used had a mass 3 a.m.u. above the quantification ion of the native analyte. One confirmation ion was also selected for $^{13}C_3$-atrazine and $^{13}C_3$-DEA, whereas two confirming ions were selected for $^{13}C_3$-DIA.

A six-point calibration curve was obtained for each analyte by plotting the ratio of the response (native ion to labeled ion) versus the ratio of the injected amounts (native to labeled). The calibration curves for all three analytes were linear up to the highest standard concentration. Each calibration curve was periodically checked by repeated analysis of a calibration standard at the beginning, during (after every 12 samples), and at the end of a sample batch.

Background signal level for the quantification ion of each analyte was estimated from the analysis of a blank calibration standard that contained only the labeled standards and assisted in improv-

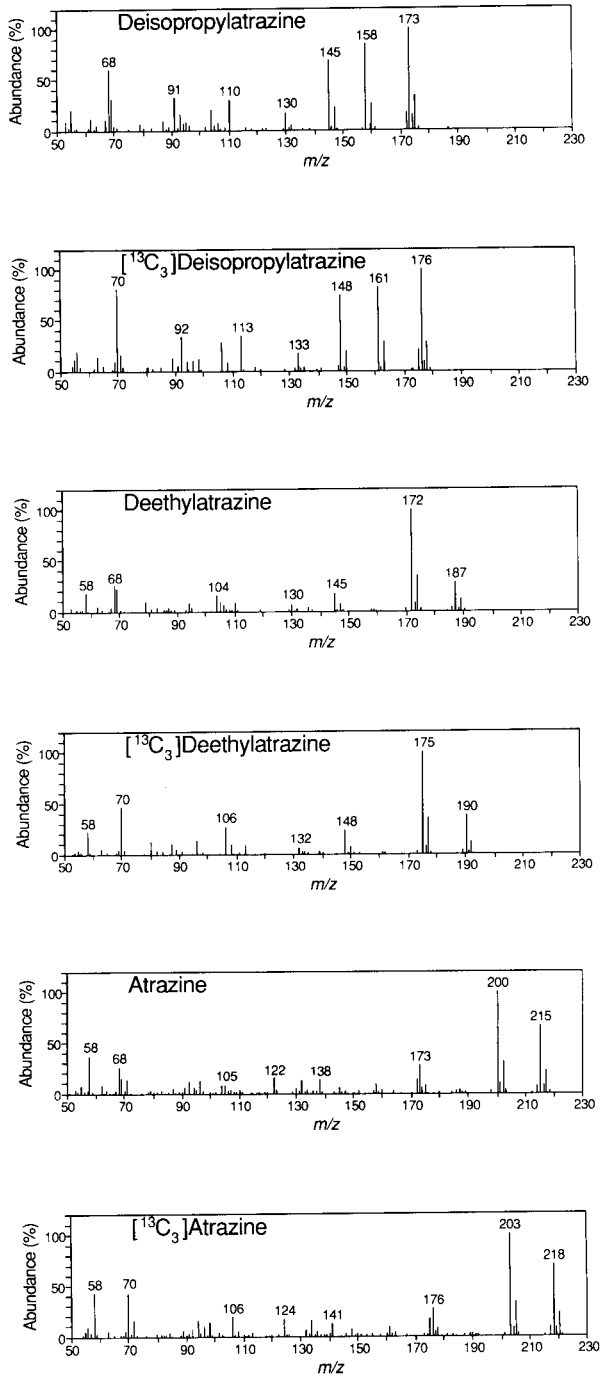

Fig. 2. Quadrupole mass spectra of the native and labeled analytes.

ing accuracy at the lowest levels. Instrument detection limits ($S/N = 5$) obtained for the analysis were 10 pg for atrazine, 8 pg for DEA and 18 pg for DIA. Method detection limits were determined by the procedure outlined by the U.S Environmental Protection Agency (USEPA) [18] and are discussed in the subsequent sections.

Solid-phase extraction

Recovery of DEA and DIA from water is poor when using either a C_{18} SPE cartridge [7,8] or conventional liquid–liquid extraction [19]. Pereira et al. [19] reported recoveries of $74 \pm 11\%$ for DEA and $34.1 \pm 0.7\%$ for DIA using liquid–liquid extraction with dichloromethane. Thurman et al. [7] reported that the 10% breakthrough capacities on C_{18} bonded silica are 300 ml and 75 ml of water for DEA and DIA, respectively. These are much lower than the 2000 ml breakthrough capacity for atrazine [7]. As a result, the recoveries obtained for extraction of 100 ml of sample were $99 \pm 5\%$, $90 + 5\%$ and $55 \pm 5\%$ for atrazine, DEA and DIA, respectively [7].

A study to determine the influence of sample volumes greater than 100 ml on recovery of atrazine, DEA and DIA included analyses of 4 samples at each of three volumes (200, 400 and 800 ml). As the sample volume increased, atrazine recovery remained constant at $95.1 \pm 8.3\%$ whereas the recovery for DEA decreased from $89.0 \pm 8.1\%$ to $63.1 \pm 4.4\%$ to $32.1 \pm 2.0\%$ and that for DIA decreased from $41.4 \pm 2.2\%$ to $24.0 \pm 2.0\%$ to $12.8 \pm 0.8\%$. These results are in agreement with previous results obtained by Thurman for 100 ml samples [7]. The reduced recovery can be compensated by isotope dilution, however, the recovery can also influence the method detection limit for that analyte. The obtained detection limits were 0.02 $\mu g\ l^{-1}$ for atrazine, 0.02 $\mu g\ l^{-1}$ for DEA and 0.10 $\mu g\ l^{-1}$ for DIA.

Analyses of 130 fortified (spiked) organic-free water samples and 70 fortified matrix samples at concentrations ranging from 0.5 to 8 $\mu g\ l^{-1}$ were evaluated over a 12-month period to determine the accuracy (bias) of the method. Biases of $+6.7 \pm 11.5\%$, $+0.3 \pm 16.3\%$, and $-21.5 \pm 26.6\%$ were obtained for atrazine, DEA and DIA, re-

spectively, in fortified organic-free samples, while biases of $+5.9 \pm 19.6\%$, $+4.6 \pm 22.1\%$ and $-2.6 \pm 24.8\%$, respectively, were obtained in fortified matrix samples. The accuracy for all analytes was very good although the low recovery of DIA in large sample volumes contributes to its poor accuracy and high variability.

Two hundred and fifty duplicate (split) samples were analyzed over the same time span to evaluate the precision of the analysis. The average relative percent differences (RPD) between duplicate samples are 6.0% ($n = 235$), 7.4% ($n = 170$) and 16.6% ($n = 61$) for atrazine, DEA and DIA, respectively.

To determine the interlaboratory reproducibility of the method, fortified organic-free water samples were analyzed at both the University of Nebraska's Water Sciences Laboratory and Midwest Center for Mass Spectrometry [5]. The results of the comparison are shown in Table 2. Three concentrations were analyzed, one concentration, 5 ng l^{-1}, was below the current method's detection limits for all three analytes whereas another concentration, 100 ng l^{-1}, was at the detection limit for DIA. In most cases, the agreement between the methods is good provided the concentrations are above the detection limit.

Supercritical fluid extraction

Past SFE methods to extract atrazine from sediments were used in sediments where mid ng g^{-1} to high $\mu g\ g^{-1}$ concentrations are commonly encountered. For these methods [14,15], various liquid phases (CO_2 and methanol), pressures (23 and 15 MPa), and temperatures (48°C and 250°C) were employed to extract the atrazine from the sediment with detection limits of approximately 50 ng g^{-1} [15] and 60 ng g^{-1} [14]. The SFE method developed here increases sensitivity by employing very mild supercritical fluid conditions (10 MPa at 43°C) to extract atrazine and its metabolites from the sediment with minimal interferences. The addition of 2 ml of methanol to the vessel prior to the extraction helped to minimize blockages in the restrictor as the initial flow was adjusted. As a result, the actual vessel concentration of methanol in the CO_2 was variable during the extraction and approached the mobile phase concentration of 4% as the initial methanol was removed. Current detection limits of 0.10 ng

TABLE 2

Interlaboratory comparison of atrazine, DEA and DIA analyses for fortified organic-free water samples

Fortified conc.	Water sciences laboratory (WSL)			Midwest center for mass spectrometry (MCMS)		
	Atrazine	DEA	DIA	Atrazine	DEA	DIA
5 ng l^{-1}						
$\bar{x}$ (ng l^{-1}) [a]	N.D. [e]	N.D.	N.D.	4.8	5.2	4.4
s (ng l^{-1}) [b]				0.1	0.2	0.5
s_{rel} (%) [c]				2.9	4.1	10.4
n [d]				6	6	6
100 ng l^{-1}						
$\bar{x}$ (ng l^{-1})	112	117	N.D.	106	131	123
s (ng l^{-1})	7	5		8	8	6
s_{rel} (%)	5.9	4.0		7.5	5.8	4.7
n	6	6		6	6	6
500 ng l^{-1}						
$\bar{x}$ (ng l^{-1})	527	543	397	488	503	489
s (ng l^{-1})	19	20	29	28	16	37
s_{rel} (%)	3.6	3.7	7.2	5.7	3.2	7.5
n	6	6	6	6	6	6
Detection limit (ng l^{-1})	20	20	100	0.2	1.0	3.0

[a] $\bar{x}$ = Average. [b] s = Standard deviation. [c] s_{rel} = Relative standard deviation. [d] n = Number of determinations. [e] N.D. = Not detected.

g^{-1} for atrazine, 0.20 ng g^{-1} for DEA and 0.50 ng g^{-1} for DIA allow for monitoring the vertical movement of the compounds in the unsaturated zone beneath the crop root zone.

Multiple extraction of an unsaturated zone sediment sample was performed to determine the precision of the SFE technique. An s_{rel} of $\pm 16\%$ ($n = 13$) was obtained for atrazine for an average concentration level of 1.91 ng g^{-1}. For DEA, an s_{rel} of $\pm 32\%$ ($n = 13$) was obtained at an average concentration of 0.25 ng g^{-1}, which is only slighty above the detection limit. For DIA, the average concentration obtained from the analyses was below the detection limit. At a spike level of 5 ng g^{-1}, a bias of $-4.9 \pm 9.3\%$ ($n = 13$) was determined for $^{13}C_3$-atrazine relative to the response standard ($^2H_{10}$-phenanthrene). Comparison of atrazine concentrations in top-soil and vadose zone sediments obtained from SFE with those obtained from methanol–water (80:20) shaking followed by water dilution and C_{18} solid-phase extraction [3] confirms that the SFE method is more efficient in removing atrazine than the liquid method with good correlation ($r^2 = 0.98$) between the two methods (Table 3).

Conclusions

Atrazine, deethylatrazine and deisopropylatrazine can be extracted by using C_{18} solid-phase cartridges at sub-μg l^{-1} levels in water and by using supercritical fluid extraction at ng g^{-1} levels in sediment. Through the use of GC–MS and isotope dilution, these methods provide both quantification and confirmation for each analyte in a single analysis. Isotope dilution also increases the quantification accuracy for analytes with low extraction efficiencies. In fortified organic-free and forified matrix water samples, the average bias for atrazine ($+6.4 \pm 14.9\%$) was slightly higher but less variable than that for DEA ($+1.8 \pm 18.7\%$). For DIA, the decrease in extraction efficiency becomes evident in both the magnitude and variability of the bias ($-14.7 \pm 27.5\%$). In sediment, the reproducibility of the SFE method for low ng g^{-1} levels of atrazine ($s_{rel} = 16\%$) is very good. The use of isotope dilution GC–MS is applicable to other organic agrichemicals once the appropriate isotopically-labeled standard is synthesized. Ideally, all analytes in a multiresidue method should be quantified by isotope dilution. However, the financial obstacles encountered in that situation would be

TABLE 3

Comparison of atrazine concentrations and $^{13}C_3$-atrazine accuracy from supercritical fluid extraction method with methanol–water extraction method for sediment samples at various depths

Core i.d.	Core depth range (ft.)	Sediment atrazine (ng g^{-1})		$^{13}C_3$-Atrazine bias (%)	
		SFE	Methanol–water	SFE	Methanol–water
1	0–2	15.8	11.6	−16	−7
1	0–2 (DUP)	16.4	11.4	−17	−6
1	4–5	0.22	0.21	−16	−20
1	8–9	0.28	0.03	−23	−31
2	1–2	23.2	21.8	+36	−11
2	8–9	0.14	0.10	−9	−18
3	1–2	30.9	29.2	+3	−17
3	4–5	1.96	1.76	−7	−26
3	4–5 (DUP)	1.83	1.71	−3	−35
3	8–9	1.26	1.20	+9	−29
4	0–1	15.9	13.3	+14	−7
4	4–5	1.95	0.19	−16	+0
4	8–9	0.27	0.25	−6	−12
Avg. bias ± S.D. (%)				−4 ± 16	−17 ± 11

hard to overcome. The methods included in this paper have been used to analyze more than 4000 water and 800 sediment samples from various locations in Nebraska.

We would like to acknowledge support from our USDA-CSRS/ARS MSEA project, the Nebraska Research Initiative, and partial support from our NSF Center Grant (No. DIR 9017262). This article has been assigned Journal Series Number 10459, Agricultural Research Division, University of Nebraska.

REFERENCES

1 Environmental Protection Agency, Fed. Regist., 49 (1984) 184.
2 V. Lopez-Avila, P. Hirata, S. Kraska, M. Flanagan, J.H. Taylor, Jr. and S.C. Hern, Anal. Chem., 57 (1985) 2797.
3 L.Q. Huang, J. Assoc. Off. Anal. Chem., 72 (1989) 349.
4 S.A. Schuette, R.G. Smith, L.R. Holden and J.A. Graham, Anal. Chim. Acta, 236 (1990) 141.
5 Z. Cai, V.M.S. Ramanujam, D.E. Giblin, M.L. Gross and R.F. Spalding, Anal. Chem., 65 (1993) 21.
6 G.A. Junk and J.J. Richard, Anal. Chem., 60 (1988) 451.
7 E.M. Thurman, M. Meyer, M. Pomes, C.A. Perry and A.P. Schwab, Anal. Chem., 62 (1990) 4043.
8 R.G. Nash, J. Assoc. Off. Anal. Chem., 73 (1990) 438.
9 A. Di Corcia and M. Marchetti, Anal. Chem., 63 (1991) 580.
10 E.G. Cotterill, Pestic. Sci., 11 (1980) 23.
11 G. Durand and D. Barceló, Anal. Chim. Acta, 243 (1991) 259.
12 H. Ghadiri, P.J. Shea, G.A. Wicks and L.C. Haderlie, J. Environ. Qual., 13 (1984) 549.
13 S.B. Hawthorne, Anal. Chem., 62 (1990) 663A.
14 V. Janda, G. Steenbeke and P. Sandra, J. Chromatogr., 479 (1989) 200.
15 P. Capriel, A. Haisch and S.U. Khan, J. Agric. Food Chem., 34 (1986) 70.
16 R.F. Spalding, Abstracts of ACS Agrochemicals Division, 197 (1989).
17 B.D. Ripley and H.E. Braun, J. Assoc. Off. Anal. Chem., 66 (1983) 1084.
18 Environmental Protection Agency, Pt. 136, App. B, 40 CFR Ch. I (7-1-89 Edition) (1989) 525.
19 W.E. Pereira, C.E. Rostad and T.J. Leiker, Anal. Chim. Acta, 228 (1990) 69.

Analytica Chimica Acta, 287 (1994) 17–24
Elsevier Science B.V., Amsterdam

Extraction and determination of butyltin compounds in shellfish by hydride generation–gas chromatography–quartz furnace atomic absorption spectrometry

F. Pannier, A. Astruc and M. Astruc

Laboratoire de Chimie Analytique, Université de Pau et des Pays de l'Adour, Avenue de l'Université, 64000 Pau (France)

(Received 9th August 1993; revised manuscript received 11th October 1993)

Abstract

The method described involves the conversion of butyltin compounds extracted from shellfish into volatile hydrides by sodium tetrahydroborate, cryogenic trapping and selective volatilization followed by on-line quartz furnace atomic absorption spectrometric detection. Several sample pretreatment procedures were compared with emphasis on their accuracy, reproducibility and respect for the speciation of tin. Digestion with 0.083 M HCl in 16.7% methanol under sonication for 1 h is proposed. The recoveries of mono-, di- and tributyltin compounds from spiked mussel and oyster samples ranged from 96 to 99% with low degradation of butyltins (< 9%). Detection limits were in the 2–3 ng Sn g^{-1} (wet weight) range. The method was applied to wild and commercial samples of oysters, mussels and scallops and fairly high concentrations of butyltin compounds were measured.

Keywords: Atomic absorption spectrometry; Gas chromatography; Butyltin compounds; Extraction; Hydride generation; Shellfish; Speciation

Butyltin compounds are extensively used in various areas of human activity. Monobutyltin (MBT) and dibutyltin (DBT) are present as additives in some polymer formulations. Tributyltin (TBT) is a biocide introduced into the environment through various ways: it is a preservative for wood and cloth and it is used as an antifouling agent in marine paints. The last application is now restricted in many countries, but nevertheless TBT is still present in aquatic environments where it is degraded slowly into DBT, MBT and inorganic tin salts. Accumulation of TBT by aquatic species (fishes, molluscs, algae) has been widely documented, with concentration factors ranging from 100 to 60 000 [1–3]. This accumulation in the food chain leads to concern over potential effects on human health through alimentation.

The toxicity of TBT and its effects at very low concentrations on marine biota (shell thickening of oysters, survival of oyster spat, imposex on gastropods, etc.) have been widely investigated [4–7]. However, the development procedures for the determination of butyltin compounds is concerned much more often with the analysis of waters and sediments than of biological material.

Correspondence to: M. Astruc, Laboratoire de Chimie Analytique, Université de Pau et des Pays de l'Adour, Avenue de l'Université, 64000 Pau (France).

SSDI 0003-2670(93)E0570-W

The main species of interest have been molluscs (oysters [8,9], mussels [10,11], scallops [12]) and a few fish (e.g., salmon [13,14], sea bass [15]).

Little effort has been devoted to the quality control of the proposed analytical procedures. Very few intercomparisons of methods have been made [16] and there is no available reference material of mollusc certified for its butyltin content. The NIES (Japan) [17] has recently produced a fish reference material certified for its TBT content, but this material must be kept frozen and its long-term stability and the possibility of transport have not been perfectly defined.

Hence there is an urgent need for the development and quality control of simple analytical procedures for the determination of butyltin compounds in marine food, especially shellfish.

A wide variety of methods for the separation and determination of butyltins have been proposed, but chromatographic methods are the most widely used, particularly those involving gas chromatography coupled to more or less specific detection methods such as flame photometric detection (FPD), flame ionization detection (FID), atomic absorption spectrometry (AAS) and mass spectrometry (MS) (Table 1).

In this paper, a simple method for the determination of butyltins in shellfish is described, based on acid leaching and analysis by HG–GC–AAS, suitable for the routine analysis of natural samples.

EXPERIMENTAL

Reagents

Di- and tributyltin chlorides were purchased from Merck and monobutyltin chloride from T& M Chemicals and all were used without further purification. Primary standard solutions (1000 mg l^{-1}) were prepared with methanol (Prolabo, Normapur) and stored for several months at 4°C in the dark; standard solutions (10 mg l^{-1}, 100 μg l^{-1}) were prepared daily by dilution in 10% HNO_3 (Merck, Suprapur) and deionized water (Millipore). Pure acetic acid and hydrochloric acid (pro analysi) were obtained from Prolabo. A 10% solution of $NaBH_4$ (Fluka, purum p.a.) was prepared weekly in 1% NaOH (Merck, Suprapur).

Analytical procedure

A small subsample (50–200 μl) of shellfish extract was introduced into the reaction flask

TABLE 1

Methods for the determination of organotin compounds in marine biological samples

Species	Compounds	Method [a]	Detection limits (as tin)	Ref.
Oysters	TBT	GFAAS	2 ng/g (5 g sample)	18
	TBT	GC–MS	8.2 ng/g	19
	TBT, DBT, MBT	GC–FPD	5–9 pg	20
	TBT, DBT, MBT	GC–FPD	2 ng/g wet sample	21
	TBT, DBT, MBT	HG–AAS	0.1–2.5 ng per 0.1 g wet sample	22
	TBT, DBT, MBT	HG–AAS	3.5 ng	23
Mussels	TBT	GC–AAS	4 ng/g wet sample	11
	TBT, DBT, MBT	GC–AAS	3 ng/g wet sample	24
	TBT, DBT, MBT	GC–FPD	5 ng/g wet sample	25
	TBT, DBT, total tin	GF–AAS	–	2, 16
	TBT, DBT	GC–FID	–	26
	TBT	GF–AAS	2 ng/g wet sample	11
Molluscs	TBT, DBT, MBT	GC–FPD–DCP	5 ng/g wet sample	27
	TBT, DBT	GC–FPD	0.08 ng	28
	TBT, DBT, MBT	GC–AAS	0.2–0.5 ng/g wet sample	29
Fish	TBT, DBT	GF–AAS	5.3 ng/g wet sample	13
	TBT, DBT	GC–FPD	3.65 ng/g dry sample	15
	TBT, DBT, MBT	GC–AAS	0.2–0.5 ng/g wet sample	29

[a] For abbreviations, see text; HG = hydride generation; GF = graphite furnace; DCP = direct current plasma.

with 100 ml of deionized water and 1 ml of acetic acid [30]. With stirring and helium flushing, organotin compounds were converted into their hydrides by addition of $NaBH_4$ via an Ismatec peristaltic pump (2.5 ml min^{-1}). Evolved hydrides were then carried by the helium flow (300 ml min^{-1}) to a glass GC column (650 × 4 mm i.d., packed with Chromosorb W HP, 10% OV-101), cooled in liquid nitrogen, where they were trapped. After removing the cooling bath, the column was then left to warm at ambient temperature for 3 min and finally electrically heated by a Gilphy 80 wire for 4 min to 180°C. Separated hydrides, flushed with helium from the GC column, were introduced into an electrically heated (950°C) quartz furnace placed in the light beam of an IL 151 atomic absorption spectrometer (λ = 286.3 nm). Hydrogen and oxygen at flow-rates of 200 and 45 ml min^{-1}, respectively, were introduced into the quartz cell where their combustion increased the sensitivity [31]. Automation of $NaBH_4$ addition, cooling in liquid nitrogen, column heating and absorption measurement was effected by a TRS 80 microcomputer, signal integration being performed with a Varian 4270 integrator.

Sample preparation

An international intercalibration conducted in 1986–87 on the determination of butyltins in tissues [16] evidenced factors of 2–3 in tributyltin and dibutyltin concentrations measured in mussel samples by different laboratories, depending on the type of instrumentation or extraction used and above all on whether the sample had been dried or not. Analysis of wet samples seems to be more convenient when it concerns routine analysis of natural samples by avoiding one step in sample preparation and because possible effects of drying or freeze-drying on tin speciation are unknown.

Sample preparation then consisted in removing the whole flesh of molluscs from shells, freezing them for 2 days and, after thawing, crushing and homogenizing a large amount of flesh in a commercial blendor (Thermomix 2200). These samples were stored at −20°C until analysis.

Spiking procedure

As there was no certified reference material available it was necessary to prepare spiked samples for recovery studies. The spiking procedure was carefully defined so that the spiked samples would be prepared long before analysis (6 months) to allow equilibration of organotin compounds with sample matrix. However, the same results were obtained with recently spiked samples. Large amounts (2 × 50 g) of spiked samples were prepared as follows: a minimum volume (to avoid matrix dilution) of spiking solution of butyltin in methanol was slowly added (2.5 ml in 1 h) to the thawed sample with stirring; the spiked sample was stirred for a further 3 h to complete homogenization. All the spiked samples were then stored frozen in open-ended glass tubes from which it is easy to remove at will the small amounts needed for analysis. During storage these tubes were closed with Parafilm caps.

RESULTS AND DISCUSSION

Extraction

Extraction of organotin compounds from the biological matrix without modifying their speciation is a preliminary step before analysis. This step should be acid or alkali digestion, liquid–liquid extraction or a combination of both [9–11,13,19,23]. Estimated recoveries of published procedures are in the range 50–100% and concern standard solutions or spiked materials [20,22,23].

Two extraction procedures already described in the literature were examined in this study. The extraction procedure with pure acetic acid, well known in the laboratory and which gives very good results for the analysis of dried sediment [30], as confirmed by Zhang et al. [32], was first applied: about 1 g of sample was mixed with 20 ml of acetic acid and agitated overnight (12–15 h) and, after centrifugation at 1800 *g* for 5 min, aliquots of supernatant were analysed. Applications to freeze-dried or wet biological material led to an abundant production of foam during hydride generation that made analysis difficult. Foaming may be prevented by addition of an-

TABLE 2

Inhibition of a 10 ng (as Sn) TBT signal by antifoaming agents (one drop of pure antifoaming agent in 100 ml of analysed solution)

Antifoaming agent	Signal area for TBT (arbitrary units)	Signal inhibition (%)
–	66840	–
Rhodorsyl 411	6100	91
Antifoam B (Sigma)	35430–40105	40–50
Others (non-commercial) [a]	2420–6500	90–96

[a] Obtained from CECA.

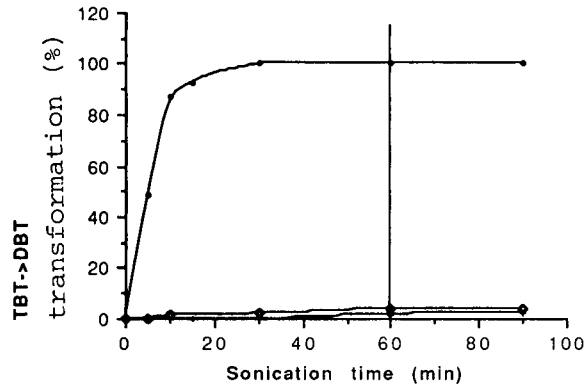

Fig. 1. Percentage degradation of TBT into DBT by HCl–MeOH during sonication of a standard solution [100 μl of a 2.5 μg (Sn) ml^{-1} TBT solution in 1 ml of MeOH + 5 ml of HCl]. HCl concentration: ● = 8.4; ◇ = 2; + = 0.1 mol l^{-1}.

tifoaming agents [22], but they were unfortunately found to inhibit the absorption signal (Table 2) so strongly that the detection limits of organotins became unacceptably high.

The second extraction procedure consisted in the addition of 1 ml of methanol and 5 ml of HCl (see below) to the wet sample followed by mechanical shaking or sonication. The volume was then adjusted to 10 ml with deionized water and an aliquot of the solution directly analysed. Under these conditions no foam formation was observed. Different concentrations of HCl have been reported: 12 mol l^{-1} [18–20], 8.4 mol l^{-1} [22], 6 mol l^{-1} [33], 3 mol l^{-1} [28] or 2 mol l^{-1} [23]. We tried 8.4, 2 and 0.1 mol l^{-1} HCl to extract butyltin compounds from a mussel sample spiked with TBT. At very low HCl concentration (0.1 mol l^{-1}) the recovery of TBT was close to 100%, but traces of DBT and MBT appeared, indicating slight degradation of the analyte (Table 3). HCl of 2 mol l^{-1} allowed the quantitative recovery of butyltins but with a significant (19%) conversion of TBT into DBT and MBT. At a high concentration of HCl (8.4 mol l^{-1}), the loss of TBT increased (33%), DBT and MBT appeared (8 and 13%, respectively) and 12% of TBT introduced was lost; this is probably due to the production of inorganic tin [Sn(IV)], which was not determined in this study. Mechanical shaking for 5 h using 8.4 mol l^{-1} HCl still gave increased TBT losses.

The same series of experiments was also run with the spiked mussel sample replaced with a standard solution of TBTCl. The results, presented in Fig. 1, indicate an even more important degradation of TBT at a high concentration of HCl (8.4 mol l^{-1}). DBT production was ca. 50% after 5 min of sonication and approached 100% after 30 min.

In contrast, low concentrations of HCl (0.1 or 2 mol l^{-1}) induced only very limited debutylation of TBT (4% in 1 h with 2 mol l^{-1} HCl).

TABLE 3

Fate and recovery of TBT in various extraction procedures applied to a mussel sample spiked with 250 ng (as Sn) g^{-1} TBTCl (each value, expressed as Sn, is the mean of five determinations)

HCl concentration (mol l^{-1})	Extraction conditions	TBT (ng g^{-1})	DBT (ng g^{-1})	MBT (ng g^{-1})	$BuSn_t$ [a] (ng g^{-1})	TBT recovery (%)	BuSn recovery (%) [b]
0.1	Sonication (1 h)	240	13	10	263	96	105
2.0	Sonication (1 h)	203	22	18	244	81	98
8.4	Sonication (1 h)	168	20	32	220	67	88
8.4	Shaking (5 h)	133	35	28	196	53	78

[a] $BuSn_t$ = TBT + DBT + MBT. [b] BuSn (%) = 100 × $BuSn_t$/250.

TABLE 4

Recovery (%) of butyltin compounds from mussel and oyster matrices (mean values for six extractions)

Matrix	TBT	DBT	MBT
Mussel	96	98	98
Oyster	97	97	99

As the best recoveries and the least degradation of TBT were observed with mild attack with 0.1 mol l^{-1} HCl, the following conditions were adopted in further work: about 1 g of wet sample was mixed with 1 ml of methanol and 5 ml of 0.1 mol l^{-1} HCl in a stoppered Pyrex flask, placed in an ultrasonic bath for 1 h and shaken two or three times during this period to break any lump formation. The solution was then transferred into a volumetric flask and diluted to 10 ml with deionized water.

This procedure was applied to mussel and to oyster samples spiked with either TBT, DBT or MBT to study the recoveries of the different butyltin compounds (Table 4). The mussel and oyster samples were spiked several months before analysis with 250 ng (Sn) g^{-1} of TBTCL, $DBTCl_2$ or $MBTCl_3$. Quantitative recoveries of butyltin compounds were observed, but nevertheless with slight degradation of TBT to DBT and MBT ($\leqslant 9\%$) or of DBT to MBT ($\leqslant 4\%$).

Analysis of standard solutions

The precision of the procedure for the three butyltin compounds was examined with standard solutions and tissue extracts (Table 5). There was no significant difference between the analysis of standard solutions and shellfish extracts.

Calibration graphs were established from chromatographic peak areas for the analysis of extracts of clean mollusc tissues spiked with standard solutions of the various butyltin chlorides. They were perfectly linear in the range of concentrations studied [2.5–1000 ng (Sn) g^{-1} in the wet sample] but the sensitivities differed, TBT being the least sensitive (Table 6). Detection limits (limit concentration; C_L) were calculated from the equation $C_L = 3S_B m^{-1}$ where S_B, the standard deviation of the blank determined from 20 blank measurements, was 5230 area units (Table 6).

TABLE 5

Precision of the analytical procedure

Method [a]	Sample	Relative standard deviation (%)		
		TBT	DBT	MBT
A	Standard solution	4	3	6
	Mussel extract	7	5	6
	Oyster extract	9	7	9
B	Standard solution	8	7	8
	Mussel extract	8	5	6
	Oyster extract	9	7	7

[a] A: five analyses of the same standard solution [50 ng (Sn) l^{-1}] or the same tissue extract [250 ng (Sn) g^{-1}]. B: Analysis of five different standard solutions [50 ng (Sn) l^{-1}] or five different tissue extracts [250 ng (Sn) g^{-1}].

For both matrices the detection limits ranged from 2.3–2.4 ng g^{-1} wet weight for MBT and DBT to 2.8–2.9 ng g^{-1} for TBT. In comparison they were in the 1 ng g^{-1} range for butyltins in dried sediments (1.2, 0.7 and 0.6 ng g^{-1} for TBT, DBT and MBT, respectively) by acetic acid leaching and analysis by the same method [34]. Instrumental detection limits for TBT, DBT and MBT were 60, 40 and 30 pg (Sn), respectively.

These concentration limits in wet samples corresponds to concentrations of 14.5 ng g^{-1} for TBT in freeze-dried oyster tissue (80% water content) and 23.5 ng g^{-1} for TBT in freeze-dried mussel tissue (88% water content).

TABLE 6

Calibration graphs and detection limits in mussel and oyster matrices

Matrix	Parameter	TBT	DBT	MBT
Mussel	m [a]	280800	329500	354000
	r [b]	0.995	1.000	0.999
	C_L [c]	2.8	2.4	2.3
Oyster	m [a]	269400	327600	330700
	r [b]	0.999	0.998	0.995
	C_L [c]	2.9	2.4	2.4

[a] Slope of the calibration graph, in area units [ng (Sn)]$^{-1}$. [b] Correlation coefficient. [c] Detection limit in ng (Sn) g^{-1} (wet weight).

Application to commercial shellfish samples

Mussel (Mytilus galloprovincialis). The method was applied to the analysis of a commercial mussel sample bought at Toulon market (France). Table 7 and Fig. 2 present the results obtained.

The ratio of degradation products to total butyltin, $BuSn_t$, (33%) is much higher than the $\leqslant 9\%$ level that could be due to degradation during the analytical procedure. DBT and MBT present in the sample not only result from degradation during the extraction procedure itself but were also initially present in the tissue. They are degradation products of TBT either ingested by the organism or produced in the organism after ingestion of TBT. The water content of the sample being 88%, a concentration of TBT of 3.93 $\mu g\ g^{-1}$ (dry weight) may be estimated, a value which is near the highest concentration on the pollution scale defined in the literature (TBT levels ranging from 0.03 [11] to 3.8 $\mu g\ g^{-1}$ [25] in mussel samples).

Scallop (Pecten maximus). The second application concerned a scallop sample bought at Brest market (France). The animals were dissected into three parts: gonad, mantle and visceral mass and adductor muscle and the extraction procedure was separately applied to each subsample. The results are presented in Table 8. Fairly high concentrations of TBT were determined in the gonad and the adductor muscle, which are the organs of prime importance for human alimentation; these concentrations are higher than the 77 ng g^{-1} found by Ishizaka et al. [28] in commercial fresh scallops in Japan. In the different parts of the animal, it may be observed that, as for the mussel sample, the $(DBT + MBT)/BuSn_t$ ratio is higher than may be accounted for by experimental artifacts. The three butyltin compounds were present in the animal and especially in the adductor muscle. This is in agreement with Davies et al. [12], who observed a gradual build-up of TBT in the adductor muscle (where the storage/detoxification system for TBT may be located) in scallops contaminated by TBT-treated nets.

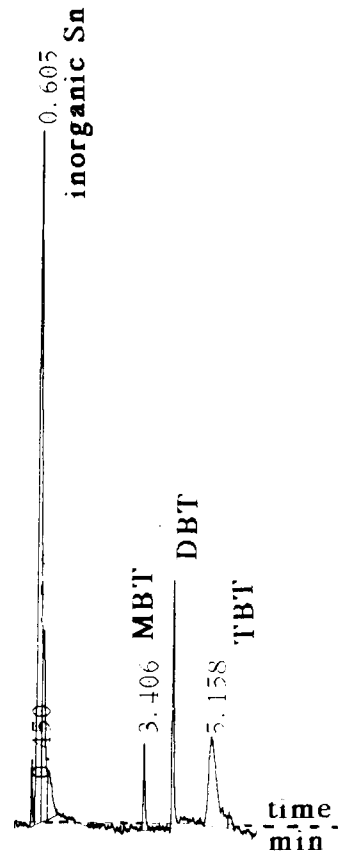

Fig. 2. Chromatogram of Toulon mussel sample.

TABLE 7

Concentrations of butyltins in a commercial mussel sample

Concentration	TBT	DBT	MBT	$BuSn_t$	$100\left(\frac{MBT + DBT}{BuSn_t}\right)$
ng (Sn) g^{-1} wet weight	193	24.5	73	291	33.5
mg (Bu_pSn [a]) kg^{-1} dry weight	3.93	0.400	0.900	–	–

[a] Bu_pSn represents either Bu_3Sn^+, Bu_2Sn^{2+} or $BuSn^{3+}$.

TABLE 8

Concentrations of butyltins in a commercial scallop sample in ng (Sn) g^{-1} (wet weight)

Tissue	TBT	DBT	MBT	$BuSn_t$	$100\left(\frac{MBT + DBT}{BuSn_t}\right)$
Adductor muscle	173	50.5	42.5	266	35
Mantle and visceral mass	109	22.5	29.5	161	32
Gonad	89	20.3	19.5	129	31
Mean value for whole animal	112	27	27.5	167	

TABLE 9

Concentrations of butyltins in a Nivelle oyster sample

Concentration	TBT	DBT	MBT	$BuSn_t$	$100\left(\frac{MBT + DBT}{BuSn_t}\right)$
ng (Sn) g^{-1} wet weight	146	42.5	50	239	38.7
mg (Bu_pSn [a]) kg^{-1} dry weight	1.8	0.42	0.37		

[a] Bu_pSn represents either Bu_3Sn^+, Bu_2Sn^{2+} or $BuSn^{3+}$.

Oyster (Crassostrea gigas). The oyster sample was collected in the Nivelle estuary (France) and the shells presented deformations typical of TBT effects (balling effect or shell thickening). Concentrations measured in the flesh are given in Table 9. These TBT levels are similar to the concentrations found by King et al. [8] in New Zealand and Batley et al. [9] in Australia but far below those measured by Rice et al. [35] and Wade et al. [25] in oysters from the US coasts, which reached up to 800 ng (Sn) g^{-1} in wet samples.

Conclusion

The procedure studied in this work allows the routine determination of butyltin compounds in shellfish with a minimum of sample handling. The first applications to real samples chosen in critical areas demonstrated the efficiency of the method and indicated the presence of tributyltin in some commercial shellfish samples at fairly high concentrations.

This study was funded by the Ministère de l'Agriculture et de la Forêt under contract No. R91/06. Thanks are due to CECA for kindly providing non-commercial antifoaming agents and C. Madec (University of Brest) for the gift of the scallop sample.

REFERENCES

1 C. Stewart and J. De Mora, Environ. Sci. Technol., 11 (1990) 565.
2 C. Zuolian and A. Jensen, Mar. Pollut. Bull., 20 (1989) 281.
3 R.B. Laughling, Oceans Proceedings 1986, Organotin Symposium, IEEE, New York, 4 (1986) 1206.
4 E.A. Dyrinda, Mar. Pollut. Bull., 24 (1992) 156.
5 M.H. Salazar and S.M. Salazar, Oceans Proceedings 1988, Organotin Symposium, IEEE, New York, 4 (1988) 1188.
6 C. Stewart, J. De Mora, M.R.L. Jones and M.C. Miller, Mar. Pollut. Bull., 24 (1992) 204.
7 J.A. Nell and R. Chvojka, Sci. Total Environ., 125 (1992) 193.
8 N. King, M. Miller and S. De Mora, N.Z. J. Mar. Freshwater Res., 23 (1989) 287.
9 G.E. Batley, M.S. Scammel and C.I. Brockband, Sci. Total Environ., 9 (1992) 301.
10 A.D. Uhler, T.H. Coogan and K.S. Davies, Environ. Toxicol. Chem., 8 (1989) 971.
11 J.W. Short and J.L. Sharp, Environ. Sci. Technol., 23 (1989) 129.
12 I.M. Davies, J.C. McKie and J.D. Paul, Aquaculture, 55 (1986) 103.
13 J.W. Short and F.P. Thrower, Mar. Pollut. Bull., 17 (1986) 542.

14 I. Martin Landa, F. Pablos and I.L. Marr, Appl. Organomet. Chem., 5 (1991) 399.
15 K. Okamoto, Biological Trace Element Research, American Chemical Society, Washington, DC, 1991, Chap. 20, p. 258.
16 M.D. Stephenson, D.R. Smith, L.W. Hall, Jr., W.E. Johnson, P. Michel, J. Short, M. Waldock, R.J. Hugget, P. Selingman and S. Kola, Oceans Proceedings 1987, Organotin Symposium, IEEE, New York, 4 (1987) 1334.
17 Certified Reference Material No. 11 "Fish Tissue", National Institute for Environmental Studies, Environment Agency of Japan, Tokyo.
18 J.L. Kacprzak, Int. J. Environ. Anal. Chem., 38 (1990) 561.
19 D.J. Hannah, T.L. Page, L. Pickston and J.A. Taucher, Bull. Environ. Contam. Toxicol., 43 (1989) 22.
20 S. Ohira and H. Matsui, J. Chromatogr., 525 (1990) 105.
21 D.J. Smith, personal communication.
22 J.S. Han and J.H. Weber, Anal. Chem., 60 (1988) 316.
23 S. Rapsomanikis and R.M. Harrison, Appl. Organomet. Chem., 2 (1988) 151.
24 Y.K. Chau, P.T.S. Wong, G.A. Bengert and J. Yaromich, Chem. Speciation Bioavail., 1 (1989) 151.
25 T.L. Wade, B. Garcia-Romero and J.M. Brooks, Environ. Sci. Technol., 22 (1988) 1488.
26 D.S. Page, Mar. Pollut Bull., 20 (1989) 129.
27 I.S. Krull, K.W. Panaro, J. Nooman and D. Erickson, Appl. Organomet. Chem., 3 (1989) 295.
28 T. Ishizaka, S. Nemoto, K. Sasaki, T. Suzuki and Y. Saito, J. Agric. Food Chem., 37 (1989) 1523.
29 D.S. Forsyth and C. Cleroux, Talanta, 9 (1991) 951.
30 V. Desauziers, F. Leguille, R. Lavigne, A. Astruc and R. Pinel, Appl. Organomet. Chem., 3 (19989) 469.
31 P.M. Sarradin, F. Leguille, A. Astruc, R. Pinel and M. Astruc, J. Anal. At. Spectrom., submitted for publication.
32 S. Zhang, Y.K. Chau, W.C. Li and A.S.Y. Chau, Appl. Organomet. Chem., 5 (1991) 431.
33 N. Cardellicchio, S. Geraci, C. Marra and P. Paterno, Appl. Organomet. Chem., 6 (1992) 241.
34 V. Desauziers, Thesis, University of Pau, Pau, 1991.
35 C.D. Rice, F.A. Espourteille and R.J. Huggett, Appl. Organomet. Chem., 1 (1987) 541.

Analytica Chimica Acta, 287 (1994) 25–34
Elsevier Science B.V., Amsterdam

Analysis of the heterogeneous rate of dissociation of Cu(II) from humic and fulvic acids by statistical deconvolution

Brett J. Stanley, Karl Topper [1] and David B. Marshall [2]

Department of Chemistry and Biochemistry, Utah State University, Logan, UT 84322-0300 (USA)

(Received 8th July 1993; revised manuscript received 28th September 1993)

Abstract

Pseudo first-order rate constant data of the dissociation of Cu(II) species from humic substances in a variety of chemical environments is considered. This data is observed to be widely heterogeneous under moderate environmental conditions, and a continuous distribution of rate constants is needed to adequately model the data. The rate constant distribution is optimally estimated with regularized least-squares and expectation-maximization (EM), and the different methods of solution yield different degrees of heterogeneity for each experiment. This behavior distinctly illustrates the pitfalls of widely heterogeneous rate constant analysis. Under these circumstances the solution of maximum entropy is dictated by the precepts of information theory. This solution corresponds to the EM solution for all the data considered in this study. The EM spectra of Cu(II) dissociation from humic and fulvic acids under various environmental conditions are reported. Interpretation of the spectra in terms of plausible humic chemistry is offered, and cautions appropriate for this type of kinetic analysis are delineated.

Keywords: Kinetic methods; Fulvic acids; Humic acids; Statistical deconvolution

The binding energetics of metal species to humus materials such as humic and fulvic acid (heretofore referred to as humics) has been extensively addressed in the literature (for a review see references 1–4). The chemical kinetics of the corresponding interactions is a useful probe of these energetics, but has received less attention [5]. There exists a dichotomy in the literature over the appropriate modelling of humic–metal equilibria and reactivity; whether to model the binding with a discrete number of classes of binding sites, or to use a continuous model of binding sites.

There is a consensus of the wide heterogeneity of binding energetics in humics owing to their polydispersive nature. This heterogeneity is due to several types of functional groups that can be found within the humic (carboxylic acids, phenolic groups, amine groups, etc.), and the flexible nature of the mass of carbon chains that interconnect these reactive sites. Due to the presence of several functional groups that can bind to a metal species such as Cu(II), the ability of metals to bind multiple ligands simultaneously, and the

Correspondence to: B.J. Stanley, Department of Chemistry, University of Tennessee, Knoxville, TN 37996-1501 (USA) (present address).

[1] Present address: College of Natural Sciences and Mathematics, Mesa State College, Grand Junction, CO 81502 (USA).

[2] Present address: Department of Chemistry, University of Idaho, Moscow, ID 83844-2343 (USA).

SSDI 0003-2670(93)E0582-R

flexibility of humics, it is conceivable that a multiplicity of binding energies may approach a continuous distribution of such energies under certain environmental conditions. On the other hand such a model of metal binding appears complex, and it may be more worthwhile to consider a discrete number (e.g. two or three) of binding sites when modelling experimental data, in order to more readily extract meaningful information.

Compounding this ambiguity is the fact that the statistical significance of these binding models decreases as the number of parameters to be fit increases. Marshall [6] showed for the case of multi-component first-order rate constant decay that high parameter variances preclude the consideration of more than three components (7 parameters), depending on the signal-to-noise ratio (S/N). Therefore if more than two or three components are needed to adequately model the data, then a problem of model selection exists.

One solution to this problem is to analyze heterogeneous rate constant data in terms of a distribution, or spectrum, and then interpret the results in terms of a model (discrete or continuous) in whatever manner one wants or needs for application purposes (e.g. prediction of transport phenomena, physicochemical descriptions, etc.). In this manner, all models (in terms of the number of components) can be considered simultaneously. Solution of first-order rate constant data in terms of rate constant distributions using formulae for the inverse Laplace transform has been done in the past [7–9]. However this is not a statistical analysis, and results in poor resolution of the distribution. Statistical analysis or regression in terms of rate constant distributions is a mathematically ill-posed problem, which means the spectra can change drastically and yield artifactual information upon the slightest perturbation in the input data. Therefore, a special approach to the analysis of heterogeneous rate constant data is needed which combines statistical integrity with the principle of parsimony, while preserving a certain aspect of generality so that the overall behavior of the data may be easily extracted. This paper presents this type of analysis for the application of dissociation of Cu(II) from humic and fulvic acids.

THEORY

The pseudo first-order dissociation of Cu(II) from humic or fulvic acid with the scheme

$$\text{Humic–Cu(II)} \rightleftharpoons \text{Humic} + \text{Cu(II)} \text{ (slow)}$$

$$\text{Cu(II)} + 2\text{PAR}^- \rightleftharpoons \text{Cu(PAR)}_2 \text{ (fast)} \quad (1)$$

where PAR^- is the colorimetric complexing agent 4-(2-pyridylazo)resorcinol, monitored experimentally via the absorbance of the Cu(PAR)_2 complex. Assuming the dissociation of Cu(II) from different binding sites occurs independently of each other, the kinetic curve, $f(t)$, can be expressed as a sum of single exponentials (i.e., $f(t) = \sum_i A_i \exp(-k_i t)$, where A is the amplitude, k is the rate constant, and t is time). To obtain the rate constant distribution, the sum is replaced by an integral

$$f(t) = \int_0^\infty F(k) \exp(-kt)\, dk \quad (2)$$

and the distribution function, $F(k)$, is deconvoluted from the single exponential kernel using quadrature.

Deconvolution may proceed statistically using the principle of least-squares. However, the ordinary least-squares (OLS) solution is unstable due to the ill-conditioned nature of the regression matrix $\mathbf{A}$ [1]

$$A_{i,j} = \exp(-k_j t_i)\Delta k \quad (3)$$

This problem is alleviated by regularizing the OLS solution. Provencher has provided a program that calculates regularized least-squares solutions for the general case of noisy linear operator equations [10–12]. Regularized least-squares stabilizes the OLS solution by implementing a smoothness criterion. The implementation of this criteria varies amongst the different algorithms that exist for this technique. Wahba [13] and

[1] A matrix is considered ill-conditioned when its condition number, defined as $c(\mathbf{A}) = \|\mathbf{A}\| \, \|\mathbf{A}^{-1}\|$ where $\|\cdot\|$ denotes any Euclidean norm, becomes very large. This definition reflects the linear system sensitivity of the $\mathbf{y} = \mathbf{Ax}$ problem, which for ill-conditioned problems is too sensitive and precludes the existence of a unique OLS solution in the presence of error.

Bates et al. [14] developed a method of cross-validation to optimally select the amount smoothing to be implemented in the least-squares solution. This method theoretically minimizes the mean-squared-error of the estimated solution in the presence of normal, or constant white noise.

Another approach to statistically deconvoluting Eqn. 2 is to derive and solve the maximum-likelihood (ML) equations for the measurement process. Maximization of the total probability of observing measurements $f(t_i)$ which originate from the model $A_i F(k)$ results in the following set of ML equations (one for each k_j)

$$\sum_{i=1}^{n}\left[\frac{A_i f(t_i)}{\sum_{j=1}^{m} A_j F(k_j)}\right] = 1 \qquad (4)$$

where n is the number of data points, and m is the number of grid points in the quadrature. An iterative algorithm to solve these equations for $F(k)$ was suggested by Shepp and Vardi [15], and is called expectation-maximization (EM):

$$F(k_j)^{l+1} = F(k_j)^{l} \sum_{i=1}^{n}\left[\frac{A_i f(t_i)}{\sum_{j=1}^{m} A_j F(k_j)}\right] \qquad (5)$$

where l is the iteration number. This algorithm was shown by Bialkowski [16] to be generally applicable to various routines of data analysis, and by Stanley et al. [17,18] for equations like Eqn. 2 (linear Fredholm integrals of the first kind).

Theoretically the Wahba solution and the EM solution should be equal at convergence, assuming the experimental errors are truly random and Gaussian in nature. Unfortunately, this is rarely the case in most experiments [19,20]. Therefore, in light of the ill-posed nature of the data analysis, it is most prudent to choose the solution of maximum entropy. The maximum entropy (MAXENT) principle states that the most probable solution to a problem is the one that is accessible in the greatest number of ways [21]. Such a solution contains the greatest amount of disorder, or the least amount of structure required by the data. This conforms to the principle of parsimony and smoothness criteria, and minimizes artifactual information. For this class of problems, ML and MAXENT solutions are equivalent [22]. Entropy can be maximally instilled into the EM solution by specifying a uniform distribution for the initial guess of the algorithm. This approach to the data analysis of heterogeneity problems of the type considered here is the most consistent with the precepts of information theory and signal processing, in which one starts with white noise and classifies only the information which is required by the data as specified by the model.

EXPERIMENTAL

All stopped-flow experiments were performed by introducing reagent grade 4-(2-pyridylazo) resorcinol (PAR^-) into a temperature-controlled cuvette containing a humic or fulvic acid solution of 120 mg/l equilibrated with the cupric ion at a specified concentration, ionic strength, and pH. The experimental temperature was 20.0 ± 0.2°C. The cuvette resided in a UV absorbance spectrophotometer (Hewlett Packard 8452a) with the detection wavelength set to the absorbance of the $Cu(PAR)_2$ complex at 508 nm. The light from the excitation source was filtered from ultra-violet radiation to minimize photodegradation. A Latahco humic acid was extracted from a northern Idaho soil and has been described by Morra et al. [23]. Standard fulvic and humic acids were obtained from the International Humic Substances Society (reference numbers 1S102F and 1S102H, respectively) [24]. The chemical analysis of these humics is presented in Table 1. The Cu(II) was prepared from reagent grade Cu pellets. The ionic strength was adjusted with $NaNO_3$, and the pH was adjusted with either 1.0 M HNO_3 or 0.50 M NaOH and buffered by 1.7×10^{-4} M $NaHCO_3$. The equilibration time was 12 h in a reciprocating shaker at 170 rpm. The PAR^- concentration was kept deliberately high at 3.6×10^{-3} M so pseudo first-order kinetics may be assumed (Eqn. 1). In separate experiments the PAR^- concentration was varied over a range of 20–50 times

TABLE 1

Selected chemical analyses of humics [a]

Component	Fulvic acid	Latahco humic acid	Standard humic acid
C	509	337	585
H	40.4	34.5	38.1
N	27.0	26.6	42.2
O	429	255	340
Ash	7.9	338	9.0

[a] Expressed on dry-weight basis in g/kg. Analysis of fulvic acid and standard humic acid reported in Ref 24. Analyses of Latahco humic acid for C, H, and N was reported in Ref. 23, while O and ash were analyzed by M-H-W Labs., Phoenix, AZ.

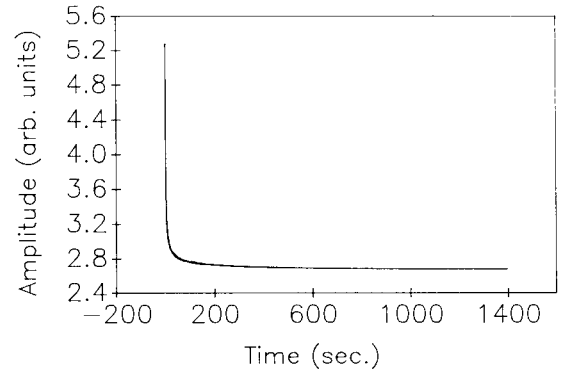

Fig. 1. Cu(II) dissociation from Latahco humic acid as a function of time. [Cu(II)] = 7.6×10^{-5} M, I = 0.02 M, pH 7.5, T = 20.0°C. Sampling rate = 10 Hz for 30 min.

the Cu(II) concentration, and no changes in the resulting kinetic spectra were observed.

The introduction of PAR^- was performed with a pneumatically driven stopped-flow apparatus (High-Tech Scientific SFA-11). The mixing time was measured as 20 ms. The sampling frequency of the experiments was set to the maximum of the spectrophotometer at 10 Hz, and the dissociation was followed for 30 min. The experiments were repeated 16 times, and the profiles signal averaged. A background stopped-flow response (< 5% of analyte signal) with no Cu(II) present in the system was subtracted from the profile. The S/N was greater than 500 for all experiments, where $S/N = A_{max}/\sigma$ with A_{max} being the maximum amplitude in the data set relative to the baseline, and σ is the standard deviation of the baseline.

The experimental 10 Hz sampling was broken down into three separate regions before data analysis, so as to reduce the total number of points to $\leqslant 2048$. This was done as follows: $t_1 \in$ [0.1,149.7] s with 1497 data points ($\Delta t = 0.1$ s, every point); $t_2 \in$ [151,500] s with 350 data points ($\Delta t = 1$ s, every 10th point); and $t_3 \in$ [505,1495] s with 200 data points ($\Delta t = 5$ s, every 50th point). In some experiments this scheme included excess baseline and the data was appropriately truncated. The dissociation profile was inverted in order to represent a decay and conform to the exponential kernel of Eqn. 2. The rate constant space analyzed was determined by the first and last data point according to the inverse Laplace transform formula of time to rate ($2/t \rightarrow k$), i.e. $k \in [1.3 \times 10^{-3}, 20]$ s^{-1}. Varying this range within reasonable values does not significantly alter the estimated distribution. The number of grid points was set to sixty.

The three statistical deconvolution methods described in the Theory section were applied to all of the data. The program of Provencher (CONTIN) was obtained from EMBL and set up to solve the inverse Laplace transform. The Wahba method (GCV) was separately programmed within the CONTIN architecture and is described in [17], but may assumably be obtained from the University of Wisconsin. The EM algorithm was coded in house, and may be obtained from the author. Execution of the programs was completed on either a 25 MHz 80386 personal computer or a SUN-4/280 computer for CONTIN and GCV. For $n = 2000$ and $m = 60$, executions times were approximately 5 min. Due to the iterative nature of the EM algorithm, a Titan-Ardent or an IBM 6000 computer was used to obtain reasonable computation times. Twenty-thousand iterations were allowed to approach the global optimum. This required approximately 2 h on the Titan, and 45 min on the IBM. [2]

[2] Massively parallel computers and computing will be the wave of the future. The EM program has recently been coded in parallel on a MasPar MP-2 computer at the University of Tennessee, and 20 000 iterations of the 2000 × 60 problem can be executed in 3 min.

The goodness-of-fit criteria mean-squared-error, defined as the summed-squared-error divided by the number of data points, was used to ascertain the quality of the fits. Discrete exponential modelling was performed by Provencher's DISCRETE program [25]. This program uses Fourier analysis to provide initial estimates of the data, and reports the best solution in terms of the number of components, based on goodness-of-fit and significance testing. If a solution with more components yields a lower fit variance but is not significantly lower than a lesser component

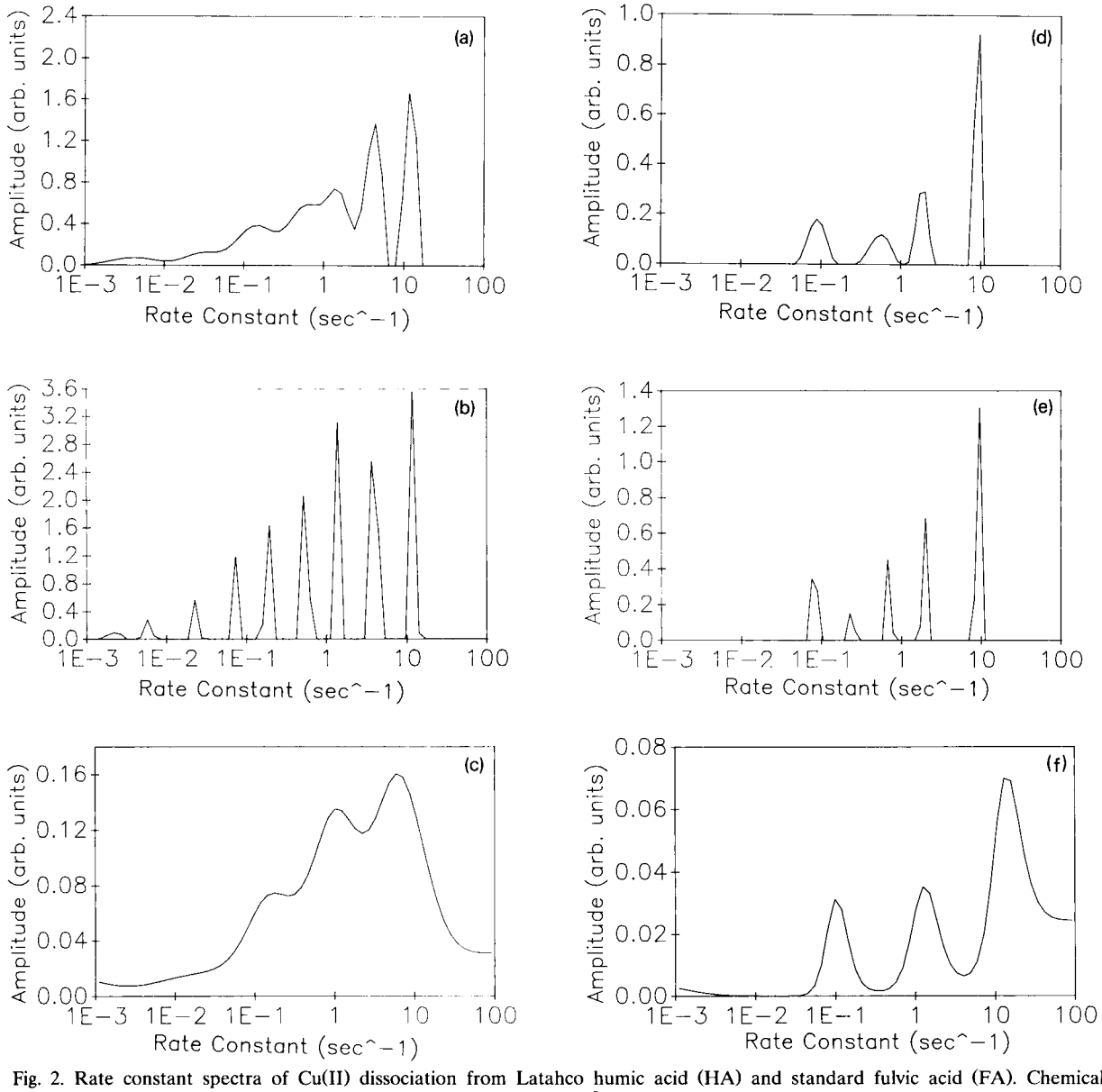

Fig. 2. Rate constant spectra of Cu(II) dissociation from Latahco humic acid (HA) and standard fulvic acid (FA). Chemical conditions exactly the same for each experiment: [Cu(II)] = 7.6×10^{-5} M, I = 0.02 M, and pH 7.5. (a) CONTIN, (b) GCV, and (c) EM estimates for HA experiment; (d) CONTIN, (e) GCV, and (f) EM estimates for FA experiment.

solution, the lesser component solution is chosen. This criterion is also used to report the 2nd, 3rd, etc. best solutions. The version obtained from EMBL reports a maximum of five components. Another version exists that can report up to nine components.

RESULTS AND DISCUSSION

A representative dissociation decay profile is shown in Fig. 1, which is of 120 mg/l Latahco humic acid, 7.6×10^{-5} M Cu(II), $I = 0.02$ M, and pH 7.5. This profile exhibits a very fast initial decay and a noticeable long-time slow decay. All the experiments look similar in this type of plot, which is very stretched. Indeed if a stretched exponential $[f(t) = A \exp(-ct^n)]$ is fit to these data, values less than 1/3 are obtained for the exponent, n. The data density of the initial decay is unfortunately limited by the sampling frequency of the spectrophotometer. Rate constants greater than 20 s^{-1} are not able to be adequately quantitated. The mixing of the PAR^- with the Cu(II)–humic system possesses a time constant of 50 s^{-1}, which is equivalent to the response time reported for $Cu(PAR)_2$ formation [7]. Therefore a faster experiment must be designed to obtain any dissociation kinetics faster than those reported here. Alternatively a decreasing kinetic signal is still observable at 30 min, and the experiment must be monitored for several hours to analyze the slowest of rates. Such extensive sampling was not judged to be pragmatic for the purposes of this study.

The deconvolution results of the data in Fig. 1 (HA) and the analogous experiment with fulvic acid (FA) using the CONTIN, GCV, and EM programs are shown in Fig. 2. Remarkably, each method yields a different picture of the hetero-

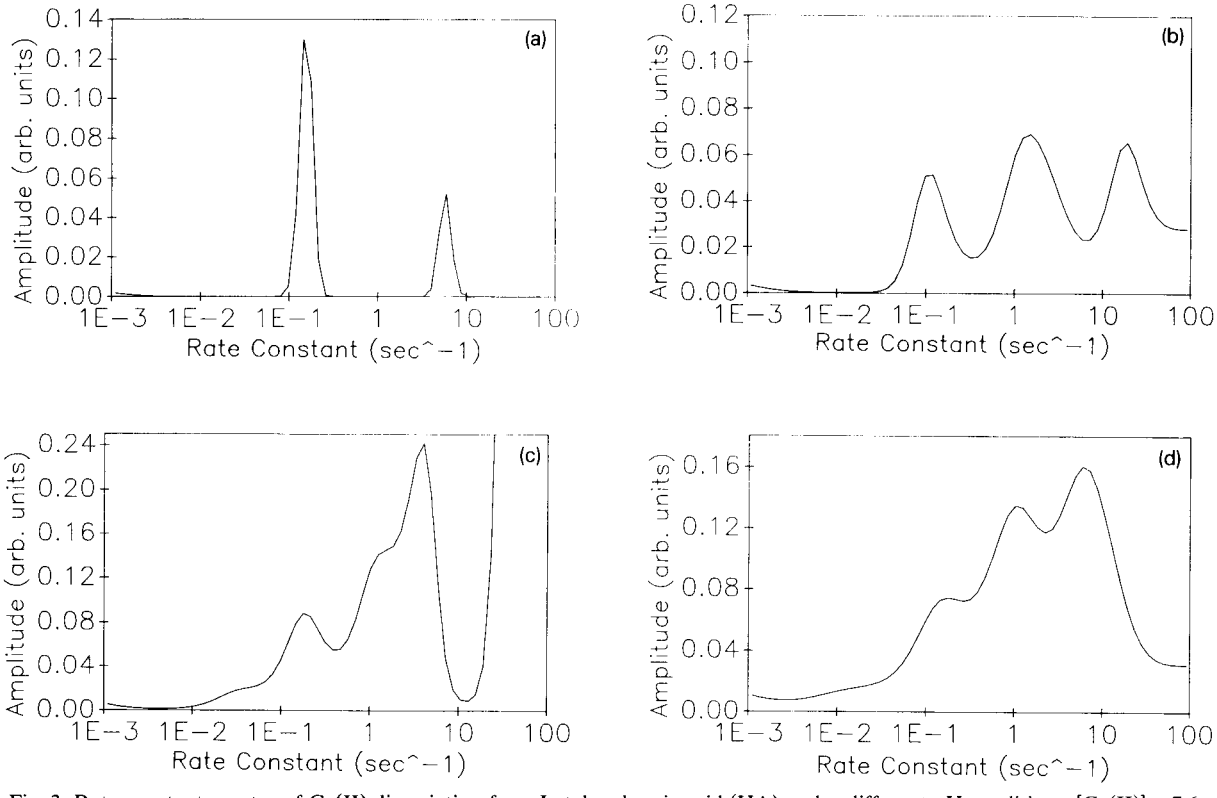

Fig. 3. Rate constant spectra of Cu(II) dissociation from Latahco humic acid (HA) under different pH conditions. $[Cu(II)] = 7.6 \times 10^{-5}$ M, $I = 0.02$ M, and (a) pH 3.5, (b) pH 5.5, (c) pH 6.5, and (d) pH 7.5.

geneity of these substances. This behavior is consistent for all the experiments under all the conditions in this study. If the DISCRETE program is executed on these data, five components are reported as the best solution for all but one set of experimental conditions to be discussed below. Thus five or more components are needed to adequately describe the data within the discrete context. The GCV distribution is the most discrete in nature of the three spectral methods, and is presumably very close to the best discrete description. These results are in contrast to previous analogous studies with Ni(II) which used the method in [7] to determine the initial estimate of a discrete model, and then refined those estimates with nonlinear least-squares [26,27]. These papers reported four components for both humic [26] and fulvic acid [27] under all conditions studied.

In order to obtain the most probable picture of the heterogeneity of dissociation, the smoothest or broadest distribution in Fig. 2 must be chosen. This corresponds to the EM solution, and does so for all data considered thus far. The reason for such significant differences in the solution with respect to method is most likely due to a non-Gaussian error distribution. Residual correlation tests were performed on the data, and were indeed found to be correlated for all methods of solution. Solutions of such widely heterogeneous distributions do not possess correlated residuals if only constant random noise is present [17]. Therefore, systematic error in the data cannot be ruled out. It is apparent that under these conditions EM further broadens the rate constant distribution and that artifactual information is minimized.

The EM rate constant distributions of Latahco humic acid as a function of pH are shown in Fig. 3, as a function of Cu(II) concentration in Fig. 4, and as a function of ionic strength in Fig. 5. The distributions as a function of humic material are

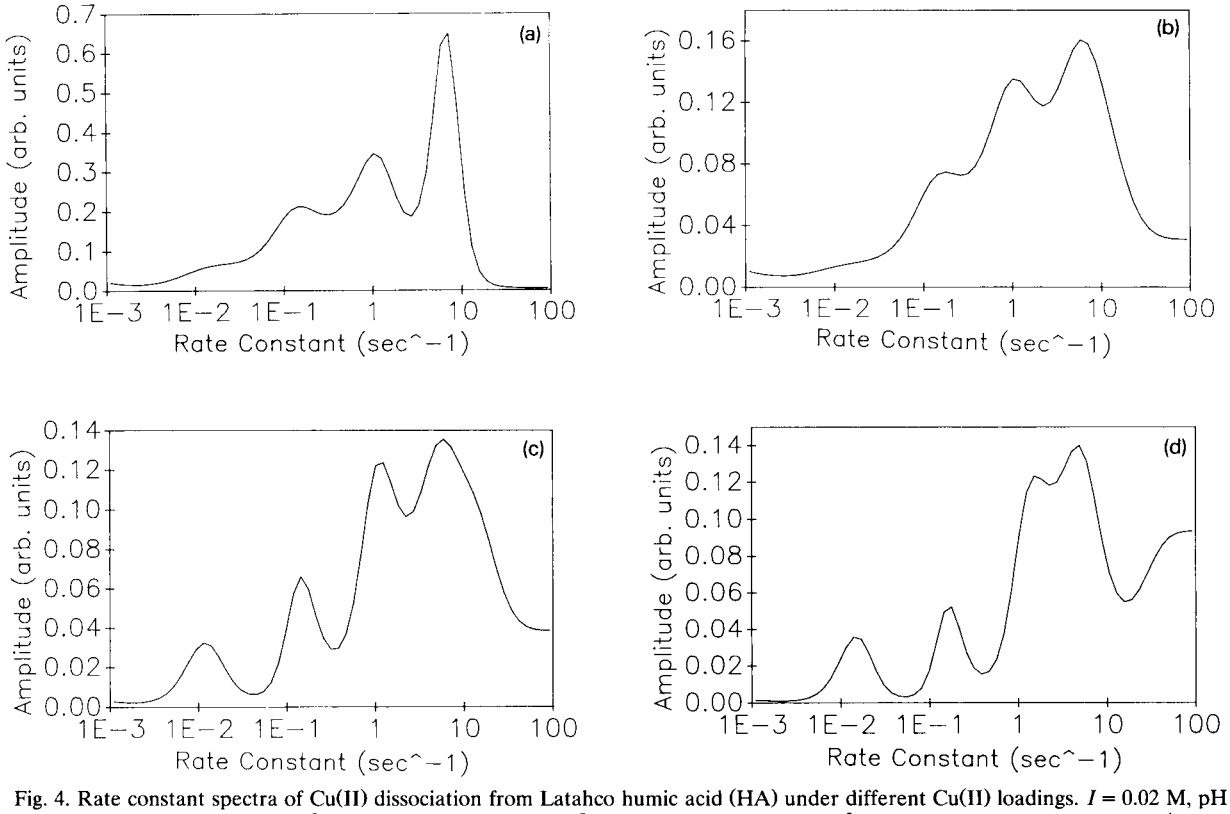

Fig. 4. Rate constant spectra of Cu(II) dissociation from Latahco humic acid (HA) under different Cu(II) loadings. $I = 0.02$ M, pH 7.5, and (a) [Cu(II)] = 3.8×10^{-5} M, (b) [Cu(II)] = 7.6×10^{-5} M, (c) [Cu(II)] = 9.5×10^{-5} M, and (d) [Cu(II)] = 1.14×10^{-4} M.

presented in Fig. 6. In general multi-modal continuous distributions appear to be the norm. Often the right-hand-side of these distributions contains significant signal amplitude or is even divergent at the endpoint. This behavior is due to the undersampling of the rate constant region 20–50 s^{-1}, which contains a large proportion of the

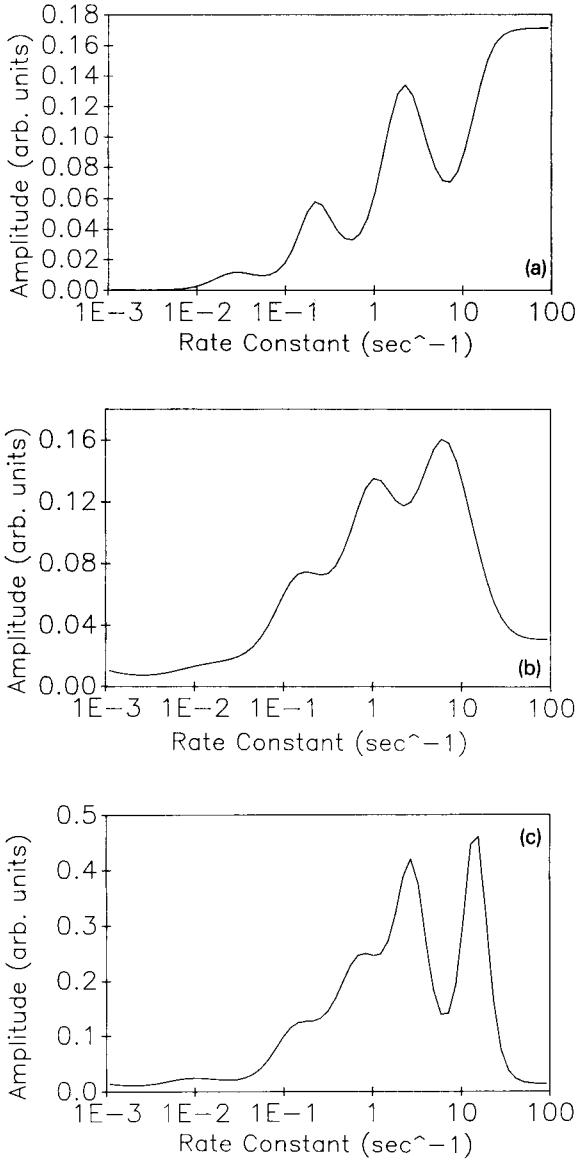

Fig. 5. Rate constant spectra of Cu(II) dissociation from Latahco humic acid (HA) under different ionic strength conditions. [Cu(II)] = 7.6×10^{-5} M, pH 7.5, and (a) $I = 0.001$ M, (b) $I = 0.02$ M, and (c) $I = 0.20$ M.

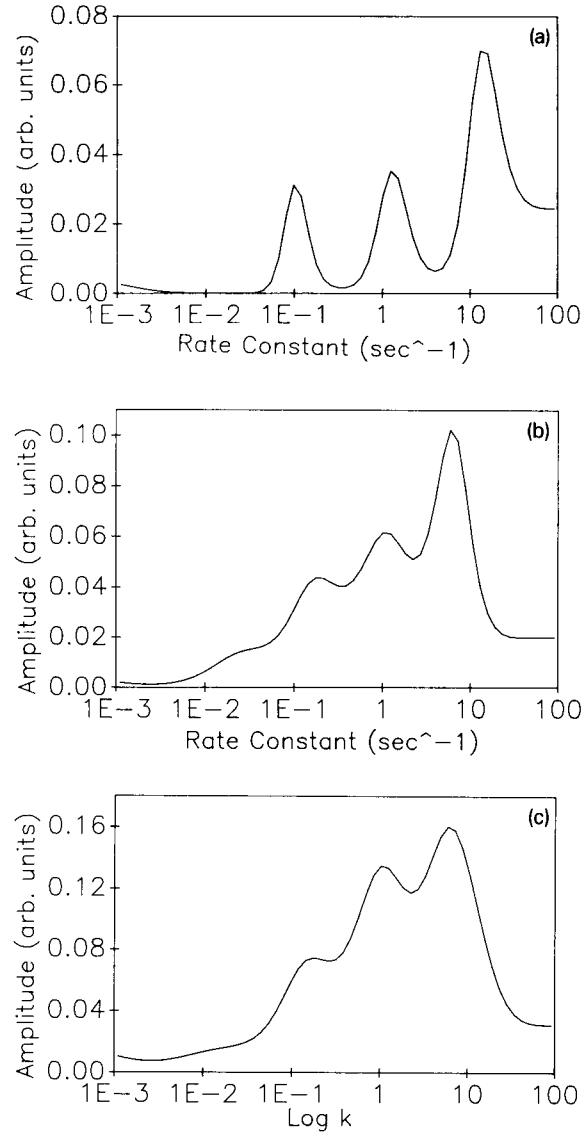

Fig. 6. Rate constant spectra of Cu(II) dissociation from different humics. [Cu(II)] = 7.6×10^{-5} M, $I = 0.02$ M, pH 7.5, and (a) standard fulvic acid, (b) standard humic acid, and (c) Latahco humic acid.

decay amplitude under many environmental conditions. Of less significant note, the left-hand-side of these distributions contains a small divergence ($< 1\%$ of total signal) of amplitude which corresponds to rate constants slower than 1×10^{-3} s^{-1}. We associate the dissociation corresponding to the faster observed rates as that corresponding

to the outer portion of the humic molecular mass which is in better contact with the outer solution, and the dissociation corresponding to the lower observed rates as that corresponding to the inner portion of the humic molecular mass which is somewhat isolated from the outer solution.

At low pH the dissociation rates of Cu(II) from Latahco humic acid are more isolated (Fig. 3). This is due to the agglutination of humic acid typically observed at low pH, which is due to the neutralization of its negative charge by occupation of the functional binding sites with protons. This effect is seen to a lesser extent as the Cu(II) concentration increases at constant pH (Fig. 4). At pH 3.5 the slow and rapid decay vanishes. In these conditions, a discrete two rate description optimally represents the data. The zeroeth and first moments of these two peaks agree with the DISCRETE parameters for a double exponential decay with $k_1 = 5.8\ s^{-1}$, $k_2 = 0.16\ s^{-1}$. Since the DISCRETE analysis resulted in a significantly lower fit variance, it is appropriate to assume a two site model classifies the data at pH < 4 [6].

As the ionic strength of the humic–Cu(II) solution is increased (Fig. 5), a consistent trend is observed: the amplitude of the fastest rates decreases while the amplitude of the lowest rates increases. This is explained as follows. As the concentration of Na^+ ions is increased around the negatively charged humic species, the electrical double layer increases in magnitude. This causes a decrease in the rate constants associated with the dissociation from these sites, which must be hydrophilic in nature. By their nature these sites are in better contact with the surrounding aqueous solution than are sites located within the interior of the humic molecular mass, which are hydrophobic in nature. Correspondingly as the ionic strength decreases, the humic molecular mass opens up to facilitate more contact or communication with the Na^+. This allows better communication of PAR^- with the Cu(II) located in the interior, increasing the rate of the slower dissociation processes. For the low pH data, the communication with the interior sites is effectively blocked as the outer double layer is quenched by protons and the humic agglutinates. The spectra do not just shift laterally, however, but change their shape as well. This is evidence that the modes of binding change in nature as the environmental conditions change.

The data presented in Fig. 6 show that fulvic acid exhibits three fairly well resolved regions of dissociation, as compared to both humic acids studied. Their first moments are $k_1 = 27\ s^{-1}$, $k_2 = 1.5\ s^{-1}$, and $k_3 = 0.11\ s^{-1}$. This is due to the lower molecular mass of fulvic acid and subsequently a lower degree of heterogeneity. The slower rates are not present to the degree of the humic acids because the interior sites are less hydrophobic than their humic acid counterparts. The difference in shape between the humic acid spectra is marginal at best. If anything, higher heterogeneity is observed in the Latahco than the standard humic acid with a larger proportion of slower rates. The Latahco humic acid does, however, significantly bind more Cu(II) than the standard humic acid, as can be obtained by integrating the distributions.

Conclusions

The differences in spectral representation or heterogeneity offered by three separate statistical deconvolution techniques clearly illustrates the difficulty in assessing the true degree of heterogeneity of the kinetics of dissociation of metals from humics. This problem is not local to these types of studies, but is representative of experiments in heterogeneous surface sorption/desorption, lifetime and charge transfer studies in heterogeneous media, etc. A consistent, foolproof, and general method for quantitatively describing such heterogeneity has not yet been developed. We feel a maximum entropy solution, achieved here with the EM algorithm, over an appropriate physical parameter space is the best offer so far.

The binding of metals by humics is most assuredly very complex and is evidenced by the movement and dependence of the spectra obtained here as a function of environmental conditions. The type of binding may change with conditions and/or be dynamic in nature. Further, more exhaustive, studies are needed to piece together the reactivity, structure, and dynamics of these substances.

REFERENCES

1 F.J. Stevenson, Humus Chemistry: Genesis, Composition, Reactions, Wiley-Interscience, New York, 1982, Chap. 14.
2 R.L. Tate, Soil Organic Matter: Biological and Ecological Effects, Wiley-Interscience, New York, 1987, Chap. 10.
3 K.H. Tan, Principles of Soil Chemistry, Marcell Dekker, New York, 1982, pp. 48–82.
4 G. Sposito, The Chemistry of Soils, Oxford University Press, New York, 1989, pp. 48–55.
5 D.L. Sparks, Kinetics of Soil Chemical Processes, Academic Press, New York, 1989, p. 119.
6 D.B. Marshall, Anal. Chem., 61 (1989) 660.
7 S.L. Olson and M.S. Shuman, Anal. Chem., 55 (1983) 1103.
8 M.S. Shuman, B.J. Collins, P.J. Fitzgerald and D.L. Olson, in R.F. Christman and E.T. Gjessing (Eds.), Aquatic and Terres trial Humic Materials, Ann Arbor Science, Ann Arbor, FL, 1983, pp. 349–370.
9 S.L. Olson and M.S. Shuman, Giochim. Cosmochim. Acta, 49 (1985) 1271.
10 S.W. Provencher, Comput. Phys. Commun., 27 (1982) 213.
11 S.W. Provencher, Comput. Phys. Commun., 27 (1982) 229.
12 S.W. Provencher, CONTIN User's Manual, Technical Report EMBL-DA07, Max-Planck-Institut fur biophysikalishe Chemie, Göttingen, 1984.
13 G. Wahba, SIAM J. Numer. Anal., 14 (1977) 651.
14 D.M. Bates, M.J. Lindstrom, G. Wahba and B.S. Yandel, Technical Report No. 775 (rev.), Department of Statistics, University of Wisconsin, Madison, WI, 1986.
15 L.A. Shepp and Y. Vardi, IEEE Trans. Med. Imag., MI-2 (1982) 113.
16 S.E. Bialkowski, J. Chemom., 5 (1991) 211.
17 B.J. Stanley, S.E. Bialkowski and D.B. Marshall, Anal. Chem., 65 (1993) 259.
18 B.J. Stanley and G. Guiochon, J. Phys. Chem., 97 (1993) 8098.
19 G.R. Phillips and E.M. Eyring, Anal. Chem., 55 (1983) 1134.
20 V.J. Clancy, Nature (London), 159 (1947) 339.
21 E.T. Jaynes, IEEE Proc., 70 (1982) 939.
22 M. Miller and D.L. Snyder, IEEE Proc., 75 (1987) 892.
23 M.J. Morra, M.O. Coracpcioglu, R.M.A. von Wandruszka, D.B. Marshall and K. Topper, Soil Sci. Soc. Am. J., 54 (1990) 1283.
24 W.L. Campbell, International Humic Substances Society list of characterization data (non-published source), USGS, Denver, CO.
25 S.W. Provencher, DISCRETE User's Manual, Technical Report (EMBL), Max-Planck-Institut fur biophysikalish Chemie, Göttingen, 1982.
26 J. Lavigne, C.H. Langford and M. Mak, Anal. Chem., 59 (1987) 2616.
27 S.E. Cabaniss, Environ. Sci. Technol., 24 (1990) 583.

Analytica Chimica Acta, 287 (1994) 35–40
Elsevier Science B.V., Amsterdam

Supercritical fluid extraction recovery studies of budesonide from blood plasma

Lars Karlsson [a], Hans Jägfeldt [b] and Dennis Gere [c]

[a] *Department of Analytical Chemistry, University of Lund, P.O. Box 124, S-221 00 Lund (Sweden)*
[b] *ASTRA-DRACO AB, P.O. Box 34, S-221 00 Lund (Sweden)*
[c] *Hewlett-Packard Company, 2850 Centerville Road, Wilmington, DE 19808 (USA)*

(Received 28th June 1993; revised manuscript received 17th September 1993)

Abstract

In this article we have studied extraction recoveries of the corticosteroid budesonide from human blood plasma. The biological material was spiked with ^{3}H-budesonide at a concentration of 93 nM. The analyte was extracted both as a pure substance and from the biological matrix. The performance of the packed column used for trapping the analytes was investigated. Special interest was focused on the performance of the trap using large concentrations of methanol in the extraction fluid. High trapping temperatures were needed for full recovery of the steroid. However, excessive temperatures were also shown to cause thermal degradation of the analyte. The extraction method sequence also had some impact on extraction recovery and repeatability. For example, some analyte loss occurred if depressurization was performed prior to trap rinsing. Reasonably high steroid recoveries, above 80%, could be obtained from the plasma samples. When pure CO_2 was used, water in the matrix modified the extraction fluid, resulting in high analyte recovery. An alternative technique was to remove the water in a first low density step. The steroid was then extracted at conditions optimal for a dry matrix in a successive extraction.

Keywords: Budesonide; Plasma; Supercritical fluid extraction; Solid phase trapping; Steroids

The monitoring of small amounts of drugs in biological material requires a highly efficient extraction of the target analyte. This is most commonly performed using one or several solid phase extraction steps. Supercritical fluid extraction (SFE) is an interesting alternative technique, normally capable of fast extractions under mild conditions. However, SFE of pharmaceuticals and drugs from biological materials presents some challenges not usually present in the extraction of volatile or semi-volatile analytes from inert matrices such as food products, polymers or even soil. The drug analytes are often polar and require aggressive extraction conditions to dissolve in supercritical carbon dioxide. In some biological samples a further difficulty is the high water content in the sample. Some papers describing SFE of large volume water samples have appeared, including extraction of diisopropyl methylphosphonate [1], phenols [2,3] and drugs [3]. Problems associated with continuous extraction of aqueous matrices are restrictor plugging [1] and that dissolved water modifies the supercritical phase making extraction conditions difficult to predict, whereas static extraction may be inefficient and slow. However, in the case of blood plasma and similar samples, sample volume is generally small, normally in the order of 1 ml. This means that the problems described above for large water samples are of less significance,

Correspondence to: L. Karlsson, Department of Analytical Chemistry, University of Lund, P.O. Box 124, S-221 00 Lund (Sweden).

SSDI 0003-2670(93)E0588-X

especially in dynamic extraction. Water may also be removed by different drying techniques, as e.g., freeze drying [4] or solid phase extraction [5].

Previously, basic investigations concerning steroid solubility in supercritical carbon dioxide have been undertaken [6,7]. Also, steroids have been extracted from various matrices, including rodent diet [8] and glass wool [9]. In these cases analyte concentration was high, in the $\mu g\ g^{-1}$ range. To our knowledge, no attempt has been made to use supercritical fluids for the extraction of corticosteroids, present at low concentrations in biological fluids. We have investigated the possibilities of using supercritical fluids for extracting small amounts of pharmaceutical drugs from human blood plasma. Three steroids with different polarities, budesonide, hydrocortisone and dexamethasone were chosen as model compounds.

EXPERIMENTAL

Equipment

The extraction system used was a Hewlett-Packard 7680T (Wilmington, DE). Liquid modifier was pumped into the pressurized carbon dioxide stream using a Hewlett-Packard 1050 quaternary LC pump, except in a few experiments where cylinders containing CO_2–methanol mixtures were used. Software for controlling the extractor and the modifier pump was developed at Hewlett-Packard. Extractions were done in the off-line mode using solid–sorbent trapping. 7-ml extraction thimbles were used throughout this work. When non-radioactive standards were used, 5 cm glass rods were inserted in the extraction thimbles, giving a remaining thimble volume of approximately 2 ml. ODS (octadecyl silica) was used as trapping material in all experiments. Trap temperature during extraction was varied between 75 and 150°C. During the depressurization step, system pressure is lowered in a controlled manner through the variable restrictor. Normally the system is depressurized prior to desorption of analytes from the trap, but the order of these two steps may be reversed. During desorption trap temperature was set to 40°C. Methanol, pumped at 1.0 ml/min to a total volume of 1.5 ml, was used as the desorption solvent. With these parameters it was shown that no analytes were eluted when repeating the desorption step.

Liquid chromatography was performed on a Hewlett-Packard 1090 liquid chromatograph with UV detection at 244 nm. The mobile phase was a mixture of 0.025 M phosphate buffer (pH 3.2) and acetonitrile in the proportions 68:32 (v/v). The column was a bonded phase C_{18} column (12.5 cm × 4.6 mm i.d., Hypersil, Hewlett-Packard) operated at a flow-rate of 1.5 ml/min. The injection volume of external standards and samples was 20 μl.

Liquid scintillation counting was done on a Packard 1500 (Chicago, IL). To each vial was added 200 μl of sample and 2 ml of Optifluor (Packard).

Chemicals

SFE-grade carbon dioxide, pure or containing methanol was used in the work reported here. Gases and mixtures were provided by Scott Speciality Gases (Plumsteadville, PA) or Air Products (Allentown, PA). Methanol was of the highest available purity.

The investigated steroids are shown in Fig. 1.

Budesonide (99.9% purity by LC) was prepared at ASTRA-DRACO (Lund). Hydrocortisone (research grade) was obtained from Serva (Heidelberg), and dexamethasone (reference

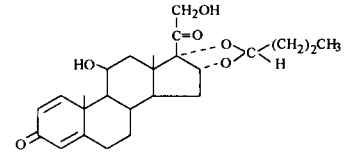

BUDESONIDE

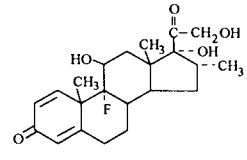

DEXAMETHASONE

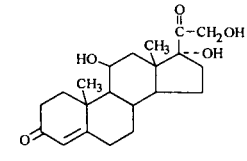

HYDROCORTISONE

Fig. 1. Compounds investigated.

standard material No. 921) from National Institute for Standards and Testing (Washington, DC).

Sample loading procedures

A methanol solution containing budesonide (3.1 mM), hydrocortisone (2.9 mM) and dexamethasone (2.3 mM) was used in the experiments with pure substances. 100 μl of this solution was pipetted onto 1/4 of a filter paper (9.0 cm Whatman 40) and placed in the extraction thimble.

For the experiments with blood plasma, tritiated budesonide (chemical purity 99.4%) was prepared at ASTRA-DRACO. The radiochemical purity was 99.3%. The ethanol stock solution contained 476 μM of ^{3}H-budesonide with a radioactivity of 35.0 MBq/ml. Plasma samples were spiked according to the following procedure. The stock solution was diluted 100 times with a 1:1 water–ethanol mixture. 200 μl of this solution was then pipetted into a volumetric flask containing 10 ml of plasma, giving a ^{3}H-budesonide concentration of 93 nM. After that, the spiked plasma solution was stirred vigorously. Filter papers (11.0 cm from S&S, Keene, NH) were rolled and placed in the cylindrical extraction vessels. 500 μl portions of spiked plasma, each with an activity of 3670 Bq, were then pipetted onto and absorbed by the filter papers in the extraction thimbles.

RESULTS AND DISCUSSION

Extractions of pure steroids

The steroids were extracted as pure substances from the thimble to elucidate solute solubility in CO_2 and CO_2–methanol phases without the influence of a matrix. The sample used here was a solution of budesonide (3.1 mM), hydrocortisone (2.9 mM) and dexamethasone (2.3 mM). 100 μl of the sample was loaded on the thimble, the solvent was allowed to evaporate and the extraction was performed. Density and temperature were set to 0.90 g/ml and 40°C, respectively. The trap temperature was 40°C and pure CO_2 was used as the extraction fluid. Liquid chromatography was used for determining extraction recoveries. Recoveries of the three steroids were 80, 66 and 30% for budesonide, hydrocortisone and dexamethasone, respectively. When the same sample

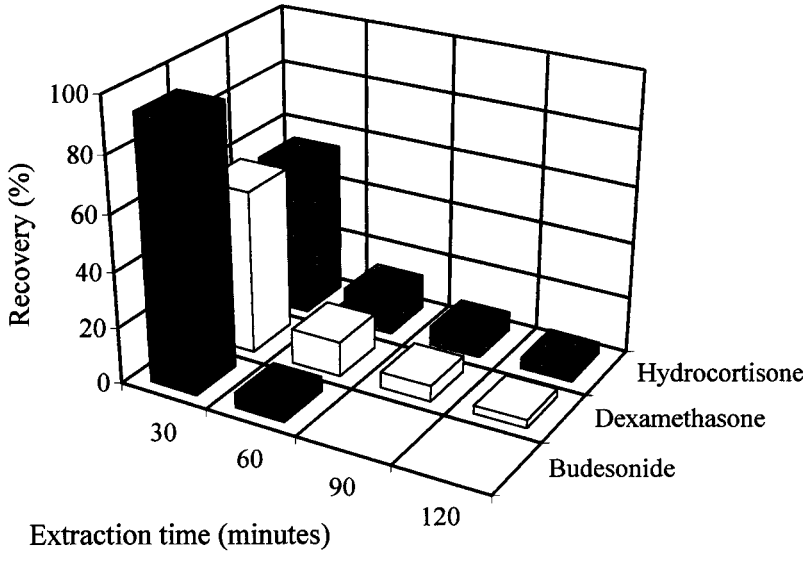

Fig. 2. Extraction time profile of the three steroids. Extraction: fluid, 5% methanol in CO_2; density, 0.90 g/ml; flow, 2.0 ml; temperature, 40°C; time, 30 min. Trapping: packing, ODS; temperature, 110°C. Rinsing: solvent, methanol; temperature, 40°C; flow, 1.0 ml/min; volume, 1.5 ml. Sample: 100 μl of a mixture of budesonide (3.1 mM), hydrocortisone (2.9 mM), dexamethasone (2.3 mM).

was loaded on filter paper in the extraction thimble, extraction recoveries were very low, less than 30%. Thus, carbon dioxide containing 5% methanol, supplied in a cylinder from the gas vendor, was tested as the extraction fluid. Repetitive extractions (30 min) were done and the recoveries are shown in Fig. 2.

The difference in polarity is quite evident from the graph. Budesonide was completely extracted after one hour, whereas the more polar dexamethasone and hydrocortisone were not fully extracted even after two hours of extraction. Here, differences in extraction recoveries are depending almost exclusively on solute solubility in the extracting phase. Diffusion properties are of limited importance since no matrix is present.

The variation in recovery of the least polar model compound budesonide with the amount of methanol in the extraction phase is shown in Fig. 3.

The recovery of budesonide in pure CO_2 is very low which is not surprising since budesonide solubility in hexane, a solvent with solvating properties similar to supercritical CO_2, is very limited. Recovery increases with the percentage of methanol and the curve levels out at approximately 10% methanol. At higher modifier concentrations the recoveries decrease. Fractions collected at the exit of the trap contained significant amounts of budesonide, indicating inefficient trapping of the analyte under such circumstances.

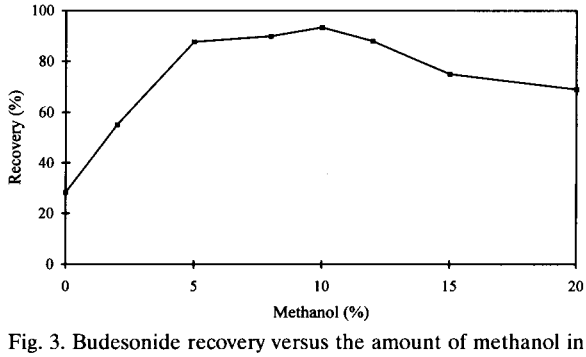

Fig. 3. Budesonide recovery versus the amount of methanol in the extraction fluid. All parameters are the same as in Fig. 2, except the methanol concentration which is varied between 0 and 20% in the extraction fluid. Sample: 100 μl of a methanol solution containing 3.1 mM budesonide.

TABLE 1

Temperature effects on the trapping efficiency of budesonide [a]

Trap temperature (°C)	Recovery (%)
75	68
100	78
125	84
150	79

[a] All parameters are the same as in Fig. 2. Sample as in Fig. 3. $n = 2$.

To investigate this problem further, trapping temperature was varied. At higher temperatures methanol is mainly present in the gaseous state and its ability to solve and elute the analytes are thereby decreased. A phase containing 15% of methanol, a concentration that resulted in a breakthrough problem in the previous experiment, was chosen for this experiment. The trap temperature was varied between 75 and 150°C and resulting recoveries are shown in Table 1.

As the temperature increases trapping becomes more efficient but there is a limit and recoveries above 90% are never reached. By increasing the temperature we have possibly created two new problems. One of them is that at a temperature of 150°C, analyte vapor pressure might be sufficiently high for the solutes to be moved through the trap with a gas chromatographic mechanism. Another problem is the temperature stability of the steroids. At 150°C thermal degradation was indicated by the fact that unknown peaks appear in the LC. The conclusion must be that raising the temperature would not solve the problem.

The trap worked well enough to trap budesonide, and full or close to full recoveries were obtained using a phase containing 10% methanol. The repeatability and recovery were also depending on the extraction method sequence. Table 2 shows that recovery was low when the depressurization step was placed in front of the rinse step.

Possibly, methanol liquefies during the depressurization period, carrying analytes through the trap. When the order of these two steps was reversed, recovery was significantly improved, although the repeatability was not so good, in the

TABLE 2

Influence of method step sequence [a]

Method	Recovery (%)	R.S.D. (%)
Extract (10% methanol) Depressurize Rinse	82	6.0
Extract (10% methanol) Rinse Depressurize	95	7.8
Extract (10% methanol) Extract (pure CO_2) Rinse Depressurize	90	4.0

[a] All parameters are the same as in Fig. 2. Sample as in Fig. 3. $n = 8$.

order of 8% (R.S.D.). Generally, when modified extraction phases are used it may be advantageous to use a short phase exchange step. Here pure CO_2 is pumped through the system between the actual extraction steps. By doing so the methanol content is always the same when a new sample is extracted. The insertion of such a step in the method sequence improved the repeatability to approximately 4% (R.S.D.).

Extractions of blood plasma samples

Spiked plasma samples containing 93 nM of budesonide were extracted with both pure and methanol modified carbon dioxide using different extraction procedures. As mentioned above, recovery of budesonide was reasonably high, almost 80%, when the non-labelled analyte was loaded simply on the thimble wall. This can be compared with Fig. 3 where the same amount loaded on filter paper gave a recovery of only ca. 28%. For plasma samples, also loaded on filter paper, analyte–matrix interactions were expected to be of even greater significance, especially as the analyte concentration in the plasma samples was several orders of magnitude lower than in the previous experiments. However, a surprisingly high recovery was found (see Fig. 4a). This is most probably due to the fact that water in plasma can act as a polar modifier of CO_2 increasing the solvent strength of the extracting fluid.

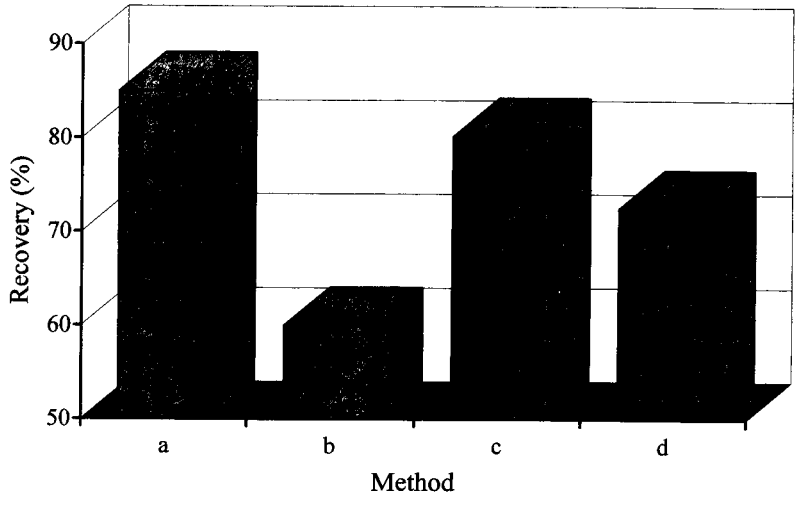

Fig. 4. Recoveries of budesonide from plasma samples. All parameters are the same as in Fig. 2. Sample: 500 μl of spiked plasma containing 93.3 nM ^{3}H-Budesonide. Time: 30 min per extraction step. Methods: (a) extract (pure CO_2, density 0.90 g/ml, trap temp. 110°C). Rinse. Depressurize. (b) Fractionated extraction with pure CO_2 (density 0.30 g/ml, trap temp. 40°C) followed by extraction with a fluid containing 10% methanol (density 0.90 g/ml, trap temp. 110°C). Rinse. Depressurize. (c) As in (b) except that the trap temperature was 110°C in all steps. (d) Fractionated extraction with pure CO_2 (density 0.30 g/ml, trap temp. 110°C) followed by a static extraction with 10% methanol as modifier (density 0.15 g/ml, trap temp. 110°C) and finally a dynamic extraction with 10% methanol as modifier (density 0.90 g/ml, trap temp. 110°C). Rinse. Depressurize.

Fractionated extraction was also tested. Water was removed in the first step, and then the target analyte was extracted using parameters optimal for extraction of the pure substance. The water removal step was done at low density, 0.30 g/ml, using pure CO_2 followed by a high density step with 10% methanol as modifier. Two methods for trapping of the analytes were used. In the first approach, trapping conditions were such that no analyte was trapped during the water removal step. In the second case optimal trapping parameters for budesonide were used also in the first extraction step. Recoveries are shown in Fig. 4b–c.

The results show that a significant amount of budesonide is removed from the extraction vessel with the aqueous phase and elutes through the trap to waste when trapping conditions are such that water can be condensed. When optimal trapping parameters were used in both extraction steps, almost the same recovery was obtained as when pure CO_2 was used to extract the wet plasma samples.

It was shown that some budesonide remained on the filter paper after the completion of the extraction. In an effort to enhance total recovery of the SFE method an additional step was included in the extraction sequence aiming to wet the matrix with methanol. Wetting techniques has been used previously with favorable results in the extraction of pesticides from soil [10]. By choosing a low density and enough methanol in the extraction fluid the sample will be wetted with liquid methanol, which is the purpose of the operation. Appropriate parameters were chosen from the phase diagram of carbon dioxide–methanol [11]. Unfortunately, as evident in Fig. 4d, recovery was not increased further when the matrix was wetted. Probably, the matrix was wetted, but the total amount of methanol might have been too high causing a breakthrough problem. Accordingly, the wetting step has to be further optimized including testing of other wetting agents, to be successful.

The authors wish to thank Dr. Ron Majors (Hewlett-Packard Company, Wilmington, DE), professor Lars-Erik Edholm (ASTRA-DRACO, Lund), Dr. Margareta Tönnesson (ASTRA-DRACO) and Dr. Lennart Mathiasson (Department of Analytical Chemistry, University of Lund) for valuable discussions.

REFERENCES

1 J. Hedrick and L.T. Taylor, Anal. Chem., 61 (1989) 1986.
2 D. Thiebaut, J.-P. Chervet, R.W. Vannoort, G.J. De Jong, U.A. Th. Brinkmann and R.W. Frei, J. Chromatogr., 477 (1989) 151.
3 J.L. Hedrick and L.T. Taylor, J. High Resolut. Chromatogr., 13 (1990) 312.
4 D.P. Ndiomu and C.F. Simpson, Anal. Chim. Acta, 213 (1988) 237.
5 H. Liu, L.M. Cooper, D.E. Raynie, J.D. Pinkston and K.R. Wehmeyer, Anal. Chem., 64 (1992) 802.
6 E. Stahl and A. Glatz, Fette, Seifen, Anstrichm., 86 (1984) 346.
7 M. Kane, J.R. Dean, S.M. Hitchen, C.J. Dowle and R.L. Tranter, Anal. Chim. Acta, 271 (1993) 83.
8 M.R. Euerby, R.J. Lewis and S.C. Nichols, Anal. Proc. 28 (1991) 287.
9 S.F.Y. Li, C.P. Ong, M.L. Lee and H.K. Lee, J. Chromatogr., 515 (1990) 515.
10 C.R. Knipe, D.R. Gere and M.E.P. McNally, in F.V. Bright and M.E.P. McNally (Eds.), ACS Symp. Series Vol. 488, American Chemical Society, Washington, DC, 1992, Chap. 18.
11 T.A. Berger, J. High Resolut. Chromatogr., 14 (1991) 312.

Analytica Chimica Acta, 287 (1994) 41–48
Elsevier Science B.V., Amsterdam

Determination of amphetamine and methamphetamine in urine with sodium 1,2-naphthoquinone 4-sulphonate using the H-point standard addition method

Pilar Campíns Falcó, Francisco Bosch Reig, Adela Sevillano Cabeza and Carmen Molins Legua

Departamento de Química Analítica, Universidad de Valencia, C / Dr. Moliner 50, 46100-Burjassot, Valencia (Spain)

(Received 21st May 1993; revised manuscript received 8th October 1993)

Abstract

The determination of amphetamine and methamphetamine in urine by the H-point standard additions method (HPSAM) is described. An extraction–spectrophotometric method for the determination of these drugs with sodium 1,2-naphthoquinone 4-sulphonate using *n*-hexane–ethyl acetate (1 : 1) as the extraction solvent is proposed. The analytes are previously extracted into *n*-hexane. Although their spectra are very similar and overlap, the H-point standard additions method provides good results for both amines. The applicability of the method when the total Youden blank is present is demonstrated. The relative errors found were less than 10%.

Keywords: UV–Visible spectrophotometry; Amphetamine; Extraction; H-point standard addition method; Methamphetamine; Pharmaceuticals; Urine

The determination of amphetamines as a drug class has been a major part of drug and toxicological analysis for many years. This drug class encompasses several different compounds, but amphetamine and methamphetamine are the most widely abused. Because of their long history of use, a significant number of studies have been made of their determination and metabolism [1–3].

The excretion of both drugs is influenced by urinary pH. Under normal conditions, methamphetamine is mainly excreted as unchanged, only a small amount being demethylated to amphetamine. The methamphetamine-to-amphetamine ratio is generally between 4 and 10 in urine samples [4–6]. The excretion of unchanged amphetamine is as much as 54% at pH 5 and as low as 2.9% at pH 8. About 30–40% of amphetamine is usually excreted unchanged in the urine within 48 h.

Most of the methods proposed in the literature for the determination of both drugs in biological samples are based on thin-layer chromatography (TLC) [7–9], gas chromatography (GC) [6,10–14] or liquid chromatography (LC) [5,15–17]. Proposed spectrophotometric methods are mainly screening tests based on the formation of ion pairs between the drugs and dyes. Extraction into organic solvents is carried out [18,19].

In 1922, Folin [20] described a method for the determination of amino acids that depends on the combination of the amino groups with sodium 1,2-naphthoquinone 4-sulphonate (NQS) in alkaline solution to form highly coloured compounds. Rosenblatt et al. [21] used NQS for the determination of ethylenimine and primary amines and

Correspondence to: P. Campíns-Falcó, Departamento de Química Analítica, Universidad de Valencia, C/Dr. Moliner 50, 46100-Burjassot, Valencia, Spain.

SSDI 0003-2670(93)E0571-N

reddish dyes were extracted into chloroform. Gürkan [22,23] applied the reaction to the investigation of sympathomimetic amines, including amphetamines, in pharmaceutical samples. Hashimoto et al. [24] used NQS for the qualitative analysis of phenethylamine derivatives by thin-layer chromatography. Endo and Imamichi [15] applied this reagent as a derivatizing agent in the determination of methamphetamine and amphetamine in urine samples by LC. Recently, Nakahara and co-workers [16,17] described the application of NQS to labelling amines in urine, plasma and saliva samples for LC with electrochemical detection.

We have proposed extraction–spectrophotometric procedures for the individual determination of amphetamine [25] or methamphetamine [26] in urine samples with NQS, selecting the best reaction conditions for each drug. Both procedures are subject to interference from the presence of the other drug. The aim of this work was to determine methamphetamine and amphetamine simultaneously in urine samples. This is of interest because a urine sample containing methamphetamine always contains amphetamine owing to the metabolism of the former drug. For this purpose the H-point standard additions method (HPSAM) developed previously [27,28] was used, which permits the analysis of binary mixtures with overlapped spectra [29] even in the presence of the total Youden blank (TYB) [28] such as occurs in these determinations [25,26]. The TYB represents the constant error of the method extrapolated to zero sample level, being independent of the size of sample taken and not attributable to the analyte. The TYB is cancelled by evaluating it using the Youden method [30] or using a urine sample from a normal subject as a placebo. The goodness of the HPSAM when the TYB is present in a real sample was also tested.

EXPERIMENTAL

Reagents

Hydrogencarbonate buffer was prepared by dissolving 8 g of sodium hydrogencarbonate (Probus) in 100 ml of distilled water. The pH was adjusted to 10 by adding the minimum amount of NaOH (10 M). This solution was then diluted to yield appropriate working solutions. A stock standard solution (0.5%, w/v) of sodium 1,2-naphthoquinone-4-sulphonic acid (Sigma) was prepared fresh for each experiment and was stored in the dark. (+)-Methamphetamine hydrochloride (Sigma) and (±)-methamphetamine hydrochloride (Sigma) stock standard solutions were prepared by dissolving 100 mg in distilled water and diluting to 100 ml. D-Amphetamine sulphate (Sigma) and DL-amphetamine sulphate (Sigma) stock standard solutions were prepared dissolving 100 mg in distilled water and diluting to 100 ml. Working standard solutions of lower concentrations were prepared daily by dilution to the appropriate volumes. Both the (+)- and (±)-isomeric forms of these drugs can be used as the reaction between NQS and methamphetamine is not specific for a particular isomeric form. *n*-Hexane (95%, LC grade) (Scharlau), ethyl acetate (LC grade) (Scharlau), concentrated ammonia solution (Probus) and hydrochloric acid (Probus) were used.

Apparatus

The organic solvent (*n*-hexane) was evaporated to dryness using a Büchi R110 rotary evaporator.

The samples were heated in a Lauda RM 20 bath, vortex mixed in a Vibromatic 384 mixer and centrifuged in a Heraeus Sepatech Medifuge.

All spectrophotometric measurements were made on a Hewlett-Packard HP 8452 A diode-array spectrophotometer furnished with quartz cuvettes of 1-cm path length.

Standard solutions

Different volumes of a stock standard solution of the analyte (amphetamine sulphate or methamphetamine hydrochloride) were added to 1 ml of hydrogencarbonate buffer (pH 10), 1 ml of 0.5% NQS and a constant volume of standard solution with a known concentration of amphetamine sulphate and methamphetamine hydrochloride and diluted to 3 ml with distilled water. The mixture was heated at 45°C for 5 min. After cooling, the mixture was shaken with the

same volume of organic solvent [*n*-hexane–ethyl acetate (1 + 1)] for 2 min and then centrifuged for 5 min. The absorbance between 190 and 820 nm of the organic phase was recorded against a reagent blank at 25°C. Three replicates were always carried out.

Urine samples

Samples of urine (5 ml, previously spiked or not with amphetamine and/or methamphetamine standard solutions) were made alkaline with 0.1 ml of concentrated ammonia solution and the free bases were extracted twice with the same volume of *n*-hexane. A small amount (50 μl) of concentrated hydrochloric acid–ethanol (1 + 6) was added to the combined *n*-hexane extracts to convert the free amines into the hydrochlorides. The solvent was evaporated to dryness and the residue was dissolved in 1 ml of distilled water, 1 ml of hydrogencarbonate buffer (pH 10) and 1 ml of 0.5% NQS. Subsequently the samples were processed in the same way as the standard solutions. Three replicates were always carried out.

H-point standard additions method

A volume of 0.3 ml of standard solution of the analyte (methamphetamine hydrochloride or amphetamine sulphate) was added to 5 ml of urine sample containing a known amount of amphetamine and methamphetamine, producing concentrations in the therapeutic range. Subsequently the samples were processed in the same way as the urine samples. Three replicates were always carried out.

RESULTS AND DISCUSSION

Consider an unknown sample containing an analyte X and an interferent Y subject to a constant bias error TYB. The determination of the concentration of X by the HPSAM under these conditions requires the selection of two wavelengths, λ_1 and λ_2, at which the interferent species Y should have the same absorbance [27,28]. Then, known amounts of X are successively added to the mixture and the resulting

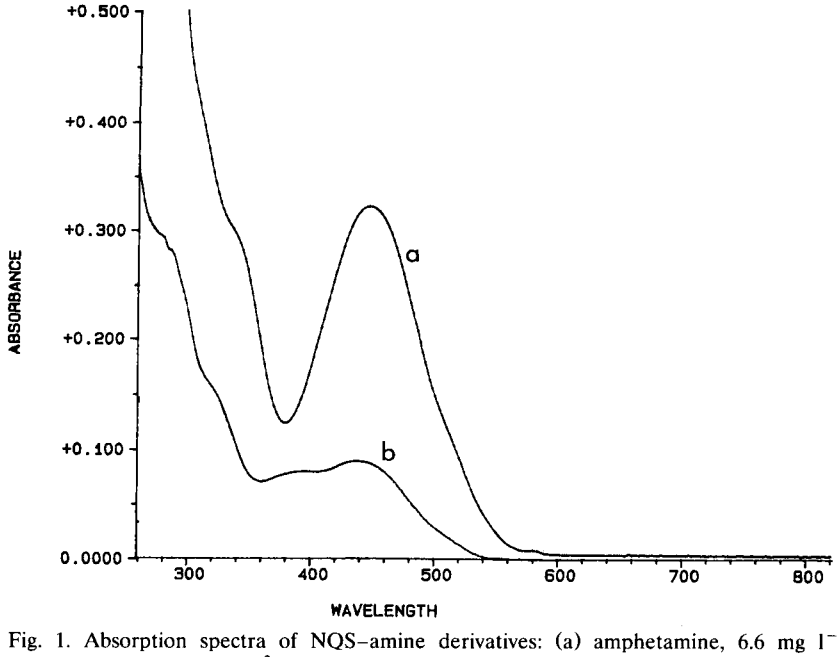

Fig. 1. Absorption spectra of NQS–amine derivatives: (a) amphetamine, 6.6 mg l^{-1}; (b) methamphetamine, 14.9 mg l^{-1}. Conditions: NQS 6.4×10^{-3} M, hydrogencarbonate buffer (pH 10), heating for 5 min at 45°C. The spectra were recorded against NQS reagent extracted into *n*-hexane–ethyl acetate (1 : 1).

absorbances are measured at the two wavelengths and applied to the following equations:

$$A(\lambda_1) = \text{TYB} + b_0 + b + M_1 C_i \quad (1)$$

$$A(\lambda_2) = \text{TYB} + A_0 + A' + M_2 C_i \quad (2)$$

where TYB (total Youden blank) is the constant bias error, which will normally be the same at the two selected wavelengths, b_0 and A_0 are the absorbances of the analyte X for the solution containing sample alone at λ_1 and λ_2, respectively, b and A' are the absorbances of Y at the same wavelengths ($b = A'$ as the two wavelengths were chosen so that the Y species has the same absorbance at both), M_1 and M_2 are the slopes of the straight lines obtained on applying the HPSAM to λ_1 and λ_2, respectively, C_i is the added X concentration and $A(\lambda_1)$ and $A(\lambda_2)$ are the absorbances measured at the two wavelengths for different points of the HPSAM. The two straight lines obtained intercept at the so-called H-point ($-C_H$, A_H), where C_H is the existing concentration of the analyte in the sample free from constant and proportional systematic errors. The ordinate value of the H-point $A_H = b + \text{TYB} = A' + \text{TYB} = A_y + \text{TYB}$ is the analytical signal due to the intercept A_y plus the TYB value. To evaluate the interferent concentration from the ordinate value of the H-point, a calibration graph or the absorbance value of an interferent standard is needed. The TYB value can be evaluated from the application of the Youden method [30,31] or by measuring the analytical signal of a placebo. It is not essential that the TYB be the same at the two selected wavelengths as it can be evaluated at both and used later to construct the HPSAM graph by plotting (A-TYB) (λ_1) and

TABLE 1

Found concentrations of amphetamine and methamphetamine in standard samples by applying the HPSAM at different pairs of wavelengths [a]

Sample concentration (mg l^{-1})		Concentration found (mg l^{-1})							
Analyte metham-phetamine	Interferent amphetamine	Analyte				Interferent			
		404–460 nm	414–458 nm	416–456 nm	420–452 nm	404–460 nm	414–458 nm	416–456 nm	420–452 nm
6.7	2.0	6.9	6.8	6.9	6.9	1.9 [b]	2.3	1.9	1.9
						1.9 [c]	2.0	1.9	1.9
10.7	2.0	11.2	11.1	11.2	11.4	2.0	2.1	1.9	1.7
						1.9	2.1	1.9	1.7
10.6	5.3	10.2	9.9	10.2	10.5	5.1	5.4	5.1	4.7
						5.2	5.6	5.2	4.8
17.2	5.3	17.5	17.4	16.7	17.9	4.3	4.6	5.4	4.1
						5.2	4.9	5.3	4.2
23.9	5.3	24.3	24.2	23.4	24.7	4.7	4.2	5.1	3.7
						4.9	3.4	5.1	3.7

Sample concentration (mg l^{-1})		Concentration found (mg l^{-1})			
Analyte amphetamine	Interferent methamphetamine	Analyte		Interferent	
		416–480 nm	428–468 nm	416–480 nm	428–468 nm
5.3	10.6	5.7	5.5	9.6 [b]	10.2
				10.2 [c]	10.3
11.9	10.6	13.0	13.0	9.6	9.6
				9.5	9.5
18.6	10.6	19.4	19.0	10.5	11.5
				10.3	10.5

[a] Conditions: NQS 6.4×10^{-3} M, hydrogencarbonate buffer (pH 10), heating for 5 min at 45°C. Extraction solvent, *n*-hexane–ethyl acetate (1:1). [b,c] Values obtained at the two wavelengths for each pair of wavelengths used in the HPSAM and from the calibration method with a single standard.

(A-TYB) (λ_2) as a function of the added analyte concentration [28].

The optimum conditions for the simultaneous determination of both drugs are 0.1 M $NaHCO_3$ (pH 10), 6.3×10^{-3} M NQS and heating for 5 min at 45°C [25,26]. The reaction products were extracted into *n*-hexane–ethyl acetate (1 : 1).

For the conditions mentioned above, the spectra of NQS–methamphetamine and NQS–amphetamine overlapped. The absorption maxima in the visible region are at 446 and 436 nm, respectively, as can be seen in Fig. 1. The visible region was chosen due to NQS reagent, and urine blank interferences are lower.

Different pairs of wavelengths where, according to the HPSAM, the absorbance of the interferent is the same were previously selected in order to test the best pair. The selected wavelength pairs were 404–460, 414–458, 416–456 and 420–452 nm for the determination of methamphetamine and 416–480 and 428–468 nm for determination of amphetamine. The two compounds were determined with each other (exclusively) as interferent.

Standard solutions of amphetamine and methamphetamine were initially tested to validate the applicability of the wavelengths chosen. In this instance the TYB value was zero. Concentrations of both compounds were added to produce concentrations of urinary samples in the therapeutic range. Table 1 summarizes the different mixtures assayed and the concentrations of analyte and interferent found. The concentration of interferent was calculated in each sample by the calibration method with a single standard and the ordinate value of the H-point (A_H).

As can be seen from Table 1, when methamphetamine is calculated as the analyte, it is well determined at the four pairs of wavelengths tested. When amphetamine is determined in these samples as interferent, similar results are obtained. Hence the HPSAM method provides accurate results for both drugs at the tested concentration ratios. When amphetamine is determined as analyte, the method also provides acceptable results and allows the determination of the concentrations existing in the samples for both compounds.

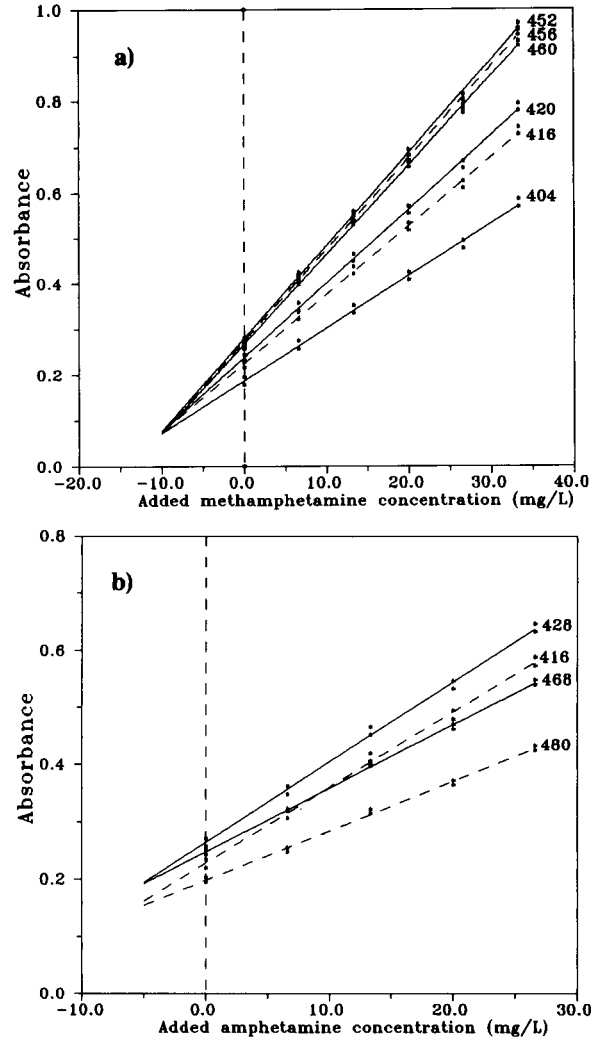

Fig. 2. HPSAM plots for methamphetamine (10.6 mg l^{-1}) and amphetamine (5.3 mg l^{-1}) in the sample: (a) added methamphetamine concentration; (b) added amphetamine concentration. Conditions: NQS 6.4×10^{-3} M, hydrogencarbonate buffer (pH 10), heating for 5 min at 45°C. The reaction products were extracted into *n*-hexane–ethyl acetate (1 + 1). The analytical signals were obtained against NQS reagent.

Figure 2 shows the HPSAM for synthetic samples at the different pairs of wavelengths chosen when methamphetamine or amphetamine was added. The sensitivity is better at 404–460 or 416–480 nm when methamphetamine or amphetamine is added, respectively, as the absorbance difference for each analyte is higher at these wavelengths. However, good results were

TABLE 2

Mean absorbance values obtained for different urine samples ($n = 16$) at different wavelengths [a]

Wavelength (nm)	Mean ± S.D.	Wavelength (nm)	Mean ± S.D.
404	0.06 ± 0.01	460	0.06 ± 0.02
414	0.05 ± 0.01	458	0.06 ± 0.02
416	0.06 ± 0.01	456	0.06 ± 0.02
420	0.06 ± 0.01	452	0.06 ± 0.02
428	0.04 ± 0.01	468	0.05 ± 0.01
480	0.06 ± 0.01		

[a] Conditions: NQS 6.4×10^{-3} M hydrogencarbonate buffer (pH 10), heating for 5 min at 45°C. Extraction solvent, *n*-hexane–ethyl acetate (1:1). The urine samples were previously extracted twice with *n*-hexane.

obtained in all instances because the experimental absorbance values are well fitted by the respective regression lines. Hence, for synthetic samples, all the pairs of wavelengths selected are suitable.

As mentioned, when these drugs are determined in urine samples the TYB is present [25,26] and must be evaluated at the different pairs of wavelengths chosen. It has been demonstrated [25,26] that the TYB value could be calculated using the Youden method [30] or with a placebo (urine sample from a normal subject).

For this purpose, different urine samples ($n = 16$) without amphetamine and methamphetamine were processed and the absorbance values found at the different wavelengths were similar (Table 2). Hence the TYB can be considered to be the same at the two selected wavelengths. Therefore, it is possible to obtain an unbiased analyte concentration directly on application of the HPSAM. The interferent concentration will be free from proportional but not from constant bias, which requires TYB evaluation.

In Table 3 are summarized the concentrations found for free urine samples spiked with different amounts of amphetamine and methamphetamine. In each instance, the analyte concentration was calculated directly from HPSAM method, which provides $A_H = A_Y$, when the analytical signal of the urine blank (TYB) has been previously subtracted. The interferent concentration was calculated from this value and from the calibration method for a single standard considering the drug recovery of the sample in the clean-up step. When low therapeutic levels of these amines are present in the sample, their determination as interferents

TABLE 3

Found concentrations of amphetamine and methamphetamine in different urine samples spiked with amphetamine and methamphetamine by applying the HPSAM at different pairs of wavelengths [a]

Sample concentration (mg l^{-1})		Concentration of analyte found (mg l^{-1})			
Analyte methamphetamine	Interferent amphetamine	404–460 nm	414–458 nm	416–456 nm	420–452 nm
3.9	1.2	–	4.1	4.1	4.1
7.9	1.2	–	7.8	8.0	8.4
11.9	1.2	–	12.1	13.1	–
10.3	3.9	10.5	10.3	9.8	10.1

Sample concentration (mg l^{-1})		Concentration found (mg l^{-1})			
Analyte amphetamine	Interferent Methamphetamine	Analyte		Interferent	
		416–480 nm	428–468 nm	416–480 nm	428–468 nm
3.9	10.3	3.8	3.2	11.2 [b]	11.5
				11.4 [c]	11.5
7.9	10.3	7.9	7.3	10.9	11.4
				11.2	11.5

[a] Conditions: NQS 6.4×10^{-3} M, hydrogencarbonate buffer (pH 10), heating for 5 min at 45°C. Extraction solvent, *n*-hexane–ethyl acetate (1:1). The urine samples were previously extracted twice with *n*-hexane. [b,c] Values obtained at the two wavelengths for each pair of wavelengths used in the HPSAM and from the calibration method with a single standard.

could be biased owing to the low values of A_H obtained. In all instances, independently of the methamphetamine-to-amphetamine ratio, the method provides accurate results for the determination of the analyte, as can be seen in Table 3.

If methamphetamine is considered as the analyte, the content of amphetamine in the sample will be low owing to the metabolism of the former drug. Then the determination of amphetamine as interferent is biased, owing to the small values of A_H. In this instance, two H-point standard additions plots might be required if it is necessary to determine both compounds. At higher contents of amphetamine and considering it as analyte it is possible to determine both drugs from a unique HPSAM plot, as can be derived from Table 3.

When only the methamphetamine or the amphetamine concentration is required, the method can be developed as a calibration method with a unique standard. The analytical signals will be $\Delta A = A_{\lambda 1} - A_{\lambda 2}$ [$A(\lambda_1)$ and $A(\lambda_2)$ are the absorbance values of the sample at the selected wavelengths for application of the HPSAM]. The analytical signals used are ΔA_m corresponding to a sample with an unknown amphetamine concentration (C_m) and ΔA_r for a reference solution with a concentration $C_r = C_m + C_{added}$ which contains the same urine volume as the sample and a known addition of amphetamine standard solution or methamphetamine standard solution (C_{added}). The analytical signal for this solution will be $\Delta A_r = \Delta A_m + \Delta A_{added}$. The unknown concentration can be obtained from the equation

$$C_m = \frac{\Delta A_m}{\Delta A_r - \Delta A_m} \times C_{added} \quad (3)$$

Table 4 gives the results obtained for urine samples using the Eqn. 3 and it can be seen that they are in agreement with those obtained using the HPSAM plots.

TABLE 4

Found concentrations of methamphetamine and amphetamine for different urine samples spiked with amphetamine and methamphetamine by applying Eqn. 3 [a]

Sample concentration (mg l^{-1})			Concentration of analyte found (mg l^{-1})			
Analyte methamphetamine	Added methamphetamine	Interferent amphetamine	404–460 nm	414–458 nm	416–456 nm	420–452 nm
3.9	6.6	1.2	4.3	4.2	4.1	4.3
	13.3	1.2	4.2	4.0	3.4	4.1
	20.0	1.2	4.4	4.1	4.1	4.2
7.9	6.6	1.2	7.7	7.3	–	7.9
	13.3	1.2	8.6	7.9	8.0	8.0
10.3	4.0	3.9	9.5	–	–	9.5
	8.0	3.9	9.3	9.3	–	10.0
	12.0	3.9	10.7	10.3	10.3	10.1
12.7	4.0	3.9	11.2	–	10.0	13.1
	8.0	3.9	14.2	–	14.6	13.2

Sample concentration (mg l^{-1})			Concentration of analyte found (mg l^{-1})	
Analyte amphetamine	Added amphetamine	Interferent methamphetamine	416–480 nm	428–468 nm
3.9	6.6	10.3	2.8	2.9
	13.3	10.3	3.5	3.2
	26.6	10.3	3.4	3.1
7.9	6.6	10.3	–	8.2
	13.3	10.3	8.7	7.5

[a] Conditions: NQS 6.4×10^{-3} M, hydrogencarbonate buffer (pH 10), heating for 5 min at 45°C. Extraction solvent, *n*-hexane–ethyl acetate (1 + 1). The urine samples were previously extracted twice with *n*-hexane.

Conclusions

The described procedure provides good results for the determination of amphetamine and/or methamphetamine in urine samples by a conventional extraction–spectrophotometric method. Although the spectra of these compounds after reaction with NQS are similar and the TYB values are present in the urine samples, their concentrations can be determined with sufficient accuracy and precision at therapeutic levels by the H-point standard additions method, even when the concentration of one of the components is many times higher than the other. As amphetamine is a metabolite of methamphetamine, urine samples containing methamphetamine always contain the other drug.

The authors are grateful to the DGICYT for financial support (Project No. PB91-0651).

REFERENCES

1 J. Caldewell, Drug. Metab. Rev., 5 (1976) 219.
2 R.L. Foltz, A.F. Fentiman, Jr. and R.B. Foltz, CG/MS Assays for Abused Drugs in Body Fluids, National Institute on Drug Abuse Research Monograph, No. 32, National Institute on Drug Abuse, Rockville, MD, 1980.
3 J. Caldwell (Ed.), Drug Dependence: Amphetamines and Related Stimulants: Chemical, Biological, Clinical and Sociological Aspects, CRC Press, Boca Raton, FL, 1980.
4 S. Shinichi, I. Takako and N. Tetsukichi, J. Chromatogr., 267 (1983) 381.
5 S.R. Binder, M. Regalia, M. Biaggi-McEachern and M. Mazhar, J. Chromatogr., 473 (1989) 325.
6 H. Tsuchihashi, K. Nakajima, M. Nishikawa, K. Shiomi and S. Takahashi, J. Chromatogr., 467 (1989) 227.
7 H. Gulyás, G. Kemény, I. Hollósi and J. Pucsok, J. Chromatogr., 291 (1984) 471.
8 J. Blakesley, D. Wood, C. Howse and J. Spencer-Peet, Ann. Clin. Biochem., 24 (1987) 508.
9 T. Daldrup and A. Rickert, Fresenius' Z. Anal. Chem., 334 (1989) 349.
10 W.R. Taylor, D.S. Le, S. Philip and N.C. Jain, J. Anal. Toxicol., 13 (1989) 293.
11 C.L. Hornbeck and J.R. Czarny, J. Anal. Toxicol., 13 (1989) 144.
12 H. Tsuchihashi, K. Nakajima, M. Nishikawa, S. Suzuki, Y. Oka and K. Otsuki, Forensic Sci. Int., 45 (1990) 181.
13 H. Tsuchihashi, K. Nakajima, M. Nishikawa, S. Suzuki, K. Shiomi and S. Takahashi, Anal. Sci., 7 (1991) 19.
14 R.O. Hughes, E.W. Broner and L.M. Smith, J. Anal. Toxicol., 15 (1991) 256.
15 M. Endo and H. Imamichi, J. Chromatogr., 196 (1980) 334.
16 Y. Nakahara, A. Ishigami and Y. Takeda, J. Chromatogr., 489 (1989) 371.
17 H. Sekine and Y. Nakahara, Eisei Kagaku, 37 (1991) 537.
18 M. Syoyama and T. Sano, Eisei Kagaku, 31 (1985) 410.
19 T. Sakai and N. Ohno, Analyst, 112 (1987) 149.
20 O. Folin, J. Biol. Chem., 51 (1922) 377.
21 D.H. Rosenblatt and P. Hlinka, J. Epstein, Anal. Chem., 27 (1955) 1290.
22 T. Gürkan, Mikrochimica Acta, I (1976) 165.
23 T. Gürkan, J. Fac. Pharm. Istambul, 16 (1980) 73.
24 Y. Hashimoto, M. Endo, T. Keido, I. Shigeko and M. Masataka, Mikrochimica Acta, II (1978) 493.
25 C. Molins Legua, P. Campíns Falcó and A. Sevillano Cabeza, Anal. Chim. Acta, in press.
26 P. Campíns Falcó, A. Sevillano Cabeza and C. Molins Legua, Fresenius' J. Anal. Chem., submitted for publication.
27 F. Bosch Reig and P. Campíns Falcó, Analyst, 113 (1988) 1011.
28 F. Bosch Reig and P. Campíns Falcó, Analyst, 115 (1989) 111.
29 P. Campíns Falcó, F. Bosch Reig and A. Molina Benet, Fresenius' J. Anal. Chem., 338 (1990) 16.
30 W.P. Youden, Anal. Chem., 19 (1947) 946.
31 M.J. Cardone, Anal. Chem., 58 (1986) 433.

Analytica Chimica Acta, 287 (1994) 49–57
Elsevier Science B.V., Amsterdam

Micellar enhanced fluorimetric determination of carbendazim in natural waters

J. Sancenón and M. de la Guardia

Department of Analytical Chemistry, University of Valencia, C / Dr. Moliner 50, 46100-Burjassot, Valencia (Spain)

(Received 1st June 1993; revised manuscript received 11th October 1993)

Abstract

A micellar enhanced flow-injection fluorimetric method was developed for the determination of carbendazim in natural water samples. The method is based on the direct injection of 500 μl of water into a three-channel flow manifold in which the samples are merged with a buffer solution and subsequently with a surfactant solution. Two alternative procedures were used: one based on the use of sodium dodecyl sulphate micelles in 0.1 M HCl, which permits a 2.6-fold enhancement of the sensitivity found in the absence of micelles to be obtained, and the other based on the use of cetyltrimethylammonium bromide in 0.1 M NaOH, which provides a 11.6-fold enhancement of sensitivity and a limit of detection of 1.3×10^{-8} M, which corresponds to 2.5 $\mu g\ l^{-1}$ of carbendazim. The recovery of carbendazim in spiked water samples of different types varied from 94 to 107%.

Keywords: Flow injection; Fluorimetry; Carbendazim; Fungicides; Micelles; Waters

Carbendazim (methylbenzimidazol-2-yl carbamate) is the major metabolite of benomyl [methyl-1-(butylcarbamoyl)benzimidazol-2-yl-carbamate]. Both compounds are very effective systemic fungicides against a wide range of fungi affecting fruits, nuts, vegetables, cereals and grapes [1].

Methods employed for the determination of carbendazim and benomyl in different matrices usually involve the use of chromatographic techniques. Numerous procedures are based on the use of liquid chromatography (LC), in reversed-phase [2], cation-exchange [3] and ion-pair [4] modes. On-line pre-concentration [5] has been applied to the preparation of samples and different detection systems, including mass spectrometry [6] have been used.

Correspondence to: M. de la Guardia, Department of Analytical Chemistry, University of Valencia, C/Dr. Moliner 50, 46100-Burjassot, Valencia (Spain).

Gas chromatography has been applied to the determination of carbendazim and related compounds using different derivatization procedures with diazomethane and diazoethane [7], trimethylanilinium chloride [8] and pentafluorobenzoyl chloride [9]. Thin-layer chromatography has been employed for the determination of carbendazim, usually combined with fluorimetric detection [10] or visual comparison [11].

Spectrophotometric methods are less commonly employed for the determination of carbendazim residues than chromatographic methods [12] but there are a few examples of the use of colorimetric [13] procedures, using chromotropic acid, derivative spectroscopy [14], isodifferential derivative spectroscopy [15], infrared spectrometry [16] and room temperature phosphorimetry [17]. Other techniques, such as classical polarography [18], voltammetry [19], enzyme-linked immunosorbent assay (ELISA) [20] and immunoassay [21] have also been employed for the determination of carbendazim and benomyl.

SSDI 0003-2670(93)E0574-Q

Only one precedent of the direct spectrofluorimetric determination of carbendazim in acidic media [22] was found, which has been applied to the determination of this compound in pesticide formulations. The aim of this work was to develop micellar enhanced procedures for the direct fluorimetric determination of benomyl and carbendazim in water samples.

Micelles are organized structures, created by the self-association of surfactant monomers, and it is well known that, in the micellar microenvironment, the fluorescence quantum yield of different molecules can be enhanced [23–28]. On the other hand, recent studies have indicated that micellar media improve analytical measurements carried out in flow systems [29] and also that flow-injection analysis (FIA) concepts provide a versatile tool for the study of the micellar interactions [30]. In this work, the micellar enhanced fluorimetric determination of carbendazim in natural waters was carried out with the use of flow injection.

EXPERIMENTAL

Apparatus

A Perkin-Elmer LS 50 luminescence spectrophotometer, equipped with a quartz flow cell of 1-cm path length and 280-μl internal volume, was employed for fluorescence measurements. A Perkin-Elmer Lambda 3 spectrophotometer and a Hewlett-Packward HP8452A diode-array spectrophotometer, equipped with a quartz of flow cell of 1-cm path length and 70-μl internal volume, were employed for absorbance measurements.

The FIA manifolds employed for the study of the interaction between pesticides and micelles and also for the fluorimetric determination of carbendazim in micellar media were similar than those employed in previous studies [28,30]. A single-channel assembly equipped with a Rheodyne Model 50 injection valve and a well stirred mixing chamber made of PTFE (with an internal volume of 790 μl) was employed to study the interaction between micelles and fluorescent molecules, as described previously [30]. In this manifold the use of a flexible vinyl tube of 2.96 mm i.d. provides a carrier flow-rate of 10.5 ml min^{-1}. All the other tubes employed in the manifold were made of PTFE of 0.8 mm i.d.

A three-channel manifold was employed for the fluorimetric determination of benomyl and its derivatives. Samples and standard solutions were injected by using a Rheodyne Model 50 injection valve with a water carrier flow-rate of 4.4 ml min^{-1}. Different buffer solutions were introduced by means of a second channel, using a carrier flow-rate of 4.2 ml min^{-1}. Both channels were joint by using a Y-shaped merging zone. Micellar solutions, at carrier flow-rates of the order of 11.2 ml min^{-1}, were introduced by a third channel and merged with the above-mentioned solutions by using a T-shaped merging zone before the measurement zone.

Reagents

Benomyl was supplied by Afrasa (Valencia) and carbendazim and other metabolites were obtained by means of the alkaline hydrolysis of benomyl. Cetyltrimethylammonium bromide (CTAB) was supplied by Merck (Darmstadt) and sodium dodecyl sulphate (SDS) by Fluka (Buchs). Other common reagents, such as NaOH, HCl, KH_2PO_4 and Na_2HPO_4, were supplied by Panreac (Barcelona).

General procedure

To study the effect of pH on the absorbance and fluorescence of carbendazim, and also for the determination of pK values, measurements were carried out in the batch mode with 8×10^{-6} M standard solutions prepared at different pH values.

The effect of surfactant concentration on the micellar enhancement of the carbendazim fluorescence was established by two procedures. In the first procedure an FIA manifold was used, equipped with a well stirred dilution chamber in which 500 μl of a solution containing 1% (w/v) surfactant and 2.6×10^{-6} M carbendazim were injected into a carrier solution of 2.6×10^{-6} M carbendazim. The FIA recording obtained, from the dispersion of the surfactant solution in the manifold, was obtained by measuring the fluores-

cence at the corresponding excitation and emission wavelengths of carbendazim. This recording provided the effect of decreasing concentration of surfactant on the fluorescence of carbendazim. In the second procedure, a series of batch measurements were carried out for solutions with different surfactant concentrations, prepared in the presence of a fixed concentration of carbendazim.

The determination of carbendazim in water samples was carried out using the three-channel FIA manifold without any pretreatment of the samples, by injecting 500 μl of sample or standard aqueous solution of carbendazim (from 5.2×10^{-7} to 26.2×10^{-7} M) into a water carrier stream, using the carrier flow-rates indicated above and the buffer and micelle concentrations appropriate for each of the systems studied.

RESULTS AND DISCUSSION

Hydrolysis of benomyl and carbendazim

The hydrolysis of benomyl (**I**) provides carbendazim (**II**) and the latter product could also be hydrolysed to 2-aminobenzimidazole (**III**):

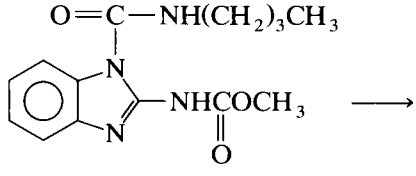

(I)

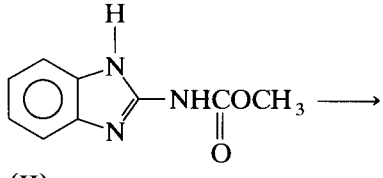

(II)

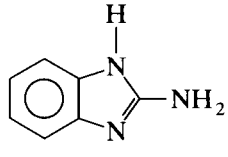

(III)

Attempts were made to carry out a study of benomyl hydrolysis, but measurements carried out in the stopped-flow mode indicated that the product degrades very rapidly to carbendazim. This process takes place in both acidic and basic media. Hence in general it is very difficult to find residues of benomyl in polluted water.

Carbendazim, the major metabolite of benomyl, is very stable in acidic and neutral conditions and it is only slowly hydrolysed in alkaline media, several days being necessary for complete hydrolysis at room temperature. For this reason, this study was focused on the developement of a fluorescence-enhanced procedure for the determination of carbendazim.

Effect of pH on the absorbance and fluorescence of carbendazim

Figure 1A and B show that the absorbance spectra of carbendazim changes strongly with pH and that three chemical forms can be identified as a function of this parameter.

A series of experiments were carried out in order to determine the pK values of carbendazim by measuring the variation of the absorbance at different wavelengths as a function of pH (Fig. 1C) and, from these measurements, values of 4.33 ± 0.05 and 10.8 ± 0.3 were established for pK_1 and pK_2 respectively. These values limit the different working zones in which the fluorescence of each chemical form of carbendazim can be evaluated.

With excitation at the maximum absorbance wavelength of carbendazim, in each of the three media considered, the fluorescence spectra in Fig. 2 were obtained and, as can be seen, the highest emission wavelength corresponds to the use of an excitation wavelength of 282 nm and an emission wavelength of 380 nm in 0.1 M HCl. On the other hand, when working in an alkaline medium, better sensitivity can be obtained at 310 nm. However, these measurements are strongly affected by the blank values.

Effect of surfactants on the absorbance and fluorescence of carbendazim

The effects of a cationic surfactant, CTAB, and an anionic surfactant, SDS, on the absorbance and fluorescence of carbendazim were studied. Other kinds of surfactant, such as

nonylphenols, and *tert*-octylphenols, which contains aromatic groups, cannot be used to improve the fluorescence measurements because they have a high residual fluorescence when short excitation wavelengths are used. Also, good results could not be obtained by using ethoxylated alcohols or ethylene oxide–propylene oxide condensates, because both types of compounds provide high blank values.

There were no significant shifts in the absorbance spectra of carbendazim in the micellar media at different pH values except in the presence of CTAB at basic pH, in which case a bathochromic shift of less than 20 nm was ob-

TABLE 1

Micellar enhancement factors obtained for the fluorimetric determination of carbendazim in different media

Medium [a]	λ(exc) (nm)	λ(nm) (nm)	MEF
0.1 M HCl	283	380	–
SDS–HCl	283	368	2.6
Neutral	288	308	–
1% (w/v) SDS	289	308	1.7
0.1% (w/v) CTAB	289	309	1.6
0.1 M NaOH	287	317	–
CTAB–NaOH	306	327	11.6

[a] SDS = sodium dodecyl sulphate; CTAB = cetyltrimethylammonium bromide.

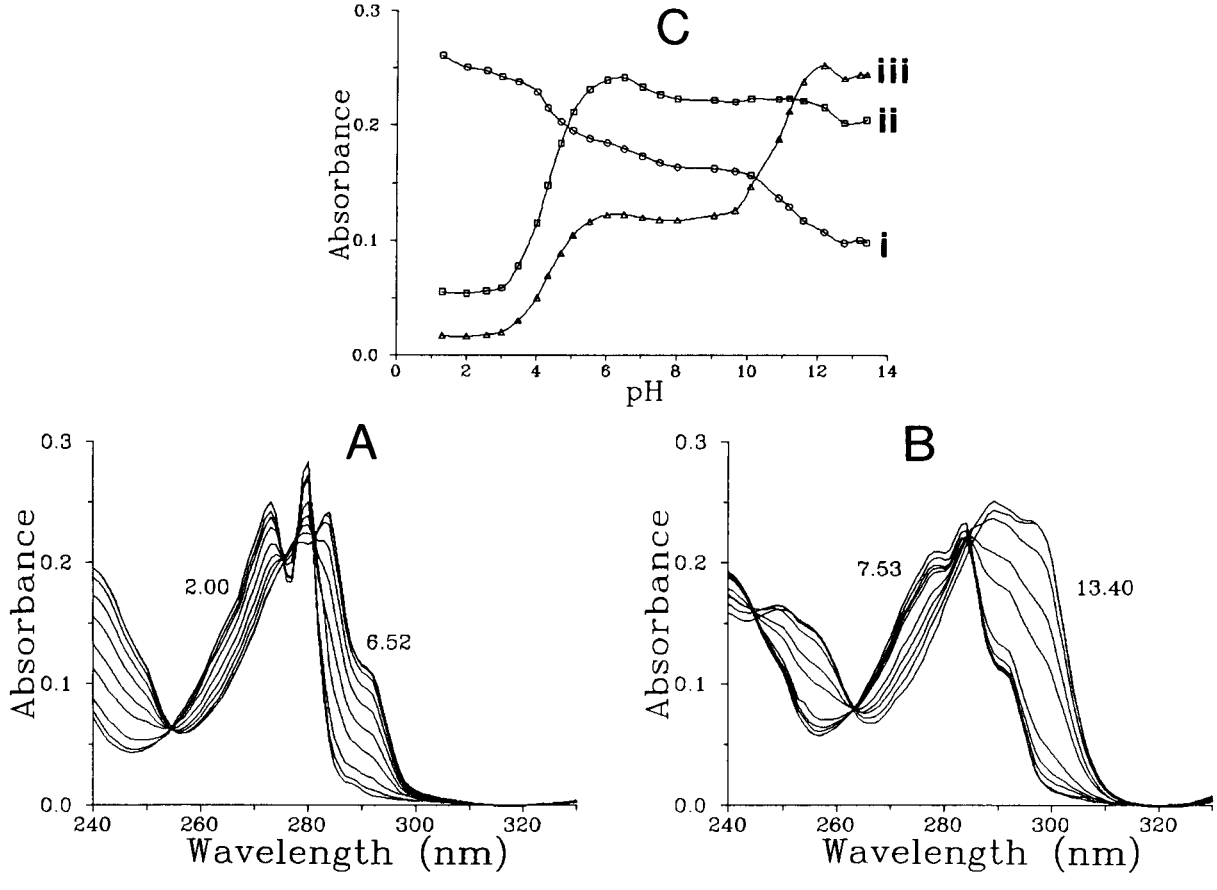

Fig. 1. Absorbance of carbendazim as a function of pH. (A) Absorbance spectra of carbendazim at different acid pH values: 2.00, 3.01, 3.49, 4.02, 4.33, 4.70, 5.05, 5.52, 6.02 and 6.52. (B) Absorbance spectra of carbendazim at different alkaline pH values: 7.53, 7.76, 9.07, 9.66, 10.11, 10.90, 11.20, 11.60, 12.19 and 13.40. (C) Absorbance of carbendazim at differents wavelengths versus pH: (i) 273; (ii) 284; (iii) 289 nm.

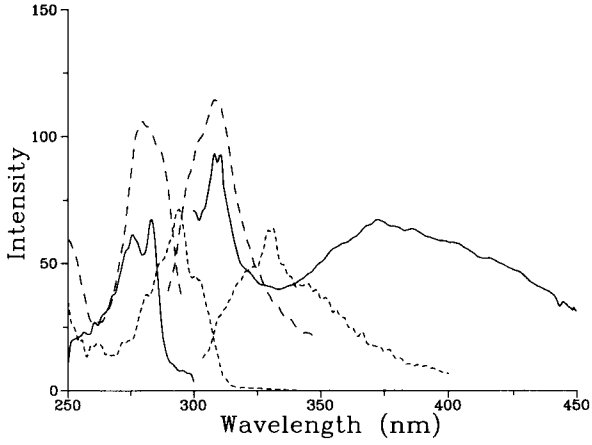

Fig. 2. Excitation and emission spectra of 3.6×10^{-6} M carbendazim solution: solid lines, in 0.1 M HCl; short dashed lines, in neutral media; long dashed lines, in 0.1 M NaOH.

served. However, the surfactants studied significantly affected the fluorescence of the different protonated forms of carbendazim.

Table 1 summarizes the values of the micellar enhancement factors (MEF) obtained in each instance, and it can be seen that in acidic media (Fig. 3A) SDS provides a ca. threefold increase in the fluorescence of carbendazim, at neutral pH (Fig. 3B) CTAB and SDS increase the fluorescence of carbendazim slightly and in basic media (Fig. 3C) CTAB provides a large enhancement of the carbendazim fluorescence.

Effect of surfactant concentration on the fluorescence of carbendazim

The effect of increasing concentration of each of the surfactants considered, CTAB and SDS,

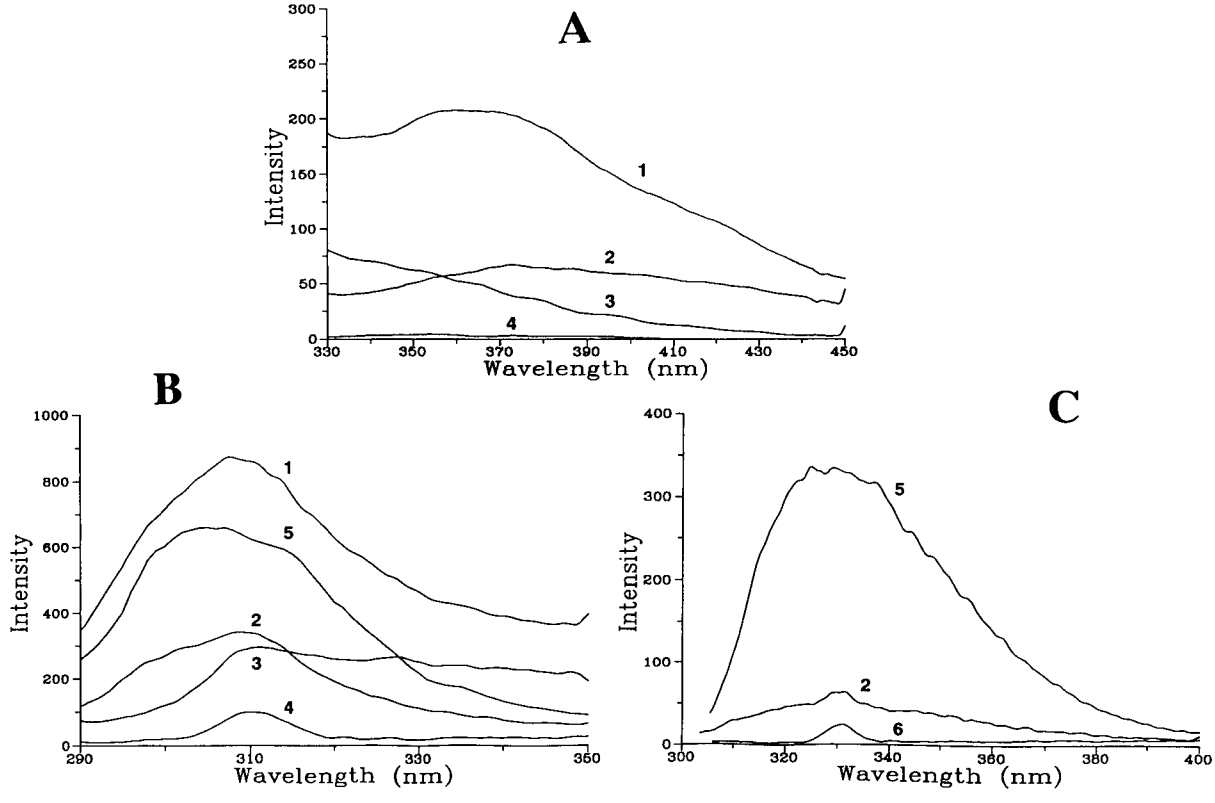

Fig. 3. Effect of ionic surfactants on the absorbance of carbendazim, (A) in 0.1 M HCl, (B) at neutral pH and (C) in 0.1 M NaOH. The different emission spectra correspond to the following solutions in the different media assayed: (1) 3.4×10^{-6} M carbendazim in 1% (w/v) SDS; (2) 3.4×10^{-6} M carbendazim; (3) 1% (w/v) SDS; (4) water blank; (5) 3.4×10^{-6} M carbendazim in 0.1% (w/v) CTAB; (6) 0.1% (w/v) CTAB.

on the fluorescence of carbendazim was studied at the pH at which the highest fluorescence enhancements were found.

Figure 4 shows, as an example, the effect of SDS concentration on the fluorescence of carbendazim in 0.1 M HCl. Results obtained by studying this effect in both the batch and flow-injection modes are reported and, as can be seen, a concentration of surfactant $\geqslant 0.5\%$ (w/v) provides a threefold sensitivity enhancement. The inset in Fig. 4B shows the FIA recordings obtained for (a) the dispersion of an HCl solution of carbendazim in a carrier flow of 0.1 M HCl and (b) for the dispersion of a carbendazim solution in concentrated SDS into a carrier flow with the same concentration of carbendazim. The presence of SDS enhances the fluorimetric measurements carried out at the typical excitation and emission wavelengths of carbendazim.

For the interaction between carbendazim and CTAB in 0.1 M NaOH, the maximum fluorescence enhancement was found for CTAB concentrations $\geqslant 0.1\%$ (w/v) and also in this instance the results obtained in the batch and flow modes are comparable.

Effect of FIA parameters

In order to develop a flow-injection procedure that simplifies the sample preparation and increases the speed of the determinations, the effects of the main FIA parameters, such as the injected sample volume and the flow-rate, on the sensitivity of the fluorescence measurements of carbendazim were studied. Other parameters, such as the coil length, were fixed at the minimum values possible in order to avoid the sample dispersion in the manifold, because the developed FIA procedure does not involve any reaction and the only objective is to change the medium by introducing organized assemblies.

Figure 5 shows, as an example, the FIA recordings obtained for different sample injection volumes of carbendazim in SDS–acid medium and using a carrier flow-rate of 4.1 ml min^{-1}. An injection volume of 500 μl provides a compromise between the maximum peak height and the

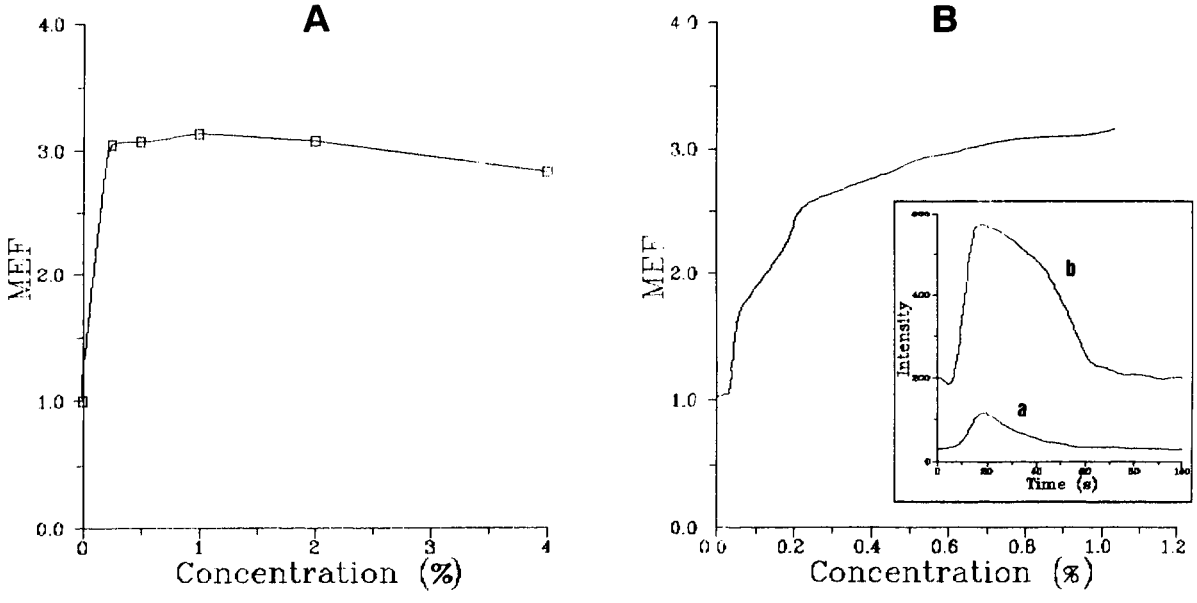

Fig. 4. Effect of the SDS concentration on the fluorescence of carbendazim in 0.1 M HCl. (A) Micellar enhancement factors (MEF) obtained by batch measurements. (B) MEF values obtained by carrying out measurements in the FIA mode. Inset: dispersion profiles obtained for the injection of (a) carbendazim in HCl and (b) an SDS solution containing carbendazim in a carrier stream with the same concentration of the pesticide.

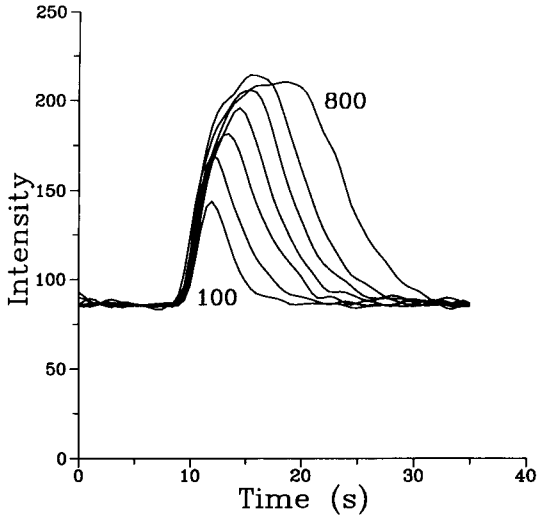

Fig. 5. Effect of the injection volume on the FIA recording obtained for 3.4×10^{-6} M carbendazim solution in 0.1M HCl in the presence of 1% (w/v) SDS. Injection volumes: 100, 200, 300, 400, 500, 600 and 800 μl.

minimun peak width. Additional increases in the injection volume do not increase the peak height significantly and only affect the width of the FIA recording, thus reducing the sample throughout.

Concerning the effect of the carrier flow-rate, it was observed that, for a total carrier flow-rate between 4 and 20 ml min^{-1}, the height of the FIA peaks remains virtually unchanged and only the peak width increases when the carrier flow-rate decreases. Therefore, in order to obtain a good sample throughput, a total carrier flow-rate of the order of 20 ml min^{-1} is recommended. To obtain this flow-rate, and taking into account the use of a three-channel assembly, a value of ca. 4 ml min^{-1} for two of these channels and ca. 11 ml min^{-1} for the third channel were selected to avoid problems in the merging zones.

Analytical features of the procedure

From the experiments carried out it can be concluded that the addition of SDS to samples containing carbendazim in 0.1 M HCl or, alternatively, the addition of CTAB to carbendazim samples in 0.1 M NaOH provides a significant enhancement of the fluorescence measurements. On the other hand, the use of a flow manifold to change the environment of carbendazim molecules and to provide the introduction of micelles can reduce other interactions that could affect the selectivity of the measurements.

Under the optimum experimental conditions, found previously, the calibration graphs for carbendazim, in both acidic and alkaline media and in the presence of SDS and CTAB, respectively, were obtained. Table 2 gives the typical equations obtained and other analytical figures of merit, such as the sensitivity, expressed as the slope of the calibration line, the limit of detection, obtained for 3σ (a probability level of 99.6%), and the relative standard deviation obtained for five independent measurements of a 2×10^{-6} M carbendazim standard solution. All of the calibration lines were obtained without correcting the blank measurements and therefore the intercept values are more or less different from zero, depending

TABLE 2

Analytical parameters of the fluorimetric determination of carbendazim in different media [a]

Medium	Calibration line	r	LOD	R.S.D. (%)
0.1 M HCl	$I_f = 10.1 + 46.9C$	0.998	7×10^{-8}(20)	2.8
SDS–HCl	$I_f = 90.4 + 123.1C$	0.9997	1.1×10^{-7}(32)	2.2
Water	$I_f = 14.2 + 72.0C$	0.9990	1×10^{-7}(28)	0.9
1% (w/v) SDS	$I_f = 74.2 + 124.6C$	0.9992	8×10^{-8}(22)	1.8
0.2% (w/v) CTAB	$I_f = 23.2 + 115.5C$	0.9993	4×10^{-8}(11)	2.2
0.1 M NaOH	$I_f = 78.3 + 25.7C$	0.997	3×10^{-7}(88)	5.4
CTAB–NaOH	$I_f = 10.3 + 297.6C$	0.9999	1.3×10^{-8}(4)	0.5

[a] Concentrations (C) in 10^6 mol l^{-1}. Repeatability values were obtained from the relative standard deviation (R.S.D.) of five independent measurements of a solution containing 2.07×10^{-6} M carbendazim. I_f = relative fluorescence in emission units; r = regression coefficient. LOD = limit of detection (3σ) (mol l^{-1}). Values in parentheses correspond to the LOD expressed in μg l^{-1} of carbendazim.

on the residual fluorescence of the reagents employed.

From the analytical features of the developed procedures, it can be concluded that, compared with the direct fluorimetric determination of carbendazim, the determination in CTAB provides an 11.6-fold enhancement in sensitivity, making it possible to obtain a limit of detection of 1.3×10^{-8} M, and that the use of SDS in 0.1 M HCl provides a sensitivity 2.6 times greater than that found in aqueous solution with a limit of detection of 1×10^{-7} M. On the other hand, both procedures provide a sample throughput of the order of 160 injections per hour.

Recovery of carbendazim in real water samples

Six synthetic samples were prepared by adding differents volumes of a stock solution of carbendazim to three different types of natural waters, then the samples were injected into the FIA manifold, carrying out the fluorescence measurements in 0.1 M HCl and in the presence of SDS with an excitation wavelength of 283 nm and an emission wavelength of 380 nm. Measurements in 0.1 M NaOH, in the presence of CTAB, were carried out with an excitation wavelength of 306 nm and an emission wavelength of 327 nm. The data in Table 3 indicate that the recovery of carbendazim varies from 94 to 107%, hence in all instances good results were obtained for the direct determination of carbendazim in the presence of all types of sample matrices assayed.

Additional experiments on the recovery of 1×10^{-6} M carbendazim added to polluted waters containing 0.8×10^{-6} M of the pesticide gave recoveries values of 102.9% in the presence of SDS and 99.3% in CTAB.

Mechanism of fluorescence enhancement of carbendazim in the presence of micelles

It is not surprising that, according to the Hartley rules, the protonated form of carbendazim ($pK_1 = 4.33$), positively charged, could interact with the anionic surfactant SDS at a pH of the medium corresponding to 0.1 M HCl. On the other hand, when the pH is very high (0.1 M NaOH), the carbendazim molecules remain deprotonated ($pK_2 = 10.8$) and so these anionic molecules could interact strongly with CTAB micelles.

The critical micelle concentration (c.m.c.) values of both surfactants were established by carrying out measurements of the surface tension of solutions with different surfactant concentrations. The c.m.c. of CTAB obtained in 0.1 M NaOH and in the presence of 2×10^{-6} M carbendazim corresponds to 0.04% (w/v) (1.1×10^{-3} M), which is higher than that obtained in pure water, 0.01% (w/v) (2.7×10^{-4} M), indicating the effect of the medium on the surfactant aggregation process. For SDS, the c.m.c. value found in 0.1 M HCl corresponds to 0.033% (w/v) (1.1×10^{-3} M), which is clearly different to that found in pure water, 0.2% (w/v) (6.9×10^{-3} M), thus indicating the strong influence of the medium on the micellation. The above c.m.c. values are clearly lower than the surfactant concentration required to obtain the best fluorescence enhancement (see

TABLE 3

Recovery of carbendazim in the FIA–fluorimetric analysis of spiked water samples by using different micellar media

Water matrix	Added (10^{-6} mol l^{-1})	In SDS–0.1 M HCl			In CTAB–0.1 M NaOH		
		Found [a] (10^{-6} mol l^{-1})	R.S.D. (%)	Recovery (%)	Found [a] (10^{-6} mol l^{-1})	R.S.D. (%)	Recovery (%)
Cistern	0.69	0.66 ± 0.03	0.4	95	0.668 ± 0.007	1	97
Cistern	1.38	1.47 ± 0.02	1	107	1.32 ± 0.01	0.7	96
Cistern	2.07	2.05 ± 0.04	1	99	1.95 ± 0.01	0.5	94
Irrigation	1.38	1.40 ± 0.03	2	102	1.40 ± 0.02	1	102
Irrigation	2.76	2.86 ± 0.04	2	104	2.72 ± 0.02	0.7	99
Well	1.38	1.33 ± 0.04	3	97	1.33 ± 0.01	0.7	97

[a] Values found are the average of three independent analyses of each spiked sample, ± standard derivation.

Fig. 4 as an example), indicating the micellar nature of the fluorescence enhancement.

Hence the analytical advantages obtained for the fluorescence determination of carbendazim in micellar media are related to the electrostatic interaction between the protonated or deprotonated molecules of carbendazim and micelles of opposite charge formed by the self-aggregation of ionic surfactant molecules.

Conclusions

The use of micellar media in the FIA–fluorimetric determination of carbendazim provides a sensitivity enhancement of these determinations and also permits direct analysis of water samples to be carried out without the need for long previous clean-up steps. The developed procedure, in the presence of CTAB micelles, provides a high sensitivity and a very low limit of detection. On the other hand, the fluorimetric determination in the presence of SDS micelles increases the sensitivity but does not improve the limit of detection owing to the high background values obtained for micellar solutions. However, the fact that these latter measurements can be carried out in 0.1 M HCl improves the applicability of the procedure and, for example, recoveries of the order of 104% were found in the determination of carbendazim at the 0.26 mg l^{-1} level in highly polluted water samples from near a river bank.

REFERENCES

1 H. Martin and C.R. Worthing, Pesticide Manual, British Crop Protection Council, Worcestershire, 5th edn., 1977.
2 G. Zweig and R.Y. Gao, Anal. Chem., 55 (1983) 1448.
3 T.D. Spitler, R.A. Marafioti and L.M. Lahr, J. Chromatogr., 317 (1984) 527.
4 D.M. Gilvydis and S.M. Walters, J. Assoc. Off. Anal. Chem., 73 (1990) 735.
5 C.H. Marvin, I.D. Brindle, R.P. Singh, C.D. Hall and M. Chiba, J. Chromatogr., 518 (1990) 242.
6 C.H. Liu, G.C. Mattern, X. Yu and J.D. Rosen, J. Agric. Food. Chem., 38 (1990) 176.
7 H. Steinwandter, Fresenius' Z. Anal. Chem., 321 (1985) 599.
8 L. Ogierman, J. Chromatogr. Sci., 19 (1981) 519.
9 S. Cline, A. Felsot and L. Wie, J. Agric. Food Chem., 29 (1981) 1087.
10 M. Baldi, G. Angiuli, A. Bovolenta and L. Zanoni, Riv. Soc. Ital. Aliment, 9 (1980) 103.
11 R. Engst and W. Schnaak, Nährung, 23 (1977) 701.
12 A. Monico-Pifarre and M. Xirau-Vayreda, J. Assoc. Off. Anal. Chem., 73 (1990) 553.
13 J.R. Rangaswamy, Y.N. Vijayashankar and S.R. Prakash, J. Food Sci. Technol., 24 (1927) 309.
14 G. Milch and E. Szabo, Acta Phys. Hung., 63 (1988) 165.
15 F. Garcia Sanchez and C. Cruces Blanco, Anal. Chem., 60 (1988) 323.
16 G. Meszlenyi, J. Kortvelyessy, E. Juhasz and M. Lelkes, Analyst, 115 (1990) 1491.
17 J.J. Vannelli and E.M. Schulman, Anal. Chem., 56 (1984) 1030.
18 Z. Xu, Y. Feng, Z. He and Y. Hou, Fenxi Huaxue, 11 (1983) 63.
19 V.N. Kavetskii and G.G. Andrienko, Zh. Anal. Khim., 41 (1986) 168.
20 W.H. Newsome and P.G. Collins, J. Assoc. Off. Anal. Chem., 70 (1987) 1025.
21 R.J. Bushway, S.A. Savage and B.S. Ferguson, Food Chem., 35 (1990) 51.
22 X. Jiang and M. Ding, Fenxi Huaxue, 17 (1989) 823.
23 C. Tanford, The Hydrophobic Effect, Wiley, New York, 1973.
24 W.L. Hinze, in K.L. Mittal (Ed.), Solution Chemistry of Surfactants, Vol. 1, Plenum, New York, 1979, p. 79.
25 E. Pelizzetti and E. Pramauro, Anal. Chim. Acta, 169 (1985) 1.
26 W.L. Hinze, H.N. Singh, Y. Baba and N.G. Harvey, Trends Anal. Chem., 3 (1984) 193.
27 J. Sancenón and M. de la Guardia, Fresenius' J. Anal. Chem., 336 (1990) 389.
28 J. Sancenón and M. de la Guardia, Quim. Anal., 4 (1992) 251.
29 B. Moreno, J.G. Perez-Paron and J. Hernandez-Méndez, Quím. Anal., 8 (1989) 23.
30 M. de la Guardia and E. Peris-Cardells, Anal. Chim. Acta, 256 (1992) 225.

Analytica Chimica Acta, 287 (1994) 59–64
Elsevier Science B.V., Amsterdam

Flow-injection analysis for total cholesterol with photometric detection

Achim Krug, Roman Göbel and Robert Kellner

Institute of Analytical Chemistry, University of Technology Vienna, Getreidemarkt 9 / 151, 1060 Vienna (Austria)

(Received 15th February 1993)

Abstract

The level of total cholesterol in human blood serum samples is determined by flow-injection analysis. A 70-μl sample is injected into a phosphate buffer stream, pH 7.0, and led through an enzymatic reactor, which contains cholesterol esterase and cholesterol oxidase immobilized on controlled pore glass. The enzymatically released hydrogen peroxide is detected with 2,2′-azinobis(3-ethylbenzthiazoline-6-sulfonate) in a peroxidase catalyzed reaction. A linear calibration is obtained in the clinically important range from 0.11 to 8.6 mmol l^{-1}. The indicator system is compared to the commonly used aminoantipyrine–phenol reagent. The potential interferents studied include bilirubin, triglycerides, haemolyzed serum, glucose, urea, uric acid, and citric acid. The accuracy of the method is established by comparison with a clinically established method based on spectrophotometric endpoint evaluation.

Keywords: Flow injection; Enzymatic methods; Spectrophotometry; Cholesterol; Serum

The determination of total cholesterol is an important task in today's clinical analysis. This is related to the context of the cholesterol level in serum and the frequency of cardiovascular diseases. The modern clinical laboratory has to carry out an increasing number of routine assays with the growing knowledge about lipid metabolism. For a fast screening of patients with a high risk of coronary heart disease the analytes triglycerides, total cholesterol and high density lipoprotein (HDL)-cholesterol are usually determined.

The standard method for clinical cholesterol assay is time and reagent consuming. It is based on the enzymatic degradation of cholesteryl esters and cholesterol followed by a spectrophotometric endpoint detection of the released hydrogen peroxide with a suitable dye reaction. The objective of this research, therefore, is to develop a cholesterol assay based on flow-injection analysis (FIA) which will have a number of advantages such as high sample throughput, use of immobilized enzymes and minimum reagent consumption.

Two different FIA methods employing electrochemical detection have already been proposed for the determination of total cholesterol. Karube et al. [1] and Yao et al. [2,3] coupled the enzyme reactors to an amperometric detector. The electrochemical approach, employing electrodes either in a sensing device or a flow system, has not yet reached the market, although considerable effort has been put into the development of enzyme electrodes for cholesterol [4]. Fernandez-Romero et al. [5] were the first to suggest several optical methods, including the stopped-flow mode, based on spectrophotometry or spectrofluorimetry. Recently 2,2′-azino-bis(3-ethylbenzthiazoline-6-sulfonate) (ABTS) has been used in a

Correspondence to: A. Krug, Institute of Analytical Chemistry, University of Technology Vienna, Getreidemarkt 9/151, 1060 Vienna (Austria).

SSDI 0003-2670(93)E0586-V

FIA procedure with a fiber optic detection cell [6]. Biosensing of total cholesterol has also been achieved with a split-flow enzyme thermistor [7].

There are several spectrophotometric methods for hydrogen peroxide employing, for example ABTS, 3-dimethylaminobenzoic acid (DMAB)–aminoantipyrine (AAP), or 3,5-dichloro-2-hydroxybenzene sulfonic acid (DCHBS)–AAP as chromogenic indicator systems. ABTS, one of the most effective known chromophores, was introduced by Kahle et al. [8], but has not been used extensively as a substrate for peroxidase-catalyzed reactions. This may have to do with its disadvantageous mechanism of dye formation. The ABTS reacts with hydrogen peroxide with the uptake of one electron to form a metastable radical cation, which undergoes slow disproportionation [9]. This is a complicating factor, when endpoint measurements are performed. Nevertheless, the disproportionation is too slow to affect initial rate studies [10,11], and it is shown here that no problems occur in a FIA system either, where the reaction time is controlled by the flow-rate of the solution and by the length of the manifold. DCHBS, which was introduced by Artiss et al. [12], and DMAB are among the most sensitive color yielding substrates which can be substituted for phenol in the oxidative coupling reaction with AAP and H_2O_2, and these are also briefly considered in this report.

EXPERIMENTAL

Materials

Cholesterol oxidase (COD) (E.C. 1.1.3.6) from *Brevibacterium* sp. with a specific activity of 6 U mg^{-1} was obtained from Scripps (San Diego, CA). Cholesterol, ABTS, DMAB, DCHBS and AAP were purchased from Sigma (Deisenhofen). Cholesterol esterase (CE) (E.C. 3.1.1.13) from pig pancreas with a specific activity of 43.7 U mg^{-1} material was obtained from Biozyme (Blaenavon), Precilip E.L. control serum was from Boehringer Mannheim (Vienna), horse radish peroxidase (POD) (E.C. 1.11.1.7) with an activity of 170 pyrogallol U mg^{-1} was from Merck (Darmstadt) and Triton X-100 was from Fluka (Buchs).

Aminopropyl-CPG (controlled pore glass) with 120/200 mesh size and a mean pore diameter of 127 nm was produced by CPG (Fairfield, NJ). All other chemicals were of analytical-reagent grade.

Immobilization of enzymes

100 mg aminopropyl-CPG were activated with 10 ml of a 2.5% solution of glutaraldehyde in 0.1 M phosphate buffer, pH 7.0, initially under reduced pressure to degas the pores of the beads. After carefully washing the CPG with buffer, the batch was divided into halves, to immobilize COD on one and CE on the other. The enzymes, 1.8 mg CE and 5.9 mg COD, were each dissolved in 2 ml of the phosphate buffer, the CPG was sus-

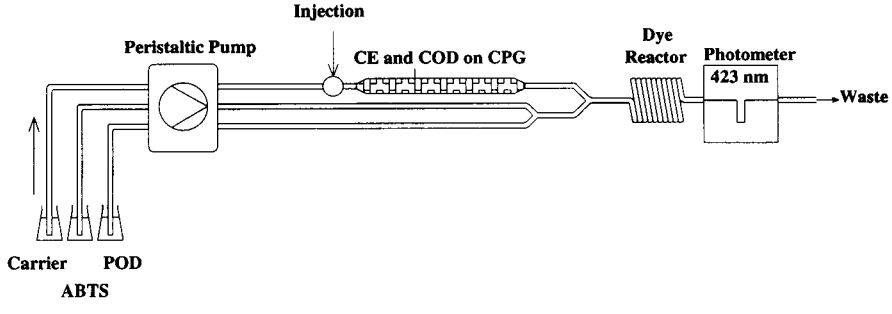

Fig. 1. FIA manifold with three channels.

pended in these solutions, and the mixtures were kept at 4°C for 24 h. Then the beads were washed with buffer and filled into the glass reactors sequentially.

Apparatus

A peristaltic pump PA-SF 5 from IKA (Staufen) was used to transport the liquids. The manifold was equipped with a low pressure PTFE injection valve 5020 from Rheodyne (Cotati, CA). A Hitachi Perkin-Elmer Model 124 spectrophotometer was fitted with a flow cell 178.010 QS from Hellma (Müllheim/Baden). All tubing had an inner diameter of 0.68 mm. The enzyme reactor consisted of a 105 × 1.5 mm i.d. glass capillary, 45 mm were filled with CE-CPG and 60 mm contained CPG with immobilized COD, so that the sample passed through the immobilized CE zone first.

The manifold consisted of a carrier stream and one or two reagent streams (Fig. 1). The reagents were not passed over the enzymatic reactors, because the leuco dyes are known to bind to enzymes and decrease the activity. The carrier as well as the solvent for the reagents consisted of a mixture of 0.1 M phosphate buffer, pH 7.0, 2-propanol and Triton X-100 in the ratio 83:13:4 (v/v/v). When measurements were performed over a period of several hours, ABTS and POD were kept in separate reservoirs and mixed shortly before merging with the carrier stream in the three-channel manifold to avoid autooxidation of the dye, which is also valid for the other color reagents employed. For measurements over a relatively short time, which is the case when the number of consecutive injections did not exceed 100, a two-channel configuration was used. The color reagents were mixed prior to the FIA run.

RESULTS AND DISCUSSION

Optimization of FIA manifold

The different parameter variations were carried out with aqueous cholesterol standards, which were prepared as described previously [11]. The enzymatic reactor used for these experiments was 80 mm long and contained immobilized COD only. Furthermore the sample volume was fixed at 70 μl, the optical path length of the flow cell was 10 mm and the absorption was measured at 423 nm.

Flow-rate, length of the coiled dye reactor and ABTS concentration were optimized using the univariate method. Three different POD concentrations (1, 5 and 10 U ml^{-1}) were tested in a preliminary study. It turned out that a concentration of 1 U ml^{-1} was too low to consume all of the generated hydrogen peroxide in a reasonable time interval. No difference was observed with both of the higher concentrations, which indicated completeness of the dye reaction. Therefore a POD concentration of 5 U ml^{-1} was chosen for all further experiments.

Several flow-rates in the range from 1.4 to 4.5 ml min^{-1} were run experimentally. At 3.0 ml min^{-1} 50 samples could be analyzed per hour. This flow-rate was used as standard. At flows below 2.0 ml min^{-1} the peak intensities were considerably greater, but large peak widths of approximately 2 min were obtained which severely decreased the sample throughput frequency. However, owing to a prolonged residence time of the sample in the enzymatic reactor, a lower detection limit can be reached with smaller flow rate. Since the clinical range of interest for cholesterol is ca. 5 mmol l^{-1}, the manifold was operated with a relatively high flow-rate.

In the next step the ABTS concentration was varied. The results are shown in Fig. 2. Below a certain dye concentration the hydrogen peroxide

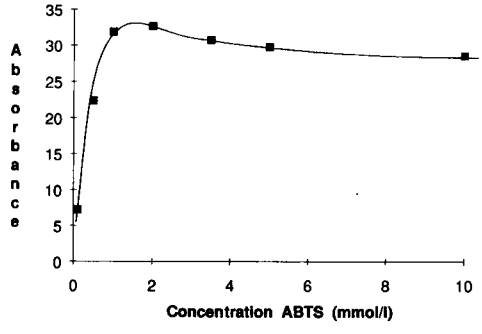

Fig. 2. Influence of the ABTS concentration on peak height absorbance ($\times 10^3$); flow-rate, 3 ml min^{-1}; 4 mmol l^{-1} cholesterol.

TABLE 1

Comparison of chromogenic substrates

Chromogenic system (conc.)	Wave-length (nm)	Calibration $slope_{(rel)}$ [a]
Phenol (3.3 mM)–AAP (3.3 mM)	500	1
DMAB (3.3 mM)–AAP (3.3 mM)	553	4.04
DCHBS (3.3 mM)–AAP (3.3 mM)	510	4.94
ABTS (1.3 mM)	423	6.09

[a] Relative to phenol–AAP chromogenic substrate.

is not consumed completely. At higher concentrations the ABTS radicals can react with excess of the dye, which yields a compound with different absorption characteristics. Therefore the signal decreases slightly with increased ABTS concentration. To measure cholesterol levels up to 12 mmol l^{-1} a minimum concentration of 3.5 mmol l^{-1} ABTS is recommended.

By varying the length of the coiled dye reactor it was established that the optimum length of the manifold is 800 mm. If the reactor is too short the color reaction is incomplete. If the reactor is too long dispersion causes peak broadening and in case of using ABTS as reagent the radicals formed decompose with time.

Study of chromogenic substrates and interfering species

For a comparison of leucodye substrates an FIA manifold with two channels was chosen. The substrates and the catalyst POD were mixed shortly before the measurements were carried out. The enzyme reactor had a length of 75 mm, 3 mg CE and 6 mg COD were co-immobilized statistically on 50 mg CPG, and the flow was adjusted to 2.2 ml min^{-1}. Table 1 displays the concentration of the chromogenic reagents, the wavelength of maximum absorption and the relative slope of the calibration graph in comparison to the original Trinder reagent, phenol-AAP, which was employed by Fernandez-Romero et al. [5]. As can be deduced from this table, the three chromogenic reagents employed in this study all surpassed the original reagent by a factor 4–6 in terms of sensitivity. This results in several additional advantages, namely a decrease of the detection limit and greater sensitivity, so that smaller concentration differences can be distinguished. In consequence the enzyme reactor can be shortened or the flow-rate increased yet still obtaining the same absorbance as with the Trinder reagent, thus resulting in a higher sample throughput frequency.

The behaviour of various commonly considered interferents present in blood was examined. The 8.6 mM standard was diluted 1:1 with carrier, and the compounds in question were dissolved in that solution. The results, which are displayed in Table 2, correspond to the measurements with ABTS as the chromogenic substrate. Triglyceride levels higher than 5 mmol l^{-1} gave a positive interference, and strongly haemolyzed sera could not be analyzed. Bilirubin did not interfere even at a concentration more than tenfold higher than normal levels. This is also true for uric acid. The method can tolerate glucose and urea at two to three times their normal concentration, and citrate can be present in 100-fold excess. Also, up to the indicated values the interfering species did not interfere when DMAB–AAP nor DCHBS–AAP were used as dye substrates.

Calibration and measurement of total cholesterol

Precilip E.L. control serum with a certified value of 8.6 ± 1.5 mmol l^{-1} was used to prepare a

TABLE 2

Interference study

Interfering species	Triglycerides	Bilirubin	Urea	Uric acid	Glucose	Citrate
Reference range (mmol l^{-1}) [a]	1.6–2.2	0.003–0.017	1.7–7.8	0.13–0.42	3.9–6.7	ca. 0.1
No interference at ⩽ (mmol l^{-1})	5.2	0.03	20	5	10	10

[a] According to [13].

series of dilutions (8.6, 7.53, 6.45, 5.38, 4.3, 3.23, 2.15, 1.08 mmol l^{-1}). All samples and standards were diluted 1:9 (v/v) with carrier and injected in triplicate at ca. 50 h^{-1}. The calibration graph was linear in the range 0.1 to 0.86 mmol l^{-1} cholesterol. The equation of the calibration is given by peak height absorbance $= 0.11 \times$ [cholesterol] (mmol l^{-1}) $- 8.2 \times 10^{-4}$. The correlation coefficient (r) of the linear regression is > 0.99 ($n = 8$). The relative standard deviation for eight replicate measurements of a serum with a cholesterol level of 5.1 mmol l^{-1} was 2.5%.

The accuracy of the FIA method was proven by comparing it to an enzymatic standard method which utilizes the Trinder reaction [13]. Forty serum samples were analyzed over the range 4–12 mmol l^{-1}, and the results were plotted against the values obtained by the clinical method. The resulting linear plot is described through the linear equation $y = 1.04x - 0.23$ ($r = 0.981$), where the values on the y-axis represent the results obtained with the standard method, and the values on the x-axis result from the FIA measurements. A few samples with extremely elevated triglyceride levels gave erroneously high cholesterol values and could therefore not be analyzed directly. The problem was solved by further dilution of the samples with a surfactant containing buffer before analysis.

Conclusion

Although several methods for the determination of free [15–17] and total [1–3,5–7] cholesterol have been suggested in the literature, clinical laboratories seem not to be interested in flow-injection analysis. One of the reasons might be the initial attention paid to electrochemical detection. Besides the perceived disadvantages of electrodes, such as interference from electroactive compounds and electrical signals, drift of the electrode and need of a reference cell, routine laboratories hesitate to change from the long established principle of spectrophotometric detection. Probably every clinical laboratory is equipped with a spectrophotometer, therefore the possibility of spectrophotometric detection was studied in this work.

Table 3 summarizes the features of the FIA methods, which have been developed until now. A comparison reveals that the present method is superior to most of the other approaches regarding sample throughput rate and the lifetime of the enzyme reactor. One advantage is related to the enhancing and stabilizing effect of the surfactants on the enzymes. Triton X-100 is the most suitable compound in this respect. The majority of the cited work reports an optimum concentration of approximately 4% Triton X-100. However, Triton X-100 interferes in electrochemical detec-

TABLE 3

Overview of FIA methodology for the determination of cholesterol in clinical samples

Method/detection	Working range	R.S.D. (%)	Stability/lifetime [a]	Sample throughput rate (h^{-1})	Ref.
Amperometry	100–400 mg dl^{-1}	2	4 months/300 assays	12	1
Amperometry	3–300 mg dl^{-1}	1.5	4 months	40 (80) [b]	2
Amperometry	5 μM–5 mM	1.8	2 months	10	3
Spectrophotometry	26–776 μmol l^{-1}	1.66	> 300 samples	60	5
Fluorescence	5–265 μmol l^{-1}	2.48	> 300 samples	60	5
Fiber optic	0.5–8.0 mmol l^{-1}	2.5–5.2	3 weeks	30 (60)	6
Thermometry	50–400 mg dl^{-1}	1.5	1 month/750 assays	20	7
Amperometry	0–80 mg dl^{-1}	1.0–3.0	3 months	(80)	15
Amperometry	10 μM–1.035 mM	5	6 weeks	(24)	16
Chemiluminescence	0.5–24 mg dl^{-1}	–	3 months	(90)	17
Spectrophotometry	0.1–8.6 mmol l^{-1}	2.5	5 months/> 850 samples	50	[c]

[a] Normally stated for 90% of initial enzyme activity. [b] Values in parenthesis are for determination of free cholesterol. [c] Present method.

tion and fluorescence measurements are impossible due to its own fluorescence. Most of the previously presented methods require sample dilution owing to their working range. For convenience a method allowing injection of undiluted serum would be preferable. In the present manifold the samples normally were injected after ten-fold dilution. The calibration graph was still linear, however, when undiluted standards were injected. The direct analysis of undiluted sera resulted in higher deviations than when using diluted specimen, probably owing to the short contact time of serum and surfactant. The Triton X-100 plays an important role in solubilizing the cholesterol and its esters in micellar form, which is not complete in the direct injection mode.

Three chromogenic systems are suggested for the detection of the enzymatically released H_2O_2 in the assay of total cholesterol. All of them exhibit higher molar absorptivities than the commonly used phenol–AAP reagent. The interference study showed that reducing species, which compete for the H_2O_2 do not interfere in concentrations more than ten times their normal levels.

This work clearly proves the advantages of enzymatic FIA over the conventional clinical method. The outstanding capabilities of FIA are high sampling frequency and low reagent consumption. The cost per analysis is effectively decreased with the employment of immobilized enzymes. One enzymatic reactor was used for over 850 measurements in a period of 5 months and the observed loss in activity was only ca. 30%.

The developed method covers the clinically interesting range and its precision lies within the accepted limits suggested by the U.S. National Institute of Health [18]. Therefore it can readily be adopted in the clinical routine work. Especially for clinical laboratories with a small to medium sample throughput capacity or for laboratories with specialized tasks an FIA manifold would provide the ideal alternative between manually performed spectrophotometric assays and an elaborate segmented flow ananlyzer.

Dr. H. Regal and his co-workers are greatly acknowledged for providing human blood serum samples including their total cholesterol values assayed with the Celichrom cholesterol reagent, which is based on the Trinder reaction.

REFERENCES

1 I. Karube, K. Hara, H. Matsuoka and S. Suzuki, Anal. Chim. Acta, 139 (1982) 129.
2 T. Yao, M. Sato, Y. Kobayashi and T. Wasa, Anal. Biochem., 149 (1985) 387.
3 T. Yao and T. Wasa, Anal. Chim. Acta, 207 (1988) 319.
4 F. Scheller and F. Schubert, Biosensors (Techniques and Instrumentation in Analytical Chemistry, Vol. 11), Elsevier, Amsterdam, 1992.
5 J.M. Fernandez-Romero, M.D. Luque de Castro and M. Valcarcel, Clin. Chim. Acta, 167 (1987) 97.
6 A. Krug, A.A. Suleiman, G.G. Guilbault and R. Kellner, Enzyme Microb. Technol., 14 (1992) 313.
7 I. Satoh and N. Teramura, Sensors Actuators B, 5 (1991) 249.
8 K. Kahle, L. Weiss, M. Klarwein and O.Z. Wieland, Fresenius' J. Anal. Chem., 252 (1970) 228.
9 R.E. Childs and W.G. Bardsley, Biochem. J., 145 (1975) 93.
10 N. Majkic and I. Berkes, Clin. Chim. Acta, 80 (1977) 121.
11 A. Krug, A.A. Suleiman and G.G. Guilbault, Anal. Chim. Acta, 256 (1992) 263.
12 J.D. Artiss, R.J. Thibert, J.M. McIntosh and B. Zak, Microchem. J., 26 (1981) 487.
13 P. Trinder, Ann. Clin. Biochem., 6 (1969) 24.
14 N.W. Tietz, Fundamentals of Clinical Chemistry, Saunders, Philadelphia, PA, 3rd edn., 1987.
15 M. Masoom and A. Townshend, Anal. Chim. Acta, 174 (1985) 293.
16 G.J. Moody, G.S. Sanghera and J.D.R. Thomas, Analyst, 113 (1988) 1419.
17 B.A. Petersson, E.H. Hansen and J. Ruzicka, Anal. Lett., 19 (1986) 649.
18 US Department of Health and Human Services, Improving Cholesterol Measurement, National Institute of Health, Bethesda, MD, 1990.

Analytica Chimica Acta, 287 (1994) 65–73
Elsevier Science B.V., Amsterdam

Surface acoustic wave sensor system for the determination of total salt content in serum

Shouzhuo Yao

New Material Research Institute, Hunan University, Changsha 410082 (China)

Kang Chen, Fangnan Zhu, Dazhong Shen and Lihua Nie

Department of Chemistry and Chemical Engineering, Hunan University, Changsha 410082 (China)

(Received 15th March 1993; revised manuscript received 8th October 1993)

Abstract

A surface acoustic wave (SAW) sensor system was constructed by combining a SAW resonator with conductive electrodes. The responses of the SAW sensor system operating at 61 MHz were investigated for different electrolyte solutions and different capacitances in series. Comparisons of SAW devices and bulk acoustic wave (BAW) devices were also made. A frequency shift (ΔF)–electrolytic conductivity (κ) equation is presented as $\Delta F = a\kappa + b$, where a can be positive or negative depending on a series capacitor. The sensor was applied to the rapid determination of the total salt content in serum.

Keywords: Acoustic methods; Sensors; Salts; Serum; Surface acoustic wave sensor

Since Wohltjen and Dessy [1] first reported the use of surface acoustic wave (SAW) devices as chemical sensors in 1979, considerable attention has been devoted to this area [2–6]. SAW devices are most frequently used for the determination of low analyte concentrations in the gas phase, and the mechanisms of operation and design are now well established [7]. Although the application of SAW devices to liquid systems is of interest, Calabrese et al. [8] found there were still some difficulties because of the acoustic energy loss if the liquid layer on the sensor was more than a few acoustic wavelengths and the higher the frequency of the device, the greater was the energy loss.

Correspondence to: S. Yao, New Material Research Institute, Hunan University, Changsha 410082, China.

In this paper a novel application of the SAW device is reported. The application is based on the theory that only when the sum of the phase angles of a loop circuit containing resistive, capacitive and inductive elements in series with an amplifier and a SAW device is a multiple of 2π rad and the loop gain is greater than 1 will oscillation be generated and supported [4]. If any element in the circuit imparts a phase delay change, the oscillator frequency will change. By analysing the frequency shift much information can be obtained about the liquid system. This is called a non-mass effect.

This paper introduces a new sensor system combining conductive electrodes with a SAW device. Conductive electrodes were selected for this combination in order to avoid the disadvantages in the normal conductivity method and to improve the sensitivity by employing a SAW device.

SSDI 0003-2670(93)E0573-P

The polarization potential that seriously affects normal conductivity measurements with a highly concentrated background does not exist because of the high oscillation frequency of the SAW device and, as the SAW device is out of contact with the solution, the frequency of the sensor system depends only on the solution permittivity and the conductivity between the two electrodes. Additionally, the frequency stability of the sensor system is much better than that of a normal SAW sensor operated directly in the analyte vapour or gas because of the large energy dissipating from the SAW surface to polymer coatings. The life span of the SAW device is therefore greatly prolonged.

Most applications of SAW devices employ the delay line configuration. Grate and Klusty [9] investigated the use of a SAW resonator device as a vapour sensor and compared the SAW resonator with a SAW delay line device. They reported that the SAW resonator device has a lower noise level, lower insert loss, narrower bandwidths and higher Q values than the delay line device. In this paper, results are reported of an investigation of a 61-MHz SAW resonator applied in a new detection system, with emphasis on its frequency behaviour with respect to electrolyte solutions. The effect of a capacitor in series with the sensor system was also investigated. As an example of its application, the results of the determination of the total salt content in serum are presented.

EXPERIMENTAL

Apparatus and reagents

The 61-MHz one-port resonator used in this study was originally manufactured by Zhuzhou Electronic Factory (Hunan), with a y,z-cut $LiNbO_3$ crystal with aluminium metallization and mounted on round 2-pin-to-5 headers with epoxy and gold wire bonds. The aluminium interdigital transducers (IDTs) were 13000 Å in thickness. The resonator was designed with an acoustic aperture and a path length of several wavelengths. On the centre of each separate $LiNbO_3$ crystal chip there were 20 pairs of IDTs with 500 reflectors placed on each side of them. The nominal insertion loss of the resonator was 6.8 dB. The whole device was epoxied with a lid to seal it from the atmosphere.

A schematic diagram of the experimental set-up is shown in Fig. 1. C_1 and C_2 are parasitic

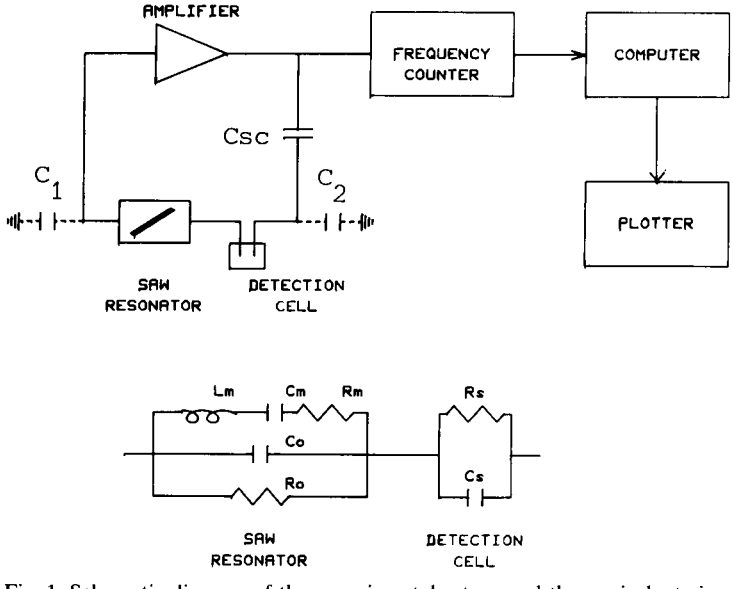

Fig. 1. Schematic diagram of the experimental set-up and the equivalent circuit of the SAW sensor system.

capacitances between the lead wires of the sensor system and the ground. The conductive electrodes were obtained from Elecoptic Device Factory (Shanghai) with cell constants near 1 cm and data presented in the paper are from this kind of conductive electrodes. The detection cell was suspended in a brass thermostated bath. The temperature was kept constant at 10°C by a Model CS501 thermostat (Laboratory Equipment Factory, Chongqin). The electrical connections between the sensor system and the oscillator board were kept as short as possible. A 12 V d.c. power supply was provided by an adjustable dual-track d.c. power supply. The frequency was measured by using a SC7201 Universal Counter at a resolution of 1 Hz and data were collected at 6 points min^{-1}.

All chemicals used were of analytical-reagent grade of 99% or greater purity. Solutions of KCl, NaCl, Na_2CO_3, $MgSO_4$ and $CaCl_2$ were prepared at precisely known concentrations near 100 mmol l^{-1}. Doubly distilled water was used throughout.

Procedure

The conductive electrodes were immersed in water stirred with a magnetic stirrer. During the experiments, the stirring speed was kept constant. A period of 30 min was needed to stabilize the whole set-up including the frequency counter and power supply. The baseline noise was determined by using frequency data collected for 5 min prior to the experiments. After the mean frequency (F_0) had been measured, 10 μl of standard electrolyte solution were injected into the water with a micro-injector. The frequency shift ($\Delta F = F_0 - F$) observed was hundreds to thousands of hertz and the response time, which mainly depends on the stirring speed, was less than 1 point (10 s). The procedure was carried out consecutively from dilute solution to more concentrated solution. The measurements were repeated for different electrolytes and the capacitor Csc was adjusted to different values (see Fig. 1).

Frequency shift vs. temperature experiments were conducted while monitoring the temperature of the detection cell and maintaining the oscillator board, including the SAW resonator, at 10°C. In most instances, temperatures were varied between 10 and 45°C at a rate of about 10°C h^{-1}. The frequency shifts were measured against temperature. Frequency shift vs. concentration experiments were also carried out at regular temperature intervals over the above period. These experiments were conducted as described. All experiments were reproducible regardless of the direction or rate of temperature change.

Serum samples obtained directly from a clinic without any pretreatment were centrifuged at 1000 rpm (500 *g*) for 10 min and the upper clear solutions were stored in a refrigerator at 4°C before use. In the determination of the total salt contents of serum samples, 0.21 ml of serum sample was diluted to 1 ml in the detection cell and tested directly according to the procedure described above for the frequency–concentration experiments. To confirm the results, standard addition experiments were also carried out with a micro-injector. The results for salt content in blood serum samples were also calculated from the linear regression equation based on former experiments.

RESULTS AND DISCUSSION

Frequency response of the SAW sensor system to electrolyte solutions

For an oscillation to be generated and supported in the oscillator of the SAW sensor system, the following two equations must be satisfied (the theory of this sensor system will be given in another paper [10]):

$$Re(A - g_0X_2) - Xe(1 + g_0X_2A) - (X_1 + X_2 + g_0X_1X_2A) = 0 \quad (1)$$

$$g_f = \frac{Re - g_0X_2(X_1 + Xe)}{X_1X_2} \quad (2)$$

where

$$X_1 = -1/(\omega C_1) \quad (3)$$

is the reactance of the parasitic capacitor C_1 and

$$X_2 = -1/(\omega C_2) \quad (4)$$

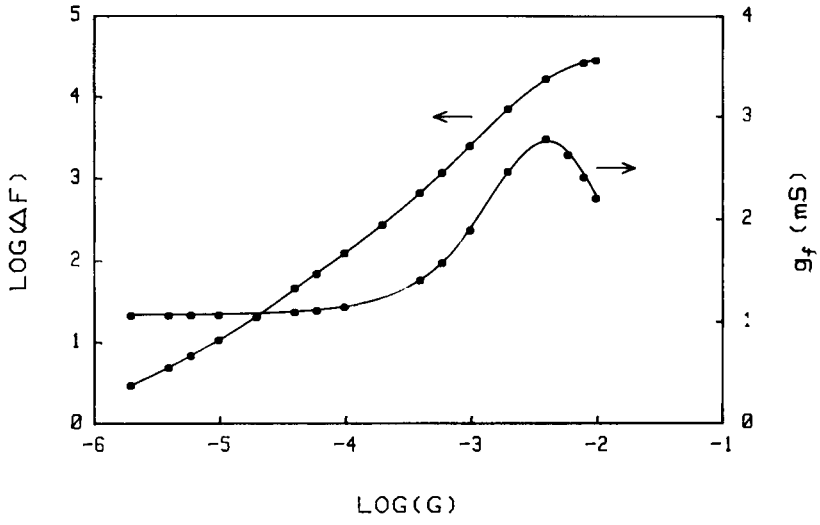

Fig. 2. Typical plots of frequency shift and transconductance as a function of solution conductivity.

that of C_2,

$$Re = G/\left[G^2 + (\omega C_s)^2\right] \quad (5)$$

$$Xe = \frac{-\omega C_s}{G^2 + (\omega C_s)^2} + \frac{\omega L_m - 1/(\omega C_m)}{1 + C_0/C_m - \omega^2 L_m C_0} \quad (6)$$

ω is the angular frequency (in rad s^{-1}), g_0 is the output conductance of the amplifier, C_m is the motional capacitance, L_m is the motional inductance, R_m is the motional resistance, R_0 is the radiation resistance and C_0 is the radiation capacitance of the SAW resonator. $G = 1/R_s$ is the conductivity of solution, C_s is the capacitance of the solution, A is the phase angle of the forward transfer admittance of the amplifier (in most instances A can be treated as a constant) and Re is the real part and Xe is the imaginary part of the

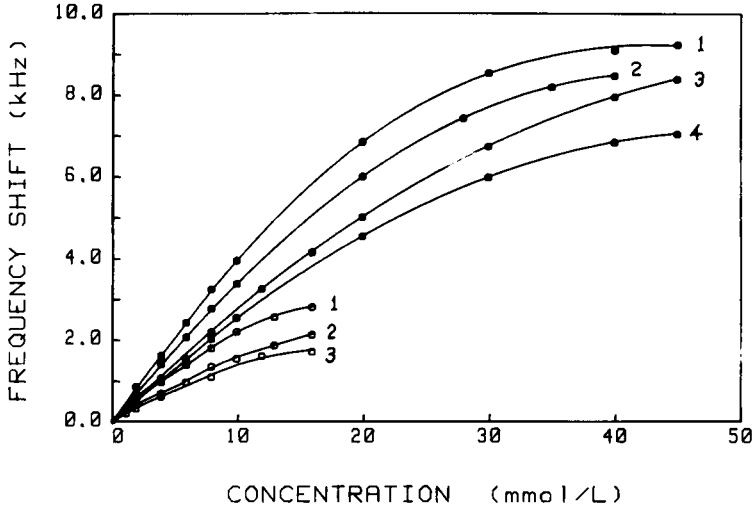

Fig. 3. Frequency shift vs. electrolyte concentration dependence at 10°C, (●) with a 20-pF Csc connected in the circuit loop and (○) without a Csc. (1) $CaCl_2$; (2) Na_2CO_3; (3) KCl; (4) $MgSO_4$. Plots for NaCl with Csc and $MgSO_4$ without Csc are similar to the above plots, but they are not shown because of overlap.

equivalent impedance of the SAW sensor system.

Equation 1 yields the necessary crystal reactance (oscillation frequency) to satisfy the phase shift requirement, while Eqn. 2 yields the forward transfer conductance (transconductance) (g_f) required for oscillation. As the real part (Re) and the imaginary part (Xe) of the sensor system vary with the conductivity of the solution (G), the frequency of the oscillator will change when the concentration of the electrolyte solution is changed. Figure 2 shows typical plots of the frequency shift and transconductance of the SAW sensor system.

The effect of the concentrations of various electrolyte solutions (KCl, NaCl, Na_2CO_3, $MgSO_4$ and $CaCl_2$) on the oscillation frequency of the SAW resonator was investigated at constant temperature and a fixed stirring speed. The frequency shifts observed versus electrolyte concentrations are plotted in Fig. 3. Data for NaCl with 20 pF in series and $MgSO_4$ without Csc are not shown because of overlap. These results show clearly that over a certain concentration range, the frequency shifts vary linearly with concentration. The capacitor Csc is an key factor influencing the linearity and the sensitivity: when a 20-pF Csc is connected in series with the conductance cell, the linearities range up to 0.02–0.03 mol l^{-1} for most salts tested; when the Csc is not included in the loop circuit, it yields a smaller linear range (up to 0.008 mol l^{-1}). The capacitor Csc was therefore connected in subsequent experiments. The slopes of the lines in Fig. 3 give the sensitivities in hertz per millimolar concentration. These values are converted into conductivity sensitivities ($d\Delta F/d\kappa$), which are defined as the incremental changes in oscillator frequency occurring in response to an incremental change in electrolytic conductivity. Linear regression equations for the frequency shifts vs. electrolytic conductivities are given in Table 1. This is an important result because for all salts tested the conduc-

TABLE 1

Dependence of frequency shift on electrolytic conductivity [a]

Electrolyte	Csc = 20 pF		No Csc	
	ΔF (Hz)	r	ΔF (Hz)	r
Na_2CO_3	$2.338\kappa - 55.83$	0.9994	$1.002\kappa + 58.42$	0.9939
$MgSO_4$	$2.115\kappa - 8.899$	0.9952	$1.002\kappa + 42.89$	0.9992
$CaCl_2$	$2.388\kappa + 20.96$	0.9997	$1.275\kappa + 122.9$	0.9932
KCl	$2.510\kappa + 20.96$	0.9980	$1.284\kappa + 44.06$	0.9976
NaCl	$2.202\kappa + 89.68$	0.9986		
Average	$2.300\kappa + 14.58$		$1.141\kappa + 67.05$	

[a] κ = Electrolytic conductivity; r is measured from no less than seven points. $d\Delta F/d\kappa$ in 10^4 Hz Ω m.

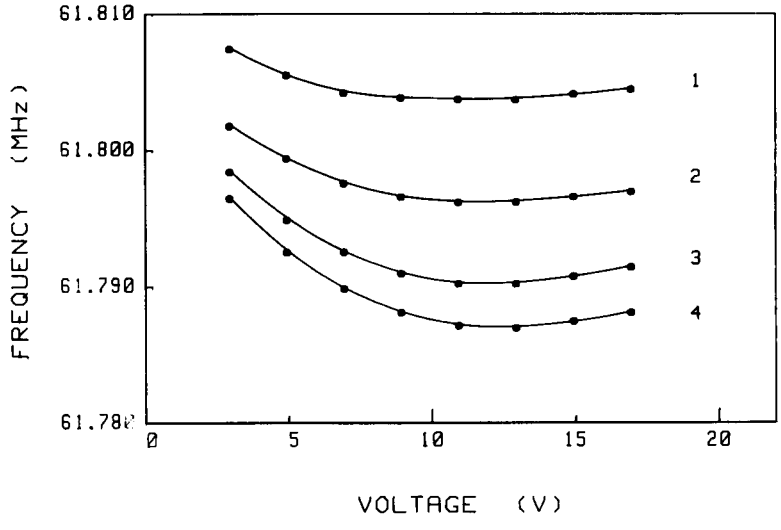

Fig. 4. Dependence of the oscillation frequency on the operating voltage at different capacitances of the Csc. Capacitor $Csc_1 < Csc_2 < Csc_3 < Csc_4$.

tivity sensitivity does not vary significantly with different kinds of salts. This implies that the response of the SAW sensor system in liquids depends linearly on electrolytic conductivity according to the following equation:

$$\Delta F = a\kappa + b \quad (7)$$

where a and b are constants depending on the SAW device and the circuit used and other experimental conditions; a can be positive or negative depending on the series capacitor Csc. The average correlations between frequency shift and electrolytic conductivity are given in Table 1.

Effect of capacitor Csc on the behaviour of the SAW sensor system

In most instances, the amplifier tends to have a considerable phase lag when it is operated at high frequency. This is undesirable for several reasons: first, the phase lag will change with temperature and supply voltage, causing oscillation frequency drift; second, it may result in free-running oscillations through the C_0 of the SAW resonator. A capacitor Csc in series with the amplifier can minimize the phase lag. It can be seen from Fig. 4 that the dependence of the frequency on supply voltage decreases with decrease in Csc capacitance, i.e., with increase in reactance of Csc. When the voltage is near 12 V, the influence of the voltage on the frequency is slight. Hence this voltage range is suitable for the sensor system.

The influence of different capacitances of Csc on the conductivity sensitivities of the SAW sensor system is shown in Fig. 5. The slopes of these plots demonstrate that Csc greatly affects the conductivity sensitivity. The oscillation frequency increases with increasing electrolytic conductivity when the capacitance of Csc is greater than a critical value, whereas it decreases when the latter has a smaller value. At the critical capacitance, the frequency does not vary significantly with electrolytic conductivity over the initial linear range, but it tends to increase with increasing electrolytic conductivity beyond this range (see Fig. 5). When the Csc capacitance reaches a certain value, the conductivity sensitivity is a maximum.

Effect of temperature on the SAW sensor system

Temperature plays a key role in detection using directly polymer-coated SAW sensors, and the temperature dependence is different for SAW devices with different oscillation frequencies. Owing to swelling effects and thermal expansion, the coated polymer also influences the temperature

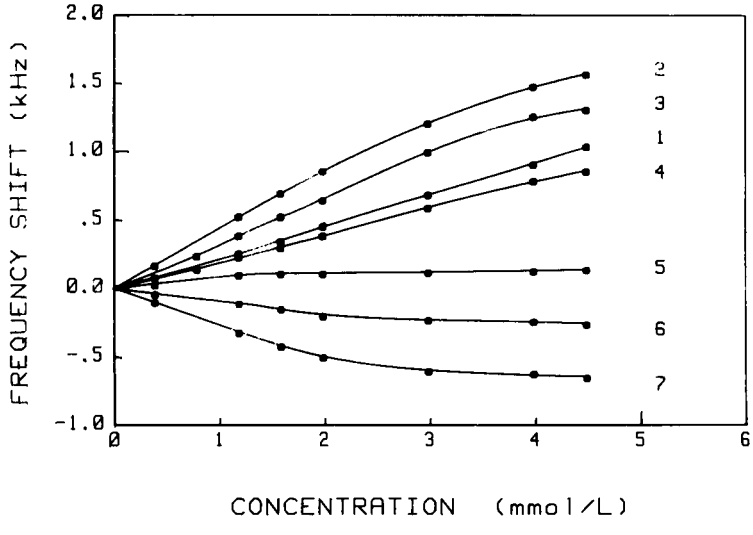

Fig. 5. Frequency shift vs. electrolyte concentration dependence for KCl at different capacitances of the Csc. Capacitor $Csc_1 > Csc_2 > Csc_3 > Csc_4 > Csc_5 > Csc_6 > Csc_7$.

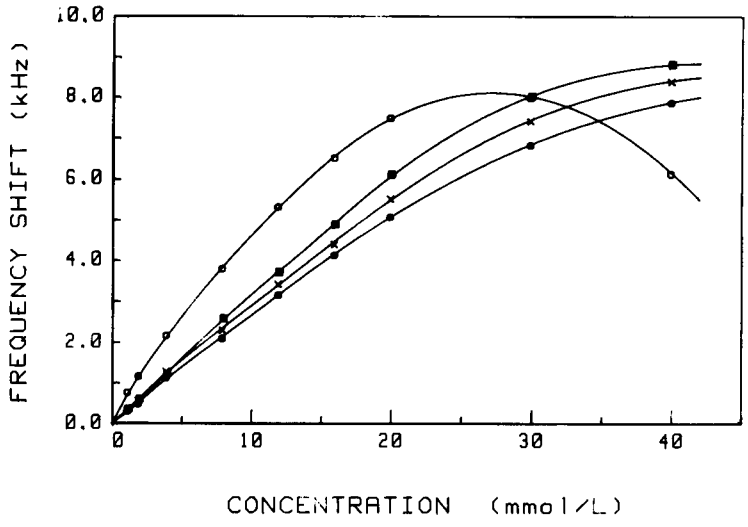

Fig. 6. Temperature dependence of the frequency behaviour of the SAW sensor system in KCl solutions. Temperature: ● = 10, × = 20; ■ = 30; ○ = 40°C.

dependence. In most instances, the temperature drifts of bare SAW delay lines are in the range of 300–750 Hz $°C^{-1}$ at room temperature. Dual delay line oscillators are widely employed for temperature compensation purposes, but the difference between the frequencies of the two sides is not completely independent of temperature but varies by 100 Hz $°C^{-1}$ [5]. In the present set-up, the oscillator board including the SAW resonator may be allowed to come to its own thermal equilibrium, which is a very stable thermal environment, so the temperature drift is far less than in previous set-ups. The oscillator frequency increases linearly with temperature at a rate of ca. 10 Hz $°C^{-1}$ when the conductive electrodes are immersed in water, and decreases by 70 Hz $°C^{-1}$ when the analyte is in a 0.02 M KCl background (Fig. 6). It is assumed that these temperature

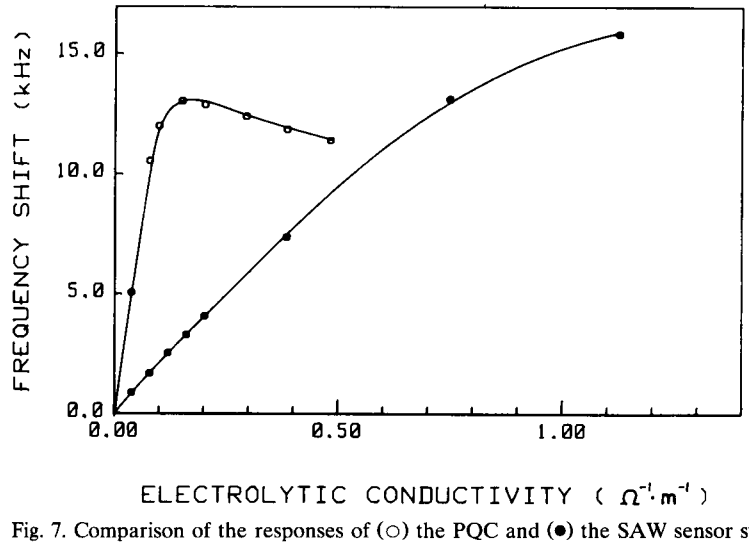

Fig. 7. Comparison of the responses of (○) the PQC and (●) the SAW sensor system in electrolyte solutions.

drifts are mainly due to changes of conductivity, dielectric constant and solution volume. The plots in Fig. 6 are in good agreement with the assumptions.

Thermal conditions make a substantial contribution to the noise levels of SAW sensors in practical use. In the present experiments, the typical noise level of the SAW sensor system was 5 Hz and the best that can be achieved with these devices is 2 Hz.

Comparisons of BAW and SAW devices

Previous work [10,11] revealed that a similar frequency–conductivity correlation also exists for bulk acoustic wave devices (BAW). To investigate this effect more thoroughly, we compared the SAW device with a 9-MHz piezoelectric quartz crystal (PQC). The experiments were made under the same conditions including the conductive electrodes. The results of frequency shift vs. electrolytic conductivity experiments using the two devices are presented in Fig. 7. It was found that the curvature with the SAW device is analogous to that with the BAW device, and the SAW device has lower conductivity sensitivity but greater linearity or dynamical range than those of the BAW device. This indicates that the SAW device has some advantages when it is used in concentrated electrolyte solutions. The following correlation was obtained for aqueous solutions of sodium chloride between 25 and 30 g l^{-1}:

$$\Delta F(\mathrm{Hz}) = 212\ C_{\mathrm{NaCl}}(\mathrm{g\ l^{-1}}) - 5268,$$

$$r = 0.9985;\ n = 12$$

where the relative frequency shift $\Delta F = F - F_0$, F_0 being the frequency response of the SAW resonator in 25 g l^{-1} NaCl solution. The concentration sensitivity is 212 Hz l^{-1} g and with the lowest noise level of 2 Hz and a signal-to-noise ratio of 3 the SAW sensor can measure at least a 0.1% concentration change if 30 g l^{-1} NaCl solution is used. This result suggests that the present set-up has the potential to be applied for process control in the alkali industry and for environmen-

TABLE 2

Determination of total salt content of serum samples [a]

Sample No.	Standard NaCl added (mmol l^{-1})	Frequency shift (Hz)	R.S.D. ($n = 3$) (%)	Concentration found (mmol l^{-1})
1	0	4618, 4640, 4662	0.47	137.43 [b]
	2	4983, 5007, 5022	0.39	138.85
	4	5330, 5339, 5378	0.48	139.70
	6	5671, 5685, 5720	0.44	140.52
2	0	4436, 4476, 4498	0.70	132.31 [b]
	2	4879, 4897, 4906	0.27	135.54
	4	5196, 5220, 5231	0.33	135.80
	6	5525, 5549, 5568	0.38	136.15
3	0	4415, 4452, 4483	0.77	131.71 [b]
	2	4863, 4873, 4890	0.27	134.98
	4	5191, 5203, 5237	0.46	135.52
	6	5516, 5550, 5572	0.51	136.10
4	0	4357, 4375, 4408	0.59	129.61 [b]
	1	4506, 4522, 4528	0.24	129.02
	2	4687, 4695, 4720	0.36	129.73
	3	4858, 4873, 4904	0.48	130.31
5	0	4414, 4430, 4446	0.35	131.11 [b]
	1	4507, 4524, 4529	0.25	129.07
	2	4689, 4720, 4728	0.44	130.08
	3	4882, 4919, 4929	0.50	131.21

[a] Cell volume, 1 ml; concentration of standard NaCl solution, 0.001 M. [b] These values were calculated by calibration method; the others were calculated by the standard addition method.

tal monitoring such as in the continuous detection of salt content fluctuations of sea water.

Determination of total salt content of serum

The main inorganic ions in serum are Na^+, Cl^-, K^+ and Ca^{2+} and the determination of the total salt content is an important test in blood chemistry. Preliminary experiments showed that the conductivity sensitivity ($d\Delta F/d\kappa$) of the SAW sensor system did not vary significantly for different salts. This makes it possible to determine the total salt content of serum directly by measuring the frequency shift. The calibration equation based on standard sodium chloride is

$$C_{NaCl} = 6.3 \times 10^{-3}(\text{mmol l}^{-1}\ \text{Hz}^{-1})\Delta F - 0.442$$

$$r = 0.9991; \quad n = 8$$

The sensitivity is 6.3×10^{-3} mmol l^{-1} Hz^{-1}. With the lowest noise level of 2 Hz and a signal-to-noise ratio of 3, the SAW sensor system can detect 0.04 mmol l^{-1} concentration variations of the total salt in serum, which is more sensitive than normal conductivity test with a high-concentration background. In order to check the accuracy of the SAW sensor system, standard NaCl solution for a normal serum sodium test was analysed; the recovery was 98.9–100.9%. Results of the determination of the total salt content of serum samples are presented in Table 2. The relative standard deviation is less than 0.8%. It was also found that blood fat has no observable influence on the determination.

Conclusions

The application of a SAW device for the detection of electrolytes in solution has been described. The relationship between oscillator frequency and electrolyte concentration was established. This SAW sensor system possesses four attributes: short response time, low temperature drift, low noise levels and high sensitivity.

The authors thank Professor Jianzhe Zhou and Professor Jianghai Zhou for helpful suggestions on circuit design. Financial support from the National Science Foundation and the Education Commission Fund of China are also gratefully acknowledged.

REFERENCES

1 H. Wohltjen and R. Dessy, Anal. Chem., 51 (1979) 1458.
2 T.N. Morrison, K.G. Schick and C.O. Huber, Anal. Chim. Acta, 120 (1980) 75.
3 B.S. Hui and C.O. Huber, Anal. Chim. Acta, 134 (1982) 211.
4 C.G. Fox and J.F. Alder, Analyst, 114 (1989) 997.
5 J.W. Grate, M. Klusty, R.A. McGill, M.H. Abraham, G. Whiting and J. Andonian-Haftvan, Anal. Chem., 64 (1992) 610.
6 M.S. Nieuwenhuizen and A. Venema, Sensors Materials, 5 (1989) 261.
7 H. Wohltjen, Sensors Actuators, 5 (1984) 307.
8 G.S. Calabrese, H. Wohltjen and M.K. Roy, Anal. Chem., 59 (1987) 833.
9 J.W. Grate and M. Klusty, Anal. Chem., 63 (1991) 1719.
10 S.Z. Yao, K. Chen and D.Z. Liu, Anal. Chim. Acta, in press.
11 S.Z. Yao, Z.H. Mo, Anal. Chim. Acta, 193 (1987) 97.
12 D.Z. Shen, W.H. Zhu, L.H. Nie, S.Z. Yao, Anal. Chim. Acta, 276 (1993) 87.

Analytica Chimica Acta, 287 (1994) 75–81
Elsevier Science B.V., Amsterdam

Chemiluminescence determination of guanine and its nucleosides and nucleotides using phenylglyoxal

Masaaki Kai and Yosuke Ohkura

Faculty of Pharmaceutical Sciences, Kyushu University 62, Maidashi, Higashi-ku, Fukuoka 812 (Japan)

Sayuri Yonekura and Masatake Iwasaki

Daiichi College of Pharmaceutical Sciences, Tamagawa-cho, Minami-ku, Fukuoka 815 (Japan)

(Received 13th July 1993; revised manuscript received 11th October 1993)

Abstract

A novel chemiluminescence method is described for the determination of guanine and its nucleosides and nucleotides. The method is based on the fluorescence reaction of the substances with phenylglyoxal in a phosphate buffer (pH 6.0) at 37°C for 20 min, followed by a chemiluminescence reaction with *N*,*N*-dimethylformamide in a weakly alkaline medium. The established conditions of the chemiluminescence reaction do not permit any development of chemiluminescence from other nucleic acid bases such as adenine, cytosine, uracil and thymine, and their nucleos(t)ides. This method is quite selective and approximately 20-fold more sensitive than the fluorimetric one; the detection limits for guanine nucleos(t)ides are 4–19 pmol ml^{-1} in the reaction mixture.

Keywords: Chemiluminescence; Guanine; Nucleosides; Nucleotides; Phenylglyoxal

Methods currently available for the determination of the nucleic acid bases and their nucleos(t)ides are based on non-specific and low-sensitive measurement of their ultraviolet absorption after chromatographic separation. These methods require no derivatization reactions of the biosubstances prior to detection [1,2]. New analytical reagents which can recognize a molecular specificity to one of nucleic acid bases and/or nucleos(t)ides become necessary for selective and sensitive determinations. Hitherto, a few fluorogenic reagents (e.g., glyoxal hydrate trimer [3], chloroacetaldehyde [4] and bromoacetaldehyde [5]) have been reported for the recognition of adenine and its nucleos(t)ides, but fluorimetry shows a relatively high level of the noise signal caused by Raman and Rayleigh scattering light due to a radiation light source.

On the other hand, chemiluminescence has the advantage of a high sensitivity and a wide linear dynamic range for analytes in quantitative analysis in comparison with fluorimetry [6,7]. Many chemiluminescence methods have been developed for the determination of various biosubstances [6,7]. The general methods utilize conventional chemiluminescent compounds (e.g., luminol, lucigenin, acridinium esters [6,7] and dioxetane analogues [8]) or peroxalate esters [6,7,9] as chemical excitation source for suitable fluorescent compounds.

In the non-chromatographic methods, immunochemical and/or enzymatic assay systems are required for acquiring selectivity to target biosubstances. For another chemiluminescence

Correspondence to: Y. Ohkura, Faculty of Pharmaceutical Sciences, Kyushu University 62, Maidashi, Higashi-ku, Fukuoka 812 (Japan).

SSDI 0003-2670(93)E0567-Q

approach, it may be important to utilize a derivatization technique that can selectively convert non-luminescent analytes to chemiluminescent derivative(s).

We previously reported that phenylglyoxal (PGO) reacts selectively with guanine and its nucleos(t)ides to yield fluorescence [10]. Recently, the reaction was found to give single fluorescent derivatives for the compounds in reversed-phase liquid chromatography [11].

In the present study, we will report that the fluorescent derivatives produced by the PGO reaction exhibit chemiluminescence in an alkaline medium in the presence of an aprotic polar solvent, *N*,*N*-dimethylformamide (DMF). The possible pathway of the reaction between PGO and guanine-containing compound to produce the chemiluminescence is shown in Scheme 1. The optimum conditions were first studied for the manual chemiluminescence measurement of guanine-nucleos(t)ides based on their PGO derivatization. Guanosine 5′-monophosphate (GMP) was used as a representative compound for optimizing the conditions. The comparison of chemiluminescence detection with fluorescence detection was also discussed with respect to the sensitivity and selectivity for the quantification of guanine and its nucleos(t)ides.

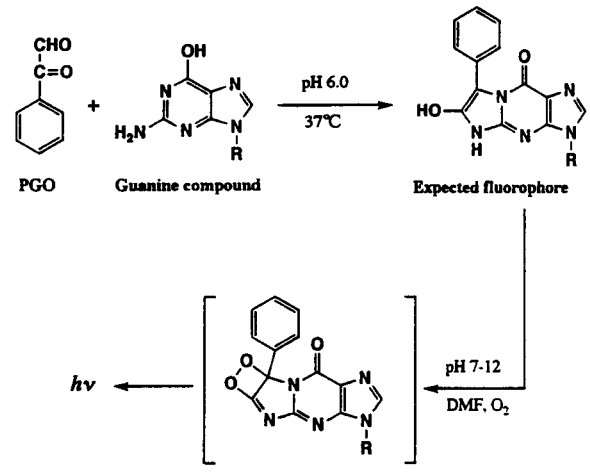

Scheme 1. Possible pathway of the fluorescence and chemiluminescence reaction between PGO and guanine compound.

EXPERIMENTAL

Chemicals and solutions

Nucleic acid bases, nucleosides and nucleotides such as GMP, guanosine 5′-diphosphate (GDP), guanosine 5′-triphosphate (GTP), 2′-deoxyGAP (dGMP), 2′-deoxyGDP (dGDP), 2′-deoxygGTP (dGTP), guanosine cyclic 3′,5′-monophosphate (cGMP), adenosine 5′-monophosphate (AMP), adenosine cyclic 3′,5′-monophosphate (cAMP), cytidine 5′-monophosphate (CMP), cytidine 5′-triphosphate (CTP), cytidine cyclic 3′,5′-monophosphate (cCMP), uridine 5′-monophosphate (UMP) and uridine 5′-triphosphate (UTP) were purchased from Seikagaku Kogyo (Tokyo). Organic solvents of methylcellosolve, DMF, dimethyl sulfoxide (DMSO) and acetonitrile were of HPLC grade (Wako, Tokyo). Other chemicals were of highest purity available.

A guanine solution (1.0 μmol ml^{-1}) was prepared by dissolving guanine hydrochloride in methylcellosolve and water (3:2, v/v), and stored at −20°C. The stock solutions (1.0 μmol ml^{-1}) of other nucleic acid bases and nucleos(t)ides were prepared in water. The solutions were diluted with water to appropriate concentrations (1.0–250 nmol ml^{-1}) when required for use. A PGO solution (0.1 M) was prepared in methylcellosolve and water (1:9, v/v).

Apparatus

Manual chemiluminescence measurements were performed on a photon-counting computer-controlled Berthold (Tokyo) Lumat LB-9501 luminometer, using 75 × 12 mm round-bottom glass tubes. Fluorescence intensities were measured manually with a Hitachi (Tokyo) F-2000 spectrofluorimeter using 1.0-ml semimicro quartz cells (10-mm length parallel to the excitation beam, 3-mm width parallel to the emission beam); spectral band widths of 10 nm were used in both the excitation and emission monochromators.

Analytical procedure

A portion (400 μl) of aqueous sample (or water for blank) was mixed with 200 μl each of 50

mM sodium phosphate buffer (pH 6.0) and 0.1 M PGO. The mixture was heated at 37°C for 20 min for derivatization. The mixture was then cooled in an ice-water bath. To 50 μl of the mixture were successively added 50 μl of 75 mM sodium phosphate buffer (pH 8.0) and 200 μl of DMF. After immediately mixing for 1 s, the chemiluminescence intensity was measured manually. The chemiluminescence intensities represent integral photon counts for 40 s.

Chromatographic system and conditions

Chromatographic separation, and fluorescence and chemiluminescence detections of the reaction products of guanine-containing compounds with PGO were carried out using a Hitachi 638-30 liquid chromatograph, a Rheodyne 7125 syringe-loading sample injector valve (100-μl loop), a Hitachi F-1000 spectrofluorimeter fitted with a 25-μl flow cell and a JASCO (Tokyo) 825-LC chemiluminescence detector. The column was a TSKgel ODS-120T (particle size 5 μm, 150 × 4.6 mm i.d.; Tosoh, Japan). The column temperature was ambient (ca. 22°C). A gradient elution of acetonitrile (5–22 %, v/v) in aqueous mobile phase containing 5 mM phosphate buffer (pH 6.5) was carried out on the column over 24 min at a flow-rate of 1.0 ml min^{-1} (Fig. 1). The column eluate was first passed through the spectrofluorimeter set at 515 nm (emission) and 365 nm (excitation), and then a mixture of DMF and 0.5 M tetra-*n*-propylammonium hydroxide aqueous solution (98:2 %, v/v) was merged with the eluate stream by a Hitachi 633 reagent delivery pump at a flow-rate of 2.0 ml min^{-1}. The chemiluminescence intensity in the resulting eluate was monitored.

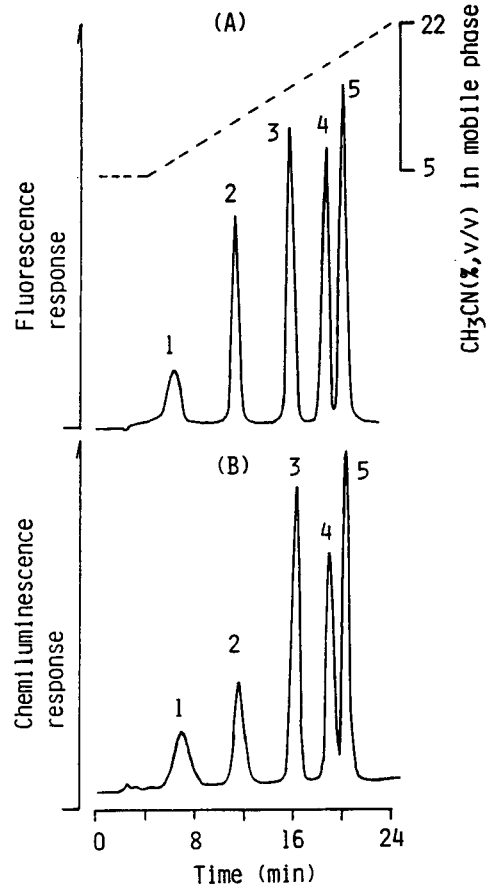

Fig. 1. (A) Fluorescence and (B) chemiluminescence detection in reversed-phase liquid chromatography of the derivatization mixture of GTP, GMP, cGMP, guanosine and deoxyguanosine with PGO. A solution of the compounds (50 nmol ml^{-1} each) was derivatized with PGO according to the analytical procedure, but with no addition of DMF and phosphate buffer (pH 8.0). A portion (50 μl) of the derivatization mixture was injected to the chromatograph. Chromatographic conditions, see in the experimental. Peaks: 1 = GTP, 2 = GMP, 3 = cGMP, 4 = guanosine, 5 = deoxyguanosine.

RESULTS AND DISCUSSION

Chemiluminescence property

Guanine and its nucleos(t)ides were derivatized with PGO to the corresponding fluorescent derivatives under the previously described conditions [11], i.e., reacting in 12.5 mM phosphate buffer (pH 6.0) at 37°C for 10–30 min. When this derivatization mixture of GTP, GMP, cGMP, guanosine and deoxyguanosine was analyzed by reversed-phase chromatography with fluorescence and subsequent chemiluminescence detection, the formed fluorescent derivatives were found to exhibit chemiluminescence in the presence of DMF containing 10 mM tetra-*n*-propylammonium hydroxide (Fig. 1).

In this experiment, the derivatives in the reaction mixture were separated on an ODS column by a linear gradient elution of acetonitrile in the

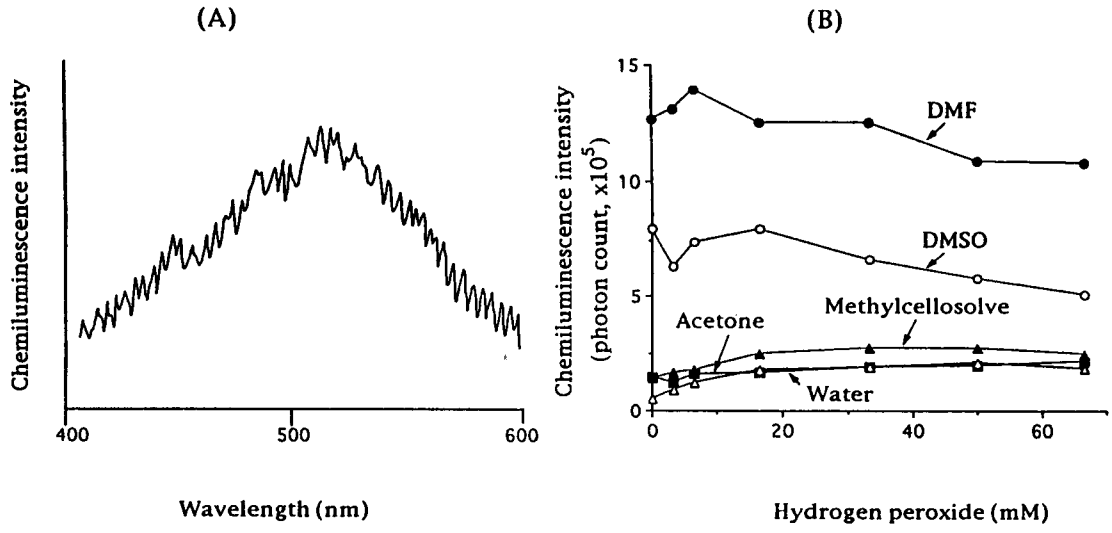

Fig. 2. (A) Chemiluminescence spectrum of the derivatization mixture of GMP, and (B) effects of hydrogen peroxide and various organic solvents on the chemiluminescence development. A GMP solution (500 nmol ml^{-1}) was treated according to the analytical procedure and then its spectrum was obtained with a spectrofluorometer at a scan rate of 200 nm per 10 s while the excitation light was turned off. For the Fig. 2B experiments, a 50 nmol ml^{-1} GMP solution was treated according to the analytical procedure for various organic solvents, except that 25 μl of hydrogen peroxide aqueous solution and 25 μl of 0.15 M phosphate buffer (pH 8.0) were used instead of 50 μl of 75 mM phosphate buffer (pH 8.0).

mobile phase containing 5.0 mM sodium phosphate buffer (pH 6.5); the elution conditions permit the separation of the respective fluorescent derivatives of guanine-nucleos(t)ides [11]. After the fluorescence detection, the column eluate was successively mixed with the alkaline DMF solu-

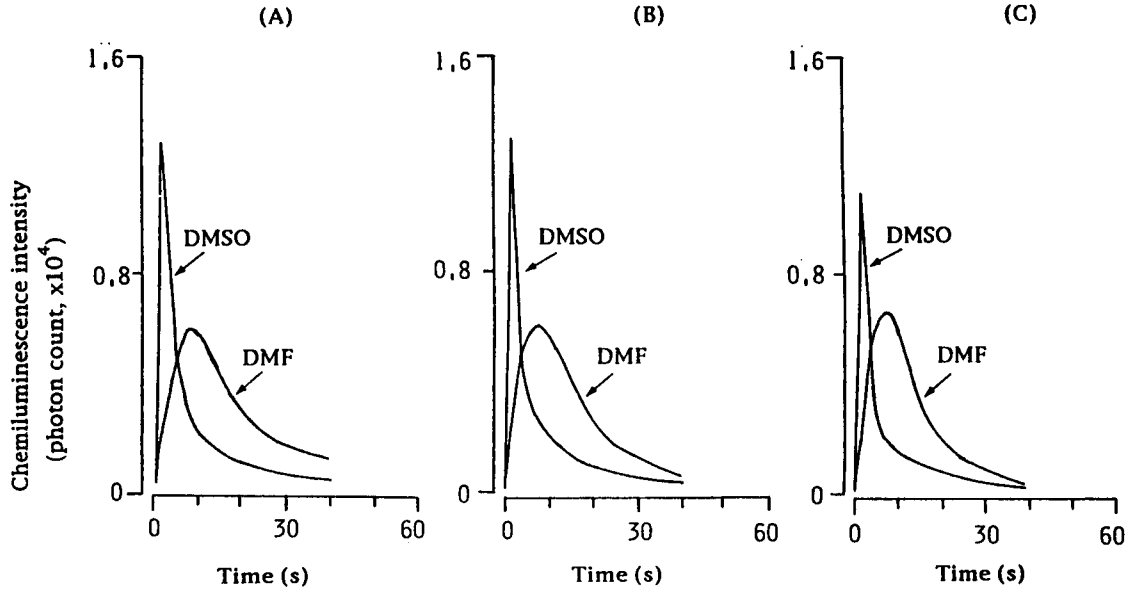

Fig. 3. Time course of the chemiluminescence intensity obtained with DMF or DMSO in the presence of (A) 0, (B) 25 and (C) 75 mM hydrogen peroxide. A GMP solution (50 nmol ml^{-1}) was treated in the same manner as for Fig. 2B.

tion for the chemiluminescence detection. The chemiluminescent peaks in the chromatogram (Fig. 1B) apparently corresponded to their fluorescent derivatives.

The chemiluminescence spectrum obtained with the GMP reaction mixture showed an emission maximum at around 515 nm (Fig. 2A); the noise in the spectrum was mainly caused by the electronic part of the spectrometer at its highest sensitivity range. This maximum emission wavelength corresponded with that of the emission maximum of the fluorescence of the GMP derivative; the fluorescence excitation and emission maxima were measured at 365 nm and 515 nm, respectively [10,11]. The data suggested that the fluorescent product is the same as the chemiluminescent product.

Conditions of chemiluminescence measurement

Chemiluminescence occurs generally in an oxidation reaction step by active oxygen species [6,7]. Figures 2B and 3 show the effects of hydrogen peroxide concentrations and aprotic solvents on the chemiluminescence efficiency. After the fluorescence reaction with PGO, the addition of 200 μl of DMF or DMSO in the analytical procedure caused a large increase in the chemiluminescence intensity (Fig. 2B). However, the addition of hydrogen peroxide (3.3–66.6 mM in the final chemiluminescence reaction mixture) did not increase significantly the intensity.

The time-dependent chemiluminescence intensity from GMP was measured in the cases of DMF and DMSO in the presence and absence of hydrogen peroxide. The time-course of the intensity showed different pattern depending on the solvent used (Fig. 3). The rate of the luminescence emission with DMSO was faster than that with DMF; the maximum photon counts were achieved at 2 and 9 s, respectively after each solvent was added. However, the rate was not affected by hydrogen peroxide concentration (Fig. 3). We examined whether molecular oxygen dissolved in the solvents was more effective on the chemiluminescence development. By using DMF and buffer solutions, treated or untreated by degassing under reduced pressure, the chemiluminescence intensity did not vary significantly in each instance. Thus, hydrogen peroxide was not employed for this chemiluminescence reaction; in the analytical procedure, the solutions treated without degassing were used for convenience.

The concentration of the aprotic solvent had a large influence on the chemiluminescence devel-

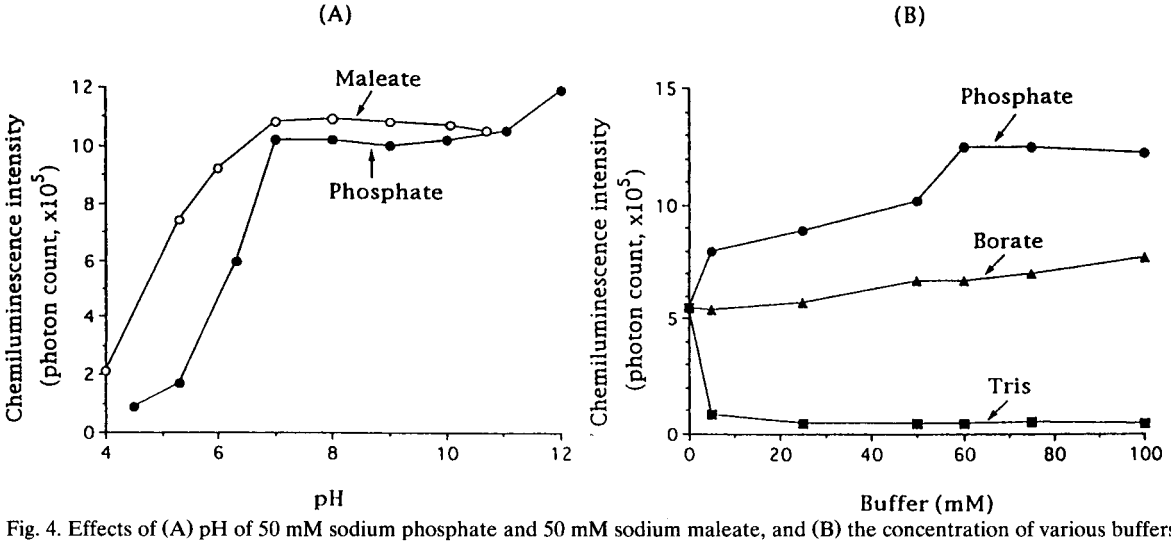

Fig. 4. Effects of (A) pH of 50 mM sodium phosphate and 50 mM sodium maleate, and (B) the concentration of various buffers (pH 8.0) on the chemiluminescence development. A GMP solution (50 nmol ml^{-1}) was treated according to the analytical procedure, except that the electrolytes at various pHs and concentrations were used instead of 75 mM phosphate buffer (pH 8.0).

TABLE 1

Effect of the concentration of aprotic solvents on the chemiluminescence development from guanosine 5′-monophosphate (GMP)

Concentration [a] (%, v/v)	Chemiluminescence intensity (photon count)	
	DMF	DMSO
0	775	344
16.6	786	373
33.3	1244	907
50.0	24 053	13 043
66.6	125 673	79 641

[a] A GMP solution (50 nmol ml^{-1}) was treated according to the procedure, but various concentrations of the aprotic solvent in the final reaction mixture were used.

opment (Table 1). The intensity increased with increasing concentrations of DMF and DMSO in the range 16.6–66.6% (v/v) in the reaction mixture (Table 1). For the analytical procedure, 66.6% of DMF was used for convenience.

Figure 4A shows the pH effect on the chemiluminescence development. Sodium phosphate and sodium maleate were used for this experiment, since these electrolytes possess buffer-action in the weakly alkaline and acidic pH regions, respectively. The maximum intensity of the chemiluminescence was observed at pH 7–12 of both the electrolytes. The time-course of the chemiluminescence intensity did not change at pH values ranging from 7 to 11; the curve profile was almost the same as that in Fig. 3.

Effect of the concentration of buffers (pH 8.0) was examined by using sodium phosphate, sodium borate and tris(hydroxymethyl)aminomethane hydrochloric acid (Tris) having strong buffer action in weakly alkaline pH region (Fig. 4B). Of the tested buffers, the phosphate buffer (pH 8.0) at concentrations greater than 60 mM had the largest effect on the chemiluminescence development; 75 mM the buffer (pH 8.0) was selected for the recommended procedure.

Selectivity and determination

Under the conditions established for chemiluminescence measurements, the following biosubstances at concentrations as high as 500 nmol ml^{-1} did not exhibit any chemiluminescence; adenine, cytosine, thymine, uracil, adenosine, cytidine, thymidine, uridine, AMP, CMP, UMP, CTP, UTP, cAMP, cCMP, hypoxanthine, xanthine, uric acid, and 20 L-α-amino acids.

However, guanine and its nucleos(t)ides produced intense chemiluminescence (Table 2). The

TABLE 2

Chemiluminescence and fluorescence intensities from guanine and its nucleos(t)ides and their detection limits

Compound [a]	Chemiluminescence		Fluorescence	
	Intensity (photon count)	Detection limit [b] (pmol ml^{-1})	Relative intensity [c]	Detection limit [b] (pmol ml^{-1})
Guanine	42 240	53	248	180
Guanosine	306 690	7	98	455
Deoxyguanosine	507 594	4	155	290
GMP	179 779	12	100	445
cGMP	201 911	11	210	212
dGMP	117 665	19	158	282
GDP	141 930	16	198	225
dGDP	171 394	13	222	212
GTP	129 226	17	200	223
dGTP	189 220	12	206	217

[a] Aqueous solutions (50 nmol ml^{-1}) of guanine-containing compounds were treated according to the analytical procedure. [b] The limit was defined as the concentration in the reaction mixture which gave a chemiluminescence or fluorescence intensity corresponding to the blank intensity plus three times its standard deviation. [c] The fluorescence intensity of the derivatization mixture without addition of DMF and the phosphate buffer (pH 8.0) was measured at an emission wavelength of 515 nm with irradiation of 365 nm, and the relative intensity from GMP was taken as 100.

selectivity of this method was identical to that of the fluorimetric determination based on the PGO derivatization [10,11]. The recommended analytical procedure for the present method could also be used for the manual spectrofluorimetric determination of these compounds. The detection limits in the present chemiluminescence and fluorescence methods were 4–53 pmol and 180–445 pmol ml^{-1}, respectively (Table 2). The sensitivity of the proposed chemiluminescence method indicated a nearly twenty-fold improvement compared to the sensitivity achieved by fluorimetry especially for the nucleos(t)ides. The chemiluminescence of guanine was weaker than that of the nucleos(t)ides, while the fluorescence intensity of guanine was highest. This discrepancy may be caused by the stability difference of each derivative depending on the presence of a ribose moiety in the chemiluminescence reaction mixture.

The calibration graphs plotted with the chemiluminescence intensities of GMP, GTP, guanine and guanosine (0, 12.5, 25, 50, 100 nmol ml^{-1}) were all linear ($n = 2$ for each plot). The regression equations for the curves were $Y = 3640X + 1056$ for GMP, $Y = 2617X - 421$ for GTP, $Y = 915X + 973$ for guanine and $Y = 5890X + 899$ for guanosine, in which Y and X represent the photon counts and their concentrations, respectively. The correlation coefficient for each straight line was in the 0.992–0.999 range. The within-day reproducibility of the chemiluminescence intensity was evaluated from the results of 20 repeated measurements of a 50 nmol ml^{-1} solution of GMP used in the procedure. The relative standard deviation was 5.7%. The temperature variation during the chemiluminescence measurements had a significant influence on the deviation. Therefore, the chemiluminescence measurement was carefully performed at a constant temperature (25°C) after the PGO derivatization reaction.

In conclusion, this study provides the first chemiluminescence method utilizing the derivatization reaction with PGO for the selective and sensitive determination of guanine and its nucleos(t)ides. The structure of the chemiluminescencing species is still unknown. The proposed method requires a simple procedure and quite mild reaction conditions, and thus may be applicable to a post-column chemiluminescence detection system in chromatography for the sensitive determination of guanine-containing compounds in complex biospecimens such as mammalian body fluids and tissues. The study is currently in progress.

This work was supported by a Grant-in-Aid for Scientific Research from the Ministry of Education, Science and Culture, Japan.

REFERENCES

1 P. Rotllan, A. Liras and P. Llorente, Anal. Biochem., 159 (1986) 377.
2 F. Arezzo, Anal. Biochem., 160 (1987) 57.
3 H. Yuki, C. Sempuku, M. Park, H. Isemura and K. Takiura, Anal. Biochem., 57 (1974) 290.
4 J.L. Sims, H.J. Salinas and M.K. Jacobson, Anal. Biochem., 106 (1980) 296.
5 H. Fujimori, T. Sasaki, K. Hibi, M. Senda and M. Yoshioka, J. Chromatogr., 515 (1990) 363.
6 K. Robards and P.J. Worsfold, Anal. Chim. Acta, 266 (1992) 147.
7 G.J. de Jong and P.J.M. Kwakman, J. Chromatogr., 492 (1989) 319.
8 S. Beck and H. Koster, Anal. Chem., 62 (1990) 2258.
9 P.J.M. Kwakman and U.A.Th. Brinkman, Anal. Chim. Acta, 266 (1992) 175.
10 M. Kai, Y. Ohkura, S. Yonekura and M. Iwasaki, Anal. Chim. Acta, 207 (1988) 243.
11 S. Yonekura, M. Iwasaki, M. Kai and Y. Ohkura, J. Chromatogr., 641 (1993) 235.

Analytica Chimica Acta, 287 (1994) 83–88
Elsevier Science B.V., Amsterdam

Determination of polyamines by liquid chromatography with aryl oxalate–sulphorhodamine 101 chemiluminescence detection

Masatoki Katayama, Hideyuki Takeuchi and Hirokazu Taniguchi

Meiji College of Pharmacy, 1-35-23, Nozawa, Setagaya-ku, Tokyo 154 (Japan)

(Received 28th June 1993; revised manuscript received 17th September 1993)

Abstract

A method for determination of polyamines based on liquid chromatography (LC) with aryl oxalate–sulphorhodamine 101 chemiluminescence detection is reported. Cadaverine, histamine, putrescine, spermine, spermidine, tyramine were separated on a Zorbax ODS column (250 × 4.0 mm i.d., 7 μm; Dupont) with methanol–acetonitrile–water (62.5 + 2.5 + 35.0, v/v) and chemiluminescence detection without derivatization. The detection limits (signal-to-noise ratio = 3) for putrescine, spermine and spermidine were 1.0×10^{-9} M, for tyramine 5.0×10^{-9} M and for histamine and cadaverine 7.0×10^{-9} M (20-μl injection) with linear calibration up to 1.0×10^{-4} M. The relative standard deviation ($n = 6$) was 4.1% at 1.0×10^{-7} M putrescine. The proposed LC method was applied to the determination of polyamines in tomatoes.

Keywords: Chemiluminescence; Liquid chromatography; Plants; Polyamines; Tomatoes

Polyamines are widespread in animals, plants and microorganisms, and increases in biogenic polyamines are observed as a consequence of metabolic processes [1]. Therefore, the determination of polyamines gives information on the freshness of foods [2,3]. Marked increases in allergies caused by histamine in the presence of polyamines [3] and the formation of strongly carcinogenic N-nitrosoamines by polyamines in the presence of nitrite have been reported [4]. A rapid and generally acceptable method for detecting decomposed polyamines is needed with a view to the prevention of allergies and the improvement of safety of foods.

Applications of gas chromatography (GC) [5,6], liquid chromatography (LC) with fluorescence detection after derivatization [7–11] and thin-layer chromatography (TLC) [12] have been reported. However, GC needed a derivatization reaction with diazomethane and TLC was not sensitive and gave poor reproducibility. LC methods using fluorescence detection after derivatization with dansyl chloride [7–9], fluorescamine [8,10] and *o*-phthalaldehyde [9,11] were sensitive, but required time-consuming sample preparation and derivatization reaction procedures.

In a previous paper [13], a sensitive flow-injection analysis (FIA) method for the determination of amines based on aryl oxalate–sulphorhodamine 101 chemiluminescence with bis[4-nitro-2-(3,6,9-trioxadecyloxycarbonyl)phenyl] oxalate (TDPO) and sulphorhodamine 101 in acetonitrile eluent was reported. This FIA method was more sensitive than LC methods using fluorescence detection after derivatization [7–11], and it could be used to determine aliphatic primary, secondary

Correspondence to: M. Katayama, Meiji College of Pharmacy, 1-35-23, Nozawa, Setagaya-ku, Tokyo 154 (Japan).

SSDI 0003-2670(93)E0591-T

and tertiary amines and imidazoles simultaneously without a derivatization process in a short time. Therefore, an FIA method combined with LC was developed and applied to the determination of polyamines in plants. In this paper, studies of LC conditions for the determination of polyamines and the application of the method to plants are reported.

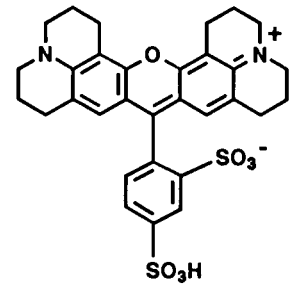

Fig. 1. Structure of sulphorhodamine 101.

EXPERIMENTAL

Reagents and materials

A polyamine stock standard solution (1.0×10^{-3} M) was prepared by dissolving 1.0×10^{-5} mol of polyamine in 0.1 ml of ethanol and diluting to 10 ml with acetonitrile.

Analytical-reagent grade chemicals were used unless indicated otherwise. Each solvent, the HPLC eluent and the reagent solution were of HPLC grade (Wako, Osaka, Japan). Sulphorhodamine 101 (Fig. 1) was of laser grade (Eastman Kodak, Rochester, NY). TDPO was purchased from Wako (Osaka). Hydrogen peroxide (30%, w/v) was purchased from Mitsubishi Gas Kagaku (Tokyo).

Apparatus

Chemiluminescence LC method. A Niti-On (Tokyo) Physcotron homogenizer was used. The LC system is illustrated in Fig. 2. A Shimadzu (Kyoto) LC-6A liquid chromatograph (pump 1) and a peristaltic pump (pump 2, PF-6) (Nihon Rikagaku, Tokyo) were used as LC and reagent pumps. Chemiluminescence was observed in a Lumi-flow LF-800 chemiluminescence detector (spiral-type flow cell, volume 160 μl) (Niti-On) and a noise cut-off filter (triacylcellulose, SC-54) (Fuji Film, Tokyo) was set in front of the photomultiplier as in the previous FIA method [13]. A Zorbax ODS column (250 mm $\times$ 4.0 i.d., 7 μm) (DuPont, Wilmington, DE) was used as the analytical column at room temperature (ca. 22°C). Eluent R_1 [methanol–acetonitrile–water (62.5 + 2.5 + 35.0, v/v, containing 1.0×10^{-2} M hydrogen peroxide)] was applied at a flow-rate of 1.0 ml min^{-1}. This eluent could used for about 30 h. Reagent R_2 (5.0×10^{-4} M TDPO and 1.0×10^{-7}

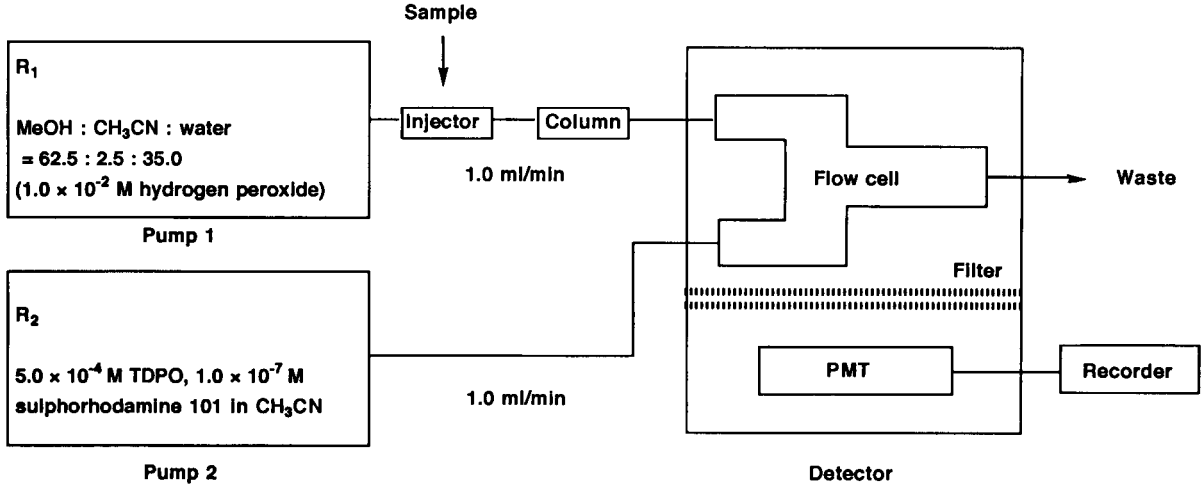

Fig. 2. Schematic diagram of LC system. Pump 1, LC pump (Shimadzu LC-6A); pump 2, peristaltic pump (Nihon Rikagaku PF-6); column, Zorbax ODS (250 $\times$ 4.0 mm i.d., 7-μm; DuPont); detector, Niti-On LF-800; PMT, photomultiplier.

M sulphorhodamine 101 in acetonitrile) was applied at a flow-rate of 1.0 ml min^{-1}. This reagent was stable for 7 days. The sample volume was 20 μl.

Fluorescence LC method. The LC comparison of polyamine contents in plants was as described [9] and the LC conditions were as follows: pump, Shimadzu LC-6A; analytical column, Zorbax ODS (250 × 4.0 mm i.d., 7 μm) (DuPont); column temperature, room temperature (ca. 22°C); eluent, acetonitrile–water (6 + 4, v/v); flow-rate, 1.3 ml min^{-1}; sample volume, 10 μl; detector, Shimadzu RF-530 fluorescence monitor [λ(ex) 350 nm, λ(em) 525 nm].

Preparation method for tomato sample

Chemiluminescence LC method. The tomato sample was prepared as described [9] with modification. A 10-g amount of cut tomato was homogenized with 10 ml of water, 10 ml of hydrochloric acid (35%, w/v) were added and the mixture was diluted to 50 ml, mixed for 30 min and filtered through a filter-paper (3-μm pore size) (Advantec, Tokyo). A 1-ml volume of 2000 μg/ml 1,6-diaminohexane solution as internal standard was added to the prepared sample solution and a 20-μl aliquot of this solution was injected into the LC system.

Fluorescence LC method. The tomato sample was prepared as described [9]. A 10-g amount of cut tomato was homogenized with 10 ml of water, 10 ml of hydrochloric acid (35%, w/v) were added and the mixture was diluted to 50 ml, mixed for 30 min and filtered through a filter-paper (3-μm pore size). A 5.0-ml aliquot of prepared sample solution was neutralized with 40% sodium hydroxide solution, the pH was adjusted to 6.0–7.0, 25 ml of 0.1 M acetate buffer solution were added and the solution was applied to an ion-exchange column (55 × 10 mm i.d., Amberlite CG-50 Type I, 100–200 mesh) (Rohm and Haas, Philadelphia, PA), which was washed with 80 ml of 0.25 M acetate buffer (pH 4.5). The polyamines were eluted with 1.0 M hydrochloric acid and 20 ml of eluate were collected. A 0.1-ml volume of 500 μg ml^{-1} 1,6-diaminohexane solution as internal standard and 0.2 g of anhydrous sodium carbonate were added to 1.0 ml of the polyamine eluent, then 1.0 ml of 10% (w/v) dansyl chloride solution in acetone was added to the mixture, which was heated at 45°C for 1 h, then 0.5 ml of 10% (w/v) proline solution was added and the mixture was allowed to stand for 10 min. The reaction solution was extracted for 1 min with 5.0 ml of toluene. A 5.0-ml volume of the toluene layer was collected and evaporated to dryness below 50°C under reduced pressure. A 1.0-ml volume of acetonitrile was added to the residue and mixed for 5 min. A 20-μl aliquot of the solution was injected into the LC system.

RESULTS AND DISCUSSION

Chemiluminescence reaction conditions

Effect of flow-rate. In the application of aryl oxalate chemiluminescence as the detection system in LC analysis, chemiluminescence reagents were added to the polyamine eluent after the analytical column and the chemiluminescence was detected by a photomultiplier [14,15]. The composition of the LC eluent from the analytical column was decided by the analytical objectives. Therefore, solvent composition and the flow-rate and concentration of the chemiluminescence reagent were the most important factors for gaining the most intense chemiluminescence. Acetonitrile was the most suitable solvent for aryl oxalate–sulphorhodamine 101 chemiluminescence [13]. The relationship between flow-rate of the LC eluent (R_1) and the chemiluminescence reagent (R_2) is shown in Fig. 3. A constant maximum chemiluminescence detector response was obtained at a flow-rate of 0.8–1.5 ml min^{-1} and a flow-rate of 1.0 ml min^{-1} was selected.

Effect of reagent concentration. The effect of TDPO, sulphorhodamine 101 and hydrogen peroxide concentrations was similar to that in the previous FIA study [13]. The lowest limit of detection was obtained at 5.0×10^{-4} M TDPO, 1.0×10^{-7} M sulphorhodamine 101 and 1.0×10^{-2} M hydrogen peroxide.

Stability of LC eluent and reagent. Eluent R_1 contained hydrogen peroxide, so the stability of the eluent was studied. It was found that eluent R_1 could be used for 30 h and no damage to the

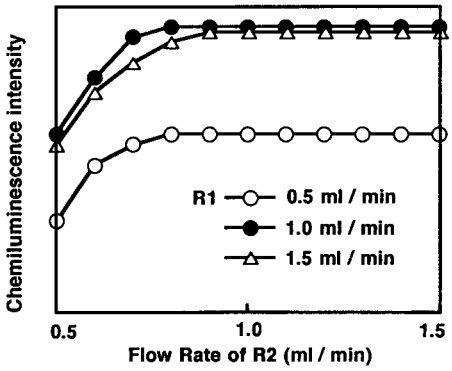

Fig. 3. Effect of flow-rates of R_1 and R_2 on the chemiluminescence intensity. Putrescine taken, 1.0×10^{-7} M.

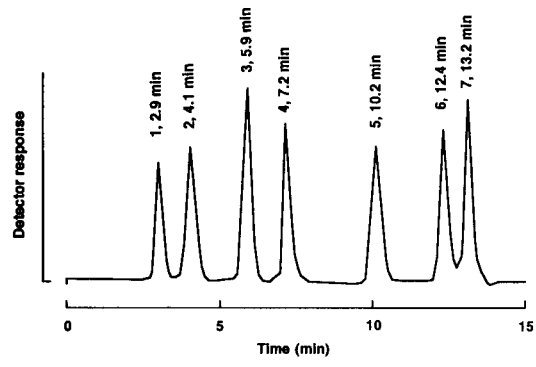

Fig. 4. Chromatogram of polyamines. Concentration of polyamine used, 1.0×10^{-7} M. Peaks: 1 = histamine; 2 = tyramine; 3 = putrescine; 4 = cadaverine; 5 = 1,6-diaminohexane (internal standard); 6 = spermine; 7 = spermidine.

LC column was observed after 3 months. TDPO and sulphorhodamine 101 reagents were stable for 7 days.

Separation of polyamines

Separation conditions. The separation conditions for polyamines (cadaverine, histamine, putrescine, spermidine, spermine and tyramine) were studied. Zorbax ODS, Zorbax C_8 and Zorbax TMS (each 250 × 4.0 mm i.d.) columns with acetonitrile, methanol, tetrahydrofuran and propan-2-ol as mobile phases were tested. Neither the Zorbax TMS nor the Zorbax C_8 column with acetonitrile, methanol, tetrahydrofuran and propan-2-ol could separate all the polyamines. The Zorbax ODS column with acetonitrile–water (7 + 3, v/v) as mobile phase could separate all the polyamines, but each peak was broad and the limit of detection of each polyamine was poor. Methanol–water (6 + 4, v/v) gave sharp peaks, but spermine and spermidine were not separated. The addition of acetonitrile to methanol–water mixtures was studied further. It was found that methanol–acetonitrile–water (62.5 + 2.5 + 35.0, v/v) was the most suitable for the separation of the polyamines. The flow-rate was set at 1.0 ml min^{-1} and each polyamine was separated within 15 min. A chromatogram of seven polyamines (1.0×10^{-7} M) obtained under the optimum conditions is shown in Fig. 4.

Determination of polyamines. The detection limits (signal-to-noise ratio = 3, 20-μl injection) for putrescine, spermine and spermidine were 1.0×10^{-9} M (20 fmol), for tyramine 5.0×10^{-9} M (100 fmol) and for histamine and cadaverine 7.0×10^{-9} M (140 fmol). The upper calibration limit of each polyamine was 1.0×10^{-4} M. The relative standard deviation ($n = 6$) was 4.1% at 1.0×10^{-7} M putrescine. The proposed method

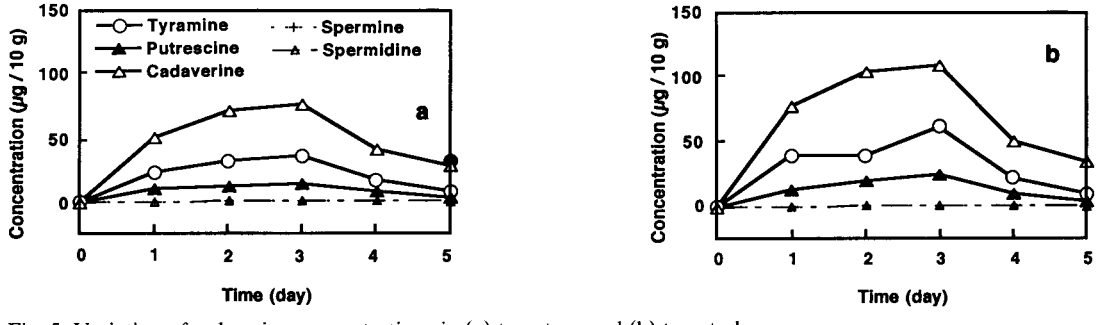

Fig. 5. Variation of polyamine concentrations in (a) tomato a and (b) tomato b.

needs no time-consuming derivatization reaction with TMS and is 25–1000 times more sensitive than the GC method [5,6]. LC after fluorimetric derivatization with dansyl chloride [7–9], fluorescamine [8,10] or *o*-phthalaldehyde [9,11] also requires handling of foul-smelling reagents such as 2-mercaptothanol and a derivatization process, but the LC method proposed here without derivatization need only a simple extraction process and is 5–100 times more sensitive than methods involving derivatization.

Application of polyamine determination in tomatoes

The proposed LC method was applied to the determination of polyamines in tomatoes.

Pretreatment of tomatoes. Each tomato was homogenized and extracted with hydrochloric acid and the extract was used as the sample solution. The LC method for the determination of polyamines in foods after derivatization with dansyl chloride method needed a clean-up process on an ion-exchange column and a derivatization process [9], but in the LC method proposed here the sample solution could be injected directly into the LC system. As a result, the analysis time was shortened by over 2 h.

Determination of polyamines. Two commercial tomato samples (a and b, purchased in different outlets) were kept at room temperature and their polyamine concentrations were determined. The polyamine contents in both samples increased with time and the highest values were observed after 3 days period (Fig. 5). The total polyamine contents after 3 days period were 108 μg in 10 g (tomato a) and 222 μg in 10 g (tomato b). The chromatograms obtained with the proposed LC method are shown in Fig. 6. The patterns of polyamine species were similar for both samples, but the contents of tyramine and putrescine in tomato a were lower than in tomato b. The histamine content was very low in both samples. The recoveries of polyamines added to tomato a were 90.0–92.9% (n = 6) (Table 1). The within-day relative standard deviations (n = 6) were 1.8–4.1%

TABLE 1

Recovery test on the application of the LC method to the determination of polyamines in tomato [a]

Polyamine	Expected concentration (μg per 10 g)	Found concentration (mean ± S.D.) (μg per 10 g)
Tyramine	1.0	0.93 ± 0.02
	10.0	9.40 ± 0.21
	100.0	93.53 ± 1.91
Putrescine	1.0	0.93 ± 0.02
	10.0	9.31 ± 0.21
	100.0	92.78 ± 2.08
Cadaverine	5.0	4.71 ± 0.14
	50.0	47.71 ± 1.24
	500.0	481.08 ± 9.21
Spermine	0.1	0.09 ± 0.00
	1.0	0.93 ± 0.01
	10.0	9.37 ± 0.21
Spermidine	0.1	0.09 ± 0.00
	1.0	0.94 ± 0.92
	10.0	9.45 ± 0.23

[a] A 10-g tomato sample was spiked at the indicated concentrations. Average values obtained from six runs.

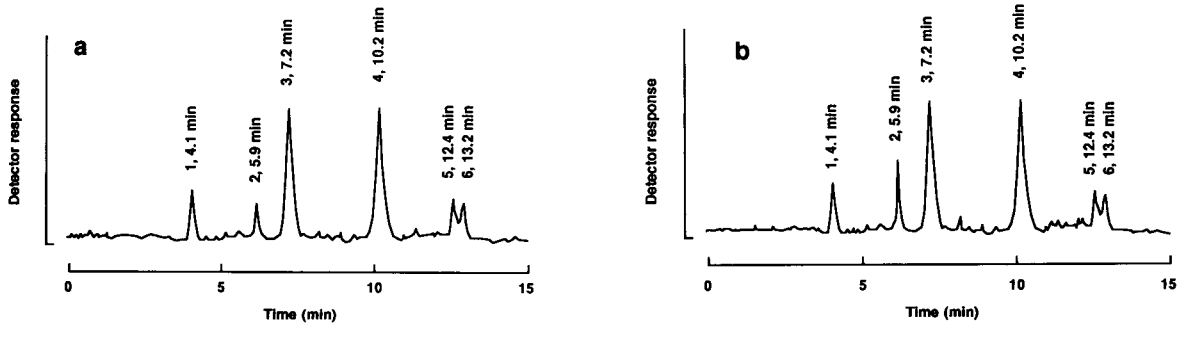

Fig. 6. Chromatograms of polyamines in (a) tomato a and (b) tomato b after standing for 3 days. Peaks: 1 = tyramine; 2 = putrescine; 3 = cadaverine; 4 = 1,6-diaminohexane (internal standard); 5 = spermine; 6 = spermidine.

and the day-to-day relative standard deviations ($n = 6$) were 3.4–4.1%. The putrescine contents in 50 samples of tomato were measured by both the proposed LC method and the LC method after derivatization with dansyl chloride [9]. The correlation coefficient was 0.98 ($n = 150$) and the regression equation was $y = 1.08x - 10.88$ (95% confidence limits for slope, $1.02 \leqslant \beta \leqslant 1.10$, and for the intercept, $-18.68 \leqslant \alpha \leqslant 3.08$), where y and x are concentrations in μg per 10 g obtained by the proposed LC method and LC method with dansyl chloride derivatization, respectively. The results show that the proposed HPLC method could be used to determine polyamines in plants, foods, drugs and biological samples.

Conclusions

The proposed LC method is simple and can be used to determine 1.0×10^{-9}–7.0×10^{-9} M levels of polyamines without the need for a derivatization reaction. It is 5–1000 times more sensitive than GC [5,6] and LC methods after derivatization [7–11]. The pretreatment process, denaturation, extraction and column-clean up process in the proposed LC method can be greatly shortened compared with conventional GC and LC methods after derivatization. Further applications of the proposed LC method to monitoring polyamines in plants, foods and biological samples, and especially monitoring damage by acid rain of plants in polluted forest areas [16–18] are expected.

REFERENCES

1 I.S.R. Albert, S.D. Mitchell and D.O. Gray, J. Chromatogr., 312 (1984) 357.
2 J.L. Mietz and E. Karmas, J. Food Sci., 42 (1977) 155.
3 S.L. Rice, R.R. Eitenmiller and P.E. Koehler, J. Milk Food Technol., 39 (1976) 353.
4 J.H. Hotchkiss, R.A. Scanlan and L.M. Libbey, J. Agric. Food Chem., 25 (1977) 1183.
5 W.F. Staruszkiewicz, Jr., and J.F. Bond, J. Assoc. Off. Anal. Chem., 64 (1981) 584.
6 G.B. Baker, J.T.F. Wong, R.T. Coutts and F.M. Pasutto, J. Chromatogr., 392 (1987) 317.
7 J.Y. Hui and S.L. Taylor, J. Assoc. Off. Anal. Chem., 66 (1983) 853.
8 C. Buteau, C.L. Duitschaever and G.C. Ashton, J. Chromatogr., 284 (1984) 201.
9 Pharmaceutical Society of Japan, Standards Methods of Analysis for Hygienic Chemists, Kanehara Shuppan, Tokyo, 1990, p. 287.
10 M. Kai, T. Ogata, K. Haraguchi and Y. Ohkura, J. Chromatogr., 163 (1979) 151.
11 N. Seiler and B. Knödgen, J. Chromatogr., 221 (1980) 227.
12 R.F. Minmchin and G.R. Hanau, J. Liq. Chromatogr., 7 (1984) 2605.
13 M. Katayama, H. Takeuchi and H. Taniguchi, Anal. Chim. Acta, 281 (1993) 111.
14 S. Kobayashi and K. Imai, Anal. Chem., 52 (1980) 424.
15 K. Imai, S. Higashidate, A. Nishitani, Y. Tsukamoto, M. Ishibashi, J. Shoda and T. Osuga, Anal. Chim. Acta, 227 (1989) 21.
16 V.R. Villanueva and A. Santerre, Water Air Soil Pollut. 48 (1989) 59.
17 A. Santerre, J.M. Mermet and V.R. Villanueva, Water Air Soil Pollut., 52 (1990) 157.
18 A. Santerre, M. Markiewicz and R. Villanueva, Phytochemistry, 29 (1990) 1767.

Analytica Chimica Acta, 287 (1994) 89–94
Elsevier Science B.V., Amsterdam

Room temperature phosphorescence of biogenic indoles in low background paper enhanced by heavy atom salts and sodium dodecyl sulfate

Simone M.C. Gioia and A.D. Campiglia

Departamento de Quimica, Universidade de Brasilia, Brasilia, DF 70910-900 (Brazil)

(Received 4th June 1993; revised manuscript received 4th October 1993)

Abstract

Room temperature phosphorescence of eight biogenic indoles was studied on matrix modified substrates. Whatman chromatography paper previously treated for background reduction was used as a solid substrate. The phosphorescence characteristics of the studied compounds were observed in the presence of sodium iodide, thallium(I) nitrate, silver(I) nitrate and lead(II) acetate. The heavy atom efficiency was increased by using sodium dodecyl sulfate in the matrix of the phosphor. The analytical figures of merit were obtained for each compound under the best experimental conditions for maximum phosphorescence emission. Limits of detection ranging from 0.9 ng (indole-2-carboxylic acid and indole-3-acetic acid) to 11.4 ng (3-methylindole) were estimated.

Keywords: Phosphorimetry; Biogenic indoles; Matrix modified substrates

Even though Roth [1] was the first to report the use of cellulose as a rigid matrix to enhance the phosphorescence emission of several compounds at room temperature, the analytical potential of solid substrate room temperature phosphorimetry (SSRTP) was only recognized after the studies performed by Schulman and Walling [2,3]. Since then, intensive work has been done to turn SSRTP into a competitive technique for the analysis of trace compounds [4,5].

A great deal of effort has been focused in the search of a suitable substrate for RTP analysis. Among the materials investigated, cellulose – in the form of filter and chromatography paper – appears to be the most convenient substrate for the technique [4,5]. One of its major characteristics is the possibility of forming hydrogen bonding with the analyte molecule. By increasing the rigidity of the matrix, the hydroxyl groups of cellulose avoid radiationless deactivation of the triplet state and favor the emission of phosphorescence [6,7]. There is, however, an important disadvantage in the use of cellulose substrates. Their phosphorescence emission, which is usually the same order of intensity as the analyte signals from relatively high concentrations, severely limits the sensitivity of SSRTP [8,9]. An effective approach to decrease this signal involves exposure of the substrate to ultraviolet radiation [10,11]. Background reductions higher than 90% have been obtained which have lowered the limits of detection from one to two orders of magnitude [11].

In addition to background reduction, the sensitivity of SSRTP can be improved by the presence of heavy atoms (HA) in the environment of the phosphor [4,5]. Frequently, the interaction between analyte and HA increases the rate of the

Correspondence to: A.D. Campiglia, Departamento de Quimica, Universidade de Brasilia, Brasilia, DF 70910-900 (Brazil).

SSDI 0003-2670(93)E0580-Z

singlet–triplet intersystem crossing mechanism, and enhances the emission of phosphorescence [4,5]. The presence of HA, however, can also increase the radiantionless rates of triplet to ground state decay and phosphorescence enhancement is not observed [12,13].

Recently, de Lima et al. [14] proposed a unique method to improve the effectiveness of HA enhancers. By employing an anionic surfactant (sodium dodecyl sulfate) in the matrix of the phosphor (carbaryl), the authors [14] observed higher HA enhancements than those obtained in the absence of the surfactant. Apparently, the long hydrocarbon chains of sodium dodecyl sulfate (NaDS) avoid the penetration of phosphor molecules into the cellulose pores and increase the interaction with HA ions at the surface of the substrate [14]. In addition, NaDS can provide other sites of interaction for the phosphor and improve the rigidity of the matrix necessary for the observation of high RTP signals [14]. The usefulness of nonionic and cationic surfactants was later studied by Ramis Ramos et al. [15]. When the emission of *o*-terphenyl was measured in the presence of these two kinds of surfactants, drastic intensity reductions were observed [15]. High enhancements, however, were obtained with NaDS and sodium decyl sulfate in the matrix of the phosphor [15]. Finally, the use of NaDS was extended to the RTP analysis of several polyaromatic hydrocarbons [16,17], phenothiazine derivatives [18] and purine related compounds [19].

In this article, a study of the RTP characteristics of eight indoles of biological interest employing NaDS as a matrix modifier surfactant is reported. Chromatography paper previously treated for background reduction [11] was used as a solid substrate. The best HA for maximum RTP signal was selected for each compound and the analytical figures of merit were obtained in the presence of the surfactant.

EXPERIMENTAL

Apparatus

An Aminco-Bowman spectrofluorimeter (SLM Instruments, Urbana, IL) equipped with an Aminco-Keirs rotating-can phosphoroscope attachment was used to collect all RTP spectra and intensity measurements. The spectrophotofluorimeter was equipped with a 150 W xenon arc lamp (Conrad-Hanovia, Newark, NJ) as excitation source, and a potted 1P21 photomultiplier (Hamamatsu, Middlesex, NJ) with a S4 spectral response as a detector. A SLM-Aminco microphotometer was used to amplify the signal. The amplified signal was fed to an *X–Y* recorder (Model 7010B, Hewlett-Packard, Palo Alto, CA). A laboratory-constructed sample holder was used for all measurements [20].

For background reduction, the paper substrate was irradiated in a Rayonet photochemical reactor (The Southern N.E. Ultraviolet Co., Middletown, CT) using five lamps with maximum wavelengths (λ_{max}) of emission at 254 nm and seven with λ_{max} at 300 nm.

The nitrogen flow employed throughout all measurements was previously passed by a silica gel bed to remove possible water vapor traces.

Reagents

Whatman No. 1 Chromatography paper was used as a solid substrate. Bidistilled (in glass) water and analytical-reagent grade chemicals were used throughout. Ethanol was obtained from Merck. Indole, 3-methylindole, 6-methoxyindole, indole-2-carboxilic acid, indole-3-carboxilic acid, indole-3-acetic acid, 5-hydroxyindole-3-acetic acid and 5-mehtoxyindole-3-acetic acid were purchased from Sigma and used as received. NaDS and sodium iodide (NaI) were from Aldrich. Thallium(I) nitrate ($TlNO_3$), lead(II) acetate (PbOAc) and silver nitrate ($AgNO_3$) were from Fluka. All were employed without further purification.

Procedure

The treatment for paper background reduction has been described in detail elsewhere [11]. Briefly, strips of chromatography paper were water extracted in a soxhlet apparatus for eight hours, introduced into quartz tubes and exposed to ultraviolet radiation for the same period of time. The strips were then removed and cut in

rectangular pieces (10 × 17 mm) to fit in the sample holder [20].

The analyte solutions were prepared in ethanol–water (10:90, v/v). By means of a microliter syringe, 3 μl of analyte were deposited on the surface of the paper substrates. In some cases, the paper had been previously spotted with 3 μl of HA solution or with 3 μl of surfactant followed by 3 μl of HA solution. The spotted substrates were vacuum dried at room temperature for approximately one hour and placed in a desiccator with P_2O_5 until measurement time. Possible light effects were prevented by covering the desiccator with aluminum foil. Prior to measurements, a flow of dry nitrogen was directed to the surface of the paper substrate for five minutes. All RTP intensities and spectra were recorded under a continuous flow of dry nitrogen to avoid possible quenching effects from oxygen and moisture [4,5].

RESULTS AND DISCUSSION

Most of the compounds selected for our studies included substituted indoles of biological interest. Determination of indolecarboxylic acids and predominantly indole-3-yl acids has long been a subject of interest in the field of plant biology [21–23] and in the medical area [24–26]. As a result, the RTP characteristics of indole, 3-methylindole, 5-methoxyindole, indole-3-acetic acid (IAA), 5-hydroxyindole-3-acetic acid (5HIAA), indole-2-carboxylic acid (I2CA) and indole-3-carboxylic acid (I3CA) have already been studied [27–31]. The SSRTP determinations were performed in a wide variety of substrates which include sodium acetate pellets [27], filter paper [28], anion-exchange filter paper [29,30], and cellulose pretreated with sodium citrate [31].

Table 1 relates the RTP characteristics of the above mentioned indoles and 5-methoxyindole-3-acetic acid (5MeIAA) on chromatography paper previously treated for background reduction. The effect of substituents caused on the RTP emission of indoles can be estimated by comparing the maximum wavelengths of the spectra and the analyte to background signal ratios (I_A/I_B).

TABLE 1

RTP characteristics of several indoles on low background substrate

Compounds [a]	λ_{exc} [b] (nm)	λ_{em} [b] (nm)	I_A/I_B [c]
Indole	288	477	1.2
3-Methylindole	290	480	1.1
5-Methoxyindole	288,290,372	462	5.9
I2CA	236,297	488	121
I3CA	281	459	2.6
IAA	284	453	2.1
5HIAA	236,299	455	6.6
5MeIAA	234,296	461	7.4

[a] Concentration used was 10^{-1} M. Spectra uncorrected for instrumental response. [b] If more than one peak was observed in the excitation spectra, the one with maximum intensity is underlined. [c] I_A = phosphorescence intensity of analyte, I_B = phosphorescence intensity of substrate. Six determinations of anlyte signals and respective blanks were employed to calculate I_A/I_B. The presicion observed was within 10 to 15%.

The differences observed in the maximum emission peaks show the important role played by the nature of the substituent group and its position in the heterocyclic ring to establish the triplet state energy of biogenic indoles. With the exception of 3-methylindole, the I_A/I_B ratios were higher for substituted compounds than the one obtained for indole. Excluding the methyl group, all the other substituents have the ability to establish hydrogen bonds with the hydroxyl groups of the paper substrate. Since hydrogen bonding (HB) increases the matrix rigidity, it is expected to observe higher RTP emission from molecules with higher probability of establishing this kind of interaction.

In addition to HB, the position of the substituent group in the heterocyclic ring also needs to be considered. The phosphorescence signal of I2CA, for instance, is approximately 47 times higher than the one emitted by I3CA. Taking a closer look at the resonance structures of I3CA, it can be noted that the carboxylic group in position 3C reduces the π electronic density in the I3CA heterocyclic ring [32]. When the same group is positioned in 2C, the withdrawing of π electrons from the ring does not occur [32]. As a result, electronic transitions to the triplet state have a higher probability to occur in I2CA than in I3CA. This effect, therefore, can be partially

TABLE 2

Phosphorescence enhancement factor for several indoles in the presence of heavy atoms and sodium dodecyl sulfate

Compound [a]	Heavy atom salt [b]	$\lambda_{exc}/\lambda_{em}$ [c] (nm)	No NaDS f [d]	NaDS f [e]
Indole	NaI	276/442	7.8	35.1
3-Methylindole	$TlNO_3$	285/488	7.5	21.1
5-Methylindole	NaI	288/464	3.6	6.4
I2CA	$TlNO_3$	294/490	15.4	14.7
I3CA	$TlNO_3$	279/433	23.8	34.9
IAA	NaI	281/442	29.0	33.0
5HIAA	NaI	294/444	28.9	64.8
5MeIAA	NaI	290/448	14.8	29.3

[a] Concentration used was 10^{-4} M. [b] For HA salt concentration see text. [c] Excitation (λ_{exc}) and emission (λ_{em}) maxima in the presence of HA. [d] HA enhancement factor in the absence of NaDS. [e] HA enhancement factor in the presence of NaDS. See text for f calculations.

responsible for the higher RTP signal emitted by I2CA.

Heavy atom and surfactant effects

The effect of HA ions on the RTP emission of the indoles was studied by taking four inorganic salts with general phosphorescence enhancers [33,34]. 1 M NaI, 0.1 M $TlNO_3$, 0.5 M $Pb(NO_3)_2$ and 0.5 M $AgNO_3$ solutions were prepared in ethanol–water (50/50, v/v) and spotted on the paper substrate prior to analyte deposition. The RTP signals in the presence of HA were then compared to those obtained in the absence of inorganic salts. When Pb(II) and Ag(II) were added to the matrix of the phosphor, no enhancement was observed. The addition of Tl(I) and iodide, on the other hand, resulted in enhancements ranging from 3.6 to 29 times depending on the analyte. 3-Methylindole, I2CA and I3CA were the only ones to show higher enhancements with Tl(I). All the other indoles emitted higher RTP intensities in the presence of iodide. The best HA enhancer for each compound is related in Table 2. The enhancement factors (f) were calculated dividing the net analyte signal in the presence of HA by the net analyte signal in the absence of HA. The lack of excitation peaks below 240 nm for I2CA, 5HIAA and 5MeIAA in the presence of HA is probably due to matrix prefilter effects [11]. NaI and $TlNO_3$ strongly absorb in the ultraviolet range where these peaks are located and cut off the intensity of the excitation energy.

The HA efficiency in the presence of NaDS was tested by spotting a 2% surfactant solution (ethanol–water, 50:50, v/v) on the paper substrates prior to HA and analyte deposition. NaDS concentration was chosen based on preliminary tests run in our laboratory. Employing indole as a model compound, we observed that higher surfactant concentrations than 2% deteriorated the analyte-to-background signal ratio. Since our observations were in agreement to previously reported data involving other kinds of compounds [15,16], we employed this surfactant concentration throughout all our studies. The last column of Table 2 shows the HA enhancement factors obtained in the presence of NaDS. The effectiveness of the HA enhancer was increased in all cases but I2CA. For this compound, the enhancement factors obtained with and without surfactant are statistically similar ($P = 0.05$; $N = 6$). Probably, Tl(I) ions increased I2CA phosphorescence quantum yield to a maximum value in the absence of NaDS. As a consequence, no further enhancement was possible even after the addition of the surfactant. Finally, no significant modifications in the RTP spectra of the studied compounds were observed due to NaDS addition. The maximum excitation and emission wavelengths were the same as those observed in the absence of surfactant within the variations of instrumental response (±2 nm).

Analytical figures of merit

Table 3 gives the AFOM obtained under experimental conditions for maximum RTP emission. The HA salts employed for each compound were the ones related in Table 2. With the exception of I3CA, all the indoles showed calibration curves with linear dynamic ranges (LDR) extended over two orders of magnitude. As expected, the slopes of the log–log calibration plots were close in unity, indicating a linear correspondence between phosphorescence intensity and analyte concentration. The correlation coefficients of the analytical curves showed that the precision was satisfactory. Relative standard devi-

TABLE 3

Analytical figures of merit of several indoles in the presence of heavy atom and sodium dodecyl sulfate

Compound [a]	LDR [b]	Slope [c]	Correlation coefficient	LOD [d] (ng)
Indole	3.5×10^2	0.93	0.994	7.5
3-Methylindole	1.1×10^2	0.95	0.988	11.4
5-Methoxyindole	3.7×10^2	0.98	0.999	1.2
I2CA	5.4×10^2	0.99	0.999	0.9
I3CA	6.7×10^2	0.98	0.976	7.2
IAA	5.8×10^2	1.10	0.998	0.9
5HIAA	2.1×10^2	0.87	0.999	2.7
5MeIAA	8.8×10^2	0.98	0.984	1.2

[a] Experimental conditions for maximum RTP signal (see text). [b] Linear dynamic range (LDR) is estimated by dividing the upper linear concentration by the limit of detection. [c] Calculated from the plot log I_p versus log C, where I_p = phosphorescence intensity and C = analyte concentration. [d] See text for limits of detection (LOD) estimates. Calculated for 3 μl sample solution.

ations ranged from 10 to 15% being better at medium and higher analyte concentrations. The limits of detection (LOD) were calculated from the equation $c = ks_b/m$, were the standard deviation of the blank average (s_b) for 16 determinations, the slope of the calibration curve (m), and $k = 3$ [35] were employed. The obtained values ranged from 0.9 (I2CA and IAA) to 11.4 ng (3-methylindole) and were comparable to those previously reported on a variety of solid substrates [27–31]. Von Wandruszka and Hurtubise [27] obtained a 50 ng LOD for 5HIAA on sodium acetate pellets. Employing iodide as a HA, Winefordner and co-workers [29,30] detected ng levels of indole, 3-methylindole, 5-methoxyindole, IAA and I2CA on DE-81 anion-exchange paper. Finally, Kuroda et al. [31], estimated 5HIAA and IAA concentrations to the pmol level on cellulose and alumina substrates, both in the presence of sodium acetate. The sensitivity obtained with our method, therefore, strongly suggests the use of low background paper and NaDS as a general matrix for the SSRTP analysis of biogenic indoles.

Conclusions

The advantages of using NaDS in the RTP analysis of biogenic indoles are shown in this paper. With the exception of I2CA, the HA efficiency was improved in all cases. The highest improvements were observed among those compounds that showed comparatively low RTP intensities in the presence of HA salts (indole and 3-methylindole). The originally high RTP signal of I2CA, on the other hand, did not have any improvement in the presence of the surfactant. These observations indicate that the efficiency of NaDS decreases in compounds with high phosphorescence quantum yields. Based on the λ_{exc} and λ_{em} maxima obtained, it can be noted that the present method is not specific for any of the studied compounds. If a selective analysis of a mixture containing these indoles is desired, a preliminary separation step will be necessary. Possibly, the method could be used as a detection technique for liquid chromatographic analysis [36,37].

The authors thank the Conselho Nacional de Desenvolvimento Cientifico e Tecnologico-CNPq for financial support. They also thank Martha P. Cloutier Dobal for linguistic advise.

REFERENCES

1 M. Roth, J. Chromatogr., 30 (1967) 276.
2 E.M. Schulman and C. Walling, Science, 178 (1972) 53.
3 E.M. Schulman and C. Walling, J. Phys. Chem., 77 (1973) 902.
4 T. Vo-Dinh, Room Temperature Phosphorimetry for Chemical Analysis, Wiley, New York, 1984.
5 R.J. Hurtubise, Solid Surface Luminescence Analysis: Theory, Instrumentation, Applications, Dekker, New York, 1981.
6 S.L. Wellons, R.A. Painter and J.D. Winefordner, Spectrochim. Acta, 30A (1974) 2133.
7 E.M. Schulman and R.T. Parker, J. Phys. Chem., 81 (1977) 1932.
8 J.L. Ward, E.L. Yen-Bower and J.D. Winefordner, Talanta, 28 (1981) 119.
9 R.P. Bateh and Winefordner, Talanta, 29 (1982) 713.
10 D.L. McAleese and R.B. Dunlap, Anal. Chem., 56 (1984) 600.
11 A.D. Campiglia and C.G. de Lima, Anal. Chem. 59 (1987) 2822.
12 W. White and P.G. Seybold, J. Phys. Chem., 81 (1977) 2035.
13 S.P. McGlynn, J. Daigre and F.J. Smith, J. Chem. Phys., 39 (1963) 675.

14 C.G. de Lima, M.M. Andino and J.D. Winefordner, Anal. Chem. 58 (1986) 2867.
15 G. Ramis Ramos, M.C. Garcia Alvarez-Coque, A.M. O'Reilly, I.M. Khasawneh and J.D. Winefordner, Anal. Chem., 60 (1988) 416.
16 M.C. Garcia Alvarez-Coque, G. Ramis Ramos, A.M. O'Reilly and J.D. Winefordner, Anal. Chim. Acta, 204 (1988) 247.
17 L.M. Perry, A.D. Campiglia and J.D. Winefordner, Anal. Chem. Acta, 415 (1989) 225.
18 L.M. Perry, A.D. Campiglia and J.D. Winefordner, Anal. Chem., 61 (1989) 2329.
19 J.J. Aaron, A.D. Campiglia and J.D. Winefordner, Anal. Chim. Acta, 236 (1990) 257.
20 A.D. Campiglia and C.G. de Lima, Anal. Chem., 60 (1988) 2165.
21 M. Bottger, K.C. Engvild and P. Kaiser, Physiol. Plant., 43 (1978) 62.
22 M. Wurst, Z. Prikryl and V. Vancura, J. Chromatogr. 191 (1980) 129.
23 V. Sjut, J. Chromatogr., 209 (1981) 107.
24 A.P. Graffeo and B.L. Karger, Clin. Chem., 22 (1976) 184.
25 M.H. Joseph and H.F. Baker, Clin. Chim. Acta, 72 (1976) 125.
26 N. Seiler, J. Chromatogr., 143 (1977) 221.
27 R.M.A. von Wandruszka and R.J. Hurtubise, Anal. Chem., 49 (1977) 2164.
28 S.L. Meyers and P.G. Seybold, Anal. Chem., 51 (1979) 1609.
29 J.J. Aaron, M. Andino and J.D. Winefordner, Anal. Chim. Acta, 160 (1984) 171.
30 M. Andino, J.J. Aaron and J.D. Winefordner, Talanta, 33 (1986) 27.
31 N. Kuroda, H. Nohta and Y. Ohkura, Anal. Chim. Acta, 197 (1987) 169.
32 L.A. Paquette, Principles of Modern Heterocyclic Chemistry, Benjamin, New York, 1968.
33 I.M. Jakoviljevic, Anal. Chem., 49 (1977) 2048.
34 T. Vo-Dinh and J.R. Hooyman, Anal. Chem., 51 (1979) 1915.
35 G.L. Long and J.D. Winefordner, Anal. Chem., 55 (1983) 713A.
36 A.D. Campiglia, A. Berthod and J.D. Winefordner, J. Chromatogr., 508 (1990) 37.
37 A.D. Campiglia, J.J. Laserna, A. Berthod and J.D. Winefordner, Anal. Chim. Acta, 244 (1991) 215.

Analytica Chimica Acta, 287 (1994) 95–100
Elsevier Science B.V., Amsterdam

Study of naphthalene and phenanthrene by microemulsion room-temperature phosphorimetry

Wei-Jun Jin, Yan-Sheng Wei, Wen-Sheng Duan and Chang-Song Liu

Department of Chemistry, Shanxi University, Taiyuan 030006 (China)

Su-She Zhang

Centre Laboratory, Shanxi Academy of Agriculture Science, Taiyuan 030006 (China)

(First received 29th April 1993; revised manuscript received 11th October 1993)

Abstract

The effect of pH on the deoxygenation rate and phosphorescence intensity in microemulsion systems was studied. It was found that more intense room-temperature phosphorescence (RTP) can be obtained and the deoxygenation time can be decreased from more that 30 min to less than 100 s if the pH is maintained in the range 7–7.5. In addition, with increase in sodium sulphite concentration the deoxygenation rate increased. Other conditions such as the concentrations of sodium dodecyl sulphate and thallium(I) nitrate were investigated in detail. For the results, the microemulsion RTP of naphthalene and phenanthrene was improved. Limits of detection of 1.3×10^{-7} mol l^{-1} for naphthalene and 7.0×10^{-8} mol l^{-1} for phenanthrene were achieved.

Keywords: Phosphorimetry; Naphthalene; Phenanthrene

Micelle-stabilized room-temperature phosphorimetry has useful applications for the determination of polycyclic aromatic hydrocarbons (PAHs), which occur widely in the environment [1–4]. However, not only is the procedure for preparing samples relatively time consuming, but also the solubilizing capability of micelle solutions for some PAHs with very low polarity is limited. Therefore, Ramos et al. [5] proposed the use of a microemulsion aqueous solution of the analyte in an apolar solvent to circumvent these problems. A microemulsion is a stable, optically transparent monodisperse system of 10–20-nm diameter droplets intermediate in size between an emulsion and a micelle. Microemulsions are formed spontaneously when appropriate amounts of water, apolar solvent, surfactant and co-surfactant are mixed together. If an apolar analyte is first dissolved in an apolar solvent and gently mixed with alcohol and an aqueous solution of the surfactant, a clear microemulsion will be obtained in a few seconds.

Chemical deoxygenation with sodium sulphite is very convenient compared with the use of nitrogen because no foaming occurs. The effect of pH on the deoxygenation rate and efficiency of sodium sulphite is strong as the SO_3^{2-} concentration is related to the H^+ concentration in the system [3,4]. In this paper, the effect of pH and other factors on the microemulsion room-temperature phosphorescence (RTP) of naphthalene and phenanthrene is reported.

Correspondence to: C.-S. Liu, Department of Chemistry, Shanxi University, Taiyuan 030006 (China).

SSDI 0003-2670(93)E0575-R

EXPERIMENTAL

Apparatus

All recordings of uncorrected luminescence spectra and measurements of RTP intensities were carried out with a RF-510 spectrofluorimeter (Shimadzu), equipped with a thermostated cell holder. pH measurements were carried out with a PHS-3C pH meter (Shanghai Overseas Chinese Instrumental Factory).

Reagents

Naphthalene (Shanghai First Reagent Factory) of LR grade was recrystallized three times. Phenanthrene was of LC grade from Fluka. Sodium dodecyl sulphate (SDS) (Shenyang Reagent Factory) of CR grade was recrystallized twice from warm 95% ethanol. A 0.5 mol l^{-1} SDS solution was prepared. Thallium(I) nitrate, sodium sulphite, sulphuric acid, *n*-heptane and 1-pentanol were all of analytical-reagent grade. Sodium sulphite aqueous solution was prepared just before use. Water was doubly distilled in a sub-boiling still.

Procedure

A microemulsion stock solution of 5×10^{-3} mol l^{-1} naphthalene or phenanthrene was prepared by dissolving 0.0320 g of naphthalene or 0.0446 g of phenanthrene in 0.5 ml of *n*-heptane, adding 0.5 ml of 1-pentanol and diluting to 50 ml with 0.5 mol l^{-1} SDS. The concentrations of *n*-heptane and 1-pentanol were 1% (v/v).

A 0.1-ml aliquot of naphthalene or phenanthrene stock microemulsion, 0.9 ml or 0.7 ml, respectively, of 0.5 mol l^{-1} SDS, 0.7 ml of 0.25 mol l^{-1} thallium(I) nitrate, 0.1 ml of 0.5 mol l^{-1} sodium sulphite and 0.8 ml or 0.5 ml, respectively, of 0.02 ml l^{-1} sulphuric acid were pipetted in turn into a 10-ml volumetric flask and diluted to volume with water. If a precipitate appears in the flask after thallium(I) nitrate is added, the flask can be warmed before other reagents are added until the precipitate disappears. After thorough mixing, the flask was placed in a constant-temperature bath (20 ± 1°C) for 10 min, then spectra were recorded or luminescence intensities were measured with a 1-cm quartz fluorescence cell. The excitation and emission wavelengths of naphthalene and phenanthrene are 285 and 515 nm and 294 and 480 nm, respectively.

RESULTS AND DISCUSSION

Luminescence spectra

Luminescence spectra of naphthalene are shown in Fig. 1a. Spectra 1 and 2 were obtained using the conditions given in this paper and in [5], respectively. The residual fluorescence peak of naphthalene is at 340 nm. The phosphorescence excitation peak is at 285 nm and the emission

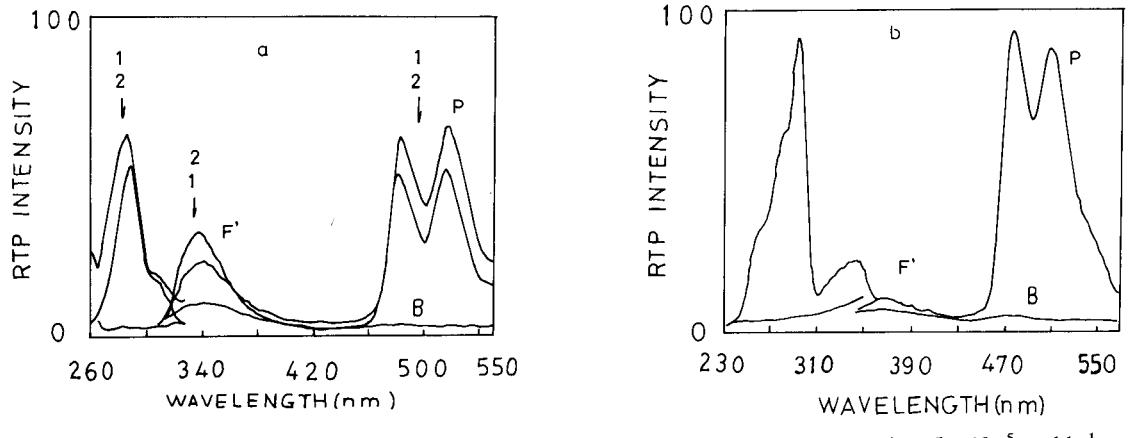

Fig. 1. Luminescence spectra of (a) naphthalene and (b) phenanthrene. Analyte concentration, 5×10^{-5} mol l^{-1}; gain, coarse (fine) 50 (50); slits, 10 nm (both excitation and emission). Spectra 1 and 2 correspond to the conditions given in this paper and in [5], respectively. P = RTP intensity; F′ = residual fluorescence intensity; B = background.

peaks are at 485 and 515 nm. Luminescence spectra of phenanthrene are shown in Fig. 1b. The residual fluorescence peak is at about 370 nm. The phosphorescence excitation peak is at 294 nm and the emission peaks are at 480 and 510 nm.

Effects of n-heptane and 1-pentanol concentrations on system stability and RTP intensities

The results indicate that stable and homogeneous microemulsions can be obtained in the range 0.5–3% (v/v) *n*-heptane or 1-pentanol. Hence 1% *n*-heptane and 1-pentanol were used throughout this work. After dilution, the *n*-heptane and 1-pentanol concentrations in the final solutions were 0.01%. Under these conditions, stable and the most intense RTP can be obtained, and the residual fluorescence is weaker than the RTP.

Effect of SDS and thallium(I) nitrate concentrations on RTP intensities

Mixing *n*-heptane, 1-pentanol and SDS aqueous solution results in the formation of oil-in-water (o/w) microemulsion. The microemulsion droplets have a spherical structure resembling that of micelles and contain a sizeable hydrocarbon core, in contrast to aqueous micelles, thus providing a highly apolar environment for dissolving relatively high concentrations of hydrophobic molecules with dimensions approaching those of many micelles [6].

In the microenvironment, phosphors, e.g., PAHs, are protected and escape partially or entirely from quenching caused by collisional deactivation. For forming spherical aggregates containing a hydrocarbon core, surfactant, the SDS concentration must be sufficient to reach or exceed a critical concentration such as the critical micelle concentration (CMC) in the micelle system. However, the critical concentration of SDS in microemulsions is unknown. The present results indicate that more intense RTP can be obtained when the SDS concentration is increased to 5×10^{-2} mol l^{-1} for naphthalene or 4×10^{-2} mol l^{-1} for phenanthrene. This must have exceeded the SDS critical concentration in microemulsions because the CMC of SDS is less than about 9×10^{-3} mol l^{-1} in a micelle system containing thallium(I) ions [1]. The RTP intensity shows a slow decrease when the SDS concentration is more than 5×10^{-2} or 4×10^{-2} mol l^{-1} for naphthalene or phenanthrene , respectively. This may be attributed to a transition of the microemulsion structure from spherical to another shape because the spherical aggregates may have a greater protecting ability against phosphors and the quenching action caused by impurities [2], especially the latter because phosphorescence is more susceptible to impurities. The residual fluorescence intensities increase slightly with increase in SDS concentration. This may be attributed mainly to the increase in viscosity because the susceptibility of fluorescence to impurities is poorer than phosphorescence.

The results show that the thallium(I) nitrate concentration corresponding to the maximum RTP intensity is 1.75×10^{-2} mol l^{-1} for both PAHs. The RTP intensity increases steadily with increasing thallium(I) nitrate concentration in the range 0–1.75×10^{-2} mol l^{-1} and decreases slightly at higher thallium(I) nitrate concentrations because the quenching action of Tl^+ on phosphors plays a major role in contrast to its heavy atom effect. However, Tl^+ as a heavy atom always causes fluorescence quenching. Therefore, the residual fluorescence intensity always decreases with increase in Tl^+ concentration. The decrease in fluorescence is rapid with less than 0.75×10^{-2} mol l^{-1} Tl^+ and becomes slow with more than 0.75×10^{-2} mol l^{-1} Tl^+.

The intensity ratios between the most intense phosphorescence and residual fluorescence peaks obtained under the same experimental conditions are $I_{P(515\ nm)}/I_{F(340\ nm)} = 5.1$ for naphthalene and $I_{P(480\ nm)}/I_{F(370\ nm)} = 7.1$ for phenanthrene.

Effect of pH and sodium sulphite concentration on RTP intensities and deoxygenation time

As shown in Fig. 2, the most intense RTP can be obtained at pH 7.1 for naphthalene or 7.5 for phenanthrene. The pH generally has little effect on the residual fluorescence of PAHs.

As shown in Fig. 3, with increasing pH from 7.1 to 8.9, the deoxygenation time increases rapidly and the RTP intensity decreases. At pH

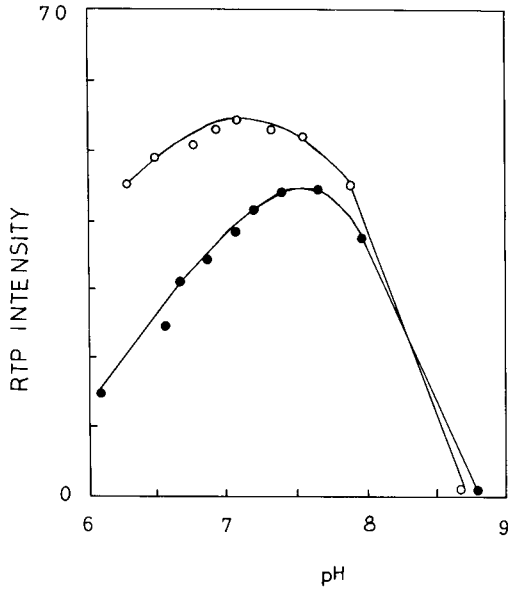

Fig. 2. Effect of pH on RTP intensities of (●) naphthalene and (○) phenanthrene.

8.9, RTP was induced only after the solution had been placed in a thermostat for 45 min. However, at pH 7.1 or 7.3 the RTP signals appeared immediately on excitation without placing the solution in thermostat. Similar results were obtained at pH < 7.1.

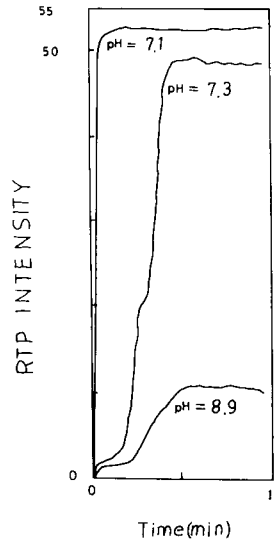

Fig. 3. Effect of pH on deoxygenation rate. Sodium sulphite concentration, 1×10^{-2} mol l^{-1}. Operation at room temperature (12°C). Before the time scan was begun under excitation, at pH 8.9 the solution must be placed in a thermostat for 45 min (no H_2SO_4 was added to the system for adjusting pH), otherwise no phosphorescence signal can be observed. The time scan can be begun at once at pH 7.1 or 7.3.

Figure 4 shows that the deoxygenation time decreases with increase in sodium sulphite concentration under the conditions given in this pa-

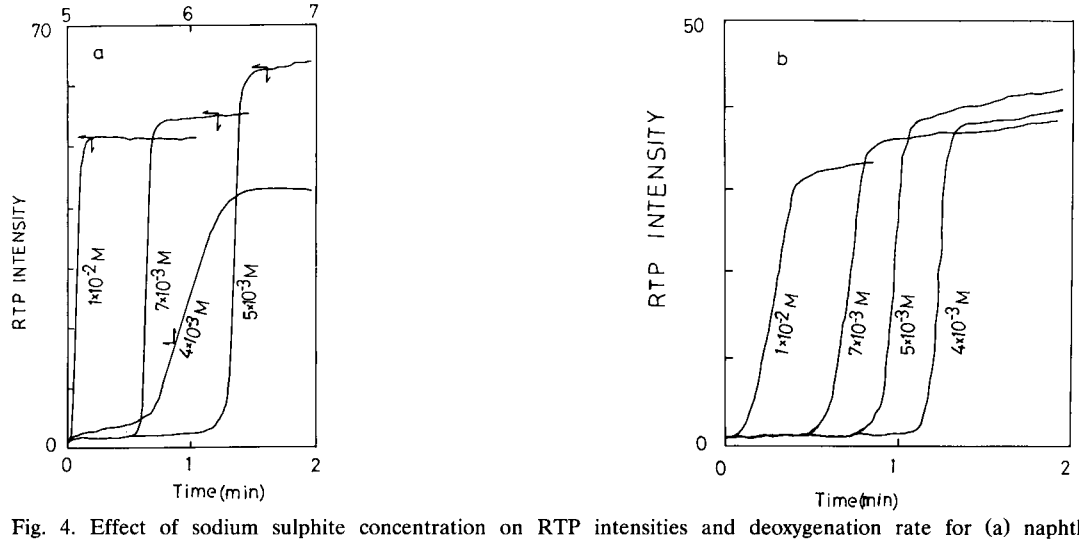

Fig. 4. Effect of sodium sulphite concentration on RTP intensities and deoxygenation rate for (a) naphthalene and (b) phenanthrene. The time scan was begun at once when the solution was ready. Concentration of sulphuric acid added: (a) 1.6×10^{-3} and (b) 1.3×10^{-3} mol l^{-1}.

TABLE 1
Calibration characteristics

Compound	Linear dynamic range (mol l^{-1})	Slope (log–log)	Relative coefficient	Detection limit [a] (mol l^{-1})	R.S.D. [b] (%)
Naphthalene	5.0×10^{-7}–2.0×10^{-5}	0.865	0.998	1.3×10^{-7}	5.6
Phenanthrene	3.0×10^{-7}–2.0×10^{-5}	0.940	0.998	7.0×10^{-8}	4.0

[a] Concentration corresponding to a signal three times the standard deviation of the blank. [b] $n = 10$; concentration levels: 4×10^{-6} mol l^{-1} (naphthalene) and 2×10^{-6} mol l^{-1} (phenanthrene).

per. In contract, the deoxygenation time is lengthened with decrease in sodium sulphite concentration. The most intense RTP is obtained with a sodium sulphite concentration of 5×10^{-3} mol l^{-1}. However, there is a decrease in phosphorescence intensity at higher sodium sulphite concentrations because excess Na^+ ions displace Tl^+ ions which are associated on the surface of the microemulsion droplets. A further decrease in the Tl^+/Na^+ ratio in the system gives rise to a decrease in the heavy atom effect of Tl^+ and leads to a decrease in phosphorescence intensity [7,8].

Chemical deoxygenation of sodium sulphite is based on the redox reaction

$$2SO_3^{2-} + O_2 \rightleftharpoons 2SO_4^{2-} \quad (1)$$

Clearly, the above the experimental results are a comprehensive result of the following equilibrium reactions:

$$SO_4^{2-} + 2H^+ + 2e \rightleftharpoons SO_3^{2-} + H_2O \quad (2)$$

$$SO_3^{2-} + H^+ \rightleftharpoons HSO_3^- \quad (3)$$

$$O_2 + 4H^+ + 4e \rightleftharpoons 2H_2O \quad (4)$$

Under acidic conditions at pH < 7, the reducing ability of sulphite ion is decreased because of the formation of HSO_3^-. Under basic conditions at pH > 7.5, although the sulphite ion concentration is higher, the reduction potential of the O_2–H_2O electrode pair is decreased, so the oxidizing ability of oxygen becomes weak. Both effects decrease the deoxygenation rate and the RTP intensity. Therefore, a moderate pH should be maintained in order to accelerate the deoxygenation reaction and enhance the RTP intensity.

Effect of temperature on RTP intensities

The RTP intensities decrease almost linearly with increase in temperature. The decrease is greater in a microemulsion system than in a micelle system [4] when the temperature increases by 5°C. The residual fluorescence intensities decrease slightly with increase in temperature. These effects are mainly related to molecular thermal motion and intermolecular energy conversion. The molecular thermal motion causes collisional deactivation of the phosphors.

Calibration data

Calibration graphs of log P vs. $-\log C$, where P is the relative phosphorescence intensity and C the concentration in mol l^{-1} of naphthalene and phenanthrene were obtained. The regression equations for naphthalene and phenanthrene are $\log P = 5.69 + 0.865 \log C$ and $\log P = 6.76 + 0.940 \log C$, respectively. Their characteristics are given in Table 1.

Conclusion

These experiments indicate that not only can RTP signals be enhanced but also the deoxygenation rate can be increased when the pH is kept under control. Hence the time of analysis can be greatly shortened. Under the conditions adopted in this work the microemulsion RTP of naphthalene and phenanthrene shows good analytical characteristics. The microemulsion RTP of other PAHs, e.g., fluoranthene and pyrene, and effect of dynamic factors on their RTP are under study.

This work was supported by the NNSF of China and the Youth Science Foundation of Shanxi Province.

REFERENCES

1 L.D. Cline Love, M. Skrilec and J.G. Habarta, Anal. Chem., 52 (1980) 754.
2 M.E. Diaz Garcia and A. Sanz-Medel, Anal. Chem., 58 (1986) 1436.
3 Y.S. Wei, C.S. Liu and S.S. Zhang, Fenxi Huaxue, 18 (1990) 228.
4 W.J. Jin and C.S. Liu, Microchem. J., 48 (1993) 94.
5 G.R. Ramos, I.M. Khasawneh, M.L. Garcia-Alvarez-Coque and J.D. Winefordner, Talanta, 35 (1988) 41.
6 E. Pelizzetli and E. Pramauro, Anal. Chim. Acta, 169 (1985) 1.
7 N.E. Nugara and A.D. King, Jr., Anal. Chem., 61 (1989) 1431.
8 W.J. Jin and C.S. Liu, Anal. Chem., 65 (1993) 863.

Analytica Chimica Acta, 287 (1994) 101–109
Elsevier Science B.V., Amsterdam

Synthesis, properties and applications of silica-immobilized 8-quinolinol

Part 1. Characterization of silica-immobilized 8-quinolinol synthesized via a Mannich reaction

Chi-Ren Lan and Mo-Hsiung Yang

Institute of Nuclear Science, National Tsing Hua University, 30043 Hsinchu (Taiwan)

(Received 9th February 1993; revised manuscript received 27th September 1993)

Abstract

A one-step Mannich reaction has been developed for the immobilization of 8-quinolinol on aminopropylsilica gel that results in a product exhibiting a capacity of 466 ± 20 μmol g^{-1} for copper(II) ions. Capacity measurements were made by copper(II) uptake and elemental analysis. Characterization of the silica bound ligands in this synthetic context including IR spectrometry, ^{13}C NMR spectrometry, acid–base properties and stabilities were presented. The effect of pH on the extraction of copper(II), nickel(II) and cadmium(II) for silica-immobilized 8-quinolinol was also evaluated.

Keywords: Atomic emission spectrometry; Infrared spectrometry; Nuclear magnetic resonance spectrometry; Mannich reaction; 8-Quinolinol; Silica-immobilized 8-quinolinol

Recently, the development of silica gel modified with organofunctional groups has been the subject of considerable interest. 8-Hydroxyquinoline (8-quinolinol), a well-characterized reagent that reacts with over 60 metal ions to form metal chelates, has been used extensively in the past in immobilized form for the preconcentration of trace levels of metal ions from natural water to increase the analyte concentrations to levels that are easily and reliably measured [1,2]. Several recent research efforts have been made to find methods of immobilizing 8-quinolinol chelating agent on the silica gel. It appears to be a conventional preparation of silica-immobilized 8-quinolinol materials by utilizing one of two similar procedures described by Hill [3] and Sugawara et al. [4]. These steps in the synthesis usually involve the silylation of the silica surface with an aliphatic aminosilane, aromatic nitro group introduction, reduction of immobilized $ArNO_2$ to immobilized $ArNH_2$, diazonium salt formation and termination in a diazo coupling to 8-quinolinol. In addition to the obviously long preparation time (3 to 4 days) involved for these immobilization procedure, the reduction step has been reported also to be troublesome [5].

Several less circuitous routes to silica-immobilized 8-quinolinol have been developed. Marshall and Mottola [6] simplified the immobilization procedure by direct introduction of the aromatic amine in the silylation step, which retained the diazo coupling reaction. Subsequently, Lührmann et al. [7] developed a single step reaction to immobilize 8-quinolinol on aminopropylsilica gel.

Correspondence to: M.-H. Yang, Institute of Nuclear Science, National Tsing Hua University, 30043 Hsinchu (Taiwan).

SSDI 0003-2670(93)E0589-Y

In this method it involved the base-catalyzed reaction of 5-chloromethyl-8-quinolinol with aminopropylsilica gel. More recently, Pyell and Stork [8] presented a more efficient method for the preparation of a silica-immobilized 8-quinolinol by immobilization of 8-quinolinol on aminopropylsilica gel by a two-step Mannich reaction.

All the improved methods of immobilization have taken steps forward to decrease the preparation time and yielded products having relatively high exchange capacities. In this study, a more direct route to the preparation of silica-immobilized 8-quinolinol is described, which employs a procedure involving a one-step Mannich reaction allowing the interaction of silica immobilized aliphatic amine, aldehyde and 8-quinolinol. The resulting silica gel has been characterized by a series of measurements including IR spectrometry, ^{13}C NMR spectrometry and acid–base properties and stabilities. The effect of pH on the extraction of copper(II), nickel(II) and cadmium (II) for the prepared material was also evaluated.

EXPERIMENTAL

Reagents

All water used was treated by reverse osmosis, mixed-bed ion exchange unit deionization, followed by double distillation in a quartz still equipped with a quartz immersion heater. All reagents were analytical grade and were used as received.

Silica gel (TLC grade, Strem Chemicals) of 100–200 mesh, 500 $m^2\ g^{-1}$ surface area, and 0.75 ml g^{-1} pore volume was used as a support for immobilizing the chelating agents. 3-Aminopropyltriethoxysilane (Strem) and 8-hydroxyquinoline (8-quinolinol) (Merck) were used.

Apparatus

A Thermo Jarrell Ash inductively coupled plasma atomic emission spectrometer, Model ICAP 9000, was used in this work. Introduction of the trace metal concentrates to the simultaneous ICP-AES was accomplished by means of an ultrasonic nebulizer (CETAC Model U-5000) equipped with a desolvation apparatus. All pH measurements were carried out with a Radiometer (Copenhagen) Model pHM82 pH meter equipped with a glass pH electrode. Microanalysis for nitrogen was performed using an Elemental Analyzer (Heraeus CHN-O-RAPID). FT-IR spectra and ^{13}C NMR spectra of silica-bound ligands were recorded by using a Model Bomen MB100 FT-IR spectrometer and a Bruker MSL200 MHz solid-state NMR spectrometer, respectively.

Immobilization procedures

The proposed method by direct attachment of 8-quinolinol to an immobilized aliphatic amine was used for the preparation of silica-immobilized 8-quinolinol. First, a 10% (v/v) solution of 3-aminopropyltriethoxysilane (100 ml) in dry acetone was allowed to incubate with the silica gel (20 g) for 4 h in a sealed PTFE flask at 45°C [3]. After the reaction was completed, the modified silica gel was transferred to a filter funnel, the reaction mixture was filtered, and the solid was washed with dry acetone and dried under vacuum.

The dried aminopropylsilica gel was added to an ethanolic solution (100 ml) containing 8-quinolinol (0.1 M) and formaldehyde (0.1 M). The immobilization reaction was completed when this mixture was refluxed in a flask for 3 days. The 8-quinolinol derivative of silica gel was filtered and washed with ethanol, and the solid was ready for use after washing three times with 100 ml of 1 M HCl and then with deionized, doubly distilled water to remove HCl.

Capacity determinations

A copper uptake study was used as an indirect measure of the amounts of active amine or immobilized 8-quinolinol on the silica surface. In this capacity determination, the amounts of copper used should be 20–50 times that of the bound ligand [9]. Typically, 40 ml of 0.05 M standard stock solution of Cu(II) in 0.2 M acetate buffer (pH 5) was added to approximately 0.2 g of the bound ligand species in a 80-ml screw cap vial. This mixture was then allowed to equilibrate for 30 min, after that an aliquot of the liquid was removed. The capacities of the dried materials

were estimated by the changes of copper concentrations in the removed solution quantified by ICP-AES. The capacity value obtained by using this procedure was believed to be the best estimate of the amount of 8-quinolinol present.

An elemental analyzer was also used for nitrogen measurement, which gave a direct measure of the total amount of immobilized organic materials.

Stability studies

The procedure described in the previous literature [6] was employed for investigating both hydrolytic and storage stability of silica-immobilized 8-quinolinol. Hydrolytic stability studies were carried out by mixing approximately 0.5 g of silica-immobilized 8-quinolinol with 40 ml of appropriate solution adjusted to integral pH values between approximately −1 and 12. After equilibration for a period of time (3–5 days), the solid was removed by filtration, rinsed with water and dried. The capacity of the dried material was then determined. Storage stability was checked by measuring the capacity of modified silica gel after 4 months of dry storage in a desiccator.

Potentiometric titrations

Potentiometric pH titrations were performed on the prepared materials. Usually, about 2 g of silica-immobilized 8-quinolinol, HCl washed and vacuum dried, was suspended in 100 ml of water containing 0.1 M $NaClO_4$. The titration was then performed with 0.01 M hydrochloric acid or 0.01 M sodium hydroxide under a nitrogen atmosphere by using a 10-ml buret. Because the reaction of the bound ligands with each increment of titrant occurs very slowly, in each titration a reasonably stable pH value can be achieved after about 2 h of stirring. The pH vs. volume titration curves of the prepared material were constructed by following the described procedure.

pH dependence of adsorption

A radiotracer technique was used to determine the adsorption yields of metal ions in sea water as a function of pH. The radiotracers ^{64}Cu, ^{63}Ni and ^{115}Cd used in this work were prepared by irradiating pure metals of interest in the open pool nuclear reactor of Tsing Hua University (THOR). The pH-dependence study was performed with the use of 20 ml of sea water sample. 1 ml of radiotracer solution was first added to the sea water sample, and the pH was then adjusted to a fixed value with HCl and NaOH. About 0.2 g of silica-immobilized 8-quinolinol was subsequently added to the sea water sample, and the whole was subjected to shaking for 30 min. The sample was then filtered through a 0.45-mm porosity filter (Gelman Sciences) under vacuum suction. The adsorption yield of the element of interest was calculated based on the activities measurement of the separated solution and the orignal solution using a Ge(Li) detector connected to a multichannel analyzer or a NaI(Tl) scintillation detector system.

RESULTS AND DISCUSSION

Immobilization reaction

A two-step synthetic procedure for silica-immobilized 8-quinolinol is shown in Fig. 1. Initially, 3-aminopropyltriethoxysilane is employed as the original group attached to the silica gel by the usual silylation reaction under mild acetone condition. The second step in the sequence used to prepare a bound chelating agent involves coupling the 8-quinolinol to the aminopropylsilica gel with a Mannich reaction. The silylation reaction, which is believed to proceed via condensation of a surface silanol with an ethoxy group of the 3-aminopropyltriethoxysilane, has been the reaction studied most because in the majority of cases the original attached moiety is the desired species. Fulcher et al. [5] reported that as the silica gel

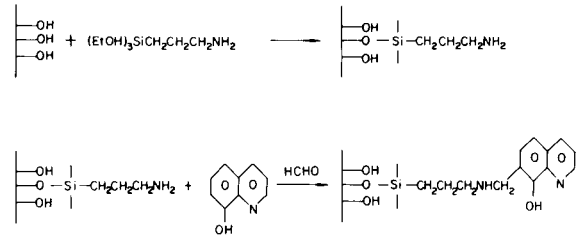

Fig. 1. Synthesis scheme for preparing silica-immobilized 8-quinolinol.

was degassed prior to vigorous refluxing with the silane in the presence of toluene, it would appear to yield aminopropylsilica gel with greater surface coverage. According to our practical experience, however, we did not find the same result when performing the silylaton in a degassed and toluene refluxing condition. Marshall and Mottola [6], on the contrary, even obtained a product with slightly higher capacities by the silylation process without degassing. In any case, in the silylation reaction it was necessary to keep the system dry so that the same capacity results would be obtained. This is because the significant amounts of water in the system could lead to hydrolytic condensation of the aminopropylsiloxane. In this work, the silylation reaction was done simply within a sealed PTFE flask and a mild, non-refluxing acetone condition was selected.

The Mannich reaction, although the exact mechanism is not known with certainty, is an effective method for the preparation of 8-quinolinol Mannich base [10,11]. The feasibility of applying the Mannich reaction to immobilize chelating agent as 8-quinolinol to silica gel has been already studied by Pyell and Stork [8]. In [8] study a two-step process was described first by allowing interaction of silylated silica gel with aqueous formaldehyde and in the subsequent step by adding the resulting product to dry ethanol solution containing 8-quinolinol for further completion of the immobilization reaction. In this study modified procedure following that of Phillips and Fernando [11] was employed for the direct immobilization of 8-quinolinol on the aminopropylsilica gel by the one-step Mannich reaction as is shown in Fig. 1.

Capacity studies

The capacities of the material prepared by various coupling reaction times ranging from three hours to five days were investigated. For the purpose of comparison, capacities were determined both by the copper(II) uptake method [5,6] and nitrogen determination [6,14]. The capacity values obtained for silica-immobilized 8-quinolinol, which can be used as an indicator of differences in the reaction efficiencies, are shown in Table 1. It can be seen that the capacities increase significantly upon increasing the reaction times. The capacity values obtained by nitrogen determination were found in reasonable agreement with those obtained by the copper(II) uptake method, and serve as evidence to indicate that copper forms a 1:1 complex with bound 8-quinolinol.

TABLE 1

Capacity measurement of the synthesized silica-immobilized 8-quinolinol prepared by different coupling reaction times

Reaction time	Capacity determination by	
	Cu(II) uptake (μmol g^{-1})	Nitrogen determination (μmol g^{-1})
3 h	255	286
6 h	303	371
24 h	391	464
3 d	456	514
5 d	489	536

There may be argument as to the validity on the capacity values which are obtained both by the copper uptake and nitrogen determination methods. For the capacity measurement by the copper uptake method, Jezorek et al. [9] have reported that the free amine site in the silica-immobilized 8-quinolinol product would apparently eventually react with Cu(II) ion at pH 4 and may thus result in higher capacity value than expected. In order to ensure that the Cu(II) was extracted only by the immobilized 8-quinolinol ligands, aminopropylsilica gel blanks were run during the capacity determinations. A similar situation may occur for the measurement of bound 8-quinolinol capacity based upon micro-determination of nitrogen and carbon. As was pointed out in the report of Kolstad et al. [14], many N- and C-containing byproducts, as impurities covalently bound to the silica surface, may be left when the conventional synthetic scheme is employed for the preparation of silica-immobilized 8-quinolinol. Consequently, it will result in an erroneously high value of bound 8-quinolinol capacity based on calculation of the measured carbon and nitrogen contents. However, with the modified coupling reaction for direct immobilization of 8-quinolinol to the aminopropylsilica gel described, the possibility of residual organic

byproducts bound to the silica surface would be considerably reduced. The capacity measurement even by nitrogen determination on the material prepared by the modified method can, therefore, reflect the true 8-quinolinol capacity. The reasonable agreement of the capacity values measured both by the methods of copper uptake and nitrogen determination, though the values obtained by the former method are seen consistently somewhat higher than the latter one, can serve to support the above explanation.

IR spectrometry

Although chemically modified silica gels have not been extensively studied by IR spectrometry, it is recognized that the IR spectrum can provide useful information for the existence of specific functional groups bonded on the silica substrate. In order to obtain IR spectra with absorption bands of useful amplitude, pellet samples without any inert binder material (e.g., KBr) were prepared.

Since much of the IR spectra were obscured by matrix absorptions which were caused by the absorbed water vapor, Si–O bands and light scattering problems by the silica gel matrix [5], the range that is useful only between 1750 and 1350 cm^{-1}. Figure 2 shows the FT-IR spectra of 3-aminopropylsilica gel and silica-immobilized 8-quinolinol. The spectrum obtained for the bound

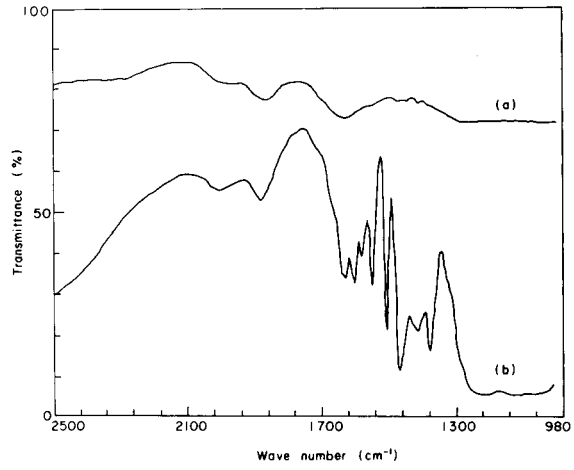

Fig. 2. FT-IR of (a) 3-aminopropylsilica gel and (b) silica-immobilized 8-quinolinol.

TABLE 2

^{13}C chemical shifts of aliphatic amine, 8-quinolinol and bound species

		Literature value[13] δ (ppm)	Measured value [a] δ (ppm)	
		aliphatic amines	3-Aminopropyl silica gel	Silica-immobilized 8-quinolinol
Propylamine	C-1	44.6	42.0	42.9
	C-2	27.4	22.2	21.0
	C-3	11.5	9.98	10.2
Methylamine	C-4	28.3		31.3
Quinoline				
	C-2	150.8		
	C-3	121.6		
	C-4	136.0		
	C-4a	128.7		
	C-5	128.3		135 ± 20
	C-6	126.9		
	C-7	129.7		
	C-8	130.0		
	C-8a	149.0		

[a] Measured by the Bruker MSL 200 MHz solid state NMR system.

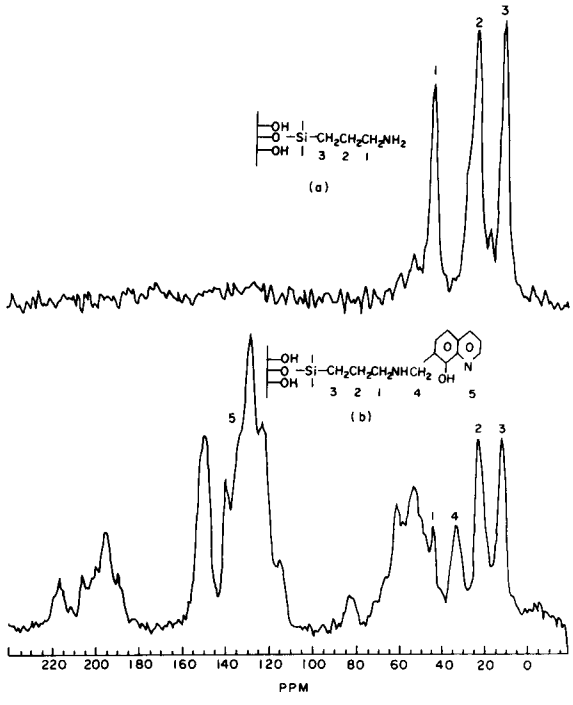

Fig. 3. Solid state ^{13}C NMR of (a) 3-aminopropylsilica gel and (b) silica-immobilized 8-quinolinol.

amine species is of little use analytically. With the introduction of additional organic functional grounds onto the bound species, more information becomes available. Some significant absorption bands are observed in Fig. 2b, among them the phenol OH band at 1375 cm^{-1} and 1462, 1504, 1578 and 1600 cm^{-1} from aromatic C = C and C = N bands [5,12].

^{13}C NMR spectrometry

In the synthetic aspects of these silica-bound ligands, the ^{13}C NMR spectra obtained for monitoring specific functional groups are of considerable importance. Figure 3 shows the solid state ^{13}C NMR spectra of 3-aminopropylsilica gel and silica-immobilized 8-quinolinol, and the measured peak values are given in Table 2. For comparison, the literature values of the ^{13}C NMR peak for aliphatic amines and quinoline are also listed in the table. Three sharp peaks appear at δ 42.0 ppm, 22.2 ppm and 9.98 ppm for the bound propylamine. For the ^{13}C NMR spectrum of silica-immobilized 8-quinolinol, aside from all the features of the 3-aminopropylsilica gel several characteristic peaks appear. Among them a multiple peaks occurred at δ 135 ± 20 ppm (quinoline) and an additional sharp peak at δ 31.3 ppm (methyl amine) [13]. These ^{13}C NMR and IR spectra can, therefore, be used as a good indication of the immobilization of 8-quinolinol onto the 3-aminopropylsilica gel via the one step Mannich reaction.

Potentiometric titrations

8-Quinolinol is an amphiprotic compound which owes its acid–base properties to the presence of both a weakly acid and a weakly basic functional group. In this study, potentiometric pH titration of aqueous suspension was performed to measure the pK_a values of silica-immobilized 8-quinolinol. Figure 4 shows the titration curves as a function of pH. To account for the effect of pH, the following reaction had been considered as a possible equilibrium for the following structure changes with pH [11].

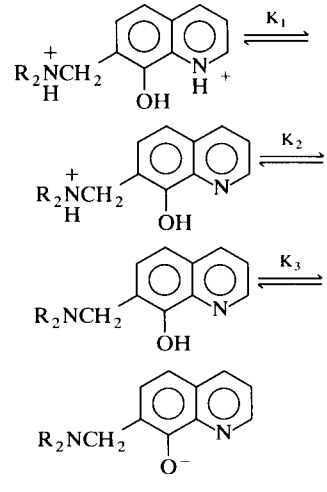

In strongly acidic solution the substituted 8-quinolinol may bind up to two protons, the first on the 8-quinolinol nitrogen and a second on the side chain nitrogen. The deprotonation process of the substituted 8-quinolinol is different from that of 8-quinolinol in which it has no equilibrium corresponding to K_2. The estimated values of pK_a for the bound 8-quinolinol from the titration curve are shown in Table 3. The literature values

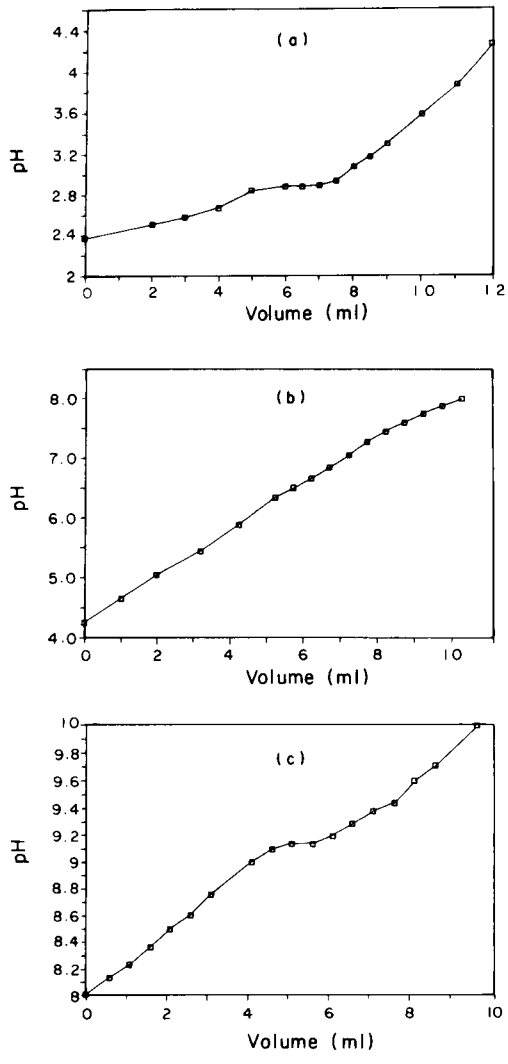

Fig. 4. Titration curves of acid washed silica-immobilized 8-quinolinol at ionic strength of 0.1 M $NaClO_4$. (a) pH 2.0–4.6 (b) pH 4.0–8.5 (c) pH 8.0–10.0. (titrant: 0.01 M NaOH).

for 8-quinolinol and its derivatives which are known to be the most similar free ligands available [11] are also listed in the table for comparison. The value of pK_1 obtained for the silica-immobilized 8-quinolinol titrated with sodium hydroxide is basically in good agreement with the substituted 8-quinolinol. However, the titration at pK_2 is complicated by the fact that protons are being removed from residual hydroxyl groups on the surface of silica gel throughout the titration process, and would thus result in a difficulty estimation of pK_2.

The relatively low pK_3 value observed for the silica-immobilized 8-quinolinol compared to other substituted 8-quinolinols may be attributed to the fact that bound 8-quinolinol is not situated far from the silanol groups and may therefore tend to "lie down" on the surface of silica gel [6]. It could be expected that a reaction of cyclic hydrogen bonding would occur between the hydroxyl group of 8-quinolinol and the rather acidic residual silanol groups. This may, consequently, considerably reduce the effective base strength of the bound 8-quinolinol in these resulted cyclic structures than those relatively free 8-quinolinol derivatives in aqueous solution in which weaker hydrogen bonding would occur only from reactions with water molecules.

Stability studies

The investigation of the hydrolytic stability of the silica-immobilized 8-quinolinol prepared is aimed at obtaining a more complete understanding of the bound chelating agent and giving a firm foundation for prediction of the behavior of this material in a variety of different circumstances. Table 4 indicates the percentage of the original capacity that is retained after equilibration with solutions of integral pH values between −1 and 12. It can be seen that the silica-immobilized 8-quinolinol is very stable even in strongly acidic solution, after equilibration for 3–5 days.

The capacity at pH 12 increases to a level higher than its original value. In the course of investigating the effect of pH on the hydrolytic

TABLE 3

Apparent acid dissociation constants for various 8-quinolinol derivatives

	pK_1	pK_2	pK_3	Ref
8-Quinolinol	4.9	—	9.7	11
Dimethylaminomethyl 8-quinolinol	2.4	7.8	11.0	11
Diethylaminomethyl 8-quinolinol	2.9	7.2	11.3	11
Piperidylmethyl 8-quinolinol	1.7	6.6	10.9	11
Silica-immobilized 8-quinolinol	2.9	ND[a]	9.2	this work

[a] ND = Exact pK value cannot be estimated from the titration curve shown in Fig. 4b.

TABLE 4
Hydrolytic stability of silica-immobilized 8-quinolinol

pH	Percent of original capacity	
	3 days	5 days
−1	104	–
0	105	96
1	101	103
2	103	99
3	99	101
4	98	96
5	97	97
6	96	95
7	96	102
8	99	100
9	96	97
10	97	98
11	98	106
12	117	133
Original capacity, μmol g^{-1}	466	459

stability of the material, at high pH range (pH 11 and 12), rapid hydrolysis of the silica framework occurred, which was indicated by the appearance of dark green color of the resulted solution. The dark green color both found in the dissolved solution and in the remaining precipitate may serve to indicate that the bound ligands remain intact. As shown in Table 4, the capacity of the material after treated with solution of various pH (from −1 to 11) not only does not appear to decrease with increasing the pH as expected, but also to a level higher than its original value at pH 12. This contradicts the previous report for the similar material prepared via other synthetic route using aminophenyltrimethoxysilane [6]. This observation may be explained on the basis of the "shielding effect" exhibited by the bound ligand for protecting the silica framework from the attack of hydroxide ion. Although the bound ligand can, to some extent, suppress the hydrolysis of the silica framework, a certain amount of dissolution of the material will not be avoidable, as is indicated by the appearance of dark green color of the solution. In view of the fact that the bond formation between silica particles tends to occur under the catalytic reaction of hydroxide ion [15], it is thus reasonable to expect that those species which are newly formed from dissolution of the silica-immobilized 8-quinolinol will undergo repolymerization to form new bond silica. Because of the "shielding effect" exerted by the ligand on the hydrolytic reaction, the newly polymerized silica can be expected to have a higher ligand density per unit surface area of the particle, and can consequently result in a higher capacity at high pH range as is shown in Table 4.

The storage stability of this material was found to be excellent as essentially no change in capacity occurred (within experimental error $\leqslant 5\%$) over a 4 month period.

pH dependence of adsorption

A study of the effect of pH on the extraction of trace metals from natural water revealed that quantitative recoveries of the sought trace metals could be obtained. The results for the extractability of Cu^{2+}, Ni^{2+} and Cd^{2+} as a function of pH are given in Fig. 5. Extractions of Cu, Ni and Cd ions gradually increased from pH 2 to 5 and then levelled off.

The direct synthetic route proved to be an efficient method for the preparation of silica-immobilized 8-quinolinol. The silica-immobilized 8-quinolinol studied offers a relatively higher exchange capacity, it is possible to demonstrate that the chelating silica gel has a great potential for the preconcentration of metal ions from natural water. Subsequently, the feasibility of using a column packed with silica-immobilized 8-quinolinol for the on-line preconcentration of trace metals from sea water in a flow system

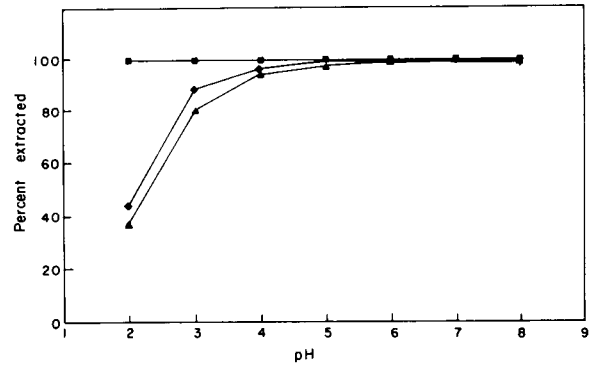

Fig. 5. Extraction of metal ions as a function of pH for the silica-immobilized 8-quinolinol. (■) Cu, (◆) Ni, (▲) Cd.

followed by determination by ICP-AES will be investigated in later experiment (Part 2, Ref. 16).

The National Science Council of Republic of China is acknowledged for the support of this work (Grant No. NSC 79-0208-M007-40).

REFERENCES

1 M.M. Guedes da Mota, F.G. Romer and B. Griepink, Fresenius' Z. Anal. Chem., 287 (1977) 19.
2 R.E. Sturgeon, S.S. Berman, S.N. Willie and J.A.H. Desaulniers, Anal. Chem., 53 (1981) 2337.
3 J.M. Hill, J. Chromatogr., 76 (1973) 455.
4 K.F. Sugawara, H.H. Weetall and G.D. Schucker, Anal. Chem., 46 (1974) 489.
5 C. Fulcher, M.A. Crowell, R. Bayliss, K.B. Holland and J.R. Jezorek, Anal. Chim. Acta., 129 (1981) 29.
6 M.A. Marshall and H.A. Mottola, Anal. Chem., 55 (1983) 2089.
7 M. Luhrmann, N. Stelter and A. Kettrup, Fresenius' Z. Anal. Chem., 332 (1985) 47.
8 U. Pyell and G. Stork, Fresenius' J. Anal. Chem., 342 (1992) 281.
9 J.R. Jezorek, C. Fulcher, M.A. Crowell, R. Bayliss, B. Greenwood and J. Lyon, Anal. Chim. Acta, 131 (1981) 223.
10 M. Tramontini, Synthesis, (1973) 703.
11 T.P. Phillips and Q. Fernando, J. Am. Chem. Soc., 75 (1953) 3768.
12 R.M. Silverstein, G.C. Bassler and T.C. Morrill, Spectrometric Identification of Organic Compounds, 3rd edn., Wiley, New York, 1977.
13 E. Breitmaier and W. Voelter, ^{13}C NMR Spectroscopy: Methods and Applications in Organic Chemistry, 2nd edn., Verlag Chemie, New York, 1978.
14 A.K. Kolstad, P.Y.T. Chow and F.F. Cantwell, Anal. Chem., 60 (1988) 1565.
15 R.K. Iler, The Chemistry of Silica, Wiley, New York, 1979.
16 C.-R. Lan and M.-H. Yang, Anal. Chim. Acta, 287 (1994) 111.

Analytica Chimica Acta, 287 (1994) 111–117
Elsevier Science B.V., Amsterdam

Synthesis, properties and applications of silica-immobilized 8-quinolinol

Part 2. On-line column preconcentration of copper, nickel and cadmium from sea water and determination by inductively-coupled plasma atomic emission spectrometry

Chi-Ren Lan and Mo-Hsiung Yang

Institute of Nuclear Science, National Tsing Hua University, 30043 Hsinchu (Taiwan)

(Received 9th February 1993; revised manuscript received 27th September 1993)

Abstract

The coupling of an on-line column preconcentration manifold with continuous flow ultrasonic nebulizer equipped with a desolvation system for simultaneous determination of metal ions by inductively coupled plasma atomic emission spectrometry (ICP-AES) is described. The silica-immobilized 8-quinolinol prepared by an improved synthetic route has been evaluated as a preconcentration material for metals in a flow system. Dynamic exchange capacities of this material were ascertained by determining the breakthrough volumes of radiotracer ^{64}Cu solution under different flow parameters. Optimization of the on-line column preconcentration with ICP-AES measurement was investigated. The feasibility of the proposed method was tested for the determination of Cu, Ni and Cd in open sea water samples. Results obtained for the determination of these elements in NASS-2 sea water sample agreed very well with certified values. The limits of detection based on a sample volume of 25 ml for Cu, Ni and Cd were 0.07, 0.054 and 0.016 ng ml^{-1}, respectively.

Keywords: Atomic Emission spectrometry; Flow system; On-line column preconcentration; Ultrasonic nebulizer; Waters

The determination of trace metal ions in sea water is important for environmental monitoring and for understanding their role in the biological and geochemical cycles of the oceans [1]. Recently, inductively-coupled plasma atomic emission spectrometry (ICP-AES) has been recommended for measurements of a large suite of elements in sea water [2]. Although the method is very sensitive, it sometimes poses problems for direct determination at the concentrations of most trace elements in sea water. The concentrations are generally low compared with their detection limits and the elements must be determined also in presence of large amounts of interfering matrix constituents [2,3]. Preconcentration of the trace metals prior to analysis may be mandatory and serves the dual purpose of removal of the interfering major elements and increasing the concentration of the trace elements. Thus, many processes such as solvent extraction [4,5], coprecipitation [6], sorption on chelating agents either on cellulose collector [7], C_{18} bonded silica gel [8] or chemically bound to a polymer chain [9–11], have been extensively studied with sea water. Each of the methods has its own advantages and the choice between them depends on the elements

Correspondence to: M.-H. Yang, Institute of Nuclear Science, National Tsing Hua University, 30043 Hsinchu (Taiwan).

SSDI 0003-2670(93)E0590-4

required to be analyzed and the method used for the detection of these elements.

During the enrichment and related steps, contaminants containing the desired trace elements may be introduced into the sample from the external source, and therefore minimization of contamination is required in order to achieve accurate analytical results, especially in inorganic trace analysis. On-line column preconcentration combined with flame atomic absorption spectrometry [12,13], inductively-coupled plasma atomic emission spectrometry [14,15], and inductively-coupled plasma mass spectrometry [15–18] are found to be useful in solving these complex analytical problems. These methods provide high enrichment factors and lower detection limits by selective extraction from the complex matrix. It not only helps in reducing the time, but also the closed system for sample handling makes it contamination-free.

In this study, metal ions released from an on-line preconcentration column containing silica-immobilized 8-quinolinol as described in Part 1 [19] are analyzed by simultaneous ICP-AES after ultrasonic nebulization. Optimization of instrumental operating conditions in ICP-AES analysis was studied, and the feasibility of on-line column preconcentration of trace amounts of Cu, Ni and Cd from sea water to decrease matrix problems was investigated. Subsequently, the proposed method which optimally combined the on-line column preconcentration with the ICP-AES measurement was employed for the determination of trace metals of interest in open sea water samples.

EXPERIMENTAL

Reagents

All water used was treated by reverse osmosis, mixed-bed ion exchange unit deionization, followed by double distillation in a quartz still equipped with an immersion heater. All reagents were analytical grade except the ammonia solution which was Merck ultra pure NH_3. High purity nitric acid and hydrochloric acid were prepared by subboiling distillation in a quartz still from reagent grade feed stocks. 0.5 M Ammonium maleate buffer solution was prepared and purified by passing through a column (50 × 4mm i.d.) packed with 0.5 g of silica-immobilized 8-quinolinol at a flow rate of 2 ml min^{-1}. The preparation of purified sea water was as follows. Coastal sea water collected was filtered through a 0.45-μm Millipore filter. After adjustment to pH 6, sea water was passed through the silica-immobilized 8-quinolinol column at a flow rate of 2 ml min^{-1} to remove metal impurities. The Merck Titrisol stock standard solution (1000 mg l^{-1}) of the elements of interest were diluted to the desired concentrations with purified sea water.

Open sea water samples from a vertical profile were collected from a station in the Pacific ocean (22° 35'N, 122° 10'E), by using Go-Flo sampling system (General Oceanics, USA). Sea water samples collected at required depths were obtained from the Institute of Oceanography, National Taiwan University. The sea water had been acidified to pH $\leqslant$ 2, and stored in precleaned polypropylene bottles. All sample preparations were carried out in a clean room equipped with laminar flow benches, providing a class 100 working environment.

All laboratory ware was thoroughly cleaned by soaking in nitric acid (1:1) at least for 24 h. Immediately prior to use, all acid washed ware was rinsed with deionized, double-distilled water.

Apparatus

The Thermo Jarrell Ash inductively-coupled plasma atomic emission spectrometer, Model ICAP 9000, was used for this work. Introduction of the trace metals concentrate for simultaneous analysis by ICP-AES was accomplished by means of an ultrasonic nebulizer (CETAC Model U-5000) equipped with a desolvation system. The instrumental operating conditions were shown in Table 1. The on-line preconcentration setup (Fig. 1) consisted of a Watson Marlow 502s minipulse peristaltic pump used for conveying dilute acid solution, two Dionex Model DQP-1 pumps used for transporting samples, buffer solution and acid eluant, two three way rotatory valves (V_1, V_2), and two silica-immobilized 8-quinolinol columns (50 × 4 mm i.d.). The measurement of transient

signals was performed by using the time scan mode, and the integration of peak area was done numerically. All pH measurements were carried out with a Radiometer Copenhagen Model pHM82 pH meter equipped with a glass pH electrode.

Column preparation

An empty column (Dionex) 50 × 4 mm i.d. was packed with silica-immobilized 8-quinolinol by the dry packing technique. The procedure consisted of a batch-wise addition of small amounts of chelating material, by hand, into a vertically mounted column. During filling, the outside of the column was tapped gently and the suction was conducted with a vacuum pump connected at the bottom end of the column, in order to facilitate settling of the particle to a dense packing and to prevent size segregation near the tube walls. The last step in column packing was to wash the column with 10 ml 1 M HCl–1 M HNO_3 mixture, 5 ml of maleate buffer solution, and then with deionized, double-distilled water. The same columns were used throughout the experiment.

Dynamic exchange capacity studies

A similar procedure, described by Marshall and Mottola [12], was employed for investigating the dynamic exchange capacities of the silica-immobilized 8-quinolinol column. The procedure for dynamic exchange capacities was performed by using radiotracer ^{64}Cu as the metal ion probe at pH 5. A test solution [137.5 μg ml^{-1}, Cu(II)] was passed through the column at various flow rates (0.5, 1, 2 and 3 ml min^{-1}). Fractions were collected in 10-ml vials at 2-ml intervals. The dynamic exchange capacities were ascertained by determining the breakthrough volumes of test solution, and the breakthrough volumes were calculated on 1% detection of relative activity of copper solution.

TABLE 1

Simultaneous ICP-AES conditions

Jarrell Ash ICAP 9000	
RF generator	
forward power	1.1 kW
reflected power	< 5 W
Gas flow	
argon coolant gas	18.0 l min^{-1}
argon plasma gas	0.5 l min^{-1}
argon carrier gas	0.8 l min^{-1}
Sample uptake rate	2.0 ml min^{-1}
View height (from coil)	18 mm

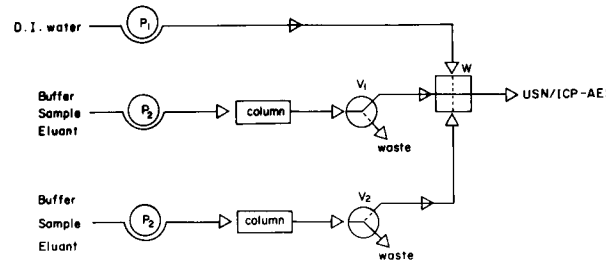

Fig. 1. Schematic diagram of manifold for the on-line column preconcentration for ICP-AES equipped with an ultrasonic nebulizer. P_1, peristaltic pump; P_2, DQP-1 pump; V_1 and V_2, three-way valves; W, four-way connector.

Sea water analyses

An ultrasonic nebulizer equipped with a desolvation system was used for the introduction of trace elements. The two-column on-line preconcentration manifold for these studies is shown in Fig. 1. In sea water analyses, one column was used for eluent to direct the output from the column to the ultrasonic nebulizer, and the other one served as a preconcentration column for introducing the sample solution. The preconcentration procedure was as following. Typically, the acidified sample (100 ml of sea water) was neutralized by using 10 ml buffer of 0.5 M ammonium maleate at pH 6.5. The buffered sample was passed through a silica-immobilized 8-quinolinol column (ca. 0.5 g dry weight, 200 mesh particle size) where some of the metals present in the sample were extracted. After a suitable washing time, the metal ions were eluted from the silica-immobilized 8-quinolinol column by introducing the 1 HCl–1 HNO_3 mixture through the acid injection valve. The eluted metals were determined by ICP-AES after ultrasonic nebulization. The resulting transient signals were recorded and integrated. The maximum flow rate allowed by the back pressure produced in the system was 2 ml min^{-1}.

RESULTS AND DISCUSSION

Dynamic exchange capacity studies

The initial total capacity of silica-immobilized 8-quinolinol is an important parameter which directly affects the feasibility of these materials used for the preconcentration of trace metals in natural water. It is usually measured under batch conditions in which an excess of a known metal ion is allowed to equilibrate with the solid chelating ion exchanger at a fixed pH and the total capacity is then determined by the amount of metal ion extracted [20]. However, in column operation, the dynamic exchange capacity is a more useful quantity. In this work, the dynamic exchange capacity of this material is ascertained by determining the breakthrough volumes of radiotracer ^{64}Cu solution by collecting the fractions and passing them directly to the Na(Tl) scintillation detector. Copper(II) is chosen as metal ion probe because it has a large formation constant with 8-quinolinol and has also been widely used in previous work [12,21]. A series of breakthrough curves for the column at various flow rates is shown in Fig. 2. Breakthrough occurs earlier at high flow rates and as the flow rate decreases the dynamic exchange capacity increases. At lower flow rates, more of the complexation sites are accessible for reaction since the longer residence

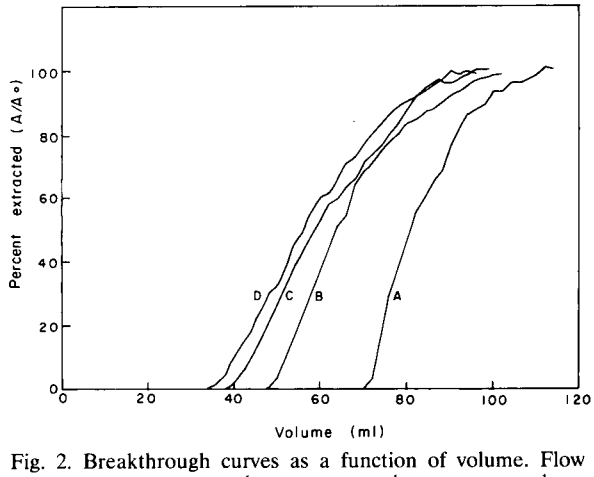

Fig. 2. Breakthrough curves as a function of volume. Flow rates are A: 0.5 ml min^{-1}; B: 1 ml min^{-1}; C: 2 ml min^{-1}; D: 3 ml min^{-1}. Test solution is 137.5 μg ml^{-1} Cu(II), pH 5. A/A_0: effluent activity/influent activity.

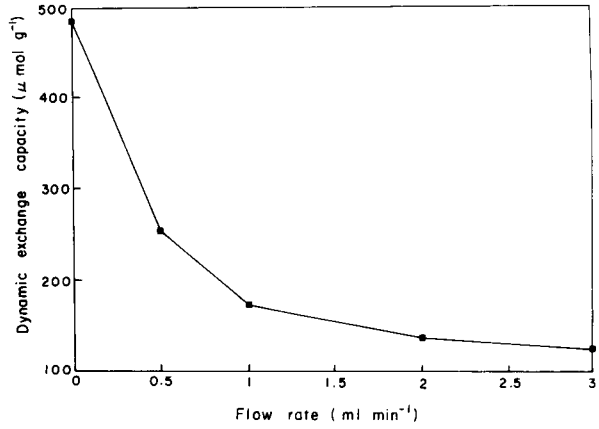

Fig. 3. Dynamic exchange capacity for copper(II) as a function of flow rate.

time of the solution in the column should increase the beneficial conditions for the rate of exchange, and then, should also result in a concomitant increasing in the dynamic exchange capacities. Figure 3 shows the dynamic exchange capacity as a function of flow rate. An approximate exponential decay in capacity is observed as the flow rate increases. At a flow rate of 2 ml min^{-1}, the dynamic exchange capacity is 138 μmol g^{-1}. For the silica-immobilized 8-quinolinol prepared by an improved synthetic route, having a relatively high exchange capacity, can be used for analytical separation of trace levels of metal ions in natural water.

Interferences studies

Elements such as calcium and magnesium in sea water at high concentrations often provide interferences in ICP-AES measurements. Thus it is desirable to investigate the extraction behaviors of different metal ions that might be presented in sea water samples. The results for the extractabilities of Cu, Ni and Cd elements in sea water as a function of pH have been investigated in Part 1 of this series [19].From these results, it is possible to concentrate trace metals completely when the investigated pH is higher than 4. Figure 4 shows the pH dependence of the signal responses of Ca and Mg retained in the column. The total amounts of Ca and Mg are estimated to be in the range of 1–3 μg, when 25 ml of sea water was passed

through the column. Generally, the dependences are similar to those obtained in the literature [12]. All the elements of interest and concomitants showed higher recoveries at high pH. However, as these extraction studies indicate that a pH 5–6 for the preconcentration of transition metal ions are effective since these ions will be combined with the immobilized ligands at such a pH, while significant amounts of alkaline earth ions will be excluded from chelation.

On-line column preconcentration / USN / ICP-AES

Berman et al. [22] reported that some trace metal ions in sea water could not be determined by ICP-AES with pneumatic nebulization using a 20-fold preconcentration as their levels in such concentrates remain below values at which reliable analysis could be performed. Fassel et al. [23], however, pointed out that a continuous flow ultrasonic nebulizer equipped with a desolvation system for generating dehydrated aerosol particles prior to their injection into analytical inductively coupled plasma could increase the detection sensitivity. However, difficulty may still be encountered for determination of trace metals in sea water by ICP-AES with pneumatic nebulization or ultrasonic nebulization due to high salt content in the sample. In order to reach the

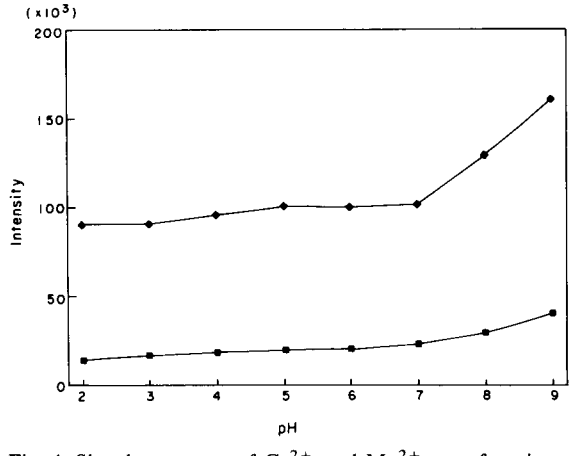

Fig. 4. Signal responses of Ca^{2+} and Mg^{2+} as a function of pH for the silica-immobilized 8-quinolinol. (♦) Ca^{2+}, (■) Mg^{2+}.

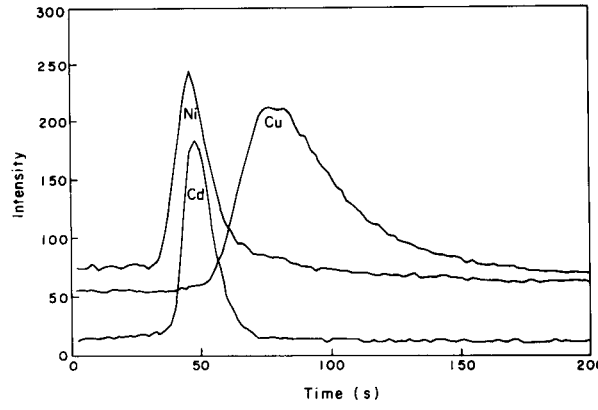

Fig. 5. Typical elution profiles for standard solution of Cu, Ni and Cd. The amounts of Cu, Ni and Cd in a 25 ml sea water sample are 125 ng, respectively.

required sensitivity as well as to avoid the interference caused by the high salt matrix, recent studies have indicated that an on-line column preconcentration technique combined with ICP-AES should be the most promising technique to sea water analyses [14,15].

Because many experimental variables are involved in the operation of the incorporation of an on-line column preconcentration/matrix separation system into a simultaneous ICP-AES equipped with ultrasonic nebulization set up, it is desirable to define the optimization steps that are taken to select compromise operating conditions. First, the compromise plasma operating conditions typically employed for simultaneous multi-element determination are used, then a compromise carrier gas flow and sample uptake rate that yielded the overall highest relative net intensity is selected for ultrasonic nebulizer. The instrumental parameters are given in Table 1. Figure 5 shows the elution characteristics of trace elements from silica-immobilized 8-quinolinol column using 1 M HCl–1 M HNO_3, the desorption of the collected trace elements at a flow rate of 2 ml min^{-1} is completed within 120 s.

Analysis of sea water

Table 2 gives the results for the recoveries of Cd, Ni and Cu from 10 ml of sea water spiked at total concentration of 100 ppb. Even at this low concentration there is nearly a 100% recovery

TABLE 2

Recovery tests carried out by spiking seawater samples with Ni, Cu and Cd (sample volume, 10 ml; ppb = $\mu g\ l^{-1}$)

	Ni		Cu		Cd	
	Spiked ($mg\ l^{-1}$)	Found ($mg\ l^{-1}$)	Spiked ($mg\ l^{-1}$)	Found ($mg\ l^{-1}$)	Spiked ($mg\ l^{-1}$)	Found ($mg\ l^{-1}$)
	100	101	100	99	100	102
	100	98	100	100	100	96
	100	99	100	102	100	100
Average:	99%		100%		99%	

(about 96–102%) for the three elements. In order to validate the method proposed in this study, a certified reference water (NASS-2, Seawater Reference Material for Trace Metals) from the National Research Council of Canada has been analyzed as a quality control material during the measurement of the elements of interest in the sea water. The analytical results are given in Table 3. The resulting values are in good agreement with the certified values. Since the preconcentration of other transition metal ions can also be effective with the immobilized 8-quinolinol at pH 5–8, the present on-line system can be expected to extend to the determination of these elements in the sea water samples.

In this study, the detection limit is defined as that concentration of analyte which gives a response equal to three times the standard deviation of the blank or background value. Blank values were measured by using sea water as the metal-free solution after passing through the silica-immobilized 8-quinolinol column. Analysis of three samples of the blank, gave the limits of detection of Cu, Ni and Cd based on a sample volume of 25 ml were 0.07, 0.054 and 0.016 ng ml^{-1}, respectively. Comparing these results with that obtained by the flow injection–ICP systems based on preconcentration with Chelex-100 resin [14,24], the detection power achievable in this work is 2–4 times better for the elements studied. Further comparison of the proposed method with the on-line preconcentration on either silica-immobilized 8-quinolinol [17] or Chelex-100 [18] followed by ICP-mass spectrometric (MS) determination reveals that in both cases the detection limits are low enough to permit the analysis of open sea water. With the ICP-MS method the preconcentration from NASS-2 sea water requires 10-ml aliquots, whereas 100-ml aliquots are needed in this work with ICP-AES as measuring instrument. The excellent resistance to swelling of silica with changes in solvents and acids is an advantage of silica-immobilized 8-quinolinol over polymer-based ion exchanger such as Chelex-100 [12]. The use of silica-immobilized 8-quinolinol, however, suffers from the disadvantage of rapid hydrolysis of the silica framework occurred at high pH range [19]. Thus, this tech-

TABLE 3

Analytical results for the determination of Ni, Cu and Cd in the reference standard seawater sample (NASS-2)

	Concentration ($\mu g\ l^{-1}$)		
	Ni^{2+}	Cu^{2+}	Cd^{2+}
Certified	0.257 ± 0.027	0.109 ± 0.011	0.029 ± 0.004
Found[a]	0.238 ± 0.038	0.119 ± 0.008	0.025 ± 0.006

[a] Results given are mean ± standard deviations ($n = 3$).

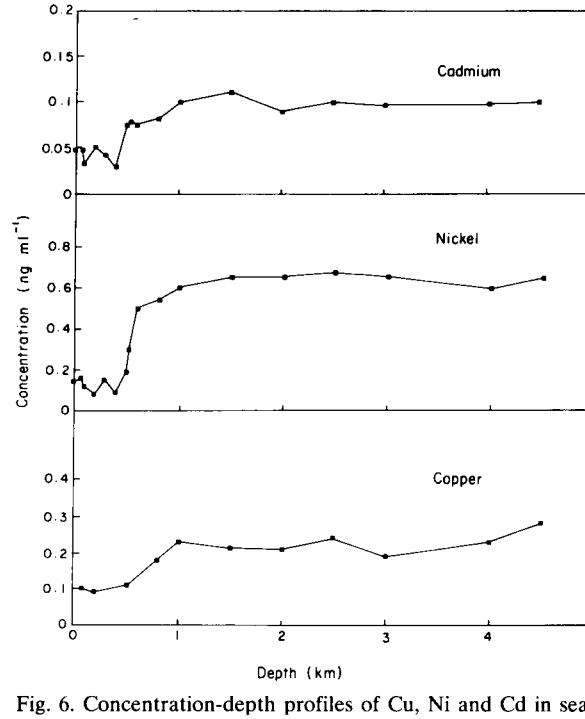

Fig. 6. Concentration-depth profiles of Cu, Ni and Cd in sea water.

nique is not applicable to all the sample solutions without a preliminary treatment prior to analysis.

The method proposed was subsequently employed for the determination of Cu, Ni and Cd in open sea water samples. The concentration-depth profiles of Cu, Ni and Cd in sea water collected from the Pacific Ocean are shown in Fig. 6. The concentrations of Cu, Ni and Cd are less depleted in surface sea water and enriched in the deep ocean. For the three metals, their characteristic vertical profiles presented in this work are similar to the vertical profiles investigated in the California current reported by Bruland et al. [25].

The authors wish to express their thanks to Professor S.C.Pai of the Institute of Oceanography, National Taiwan University for providing the open sea water samples collected from the Pacific ocean. We thank the National Science Council of the Republic of China for the support of this work (Grant No. NSC 81-0208-M007-106)

REFERENCES

1 G. Bearman, Ocean Chemistry and Deep-sea Sediments, 1st edn., Pergamon Press, New York, 1989.
2 M. Thompson and J.N. Walsh, Handbook of Inductively Coupled Plasma Spectrometry, 2nd edn., Chapman and Hall, New York, 1989.
3 T. Akagi, K. Fuwa and H. Haraguchi, Anal. Chim. Acta, 177 (1985) 139.
4 E. Mentasti, A. Nicolotti, V. Porta and C. Sarzanini, Analyst, 114 (1989) 1113.
5 J.M. Lo, Y.P. Lin and K.S. Lin, Anal. Sci., 7 (1991) 455.
6 M. Hiraide, T. Ito, M. Bara, H. Kawaguchi and A. Mizuike, Anal. Chem., 52 (1980) 804.
7 P. Burba and P.G. Willmer, Fresenius' Z. Anal. Chem., 329 (1987) 539.
8 H. Watanabe, K. Goto, S. Taguchi, J.W. McLaren, S.S. Berman and D.S. Russell, Anal. Chem., 53 (1981) 738.
9 R.E. Sturgeon, S.S. Berman J.A.H. Desaulniers, A.P. Mykytiuk, J.W. McLaren and D.S. Russell, Anal. Chem., 52 (1980) 1585.
10 C.J. Cheng, T. Akagi and H. Haraguchi, Bull. Chem. Soc. Jpn., 58 (1985) 3229.
11 V. Dupont, Y. Auger, C. Jeandel and M. Wartel, Anal. Chem., 63 (1991) 520.
12 M.A. Marshall and H.A. Mottola, Anal. Chem., 57 (1985) 729.
13 E. Beinrohr, M. Cakrt, J. Garaj and M. Rapta, Anal. Chim. Acta, 230 (1990) 163.
14 S. Caroli, A. Alimonti and F. Petrucci, Anal. Chim. Acta, 248 (1991) 241.
15 Z. Horvath, A. Lasztity and R.M. Barnes, Spectrochim. Acta Rev., 14 (1991) 45.
16 M.R. Plantz, J.S. Fritz, F.G. Smith and R.S. Houk, Anal. Chem., 61 (1989) 149.
17 D. Beauchemin and S.S. Berman, Anal. Chem., 61 (1989) 1857.
18 E.M. Heithmar, T.A. Hinners, J.T. Rowan and J.M. Riviello, Anal. Chem., 62 (1990) 857.
19 C.R. Lan and M.H. Yang, Anal. Chim. Acta, 287 (1994) 101.
20 M.A. Marshall and H.A. Mottola, Anal. Chem., 55 (1983) 2089.
21 N. Prakash, G. Csanady, M.R.A. Michaelis and G. Knapp, Mikrochim. Acta, 111 (1989) 257.
22 S.S. Berman, J.W. McLaren and S.N. Willie, Anal. Chem., 52 (1980) 488.
23 V.A. Fassel and B.R. Bear, Spectrochim. Acta, 41B (1986) 1089.
24 S.D. Hartenstein, J. Ruzicka and G.D. Christian, Anal. Chem., 57 (1985) 21.
25 K.W. Bruland, R.P. Franks, G.A. Knauer and J.H. Martin, Anal. Chim. Acta, 105 (1979) 233.

Analytica Chimica Acta, 287 (1994) 119–145
Elsevier Science B.V., Amsterdam

Limit of discrimination, limit of detection and sensitivity in analytical systems

Ricard Ferrús and Maria Rosa Egea

Escola Tècnica Superior d'Enginyers Industrials, Universitat Politècnica de Catalunya, Colom 11, E-08222 Terrassa, Barcelona (Spain)

(Received 8th February 1993; revised manuscript received 1st October 1993)

Abstract

The limit of discrimination is the minimum increase in analyte amount in the test portion which secures, with a high probability, analytical signals significantly different from those given by the original analyte amount. The analyte addition technique is applied to measure the limit of discrimination. The Hubaux and Vos methodology for measuring the limit of detection is followed to obtain the limit of discrimination from the plot of analytical signal vs. added analyte amount. According to Currie, the limit of discrimination in the matrix blank is the limit of detection. When matrix blanks are not available, the limit of detection can still be measured as the limit of discrimination in the solvent, provided that matrix effects are absent. This absence can be shown by comparison of the limits of discrimination in the laboratory sample, in an analyte solution giving about the same signal as the laboratory sample and in the solvent. This check is not possible in analytical systems showing a sensitivity change near the limit of detection. An extension of the Hubaux and Vos methodology is proposed for measuring the limit of detection in the presence of strong sensitivity changes. Four analytical methods showing sensitivity changes to different extents are applied for the sake of demonstration to determine the sulphate ion concentration in tap water. The Hubaux and Vos, Kaiser and method detection limit methodologies are compared. The differences between the analytical signal, analytical result and analyte amount standard are emphasized. Bias introduced by the calibration standards can be shown through erratic regression residuals.

Keywords: Limits of detection; Limits of discrimination; Sensitivity; Sulphate

Discrimination is binary classification after inspection. Because exhaustive inspection is generally excluded for economic reasons, classification of a lot [1] follows after inspection of representative samples. This introduces an uncertainty expressed as sampling variance. In addition, there is also the uncertainty bound to the inspection itself. Both sources of variation, sampling and inspection, are independent, and the total variance is the sum of the sampling plus inspection variances. The situations addressed in this paper are concerned with inspection by measurement of continuous variables.

The measurement of a continuous variable is always based on the assumed biunivocal relationship between a signal (scale reading, instrument response) and a level of the variable within a working or dynamic range. Strictly, the measurement consists in finding a standard that gives the same signal as the unknown. However, the number of available standards generating signals at different levels is necessarily limited. This is why a bracketing technique [2] is used, giving rise to the familiar calibration function, which gives the signal as a function of the level of the variable. From now on the variable is the analyte amount

Correspondence to: R. Ferrús, Escola Tècnica Superior d'Enginyers Industrials, Universitat Politècnica de Catalunya, Colom 11, E-08222 Terrassa, Barcelona (Spain).

SSDI 0003-2670(93)E0569-S

in the test portion [1], when performing a quantitative chemical analysis.

Because of the total variance quoted above, the signal relating to a given analyte amount is univocal only to some extent. This situation is dealt with by considering a signal range in which there is a high probability of finding the signal value generated from an analyte level in the laboratory sample. A biunivocal relationship still holds for the central signal value, X_0, of the signal distribution. The central value can be estimated as the mean of several signals arising from the same amount of analyte. This estimate should properly be quoted not as a single figure, but rather as an interval within which we are confident that the signal related to an analyte amount, q_0, lies [3]. Conversely, X_0 refers to q_0, the analyte amount in the test portion, which is estimated as an equivalent to X_0 through the calibration function. This estimation is the analytical result. It is different from q_0. For the purpose of this paper, the analytical result is just the analytical signal expressed in analyte amount units [4], the calibration function being used for this conversion. Calibration, whether it is remote (e.g., gravimetry), intermittent (e.g., molecular absorption spectrometry) or immediate (e.g., atomic absorption spectrometry), is always present in the analytical measurement process. Between the analytical signal and the analytical result there is always the calibration step. Both signal and result share the condition of a random variable. On the other hand, the analyte amount in the test portion is not a random variable. The only possible relationship between this amount and an analytical signal is when the latter stands as the limit of a probability interval for signals generated from the known analyte amount, i.e., from the standard. We shall always go here from standard to signal, never the other way round. Even in cases where it might seem that an analyte amount is derived from a signal, it will not be so, because the analyte amount will be assumed a priori as that giving rise to a signal interval limited by the signal value. Unfortunately, the difference between analytical result and analyte amount or concentration in the laboratory sample [1] is frequently overlooked. Liteanu and Rîcă avoided this pitfall by denoting the analysis result as c and the true value as either c' [5] or $\hat{c}$ [6].

Altshuler and Pasternak [7] pointed out the difference between the object of a measurement and the result of the measurement in a particularly misleading case, that of a radioactivity counter, because both the object and the result belong to the same physical quantity, i.e., events per unit time. In cases such as this it is customary to speak of the "measured" or "receiver" signal and of the "true" or "sender" signal. Fortunately, there is no need for such qualifications in chemical analysis, as the object of the measurement, either the analyte amount or its concentration, is clearly different from the "receiver" signal or instrumental response. On the other hand, the distinction between analyte amount q in the test portion and analyte concentration c' in the laboratory sample is irrelevant to the purpose of this paper. Only the former will be used here.

The discrimination of a lot is implemented by comparing with a critical value the analytical signal obtained from the statistical sample representing the lot. Obviously, this critical or decision value is always an analytical signal. It is important to consider how it is fixed. In discrimination through quantitative chemical analysis there is always a given analyte amount, q_0, taken as a reference. From previous information, which may include the use of standards, it is known that lots having q_0 in the test portion show a value X_0 as the most frequent signal. This is the central signal value pertaining to q_0. After sampling and measurement on an unknown, a mean value $\bar{X}$ results and it is compared with X_0, in order to decide whether the difference $\bar{X} - X_0$ can be explained as being due to the sampling/measurement variance only. Should this be the case it is said that the null hypothesis $\bar{X} - X_0 = 0$ cannot be rejected. This operation is called hypothesis testing. It is performed by comparing the statistic $(\bar{X} - X_0)/s$ (where s is the standard error of the difference $\bar{X} - X_0$) with a critical value obtained from a table prepared by statisticians. The use of the table implies the assumption of a statistical model describing the frequency distribution of signal values, X, as a function of the value. In this paper the assumed model is the Student t-distri-

bution. This assumption is usually safe when comparing means. The critical value to decide the outcome of the statistical test is a function of both the degrees of freedom in the standard error, s, and the accepted probability α of rejecting the null hypothesis when the analyte contents in the test portion is actually q_0. The critical value, X_c, is bound to the accepted probability α. Signals generated from q_0 and larger than X_c are expected to occur $100\alpha\%$ of the time. Rejecting the null hypothesis in this case is designed as an error of the first kind, or a type I error.

It is possible to make the drawbacks bound to this type of error more unlikely by choosing α sufficiently small, but then, by so doing, the possibility is increased of making an error of the second kind, or type II error, i.e. of concluding that the null hypothesis cannot be rejected, in a situation where the test portions have an analyte amount different from q_0, because the signal of the measurement under consideration does not surpass X_c, in the direction expected from the difference between q_0 and the actual amount. The probability of a type II error is denoted as β.

When the null hypothesis is discredited, it is frequently said that it should be rejected in favour of the alternative hypothesis, expressed as either $\bar{X} > X_0$ or $\bar{X} < X_0$. However, it would be better just to state that the null hypothesis is discredited, without mentioning the alternative hypothesis. Only in those cases where the discredit of $\bar{X} = X_0$ means $\bar{X} = X_p$, X_p being another central value, should the alternative hypothesis be considered. A familiar example of such a situation is the discrimination (diagnosis) of a patient population into two classes, healthy and ill [8]. Radiocarbon concentrations for living matter and fossil fuel carbon, or trace element concentrations characteristic of certain ore bodies, are quoted by Currie [9] as additional examples of alternative hypotheses fixed by Nature. The distance between the respective central values or centroids is determined for any analytical method, and the critical value is located somewhere between the centroids, in such a way that the losses to society, made up of medical care for the healthy plus non-acceptance of the ill, are set to a minimum. This situation is described by means of the receiver operating characteristic (ROC) curves, a methodology borrowed from the statistical theory of signal detection. The ROC curves give the probability, 1-β, of correct discrimination of a signal (i.e., the ill patient is discriminated as ill), as a function of the probability, α, of wrong discrimination of the background (i.e., the healthy patient is discriminated as ill). The parameter in the family of ROC curves is the discriminating power, defined as the ratio of the distance between centroids to s, the pooled standard deviation, taken as a measure of the scattering about the centroids. The use of the ROC graph begins with choosing an acceptable value for α, then a vertical line is drawn at this abscissa and the intercept with the curve having the corresponding discriminating power value gives, on the ordinate axis, 1-β, the power of the analytical method. Should the power be insufficient, i.e., β too large, it can be improved by decreasing the standard deviation of the measurement process. This is usually done by increasing m, the number of repeats to obtain $\bar{X}$, since the standard error of the mean is proportional to $m^{-1/2}$.

There is another situation where it is useful to consider explicitly an alternative hypothesis. It deals with the smallest signal difference, δ, that it is important to detect [10]. This minimum difference will be considered here from the point of view of quantitative chemical analysis. If q_0 is the analyte amount taken as reference for the null hypothesis, and X_0 its central signal value, another central value is defined as $X_p = X_0 + \delta$, while q_p is the analyte amount referred to by X_p. After deciding on economic grounds the value of α, a tentative value of m is proposed, and then the critical signal value to discriminate q_p from q_0, with probability α of an error of the first kind, is

$$X_c = X_0 + s_0 t_\alpha / m^{1/2} \quad (1)$$

where s_0 is the standard deviation of signals generated from q_0 and t_α is taken from the table of probability points of the t-distribution (single-sided). Expressing X_c now in terms of the alternative central value, X_p, and the probability β of a type II error, we have

$$X_c = X_p - s_p t_\beta / m^{1/2} \quad (2)$$

where s_p is the standard deviation of signals generated from q_p. From Eqns. 1 and 2,

$$\delta = X_p - X_0 = (s_0 t_\alpha + s_p t_\beta)/m^{1/2} \quad (3)$$

and

$$m = \left[(s_0 t_\alpha + s_p t_\beta)/\delta\right]^2 \quad (4)$$

The value of δ given by Eqn. 3 is bound to $q_p - q_0$, the limit of discrimination [9]. This limit is a performance characteristic of a measurement process where m is fixed.

Conversely, Eqn. 4 gives a clue to designing a measurement process tailored to measure δ, the minimum difference that it is important to detect. It gives the number m of repeats needed to discriminate between analyte amounts differing by $q_p - q_0$ or more, with the accepted error probabilities α and β. Since t_α and t_β depend on m, the latter is calculated by iteration from Eqn. 4.

These relationships between q_0, q_p, α and β are better shown by means of the operating characteristic or power curves (Fig. 1) [10]. Each curve pertains to a given measurement process. The choice of α is a preceding step regulated by economic reasons which have nothing to do with the measurement process itself. This is why all the measurement processes, devoted to the solution of the same problem, share the initial point in the graph. The term $1 - \alpha$ is the probability of acceptance of the null hypothesis. The fact that the quantities on the abscissa are analyte amounts means that, at some earlier stage before drawing the power curve, measurement on standards, i.e., calibration, has taken place. Once the probability density function for the analytical signals has been agreed upon and the parameters s_0 and s_p have been measured, the power curve is determined by two points. The straightforward choice is $(q_0, 1 - \alpha)$ and (q_p, β).

Altshuler and Pasternak [7] directly applied the power curves to define the limit of detection in the measurement of radioactivity. Liteanu and Rîcă [5,6] did the same thing for chemical analysis, labelling the power curves as detection characteristic curves, and viewing the discriminating power as a signal-to-noise ratio. The types of power curve applied by all these workers differ

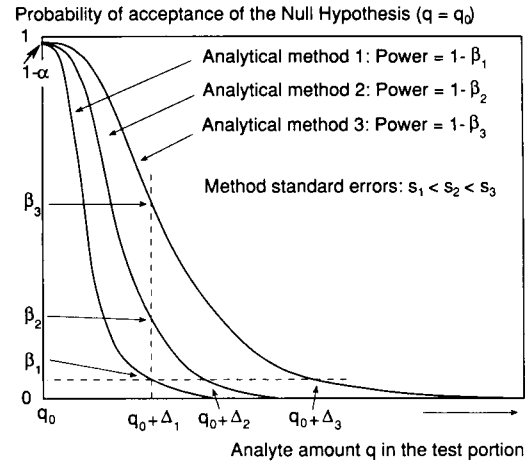

Fig. 1. Operating characteristic curves (power curves) of three analytical methods. They are useful for comparing the powers of different tests (analytical methods in the present case) to measure the increase, Δ (limit of discrimination), in the analyte amount, that it is important to detect through the analytical-signal difference δ, with allowed probabilities α and β of errors of type I and II, respectively, (analytical methods 1, 2 and 3, have different powers to secure a limit of discrimination Δ_1, dashed vertical line). Comparisons of limits of discrimination at constant power between methods (limits of discrimination Δ_1, Δ_2, Δ_3 at constant power for three different methods, dashed horizontal line), or changes of power following changes in the limit of discrimination aimed at (discrimination limits Δ_1 and Δ_2, require different powers $1 - \beta_2$ and $1 - \beta_1$, respectively, from analytical method 2), are of secondary usefulness. What really matters is the comparison between powers of different tests (different analytical systems) to secure a predeterminate limit of discrimination.

from Fig. 1 by bearing on the ordinate axis the probability $1 - \beta$ (P_{11} according to Liteanu and Rîcă) instead of a general acceptance probability, be it either $1\text{-}\alpha$ or β, and α (P_{10} according to Liteanu and Rîcă) on the abscissa, instead of analyte amounts. Figure 1 is preferred here in order to take advantage of a well worked out procedure usually applied in chemical industry [10].

As pointed out by Currie [9], the limit of discrimination at zero analyte amount is the limit of detection. This view opens up the way for applying to the limit of discrimination the experience gathered from the study of the limit of detection. The Hubaux and Vos methodology [11] for measuring this limit is the one preferred in

this paper. It is a widely accepted methodology [12]. Its implementation requires a set of standards with analyte contents bracketing the prospective limit of detection. When matrix-matching standards are not available, it is still possible to use surrogate standards, if the laboratory samples to be analysed can be treated by means of the analyte addition technique. The lack of matrix matching can give rise to matrix interference. This interference can be diagnosed by comparison among the limits of discrimination measured on different substrata, as will be described later. In cases where the system shows changes in sensitivity near the limit of detection [13], the study of matrix interference through limits of discrimination is not possible. The changes in sensitivity can be disclosed by means of the Youden one-sample regression analysis [14], i.e., the regression of analytical signals on increasing test portions of the laboratory sample.

The description of how to monitor both sensitivity changes by way of the Youden blank and matrix interferences through the limit of discrimination is the main purpose of this paper. However, before focusing on these matters, three different approaches for measuring limits of detection will be discussed in the light of the fundamental distinction between analytical result and analyte amount in the test portion. Also, the instrumental limitations or instrument thresholds and the concept of the analytical system will be considered.

HUBAUX AND VOS APPROACH TO THE MEASUREMENT OF THE LIMIT OF DETECTION AND ITS IMPLEMENTATION

In a previous paper [4] we emphasized the essential difference between the limit of detection, such as this term was used by Kaiser [15] as a translation of his Nachweisgrenze [16], and the limit of guarantee for purity, Garantiegrenze für Reinheit, [17]. Currie [18] uses decision limit for Nachweisgrenze and detection limit for Garantiegrenze für Reinheit, as do Hubaux and Vos [11]. We shall follow the same terminology in this paper, without losing sight of the difference between either the analytical signal or the analytical result, and the actual analyte amount in the test portion. While referring to a tutorial by Kirchmer [19], Currie [9] expressed this difference as follows: "...a crucial distinction is noted: that is, the detection decision is made in reference to an observed, random experimental outcome (estimated concentration), whereas the detection limit refers to the underlying true concentration which the chemical measurement process is capable of detecting". This distinction is straightforward in the Hubaux and Vos methodology [11] for measuring limits of detection, since the limit of detection lies on the same axis where the analyte amount in the standards is plotted, while the critical signal value or decision limit is on the analytical signal or instrumental response axis. The probability density distribution curve is located in a third dimension. The usual illustration when discussing limits of detection, i.e., the standing bell on horizontal line, is misleading because the abscissa axis is shared by both the analyte amount and the analytical results calculated through the calibration line from instrumental responses.

Another important advantage in the Hubaux and Vos approach is that it does not rely on the blank signal variation. It can be implemented in situations where the response observed on a blank is steady, as is often the case in chromatographic methods. Bailey et al. [20] measured detection limits of intermediates and side reaction products in two food dyes by means of liquid chromatography, following Hubaux and Vos, without allowing for the fact that the photometric response observed on a blank is virtually a horizontal straight line. In spite of this, they succeeded in measuring the limits of detection for all the compounds tested (nine), because in all instances the limit of detection gave higher results than the lowest contents of analyte in the standards used.

The implementation of the Hubaux and Vos methodology [11] is based on external standards. Whenever possible, reference materials with analyte levels bracketing the limit of detection should be used. As the limit of detection in a routine analytical procedure is expected to be much higher than the limit of detection in the definitive

procedure, the one which is applied to prepare the certified reference materials, there is no difficulty in thinking of such materials as having an analyte contents even lower than the target limit of detection. However, reference materials related to a given laboratory sample are in general not available. Their scarcity leads in most instances to the impossibility of determining the limit of detection under matrix-matching conditions.

A surrogate for certified reference materials could be prepared by means of the analyte addition technique on a blank. A blank is a material identical with the laboratory sample, but having no analyte or, more correctly, no detectable analyte amount. Again, the availability of such a material is extremely rare. It is at one's disposal only when monitoring either the levels of an additive [21] or contamination by just one pollutant [22]. This is why it is convenient to use special terms, such as placebo [23], field blank [24] or matrix blank [25], to describe the true blank.

In analytical systems where the analyte addition technique cannot be applied to give an added analyte identical with that indigenous to the laboratory sample, there is no possibility of implementing the Hubaux and Vos approach without appropriate certified reference materials.

KAISER'S APPROACH

Kaiser [16] reported in 1947 his results on three analytical systems made up of a matrix of aluminium with small amounts of zinc and other metals, calibration by measuring the zinc contents using wet chemistry methods and three emission spectroscopy methods, two with sparks at different magnetic autoinduction and the third with arc excitation. The dynamic range given by the standards was 0.03_3–0.40% Zn. The Nachweisgrenzen were calculated according to

$$3s_B/S \quad (5)$$

where S is the sensitivity as measured in the range 0.03_3–0.40% Zn. The standard deviation of the blank signal, s_B, was obtained by scanning with a densitometer the photographic emulsion near the 334.50-nm zinc line. Therefore, the blank here is not the reading at 334.50 nm when an aluminium sample without zinc is excited, that is, a matrix blank, but an instrumental blank obtained by recording the background noise. The "limits of detection" calculated from Eqn. 5 were 0.02% Zn (spark lower induction), 0.007% Zn (spark higher induction) and 0.0004% Zn (arc). Note that these results are in fact limits of decision, analytical signals expressed in analytical result units. All of them are below the dynamic range covered by the standards. In situations such as this the blank test portion is usually much closer to the limit of detection than the available standard with the lowest analyte content. This justifies the importance of the blank measurements in Kaiser's approach.

Without appropriate standards, whenever the analyte addition technique cannot be applied, the reference $q_0 = 0$ corresponding to a blank is the only one available to define the limit of detection by way of hypothesis testing. This requires reasonable assumptions on the extrapolated sensitivity to be entered into Eqn. 5. Long and Winefordner [26] improved the model by introducing the uncertainty of the sensitivity S in Eqn. 5, again by way of extrapolation.

Data reported in this paper are substituted in Eqn. 5, after changing 3 to $2 \times 2.46 = 4.92$, to give a value for the limit of detection (Appendices B and C).

METHOD DETECTION LIMIT

Liteanu and Rîcă [6] applied an expression analogous to Eqn. 5 with the essential difference of measuring the signal standard deviation on a sample with an analyte contents near the limit of detection, 0.007% tungsten in steel, instead of the standard deviation on the blank. S was taken from a calibration line covering the range 0.000–0.105% tungsten, and 6 was substituted for 3 in Eqn. 5.

The same approach has been proposed under the name of method detection limit [27], a misnomer according to Kirchmer [19]. It is applied to trace analyses for waste waters. Contrary to the

case with tungsten alloy, no matrix matching standards are available, but surrogate standards can be applied by spiking either the test portion or reagent water with pure analyte, which is not possible with Kaiser's aluminium samples or with steel samples.

The method detection limit is given as an experimental design intended to measure limits of detection in "the detection mode", that is, the limit of detection is not approached from a position of "non-detectable analyte" (the blank), but from a more realistic one of "small analyte amount near the detection limit". The standard deviation of the analytical signal is obtained from seven repeats, the change from analytical signal to analytical result units is made through the sensitivity S, as measured in a calibration range far above the limit of detection, and Eqn. 5, that of Kaiser's approach, is applied with a small variation, i.e., 3.14, the t-value for seven repeats and 1% significance, one-sided, is substituted for 3. This modification joins the obvious one of substituting s_C, the standard deviation measured "in the detection mode" for s_B, the corresponding value "in the blank mode", i.e., measured on the blank.

Both Kaiser's and the method detection limit approaches share the shortcoming of obtaining S in Eqn. 5 by extrapolation. The method detection limit includes recovery experiments as a check against this source of error. This type of check monitors sensitivity differences between standards and sample [28].

In cases where the measured level of analyte is more than five times higher than the calculated detection limit, the calculated value is discarded (this rule results from the fact that the standard deviation may change with the analyte level). Then a limit of detection is determined by spiking reagent water with analyte. If the analyte amount in the sample remains below a level ten times higher than the limit of detection in reagent water, the latter is retained. This rule seems to indicate that the matrix increases the random scattering of the results.

The application of the preceding rules requires that the analyte amount in the test portion be known, which in turn demands a blank-corrected signal. However, blank corrections are usually not needed in this methodology. It was originally designed to be applied with fifteen chromatographic methods, three of them employing a mass spectrometer as a detector. In analytical methods including chromatographic techniques the analytical signals are usually obtained by integrators giving the area of a peak rising above a background, so that the signal comes out as background corrected [19], and no blank correction is considered necessary most of the time, provided that no analyte alien to the test portion enters the analytical system. On the other hand, it is suggested in the original paper that one should remove the interference due to co-elution of chromatographic peaks through blank measurements. However, the term blank measurement should be restricted to the measurement on a blank test portion within the same analytical system. Peak co-elution is a case of direct matrix interference, which cannot be corrected for without moving to another analytical system [23,29,30].

When no standards enter the measurement of a limit of detection, apart from those applied to obtain the calibration function in a dynamic range far above the limit, the calculated limit is just an analytical signal. The method detection limit is usually interpreted as such. Therefore, it is to be used as a critical signal value to discriminate samples after analysis, by comparing the resulting signal with the critical value. Thus, it has been remarked [19,31] that the method detection limit has a probability $\alpha = 0.01$ of an error of the first kind (false positives) and a probability $\beta = 0.50$ of an error of the second kind (false negatives). However, should standards be available as certified reference materials, as surrogate standards in the case of no matrix effects, or as unknowns analysed by means of a definitive method, then the method detection limit would be a limit of detection with critical signal value 0.000, $\alpha = 0$ and $\beta = 0.01$. This situation reminds us of Feigl's definition of his Erfassungsgrenze [32] as "jene Konzentration..., in welcher eine Reaktion bei einer Serie von Versuchen noch anstandslos gelingt". Only false negatives are contemplated here, because the wealth of information brought by a positive spot test to the analyst's retina

makes false positives more unlikely. This situation is met with again, for example, in chromatographic peaks detected through a mass spectrum. This bring us to the situation where an analyte that is not indigenous to the test portion becomes the limiting factor in the way towards lower limits of detection [33].

A comparative study of the Hubaux and Vos and method detection limit approaches was made by Grant et al. [31] by measuring synthetic samples.

INSTRUMENT THRESHOLDS

Kaiser [17] considered the situation where the measurements on the blank give repeatedly a zero analytical signal. This situation is explained as being due to the instrument being too coarse to discriminate between zero analyte amount and any analyte amount up to a value called the threshold value. Currie [34] deals with the same problem as originating in proprietary "black boxes" incorporated in the instrument. A possible solution to this problem, provided that the laboratory sample can be spiked, is to include in the analytical method the addition of a given amount of standard analyte, sufficient to surpass slightly the scale threshold. Then the limit of discrimination is measured. Should the limit thus found be lower than an order of magnitude below the scale threshold, it is ignored, and the threshold is taken as the limit of detection. Otherwise the limit of discrimination plus the scale threshold is the limit of detection.

In addition to the scale threshold, there is still another type of instrumental limitation, which could be called a threshold degree. It was pointed out by Gottschalk [35], when from 24 titrimetric measurements of mercury(II) ions with a 0.2 M solution of sodium diethyldithiocarbamate, a standard deviation of 0.009 ml of titrant solution was obtained. This was below the minimum reading difference, 0.02 ml. In cases such as this there is no possibility of applying statistics to the evaluation of the experimental results, because the reading device does not follow the random fluctuations of the signal. When discussing the effects of rounding and truncation, Currie [9] indicates that scale divisions (minimum reading differences) much smaller than $\sigma/4$ are required.

ANALYTICAL SYSTEM

Kaiser and Specker [36] looked upon the limit of detection as an objective performance characteristic, Güteziffer, of an analytical procedure. This contention requires an accurate description of the "complete analytical procedure". Thompson and Howarth [37] followed this view and defined the analytical system as characterized by the laboratory sample with the analyte in a given matrix, the exactly defined analytical procedure and the particular instrument used. Unfortunately, "the exactly defined analytical procedure" must include parameters such as the number of repeats, the number and distribution of the standards along the dynamic range and the statistical significance levels. Therefore, the number of possible analytical systems is practically limitless, and to look upon the limit of detection as a performance characteristic is impractical.

On the other hand, the introductory discussion relates a signal variation, δ, with an analyte amount increment, $q_p - q_0$. The relationship between these two quantities is monitored by means of the power curves (Fig. 1). The power curves are useful when designing a cost-effective measurement process. The design is obviously a problem-oriented one. It would be convenient to isolate the problem-oriented part within the analytical system. Therefore, the analytical system could be defined by (i) the laboratory sample with the analyte in a given matrix, (ii) the sample treatment prior to obtaining the analytical signal [1], (iii) the analytical method [38] and (iv) the experimental design and evaluation.

Part (i) is determined by the customer. Part (ii) follows from (i) and is oriented towards (iii). Part (iii) depends on the laboratory resources. Parts (i), (ii) and (iii) fix the limit of detection within one order of magnitude. If we are content with this gross estimation then, certainly, the limit of detection can be accepted as a performance characteristic of the chemical measurement process,

provided that part (iv) is left out when defining such a process. Finally, part (iv) is determined by external factors, i.e., the choice of α and β probabilities and, simultaneously, by the "fine tuning" which decreases the limit of detection and, in general, the limit of discrimination, at the cost of more technician hours. The last point is considered further in Appendix F.

LIMIT OF DISCRIMINATION

It is the minimum increase in analyte contents in a test portion from the laboratory sample that is required to secure an analytical signal significantly different from the signal generated in the non-spiked test portion. We are not dealing now with the minimum signal difference that it is important to detect, δ in Eqn. 4, but with the smallest difference that can be detected, δ in Eqn. 3. The limit of discrimination is measured by means of the analyte addition technique on the laboratory sample, as shown in Fig. 2. The confidence bands in Fig. 2 are drawn according to the equation [39]

$$X = a + b\Delta \pm st\left[1/m + 1/n + (\Delta - \bar{\Delta})^2 \Big/ \sum_{i=1}^{n} (\Delta_i - \bar{\Delta})^2\right]^{1/2} \quad (6)$$

where Δ is the analyte spike in the laboratory sample (independent variable in the regression, the predictor), X the analytical signal (the function in the regression, the regressor), a the intercept of the regression straight line, which is estimated by least squares, b the slope or sensitivity, s the estimate of the residual standard deviation, t the probability point of Student's t distribution, one-sided 1.0% significance, n the number of experimental points from which the least-squares straight line is estimated, m the number of measurements to obtain an average value of the signal, as additional measurements on either the standard or the unknown, once the regression line has been completed, Δ_i the ith spike and $\bar{\Delta}$ the mean value calculated from $\Sigma\Delta_i/n$. Two experimental designs are applied to obtain the estimates by least squares, one with $j = 3$ spike levels and $r = 10$ repeats at each level, $n = 30$, and another with three levels and three repeats per level, $n = 9$. The respective t-values are 2.47 and 3.00. Once the n pairs (Δ, X) have been obtained, Fig. 2 is drawn and the limit of discrimination is defined as the spike chosen a priori to give the signal upper confidence limit from the laboratory sample, in short, the critical signal value, as shown in Fig. 2. Therefore, the limit of discrimination is the minimum spike which has a probability not higher than 1% of giving rise to a signal equal to or lower than the signal upper confidence limit of the one-sided 99% prediction interval. The above definition can be developed in current statistical terminology as follows. By accepting a 1% probability ($\alpha = 0.01$) of concluding from an analytical signal increase that a test portion has been spiked, when actually it has not been so (error of the first kind), the upper limit of the two-sided 98% prediction interval is set as a critical or decisive signal value. Then the limit of discrimination is the spike, expressed in analyte amount units, which gives rise to an analytical signal lower than the critical value in 1% of the measurements, i.e., once in 100 times it leads to the wrong conclusion that the test portion has not been spiked (error of the second kind, $\beta = 0.01$). The limit of discrimination thus found belongs to a particular analytical system (laboratory sample, plus way of treating the sample, plus

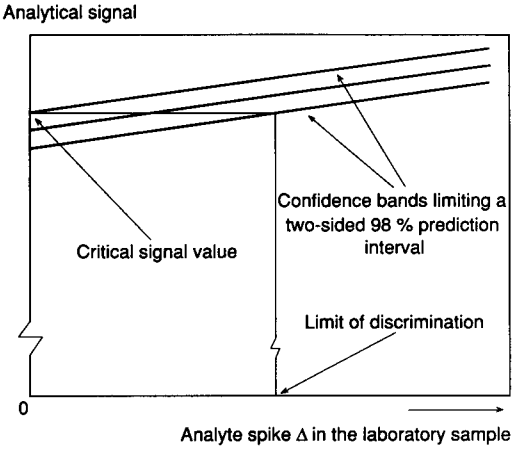

Fig. 2. Measurement of the limit of discrimination in analytical systems.

analytical method, plus experimental design, plus chosen significance levels).

The way from Eqn. 6 to the critical signal value, CRITIC, and to the limit of discrimination, DISCRM, is discussed in Appendix A.

The measurements related to Fig. 2 can be easily implemented, provided that the conditions for the analyte addition technique are fulfilled, i.e., that the analyte is available in pure form and that the added analyte is identical with that in the laboratory sample, at least as a signal contributor. The analyte addition technique is used for different purpose here, as compared with the general application to remove the interactive matrix interference [40] form the analytical result (standard addition method).

The limit of discrimination is applied in this paper to ascertain the importance of matrix effects when looking for a breakthrough to measure limits of detection, in cases where appropriate matrix-matching standards are not available. In addition, it could be used to compare two analytical systems. In this sense it is related to a "sensitivity" defined by Stiehler and Mandel [41] for the purpose of comparing test methods. As shown in Appendix F and expected from Fig. 2, there is a strong positive correlation between the limit of discrimination and the ratio s/b, where s is the residual standard deviation and b the slope of the calibration line (IUPAC sensitivity). On the other hand, Stiehler and Mandel's "sensitivity" is defined as the ratio of the slope of the calibration line to the standard deviation of the signal obtained on an unknown. However, the application of this approach to compare test methods in the case of quantitative chemical analysis is as follows. Two unknowns with different analyte amounts in the test portion are repeatedly measured by methods A and B. The recorded signal differences between unknowns are ΔA and ΔB, respectively, while the standard deviations are s_A and s_B. If the ratio $(\Delta A/\Delta B)/(s_A/s_B)$ is greater than 1, method A is more discriminating than method B. No standards are needed for the comparison, which will be meaningful only if the calibration steps are not decisive. This is so because the ratio quoted above to compare both methods relies on signals only.

LIMIT OF DETECTION

The limit of detection is the limit of discrimination in an analytical system at zero analyte amount [9]. The laboratory sample has no detectable analyte amount now, i.e., the laboratory sample is the matrix blank. Should matrix blanks be unavailable, we are still left with the possibility of performing the measurements on a solvent blank. The price to be paid for this expediency is to face the uncertainties derived from a lack of matrix matching. This difficulty is dealt with by having resource to the comparison between the limit of discrimination values measured on three different substrata: the laboratory sample, an analyte solution which gives about the same analytical signal as the laboratory sample and the solvent. Agreement between the three values would indicate the absence of matrix effects.

The definition for limit of discrimination has been chosen such that at zero analyte amount it becomes the limit of detection, as defined by Hubaux and Vos [11]. The critical signal value, obtained as the intercept of the upper confidence band and related to the non-spiked laboratory sample, becomes the Hubaux and Vos decision limit. Here the blank is just another standard, the zero added analyte level in the regression calculations leading to the limit of detection.

EXPERIMENTAL

In order to demonstrate how to measure the limit of discrimination by applying the methodology outlined earlier to reach the limit of detection, four different although closely related analytical systems are considered. They have in common the analyte, sulphate ion, the laboratory sample, tap water, and the main features of the analytical method, indirect spectrophotometry of sulphate ion with analytical signal due to absorption by dichromate ion at 350 nm, and based on the following sequence of reactions:

$$(SO_4^{2-})_{\text{analyte}} + (Ba^{2+})_{\text{total reagent}} + (Cr_2O_7^{2-})_{\text{total reagent}} \longrightarrow BaSO_4$$

$$+ (Ba^{2+})_{\text{excess reagent}} + (Cr_2O_7^{2-})_{\text{total reagent}} \quad (7)$$

$$BaSO_4 + (Ba^{2+})_{\text{excess reagent}} + (Cr_2O_7^{2-})_{\text{total reagent}} \xrightarrow[\text{basic medium}]{\text{change to}} BaSO_4 + BaCrO_4$$

$$+ (CrO_4^{2-})_{\text{excess reagent}} \quad (8)$$

$$BaSO_4 + BaCrO_4 + (CrO_4^{2-})_{\text{excess reagent}} \xrightarrow[\text{filtration}]{}$$

$$(CrO_4^{2-})_{\text{excess reagent}} \quad (9)$$

$$(2\ CrO_4^{2-})_{\text{excess reagent}} \xrightarrow[\text{acid medium}]{\text{change to}}$$

$$(Cr_2O_7^{2-})_{\text{excess reagent measured at 350 nm}} \quad (10)$$

According to this sequence of reactions, the absorbance measured at 350 nm should increase linearly with increasing amount of sulphate ion in the test portion.

More than 50 papers, published between 1862 and 1976, dealing with analytical methods based on reactions 7–9 have been discussed elsewhere [42]. Two of them [43,44] bear a closer relationship to the four analytical methods applied in this paper. Hinman [43] added simultaneously both reagents in reaction 7 as a solution of barium chromate in hydrochloric acid, used ammonia in reaction 8, and measured by titrimetry the Cr(VI) related to the sulphate ion. Egami and Takahashi [44] added a barium chloride solution in reaction 7, and then sodium acetate and potassium dichromate in reaction 8; finally, the Cr(VI) was measured spectrophotometrically.

The four analytical methods chosen in this paper for demonstration purposes are designated A, B, C and D. Method A illustrates the situation where the sensitivity change is strong enough to go from a positive to a negative slope. Methods B and C provide examples of milder effects, and in method D the sensitivity change has been removed.

Analytical method A (Hinman acetate; short standing before filtration)

A measured volume of either tap water or standard sodium sulphate solution is introduced into a dry 125-ml conical flask and the volume is completed to 50 ml with reagent water. The tare of the flask plus a magnetic bar is previously registered. Magnetic stirring is started so that a vortex just reaching the bar is formed. A 10-ml volume of Hinman's reagent is added with a pipette and the stirring is maintained for 15 min, followed by a 45-min period without stirring. Next, the stirring is started again and 25 ml (graduated cylinder) of 0.36 M sodium acetate are added. The stirring is discontinued after 1 min, followed by a 10-min period of rest. The conical flask with its contents is weighed to 0.01 g with a Mettler PE200 balance and by tare subtraction Δm is obtained. Δm is a measure of the solution volume in the conical flask, since density differences between runs are considered to be negligible. A portion of the solution is filtered with Whatman 42 paper, the first 20 ml of filtrate are discarded and the rest is collected in a dry test-tube, from which 10 ml are taken with a pipette and transferred into dry 50-ml conical flask, followed by 10 ml (pipette) of 165 mM perchloric acid. Finally, the absorbance at 350 nm is measured in 10-mm glass cells, with water in the reference cell, with a Pye Unicam SP8-300 spectrophotometer. The product $\Delta m \times$ absorbance is taken as the analytical signal.

Analytical method B (Hinman acetate; long standing before filtration)

This is the same as method A, but with a wait of 24 h before filtration instead of the 10 min in method A.

Analytical method C (Hinman ammonia)

This is implemented like method A but with alkalinization with 0.36 M ammonia solution.

Analytical method D (no sensitivity change)

This method is the same as method C, after replacing the sentence "A 10-ml volume of Hinman's reagent...without stirring." by "A 10-ml volume of 14 mM barium chloride in 250 mM hydrochloric acid is added with a pipette and the stirring is maintained for 15 min, followed by a 45-min period without stirring. Then 10 ml of 10 mM potassium dichromate are added."

Youden one-sample regression

The measurements are obtained by applying the pertinent analytical method to several test

portions of different size. Since linear relationships are sought in this treatment, three runs are performed at each test portion level so as to have sufficient data for lack-of-fit tests [45]. Solvent blank measurements are run in parallel with those on test portions.

Measurements of the limit of discrimination, designed to ascertain matrix effects

A 50.0-ml volume of tap water is spiked with 0.00, 1.00 or 2.00 ml of sodium sulphate solution containing 250 mg l^{-1} SO_4^{2-} using a microburette. In another series of measurements 50.0 ml of a 153 mg l^{-1} SO_4^{2-} sodium sulphate solution are spiked in the same way. Finally, the limit of discrimination of the solvent is measured by diluting 0.00, 12.0 or 19.9 ml of 25.1 mg l^{-1} SO_4^{2-} sodium sulphate solution with reagent water to 50.0 ml. Analytical method D (no sensitivity change) is applied in all three series of measurements, with ten replicates at each analyte level.

Measurement of the limit of detection in the case of a mild change in sensitivity

A volume of 0.00, 10.0 or 20.0 ml of a 40.0 mg l^{-1} SO_4^{2-} solution is diluted to 50.0 ml with reagent water and submitted to analytical method B, with three replicates at each analyte level.

Measurement of the limit of detection in the presence of a strong change in sensitivity

In the series designed to measure the limit of decision, 0.00, 3.0 or 6.0 ml of a sodium sulphate solution containing 40.0 mg l^{-1} SO_4^{2-} are diluted to 50.0 ml with reagent water, then analytical method A is applied. In a complementary series to measure the limit of detection, once the critical signal value is known, 10.0, 20.0 or 30.0 ml of a 200 mg l^{-1} SO_4^{2-} solution are used instead. Three replicates are performed at each analyte level.

Experimental design

r Replicates at j analyte levels result in $n = r \times j$ measurements within a series; the measurements are run in random order.

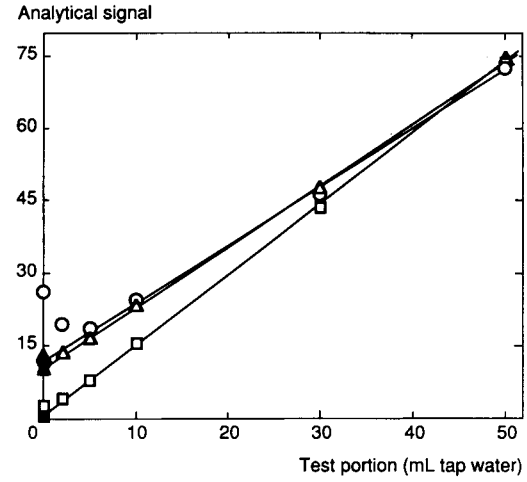

Fig. 3. Slope changes at small test portions, as observed from the Youden one-sample plot. They indicate sensitivity changes in the respective calibration lines. Analytical methods: ○ = A, Hinman acetate with 10-min digestion before filtration; △ = B, Hinman acetate with 24-h digestion before filtration; □ = C, Hinman ammonia with 10-min digestion before filtration. Total Youden blanks obtained by extrapolation from the 10–50-ml tap water range ($n = 9$ regression points, triplicates at 10, 30 and 50 ml, respectively, tap water, 95% confidence intervals): ● = 11.2 ± 2.3; ▲ = 9.5 ± 1.1; ■ = 1.05 ± 1.29. Solvent blanks (open symbols at zero test portion, average from nine replicates, 95% confidence intervals): ○ = 26.2 ± 2.4; △ = 11.95 ± 0.17; □ = 3.5 ± 0.16.

Reagents

Hinman's reagent is prepared with 3.464 g of Panreac barium chromate dissolved in 264 mM hydrochloric acid and diluted to 1000 ml with the same acid. Chlorine odour was never noticed while using these solutions. The 0.36 M ammonia is kept in a carbonate-free condition [46] by taking 2.50 g of calcium carbonate, dissolving it in excess hydrochloric acid, evaporating to dryness, dissolving the residue in a small volume of water and adding the calcium ion solution to the concentrated ammonia before diluting with water to 1000 ml. Unless stated otherwise, all reagent solutions were prepared with Merck analytical-reagent grade chemicals. Reagent water prepared from deionized water by distillation in an all-glass apparatus was used throughout.

RESULTS AND DISCUSSION

Figure 3 shows the Youden one-sample plot when applying analytical methods A, B and C. The best available blank correction [14], in a given working range, is the total Youden blank, which is obtained by extrapolating to zero test portion the Youden one-sample plot. The working range is defined in the present case by 10 and 50 ml of tap water. Therefore, the total Youden blank is obtained by extrapolating to zero test portion the least-squares straight line, defined by the analytical signals at 10, 30 and 50 ml of tap water. Total Youden blanks are shown by filled points in Fig. 3. Outside the 10–50-ml tap water range, the sensitivity shows a decrease as the test portions become smaller. The effect is more pronounced with method A, where the sensitivity even changes its sign. The extent of the sensitivity change can be established by comparison be-

TABLE 1

Data for a Youden one-sample plot showing constant slope: analytical method D, barium chloride–potassium dichromate–ammonia; 10-min standing before filtration; excess of chromate ion over barium ion

	Test portion (ml tap water)	Analytical signal (absorbance × g treated sample)	Test portion (ml tap water)	Analytical signal (absorbance × g treated sample)	Test portion (ml tap water)	Analytical signal (absorbance × g treated sample)
	0.70	45.87	25.0	82.87	50.0	118.4
		45.75		82.38		119.5
		45.46		81.78		119.7
		48.09		82.56		120.0 [b]
		48.43		83.40		118.6
		46.21		82.88		119.9
		46.02		82.31		119.7
		46.68		81.94		120.5
		45.95		83.24		119.1
		45.95		82.04		120.1
Mean values		46.44		82.54		119.5
Standard deviation		1.01		0.55		0.66

Statistic for the lack-of-fit test [45]: 0.05. Critical value (1% significance): 7.68. Non-significant lack of fit to a straight line

Total Youden blank: 45.43 ± 0.45 [a]

	0.00	45.20	0.00	44.88	0.00	44.62
		44.92		44.74		44.45
		45.65		45.22		44.63
		44.63		45.26		44.76
		45.36		45.29		45.43
		44.39		45.07 [b]		44.72
		44.83		45.99		45.02
		45.43		44.34		44.73
		45.41		44.80		44.63
		45.88		45.38		44.72
Mean values		45.17		45.10		44.77
Standard deviation		0.47		0.45		0.27

Grand mean for the 30 solvent blanks: 45.01
Standard deviation: 0.43
Solvent blank: 45.01 ± 0.16 [a]

[a] 95% confidence interval. [b] Substitution for an outlier value.

tween the solvent blank measure (empty points at zero test portion in Fig. 3) and the total Youden blank.

The kinetic nature of the changing sensitivity effect is shown by the fact that in method B 24 h are allowed for the precipitation described by Eqn. 8, whereas in method A only 10 min are left before filtration. Once the solution has been filtered it remains transparent and gives a steady absorbance reading at 350 nm, thus showing that the filtration cuts off the formation of precipitate. The kinetic effect is even less pronounced with method C, where ammonia is used to cause the precipitation of barium chromate, instead of the acetate ion, which is a weaker base.

The Hinman reagent used in methods A, B and C carries Cr(VI) and Ba in nearly equimolar amounts (nearly, because some coprecipitation of either soluble chromates or soluble barium salts is unavoidable when preparing barium chromate). Complete precipitation of barium chromate according to Eqn. 8 leaves very little or no chromate ion in solution when measuring on either blanks or test portions with small sulphate amounts. On the other hand, method D is implemented by adding 140 μmol of Ba^{2+} and 200 μmol of Cr(VI), so that an excess of Cr(VI) is secured even when measuring on a blank. The excess of Cr(VI) suppresses the kinetic effect, as the data in Table 1 show by the complete agreement between the solvent blank measure and the total Youden blank.

After having secured an analytical method which gives a Youden one-sample plot with constant slope all the way down to zero test portion, it is possible to check for the absence of matrix effects. This absence is required if valid measurements of the limit of detection are to be obtained from surrogate standards. As pointed out before, this is done by measuring the limit of discrimination on the laboratory sample, on a solution having an analyte content nearly equal to that in the laboratory sample and on the solvent. The pertinent data are given in Table 2.

Comparison between the results in the laboratory sample series with those in the analyte solution gives information on matrix effects. This has already been done by Henning and Jackson [47]

TABLE 2

Limits of discrimination with analytical method D [separate addition of Cr(VI) and Ba, the former being in excess] on the laboratory sample (tap water), on a solution of 153 mg l^{-1} SO_4^{2-} and on the solvent (reagent water)

	Analyte spike (mg SO_4^{2-})	Analytical signal (absorbance × g treated sample)	Analyte spike (mg SO_4^{2-})	Analytical signal (absorbance × g treated sample	Analyte spike (mg SO_4^{2-})	Analytical signal (absorbance × g treated sample)
Laboratory sample (tap water)	0.000	109.14	0.250	111.26	0.500	113.53
		108.58		111.98		113.45
		109.16		110.78		113.39
		109.53		111.46		113.08
		109.18		111.61		113.04
		109.19		110.67		113.84
		109.44		111.88		113.35
		109.13		111.22		113.51
		109.11		111.26		113.54
		109.06		110.70		112.70

Statistic for the lack-of-fit test [45]: 0.06. Critical value (1% significance): 7.68. Non-significant lack of fit to a straight line
Residual standard deviation, s: 0.352 signal units
Spike sum of squares: $\Sigma(\Delta_i - \bar{\Delta})^2 = 1.250$ (mg SO_4^{2-})^2
Sensitivity: 8.38 signal units (mg SO_4^{2-})$^{-1}$
Critical signal value (signal upper confidence limit [a], unspiked test portion): 110.07 signal units
Limit of discrimination in method D on the laboratory sample (tap water): 0.21 mg SO_4^{2-}

TABLE 2 (continued)

	Analyte spike (mg SO_4^{2-})	Analytical signal (absorbance × g treated sample)	Analyte spike (mg SO_4^{2-})	Analytical signal (absorbance × g treated sample	Analyte spike (mg SO_4^{2-})	Analytical signal (absorbance × g treated sample)
Solution of 153 mg l^{-1} SO_4^{2-}	0.000	109.23	0.250	110.95	0.500	113.89
		109.70		111.49		114.02
		109.55		111.73		113.57
		109.14		111.40		113.79
		108.97		111.57 [c]		113.85
		108.68		111.10		113.35
		109.66		110.74		114.29
		109.24		112.32		113.89
		109.77		111.57		114.13
		109.89		112.02		113.88

Statistic for the lack-of-fit test: 0.82. Critical value (1% significance): 7.68. Non-significant lack of fit to a straight line
Residual standard deviation, s: 0.387 signal units
Spike sum of squares: $\Sigma(\Delta_i - \bar{\Delta})^2 = 1.250$ (mg SO_4^{2-})^2
Sensitivity: 8.97 signal units (mg SO_4^{2-})$^{-1}$
Snedecor F-test: $(0.387/0.352)^2 = 1.21 < F_{28}^{28}(1\%) = 2.48$). The hypothesis of non-significant (1%) matrix contribution to the analytical signal random error cannot be rejected
Pooled residual standard deviation: $[(28 \times 0.352^2 + 28 \times 0.387^2)/(28 + 28)]^{1/2} = 0.370$ signal units
Standard error of the sensitivity difference: $0.370\,(1/1.250 + 1/1.250)^{1/2} = 0.468$ signal units
t-Test for sensitivity difference [b]: $(8.97 - 8.38)/0.468 = 1.26 < t$ (56 degrees of freedom) = 2.00. The hypothesis of non-significant interactive matrix interference cannot be rejected
Critical signal value (signal upper confidence limit [a], unspiked test portion): 110.33 signal units
Limit of discrimination in method D on the solution of 153 mg l^{-1} SO_4^{2-}: 0.22 mg SO_4^{2-}

Solvent (reagent water)	0.000	46.97	0.300	49.08	0.500	51.15
		46.85		49.21		51.99
		46.67		49.65		51.24
		46.62		50.11		51.43
		46.08		49.43		51.99
		46.39		50.57		51.38
		46.59		48.77		50.80
		47.35		48.97		52.22
		46.70		49.08		50.81
		46.64		49.33		50.81

Statistic for the lack-of-fit test: 0.08. Critical value (1% significance): 7.68. Non-significant lack of fit to a straight line
Residual standard deviation, s: 0.476 signal units
Spike sum of squares; $\Sigma(\Delta_i - \bar{\Delta})^2 = 1.267$ (mg SO_4^{2-})^2
Sensitivity: 9.37 signal units (mg SO_4^{2-})$^{-1}$
Snedecor F-test: $(0.476/0.387)^2 = 1.51 < F_{28}^{28}(1\%) = 2.48$. The hypothesis of non-significant (1%) analyte contribution to the analytical signal random error cannot be rejected
Pooled residual standard deviation: $[(28 \times 0.387^2 + 28 \times 0.476^2)/(28 + 28)]^{1/2} = 0.432$ signal units
Standard error of the sensitivity difference: $0.432\,(1/1.250 + 1/1.267)^{1/2} = 0.545$ signal units
t-Test for sensitivity difference [b]: $(9.37 - 8.97)/0.545 = 0.73 < t$ (56 degrees of freedom) = 2.00. The hypothesis of non-significant sensitivity variation with the analyte concentration level (0 to 153 mg SO_4^{2-}) cannot be rejected
Critical signal value (signal upper confidence limit [a], unspiked test portion): 47.89 signal units
Limit of discrimination in method D on the solvent (reagent water): 0.26 mg SO_4^{2-}

[a] One-sided 99% confidence interval. [b] Two-sided 5% significance test. [c] Substitution for an outlier value.

by comparing just the sensitivities. They concluded that matrix effects were absent in the determination of molybdenum in plant tissue by electrothermal atomic absorption spectrometry. The conclusion is based on the fact that the sensitivity is the same in both the laboratory sample and the solvent, thus making unnecessary the standard addition method. Klein and Hach [29] found that the standard addition method removes only a particular kind of matrix interference. Cardone [23] described the non-removable component as a direct matrix interference. This component does not change with the analyte amount, so that, according to the definition outlined in Fig. 2, the level of the direct matrix interference does not affect the limit of discrimination. Only its contribution to the precision of the measurements can be important in this respect, because it might change the residual standard deviation, s in Eqn. 6, thus modifying the gap between confidence bands in Fig. 2.

On the other hand, the matrix-interference component changing with the analyte amount (interactive matrix interference) is the one actually checked by Henning and Jackson. It influences the limit of discrimination in two ways, i.e., through a sensitivity variation and, perhaps, through a change in the residual standard deviation. The sensitivities with and without the matrix, b_1 and b_2 respectively, are compared by means of a t-test. The pertinent statistic [39] is

$$(b_1 - b_2) \Big/ \left(s_{1/2} \left\{ \left[1 \Big/ \sum_{i=1}^{n} \left(\Delta_i - \bar{\Delta} \right)^2 \right]_1 + \left[1 \Big/ \sum_{i=1}^{n} \left(\Delta_i - \bar{\Delta} \right)^2 \right]_2 \right\}^{1/2} \right) \qquad (11)$$

where $s_{1/2}$ is the pooled residual standard deviation. The sums of squares have the same meaning as in Eqn. 6. The calculation of this statistic is detailed in Table 2.

Therefore, comparison between series of measurements such as those in Table 2 for the laboratory sample and for the analyte solution gives information about the existence of an overall matrix interference (changes in the confidence-band gap), direct plus interactive, indiscriminately, and about the existence of the interactive interference (changes in the sensitivity). In the analytical systems chosen for demonstration purposes in this paper, it comes out that neither the direct nor the interactive interference is important, because of non-significant variation in the statistical sample estimates for either the residual standard deviation, s in Eqn. 6, or the sensitivity, b in Eqn. 6, respectively.

After having shown that matrix effects are not important, joint consideration of the limit of discrimination in both the analyte solution and the solvent is pertinent to ascertain whether the latter can be taken as the detection limit in the analytical system under study. In the chosen demonstration case the residual standard deviation remains unchanged when the analyte concentration goes from 153 mg l^{-1} SO_4^{2-} to zero. Also the sensitivity does not change, a result which is to be expected from the data in Table 1, where it is shown for analytical method D that the Youden one-sample plot is a straight line all the way from 50 ml of tap water to zero test portion.

Once the limit of discrimination has been shown to be unaffected by either matrix or analyte-level effects, it only remains to assume an absence of interaction [48], i.e., to assume that the effects on the analytical signal are both independent and additive, in order to conclude that the limit of discrimination on the solvent can be taken as the limit of detection in the analytical system defined by analytical method D, tap water as the laboratory sample, three repeats at three equally spaced levels and $\alpha = \beta = 0.01$.

As neither sensitivity variations nor residual standard deviation changes are significant, it may be concluded that the three limits of discrimination in Table 2 are in agreement, so that the limit of detection sought is 0.3 mg SO_4^{2-} (see also Appendix E).

In cases where sensitivity changes near the limit of detection can be removed by means of analytical method modifications, such as those leading to analytical method D, the experimental design just described validates the limit of detection measured by means of surrogate standards, after showing that significant matrix interference

is absent. Such a validation is not possible in analytical systems showing unremovable sensitivity changes. However, the Hubaux and Vos methodology is still useful for these systems, provided that a working range starting at zero analyte amount can be found which meets two requirements: first, that the experimental points do not show a significant lack of fit to a straight line due to an inappropriate regression model (Appendix D) and, second, that the limit of detection falls inside the chosen working range. This is the situation illustrated in Fig. 4, which belongs to a case of mild sensitivity change (data in Table 3).

Situations with a strong sensitivity change are also amenable to the Hubaux and Vos methodology, by considering two working ranges, one for the measurement of the critical signal value and the other for finding the limit of discrimination, as shown in Fig. 5 (data in Table 3).

In analytical systems with available matrix blanks, Figs. 4 and 5 could have been obtained by spiking the matrix blank instead of the solvent, so that the critical signal value and the limit of discrimination might have been taken as the Hubaux and Vos decision limit and detection limit, respectively. Without available matrix blanks, the limit of discrimination in either Fig. 4 or Fig. 5 might still be taken as an approximate limit of detection in which matrix effects are not allowed for.

Levelling-off effects at the lower end of the calibration graph, as typified by the quinine sulphate system [13] and the electrode calibration graphs, are examples of strong sensitivity changes.

TABLE 3

Measurement of the limit of discrimination in analytical systems with sensitivity changes near the limit of detection

	Analyte amount (mg SO_4^{2-})	Analytical signal (absorbance × g treated sample)	Analyte amount (mg SO_4^{2-})	Analytical signal (absorbance × g treated sample)	Analyte amount (mg SO_4^{2-})	Analytical signal (absorbance × g treated sample)
Mild sensitivity change: analytical system B; Hinman acetate, 24-h standing before filtration						
	0.000	11.77	0.400	12.63	0.800	16.11
		10.98		12.39		15.29
		11.33		13.08		15.48
Statistic for the lack-of-fit test [45]: 8.14. Critical value (1% significance): 13.74. Non-significant lack of fit to a straight line						
Residual standard deviation, *s*: 0.559 signal units						
Sensitivity: 5.3 ± 1.3 [a] signal units (mg SO_4^{2-})$^{-1}$						
Limit of discrimination: 0.7 mg SO_4^{2-}						
Strong sensitivity change: analytical system A; Hinman acetate; 10-min standing before filtration						
Lower dynamic range segment:	0.000	28.82	0.120	26.27	0.240	19.13
		31.45		22.35		19.53
		31.08		20.64		19.34
Statistic for the lack-of-fit test: 1.88. Critical value (1% significance): 13.74. Non-significant lack of fit to a straight line						
Residual standard deviation, *s*: 1.975 signal units						
Sensitivity: −46.3 ± 16 [a] signal units (mg SO_4^{2-})$^{-1}$						
Critical signal value (signal upper confidence limit [b], unspiked test portion): 36.55 signal units						
Higher dynamic range segment:	2.00	28.99	4.00	41.85	6.00	57.99
		31.34		47.92		53.11
		28.95		47.24		59.01
Statistic for the lack-of-fit test: 1.56. Critical value (1% significance): 13.74. Non-significant lack of fit to a straight line						
Residual standard deviation, *s*: 2.870 signal units						
Sensitivity: 6.74 ± 1.4 [a] signal units (mg SO_4^{2-})$^{-1}$						
Limit of discrimination: 5 mg SO_4^{2-}						

[a] 95% confidence interval, two-sided. [b] 99% confidence interval, one-sided.

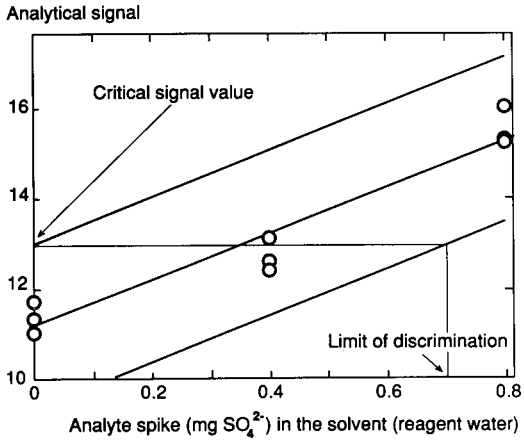

Fig. 4. Measurement of the limit of discrimination on the solvent in a case of mild sensitivity change near the limit of detection. Analytical method B, Hinman acetate, long standing time before filtration.

The authors thank Mercè Pintado for unpublished results and Marina Castellví for most of the experimental results reported here.

APPENDIX A

Computations for the limit of discrimination

First, the value CRITIC is obtained by making $\Delta = 0$ in the equation of the upper confidence band:

$$X = a + b\Delta + st_{\text{upp}}\left[1/m + 1/n + (\Delta - \bar{\Delta})^2 / \sum_{i=1}^{n} (\Delta_i - \bar{\Delta})^2\right]^{1/2} \quad \text{(A1)}$$

which results in

$$\text{CRITIC} = a + st_{\text{upp}}\left[1/m + 1/n + \bar{\Delta}^2 / \sum_{i=1}^{n} (\Delta_i - \bar{\Delta})^2\right]^{1/2} \quad \text{(A2)}$$

Substitution of CRITIC for X in the equation of the lower confidence band:

$$X = a + b\Delta - st_{\text{low}}\left[1/m + 1/n + (\Delta - \bar{\Delta})^2 / \sum_{i=1}^{n} (\Delta_i - \bar{\Delta})^2\right]^{1/2} \quad \text{(A3)}$$

makes Δ become the limit of discrimination, DISCRM:

$$\text{CRITIC} = a + b(\text{DISCRM}) - st_{\text{low}}\left[1/m + 1/n + (\text{DISCRM} - \bar{\Delta})^2 / \sum_{i=1}^{n} (\Delta_i - \bar{\Delta})^2\right]^{1/2} \quad \text{(A4)}$$

Isolating the term with the square root in Eqn. A4, squaring the resulting equation, developing the square of the difference between DISCRM and Δ and rearranging gives

$$\text{COEFFA}(\text{DISCRM})^2 + \text{COEFFB}(\text{DISCRM}) + \text{COEFFC} = 0 \quad \text{(A5)}$$

where

$$\text{COEFFA} = b^2 - (st_{\text{low}})^2 / \sum_{i=1}^{n} (\Delta_i - \bar{\Delta})^2 \quad \text{(A6)}$$

$$\text{COEFFB} = 2b(a - \text{CRITIC})$$

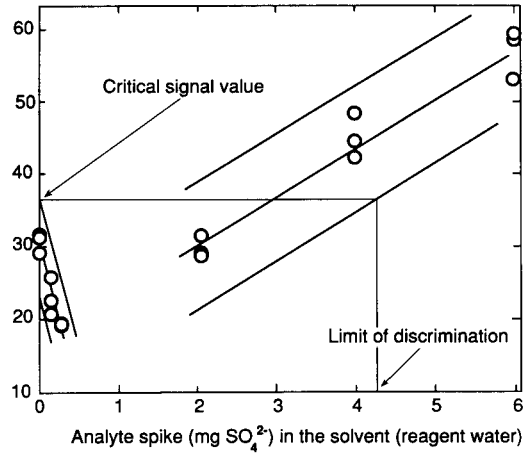

Fig. 5. Measurement of the limit of discrimination on the solvent in a case of strong sensitivity change near the limit of detection. Analytical method A, Hinman acetate, short standing time before filtration. Room temperature, 290–291 K.

$$+ 2(st_{low})^2\bar{\Delta}/\sum_{i=1}^{n}(\Delta_i - \bar{\Delta})^2 \quad \text{(A7)}$$

and

$$\text{COEFFC} = (a - \text{CRITIC})^2 - (st_{low})^2\left[1/m + 1/n + \bar{\Delta}^2/\sum_{i=1}^{n}(\Delta_i - \bar{\Delta})^2\right] \quad \text{(A8)}$$

Bearing in mind the value of $a - \text{CRITIC}$, obtained from Eqn. A2, it comes out that COEFFC is zero, in cases where $t_{upp} = t_{low}$. This reduces the second-degree equation, Eqn. A5, to

$$\text{COEFFA}(\text{DISCRM})^2 + \text{COEFFB}(\text{DISCRM}) = 0 \quad \text{(A9)}$$

and

$$\text{DISCRM} = -\text{COEFFB}/\text{COEFFA} \quad \text{(A10)}$$

In the general case DISCRM is calculated from

$$\text{DISCRM} = \left\{-\text{COEFFB} + \left[(\text{COEFFB})^2 - 4(\text{COEFFA})(\text{COEFFC})\right]^{1/2}\right\} / [2(\text{COEFFA})] \quad \text{(A11)}$$

The plus sign before the square root was chosen according to the nature of the coefficients of Eqn. A5, as given by Eqns. A6–A8, bearing in mind that DISCRM must result in a value above zero.

In analytical methods where the sensitivity is negative, the critical value, CRITIC, is obviously defined on the lower confidence band, so that Eqn. A2 becomes

$$\text{CRITIC} = a - st_{low}\left[1/m + 1/n + \bar{\Delta}^2/\sum_{i=1}^{n}(\Delta_i - \bar{\Delta})^2\right]^{1/2} \quad \text{(A2')}$$

Also, there is a change for the limit of discrimination, DISCRM, which now is based on the upper confidence band. Therefore, Eqn. A4 should be replaced by

$$\text{CRITIC} = a + b(\text{DISCRM}) + st_{upp}\left[1/m + 1/n + (\text{DISCRM} - \bar{\Delta})^2/\sum_{i=1}^{n}(\Delta_i - \bar{\Delta})^2\right]^{1/2} \quad \text{(A4')}$$

All other equations, from A5 to A11, remain exactly the same as for the usual situations with positive sensitivities, after substitution of t_{upp} for t_{low} in Eqns. A6, A7 and A8.

Finally, in cases with strong sensitivity changes near the limit of detection, as illustrated in Fig. 5, the DISCRM calculation is performed in two steps. First, CRITIC is obtained according to Eqn. A2. The FORTRAN code gives simultaneously zero as a meaningless result for DISCRM, in cases with $t_{upp} = t_{low}$. The reason is because the strong sensitivity change makes the slope of the regression line, b, go from positive to negative, whereas the difference $a - \text{CRITIC}$ retains its negative sign. This makes COEFFB change its sign, according to Eqn. A7. Now COEFFC is zero and $-\text{COEFFB}$ has changed its sign, so that Eqn. A11 gives zero, the trivial root in Eqn. A9. The pertinent DISCRM value comes from a second dynamic range at higher spikes. The CRITIC value resulting from the lower range is now entered as a constant, $-\text{COEFFB}$ is again negative, COEFFC is no longer zero, because we are in the second regression line, and Eqn. A11 renders the value of DISCRM for this situation with strong sensitivity changes.

APPENDIX B

The blank as a control measurement

The primary measurement data obtained with analytical method D on the solvent are given in Table 4. The experimental design addressed the possibility of time-dependent additive fluctuations in the signal. Therefore, each measurement on a standard was paralleled with a measurement on a blank, so that the difference between the two measurements, the blank-corrected signal,

TABLE 4

Primary data for analytical method D on simplified matrix (the solvent), blank-corrected signals and Snedecor F-test for testing for the need for the blank in parallel as a control of time-dependent additive effects on the signal (analytical method D, barium chloride–potassium dichromate–ammonia; 10-min standing before filtration; excess of chromate ion over barium ion)

	Analyte spike (mg SO_4^{2-})	Analytical signal (absorbance ×g treated sample)	Analyte spike (mg SO_4^{2-})	Analytical signal (absorbance ×g treated sample)	Analyte spike (mg SO_4^{2-})	Analytical signal (absorbance ×g treated sample)
Raw signals	0.100	47.52	0.300	49.08	0.500	51.15
		47.68		49.21		51.99
		47.03		49.65		51.24
		47.12		50.11		51.43
		47.16		49.43		51.99
		47.76		50.57		51.38
		47.16		48.77		50.80
		47.31		48.97		52.22
		47.36		49.08		50.81
		47.45		49.33		50.81
Sample estimation of the variance, s^2		0.061		0.307		0.279
Blank signals	0.000	46.76	0.000	46.53	0.000	46.97
		46.76		46.72		46.72
		46.53		46.86		46.85
		46.49		46.67		47.08
		46.62		46.45		47.57
		46.08		47.03		46.39
		46.34		46.44		46.59
		47.35		46.70		46.53
		46.62		46.24		47.08
		46.57		46.64		46.64
Sample estimation of the variance, s^2		0.108		0.051		0.120
Blank-corrected signals	0.100	0.76	0.300	2.55	0.500	4.18
		0.92		2.49		5.27
		0.50		2.79		4.39
		0.63		3.44		4.35
		0.54		2.98		4.42
		1.68		3.54		4.99
		0.82		2.33		4.21
		−0.04		2.27		5.69
		0.74		2.84		3.73
		0.88		2.69		4.17
Sample estimation of the variance, s^2		0.184		0.185		0.351
Snedecor F-test [a]		$\frac{0.061 + 0.108}{0.184} < 1$		$\frac{0.307 + 0.051}{0.185} = 1.94$		$\frac{0.279 + 0.120}{0.351} = 1.14$

[a] Critical value for the F-test, significance 5%, nine degrees of freedom in each variance estimate: 3.18. The hypothesis of random error independence between raw signals and blank signals is not discredited. The measurement of the blank in parallel is not required.

could be considered as free from the time-dependent fluctuations. On the other hand, in the absence of any time effect the raw signal and the blank signal will be independent, so that the variance of the net signal, which is the difference between the raw and blank signals, will be equal to the sum of the variances of the two primary measures. The hypothesis of the independence of random error in raw and blank signals is statistically tested by means of an F-test, which is detailed at the end of Table 4. The outcome of the test is that the hypothesis of independence is not discredited. Accordingly, there is no need to use the blank as a control in parallel. This is advantageous because it saves time and, also, because the blank can be used along with the other standards in the determination of the limit of detection following Hubaux and Vos [11].

APPENDIX C

The limit of detection according to Kaiser

The 30 blank measurements shown as unnecessary because the random fluctuations are not time dependent, thus making superfluous the paired standard–blank measurement design, can now be used to approach the limit of detection according to Kaiser. The available 30 blanks come from an analytical method proved to be without sensitivity changes near the limit of detection. Also, a sensitivity is available which pertains to the dynamic range where the limit of detection is to be measured, so that no extrapolation is necessary to obtain S in Eqn. 5. Finally, the limit of detection measured on the solvent can be accepted, because of the absence of matrix effects shown by comparison among limits of discrimination (see Results and Discussion).

X_0 and s_0 in Eqn. 1 are 46.69 and 0.3128, respectively, the mean and standard deviation of the blank as obtained from the $n = 30$ measurements. Taking $\alpha = 0.01$ and $m = 1$ (m is the number of measurements on the unknown, which will be averaged in routine control in order to compare the mean with the critical value X_c given by Eqn. 1; m is different from n, the number of measurements designed to obtain the central value X_0 and the standard deviation s_0); t for 29 degrees of freedom, $\alpha = 0.01$, one-sided test, is 2.46. Thus we obtain $X_c = 46.69 + 0.3128 \times 2.46 = 47.46$ signal units. Assuming $s_0 = s_p$ and taking $\beta = 0.01$, Eqn. 3 gives the minimum detectable signal increase, 1.54 signal units. Applying the sensitivity in Table 5, 9.58 signal units (mg SO_4^{2-})$^{-1}$, we have 0.16 mg SO_4^{2-} as the limit of detection, i.e., the limit of guarantee of purity in Kaiser's terms.

APPENDIX D

Function of the lack-of-fit test when determining limits of discrimination

Ten blank signals were selected at random from the values in Table 4 and entered in the calculation together with the values at 0.100, 0.300 and 0.500 mg SO_4^{2-}. The results are given in Table 5. Also, data from Liteanu and Rîcă [6] relating to the measurement of tungsten in standard samples of steel were subjected to the same computer program, in order to discuss the function of the lack-of-fit test when measuring the limit of detection.

A significant lack of fit to the assumed straight-line model may be due to one or more of three different causes: (1) a systematic signal bias causing a displacement of the mean value bound to a given analyte level in the standard, (2) a calibration function other than the first-order polynomial assumed before least-squares fitting and (3) an error in the analyte level assigned to one or more standards. Source (1) is unlikely when all standards are treated alike, the number of repeats on the standards is high and the repeat order among the standards is decided at random. Therefore, source (1) is ruled out for the tungsten measurements. Source (2), when it is the only one to cause the significant lack of fit, results in a symmetrical distribution of residuals around the fitted straight line, i.e., at both extremes in the regression line the same number of residuals having the same sign are found, while the central part is taken by the residuals with the reversed sign. This "sign test" requires four or more analyte levels in standards. Gradual departure from

TABLE 5

Measurement of the limit of detection according to Hubaux and Vos [11], using four standards including the blank (analytical method D, barium chloride–potassium dichromate–ammonia; 10-min standing before filtration; excess of chromate ion over barium ion)

	Standard sulphate ion added to the solvent (mg)			
	0.000	0.100	0.300	0.500
	Analytical signal (absorbance × g treated sample)			
	46.97	47.52	49.08	51.15
	46.85	47.68	49.21	51.99
	46.67	47.03	49.65	51.24
	46.62	47.12	50.11	51.43
	46.08	47.16	49.43	51.99
	46.39	47.76	50.57	51.38
	46.59	47.16	48.77	50.80
	47.35	47.31	48.97	52.22
	46.70	47.36	49.08	50.81
	46.64	47.45	49.33	50.81
Mean	46.69	47.36	49.42	51.38
Standard deviation	0.337	0.246	0.554	0.528
Residual of the mean	0.13	−0.16	−0.01	0.07
Standard deviation about the regression		0.437		
Sensitivity (95% confidence interval)		9.58 ± 0.73		
Intercept (95% confidence interval)		46.56 ± 0.22		

Lack-of-fit test [45]: 1.15 to be compared with 5.25. Non-significant lack of fit (1%)
The limit of decision is 47.65 analytical signal units (99.0% upper confidence band)
The limit of detection is 0.23 mg SO_4^{2-} (99.0% lower confidence band). It is inside the dynamic range

Emission spectrometric calibration data for tungsten, obtained by repeated recording for four standard samples of steel [6]

	Percentage of tungsten in the standard			
	0.000	0.001	0.006	0.012
	Analytical signal (arbitrary units)			
	111	117	119	138
	113	112	124	133
	112	115	118	133
	113	113	120	133
	112	116	120	135
	115	118	123	135
	116	116	120	138
	115	117	120	134
	115	116	120	133
	111	114	118	130
	111	115	117	133
	110	115	118	130
Mean	112.8	115.3	119.8	133.8
Standard deviation	1.992	1.723	2.050	2.527
Residual of the mean	0.316	1.153	−2.745	1.277
Standard deviation about the regression		2.637		
Sensitivity (95% confidence interval)		1663 ± 161		
Intercept (95% confidence interval)		112.5 ± 1.1		

Lack-of-fit test: 14.51 to be compared with 5.12. Significant lack of fit (1%)
The limit of decision is 119 analytical signal units (99.0% upper confidence band)
The limit of detection is 0.0078% tungsten (99% lower confidence band). It is inside the dynamic range

the straight-line model is better recognized from a graphical plot. Finally, source (3) is shown by the erratic sign of the residuals. The calibration on steel standards shows a significant lack of fit, which seems to be traceable to source (3). The discrimination between sources (2) and (3) is increasingly more certain as the number of analyte levels in the calibration line increases. In addition

TABLE 6

Repeatability of the limit of detection (analytical method D, barium chloride–potassium dichromate–ammonia; 10-min standing before filtration; excess of chromate; experimental design, three analyte levels in the standards, three repeats at each level)

	Standard sulphate ion added to the solvent (mg)		
	0.000	0.300	0.500
	Analytical signal (absorbance × g treated sample)		
	46.97	49.08	51.15
	46.62	50.11	51.43
	46.59	48.77	50.80
Mean	46.73	49.32	51.13
Standard deviation	0.211	0.702	0.316
Residual of the mean	0.012	−0.031	0.018
Standard deviation about the regression	0.427		
Sensitivity (95% confidence interval)	8.79 ± 1.64		
Intercept (95% confidence interval)	46.71 ± 0.55		
Lack-of-fit test [45]: 0.02 to be compared with 13.74. Non-significant lack of fit (1%)			
The limit of decision is 48.17 analytical signal units (99.0% upper confidence band)			
The limit of detection is 0.32 mg SO_4^{2-} (99.0% lower confidence band). It is inside the dynamic range			
	46.85	49.21	51.99
	46.08	49.43	51.99
	47.35	48.97	52.22
Mean	46.76	49.20	52.07
Standard deviation	0.640	0.230	0.133
Residual of the mean	0.195	−0.487	0.562
Standard deviation about the regression	0.540		
Sensitivity (95% confidence interval)	10.42 ± 2.07		
Intercept (95% confidence interval)	46.57 ± 0.70		
Lack-of-fit test: 6.77 to be compared with 13.74. Non-significant lack of fit (1%)			
The limit of decision is 48.41 analytical signal units (99.0% upper confidence band)			
The limit of detection is 0.34 mg SO_4^{2-} (99.0% lower confidence band). It is inside the dynamic range			
	46.67	49.65	51.24
	46.39	50.57	51.38
	46.70	49.08	50.81
Mean	46.59	49.77	51.14
Standard deviation	0.171	0.752	0.297
Residual of the mean	−0.117	0.293	−0.176
Standard deviation about the regression	0.501		
Sensitivity (95% confidence interval)	9.23 ± 1.92		
Intercept (95% confidence interval)	46.70 ± 0.65		
Lack-of-fit test: 1.73 to be compared with 13.74. Non-significant lack of fit (1%)			
The limit of decision is 48.42 analytical signal units (99.0% upper confidence band)			
The limit of detection is 0.36 mg SO_4^{2-} (99.0% lower confidence band). It is inside the dynamic range			
Mean of three values for the limit of detection: 0.340 mg SO_4^{2-}			
Standard deviation: 0.0200. t-Value, two degrees of freedom, 95% probability, two-sided: 4.303			
95% confidence interval: 0.34 ± 0.09 mg SO_4^{2-}			

to the levels shown in Table 5, there are three more levels available, at 0.048, 0.077 and 0.105% tungsten, with twelve signals registered at each level. A regression on seven levels gives again a significant lack of fit, 8.06 for the lack-of-fit statistic against 3.26 for the critical value. The highest residual is −2.09 signal units, again at 0.006% tungsten, followed by 1.69 at 0.012% tungsten. The immediate inference is that the "0.006%" standard has a lower and the "0.012%" standard a higher analyte content. By applying the slope from the seven-level regression, 1539 signal units (percentage of tungsten)$^{-1}$, the corrected values 0.005 and 0.013 are obtained and substituted for the nominal values. The result is a non-significant lack of fit, for both the 4×12 and the 7×12 design, lack-of-fit statistic 2.64 to be compared with the critical value of 5.12 for the first design, slope 1574 instead of 1663 in Table 5, limit of decision 118 and limit of detection 0.0067% instead of 0.0078% in Table 5. However, as the result cannot be better than the standard, the corrected value is 0.007% tungsten instead of 0.008%.

APPENDIX E

Repeatability of the limit of detection

Returning to the Hubaux and Vos approach, it is important to give some indication about the confidence intervals of the reported values for the limit of detection. As these values result from a limited number of measurements, a sampling fluctuation exists, which can be estimated from a number of independent measurements of the limit of detection. Three such measurements are selected from the 10×3 array of analytical signals reported in the last third of Table 2, to measure the limit of discrimination in the solvent. The selection results in three 3×3 arrays made up, respectively, of the rows 1–4–7, 2–5–8 and 3–6–9. Even though the measurements giving rise to the 10×3 array were made in random order, the reported signals within each column are in order of acquisition. The way of forming the 3×3 arrays was designed to prevent, as far as possible, the presence of consecutive measurements in the same array. Data and confidence interval are given in Table 6.

APPENDIX F

Lowering the limit of detection in routine monitoring

An estimation of the uncertainty of the limit of detection, such as that obtained in Appendix E, would suffice to know whether this limit is safely below the regulatory level to be adhered to. Horwitz [49] expressed this view by saying that the primary purpose of determining the limit of detection is to stay away from it. However, the requirement for periodic checks in continuous monitoring continuously increases the available information, which can be handled via control charts. This gives the opportunity of refining the measurement process by information feedback. The limit of detection is a particular case of the limit of discrimination. Joint consideration of Fig. 2 with assumed parallelism between confidence bands and the regression line, Eqn. 6 and Thales' theorem, show that the limit of discrimination is proportional to s/b. From the twelve measurements of the limit of discrimination in sulphate ion systems reported in this paper, it results that the correlation coefficient [50] between s and b is −0.10, which means that no significant correlation exists between the two variables, after comparison with 0.576, the critical value for twelve pairs of observations and 5% significance. This result justifies the convenient monitoring of s and b through control charts, each variable in its own chart. As expected, the correlation between the limit of discrimination and the ratio s/b is significantly high, 0.97. The correlation coefficient between limits of discrimination and s is 0.70, and that between limits of discrimination and $1/b$ is 0.81.

Hubaux and Vos [11] discussed how to obtain lower limits of detection by increasing the number of standards, by replication of the unknown, m in Eqn. 6, by choosing the range of analyte content in the standards, and also the repartition of the analyte contents along the dynamic range. The recommended repartition is a three-level dis-

tribution, with the lowest level having all standards but two. This accumulation of standards at the lower end of the dynamic range is preferred because of the expectation that the limit of detection has to be near this end. This is not necessarily so. The repartition chosen in this paper is three equidistant levels with the same number of repeats at each level. This favours the lack-of-fit test and also Cochran's test for variance homogeneity [51], which requires the same number of repeats at each level. The computer program applied includes a warning message for significant heteroscedasticity at 1% significance. In this case the message would appear between the standard deviation and the residual of the mean lines in the computer output (Tables 5 and 6).

In cases where the measurement process is sufficiently under control, the choice of m, the number of repeats on the unknown, might be an interesting resource to keep the limit of detection safely below the regulatory level, without having to move to another, more expensive, instrumental

TABLE 7

Limits of decision and limits of detection for blank-corrected analytical signals [barium chloride–potassium dichromate–ammonia; 10-min standing before filtration; excess of chromate; 10 × 3 and 3 × 3 experimental designs; 99.0% confidence bands; non-significant (1%) lack of fit in all cases]

	Standard sulphate ion added to the solvent (mg)		
	0.100	0.300	0.500
	Blank-corrected analytical signal (absorbance × g treated sample)		
10 × 3 array of blank-corrected analytical signals from Table 4			
Mean	0.74	2.79	4.54
Standard deviation	0.430	0.430	0.593
Standard deviation about the regression: 0.487			
Sensitivity (95% confidence interval): 9.49 ± 1.11			
The limit of decision is 1.13 blank-corrected analytical signal units			
The limit of detection is 0.26 mg SO_4^{2-}			
Rows 1, 4 and 7 from the 10 × 3 array			
Mean	0.74	2.77	4.25
Standard deviation	0.097	0.588	0.091
0.9513 is greater than 0.9423. Significant heteroscedasticity (1%)			
Standard deviation about the regression: 0.356			
Sensitivity (95% confidence interval): 8.78 ± 1.71			
The limit of decision is 1.25 blank-corrected analytical signal units			
The limit of detection is 0.28 mg SO_4^{2-}			
Rows 2, 5 and 8 from the 10 × 3 array			
Mean	0.47	2.58	5.13
Standard deviation	0.484	0.364	0.647
Standard deviation about the regression: 0.488			
Sensitivity (95% confidence interval): 11.63 ± 2.35			
The limit of decision is 1.02 blank-corrected analytical signal units			
The limit of detection is 0.29 mg SO_4^{2-}			
Rows 3, 6 and 9 from the 10 × 3 array			
Mean	0.97	3.06	4.37
Standard deviation	0.624	0.419	0.630
Standard deviation about the regression: 0.563			
Sensitivity (95% confidence interval): 8.49 ± 2.71			
The limit of decision is 2.31 blank-corrected analytical signal units			
The limit of detection is 0.46 mg SO_4^{2-}			

technique. Provided that the number of standards is not too small, and that the limit of detection lies closer to the average analyte level in the standards, the relationship between m and the limit of discrimination is close to the reciprocal square root, as in the analogous situation related to Eqn. 3.

Finally, even in situations where no signal drift is apparent, as shown by the Snedecor test in Table 4, it might be considered cost effective to improve the reliability by working with blank-corrected signals. Table 7 gives the limits of decision (critical signal values) and the limits of detection pertinent to this situation. At this starting point some degree of independence from the assumed statistical model would be reasonable. It could be decided, for example, to begin with by rejecting all lots with samples giving a blank-corrected signal higher than 1.0, the limit of decision, thus guaranteeing for the accepted lots an analyte content lower than 0.5 mg SO_4^{2-}, the rounded-off limit of detection. In this example the sampling variance is considered to be negligible as compared with the measurement variance.

REFERENCES

1 W. Horwitz, Pure Appl. Chem., 62 (1990) 1193.
2 International Union of Pure and Applied Chemistry, Compendium of Analytical Nomenclature. Definitive Rules 1987, Blackwell, Oxford, 2nd edn., 1987.
3 A.C. Bajpai, I.M. Calus and J.A. Fairley, Statistical Methods for Engineers and Scientists. A Student's Course Book, Wiley, Chichester, 1979, p. 173.
4 R. Ferrús and F. Torrades, Analyst, 110 (1985) 403.
5 C. Liteanu and I. Rîcă, Mikrochim. Acta, II (1975) 311.
6 C. Liteanu and I. Rîcă, Statistical Theory and Methodology of Trace Analysis, Horwood, Chichester, 1980, Chap. 7.
7 B. Altshuler and B. Pasternak, Health Phys., 9 (1963) 293.
8 D.L. Massart, A. Dijkstra and L. Kaufman, Evaluation and Optimization of Laboratory Methods and Analytical Procedures, Elsevier, Amsterdam, 1980, Chap. 25.
9 L.A. Currie, in L.A. Currie (Ed.), Detection in Analytical Chemistry. Importance, Theory, and Practice, American Chemical Society, Washington, DC, 1988, Chap. 1.
10 P.L. Smith, in O.L. Davies and P.L. Smith (Eds.), Statistical Methods in Research and Production, Longman, London, 1980, Chap. 5 and 11.
11 A. Hubaux and G. Vos, Anal. Chem., 42 (1970) 849.
12 G.T. Wernimont, Use of Statistics to Develop and Evaluate Analytical Methods, Association of Official Analytical Chemists, Arlington, VA, 1987, Section 3.4.6.
13 J.D. Ingle, Jr., and R.L. Wilson, Anal. Chem., 48 (1976) 1641.
14 M.J. Cardone, J. Assoc. Off. Anal. Chem., 66 (1983) 1283.
15 H. Kaiser, Anal. Chem., 42, No. 4 (1970) 26A.
16 H, Kaiser, Spectrochim. Acta, 3 (1947) 40.
17 H. Kaiser, Fresenius' Z. Anal. Chem., 209 (1965) 1.
18 L.A. Currie, Anal. Chem., 40 (1968) 586.
19 C. Kirchmer, in L.A. Currie (Ed.), Detection in Analytical Chemistry. Importance, Theory, and Practice, American Chemical Society, Washington, DC, 1988, Chap. 4.
20 C.J. Bailey, E.A. Cox and J.A. Springer, J. Assoc. Off. Anal. Chem., 61 (1978) 1404.
21 A. Montag, Fresenius' Z. Anal. Chem., 312 (1982) 96.
22 G. Mücke, Fresenius' Z. Anal. Chem., 320 (1985) 639.
23 M.J. Cardone, J. Assoc. Off. Anal. Chem., 66 (1983) 1257.
24 M. Thompson, Anal. Proc., 24 (1987) 355.
25 R.L. Watters and L.J. Wood, in L.A. Currie (Ed.), Detection in Analytical Chemistry. Importance, Theory, and Practice, American Chemical Society, Washington DC, 1988, Chap. 16.
26 G.L. Long and J.D. Winefordner, Anal. Chem., 55 (1983) 712A.
27 J.A. Glaser, D.L. Foerst, G.D. McKee, S.A. Quave and W.L. Budde, Environ. Sci. Technol., 15 (1981) 1426.
28 D.L. Massart, A. Dijkstra and L. Kaufman, Evaluation and Optimization of Laboratory Methods and Analytical Procedures, Elsevier, Amsterdam, 1980, p. 55.
29 R.K. Klein Jr. and C. Hach, Am. Lab., 9, July (1977) 21.
30 L.B. Rogers, in L.A. Currie (Ed.), Detection in Analytical Chemistry. Importance, Theory, and Practice, American Chemical Society Washington, DC, 1988, Chap 5.
31 C.L. Grant, A.D. Hewitt, T.F. Jenkins, Am. Lab., 23, February (1991) 15.
32 F. Feigl, Mikrochemie, 1 (1923) 4.
33 W.R. Kelly and J.D. Fasset, Anal. Chem., 55 (1983) 1040.
34 L.A. Currie, in D.A. Kurtz (Ed.), Trace Residue Analysis. Chemometric Estimation of Sampling, Amount, and Error, American Chemical Society, Washington, DC, 1985, Chap. 5.
35 G. Gottschalk, Statistik in der Quantitativen Chemischen Analyse, Enke, Stuttgart, 1962, p. 103.
36 H. Kaiser and H. Specker, Fresenius' Z. Anal. Chem., 149 (1956) 46.
37 M. Thompson and R.J. Howarth, Analyst, 101 (1976) 690.
38 J.K. Taylor, Anal. Chem., 55 (1983) 600A.
39 R.H. Woodward, in O.L. Davies and P.L. Goldsmith (Eds.), Statistical Methods in Research and Production, Longman, London, 4th edn., 1980, Chap. 7.
40 R. Ferrús and F. Torrades, Anal. Chem., 60 (1988) 1281.
41 R.D. Stiehler and J. Mandel, Anal. Chem., 29, No. 4 (1957) 17A.
42 M.R. Egea, Dissertation, University of Barcelona, Barcelona 1985.
43 C.W. Hinman, Am. J. Sci. Arts, 114 (1867) 478.

44 F. Egami and N. Takahashi, Bull. Chem. Soc. Jpn., 38 (1957) 373.
45 N.R. Draper and H. Smith, Applied Regression Analysis, Wiley, New York, 2nd edn., 1981, Chap. 1.
46 C. Urbach, Mikrochemie, 14 (1934) 321.
47 S. Henning and T.L. Jackson, At. Absorpt. Newsl., 12 (1973) 100.
48 O.L. Davies (Ed.), The Design and Analysis of Industrial Experiments, Longman, London, 2nd edn., 1979, Chap 7.
49 W. Horwitz, in L.A. Currie (Ed.), Detection in Analytical Chemistry. Importance, Theory, and Practice, American Chemical Society, Washington, DC, 1988, Chap. 16.
50 A.C. Bajpai, I.M. Calus and J.A. Fairley, Statistical Methods for Engineers and Scientists. A Students' Course Book, Wiley, Chichester, 1979, pp. 368–384.
51 W.J. Dixon and F.J. Massey, Jr., Introduction to Statistical Analysis, McGraw-Hill, New York, 4th edn., 1983, Chap. 15

PUBLICATION SCHEDULE FOR 1994

	S'93	O'93	N'93	D'93	J	F	M	A	M			
Analytica Chimica Acta	281/1 281/2 281/3	282/1 282/2 282/3	283/1 283/2	283/3 284/1 284/2	284/3 285/1-2 285/3	286/1 286/2 286/3	287/1-2 287/3 288/1-2	288/3 289/1 289/2	289/3 290/1-2 290/3			
Vibrational Spectroscopy		6/1			6/2		6/3		7/1			

INFORMATION FOR AUTHORS

Detailed "Instructions to Authors" for *Analytica Chimica Acta* was published in Volume 256, No. 2, pp. 373–376. Free reprints of the "Instructions to Authors" of *Analytica Chimica Acta* and *Vibrational Spectroscopy* are available from the Editors or from: Elsevier Science B.V., P.O. Box 330, 1000 AH Amsterdam, The Netherlands. Telefax: (+31-20) 5862459.

Manuscripts. The language of the journal is English. English linguistic improvement is provided as part of the normal editorial processing. Authors should submit three copies of the manuscript in clear double-spaced typing on one side of the paper only. *Vibrational Spectroscopy* also accepts papers in English only.

Rapid publication letters. *Letters* are short papers that describe innovative research. Criteria for letters are novelty, quality, significance, urgency and brevity. Submission data: max. of 2 printed pages (incl. Figs., Tables, Abstr., Refs.); short abstract (e.g., 3 lines); *no* proofs will be sent to the authors; submission on floppy disc; *no* revision will be possible.

Abstract. All papers and reviews begin with an Abstract (50–250 words) which should comprise a factual account of the contents of the paper, with emphasis on new information.

Figures. Figures should be prepared in black waterproof drawing ink on drawing or tracing paper of the same size as that on which the manuscript is typed. One original (or sharp glossy print) and two photostat (or other) copies are required. Attention should be given to line thickness, lettering (which should be kept to a minimum) and spacing on axes of graphs, to ensure suitability for reduction in size on printing. Axes of a graph should be clearly labelled, along the axes, outside the graph itself. All figures should be numbered with Arabic numerals, and require descriptive legends which should be typed on a separate sheet of paper. Simple straight-line graphs are not acceptable, because they can readily be described in the text by means of an equation or a sentence. Claims of linearity should be supported by regression data that include slope, intercept, standard deviations of the slope and intercept, standard error and the number of data points; correlation coefficients are optional.
Photographs should be glossy prints and be as rich in contrast as possible; colour photographs cannot be accepted. Line diagrams are generally preferred to photographs of equipment. Computer outputs for reproduction as figures must be good quality on blank paper, and should preferably be submitted as glossy prints.

Nomenclature, abbreviations and symbols. In general, the recommendations of IUPAC should be followed, and attention should be given to the recommendations of the Analytical Chemistry Division in the journal *Pure and Applied Chemistry* (see also *IUPAC Compendium of Analytical Nomenclature, Definitive Rules*, 1987).

References. The references should be collected at the end of the paper, numbered in the order of their appearance in the text (*not* alphabetically) and typed on a separate sheet.

Reprints. Fifty reprints will be supplied free of charge. Additional reprints (minimum 100) can be ordered. An order form containing price quotations will be sent to the authors together with the proofs of their article.

Papers dealing with vibrational spectroscopy should be sent to: Dr J.G. Grasselli, 150 Greentree Road, Chagrin Falls, OH 44022, U.S.A. Telefax: (+1-216) 2473360 (Americas, Canada, Australia and New Zealand) or Dr J.H. van der Maas, Department of Analytical Molecular Spectrometry, Faculty of Chemistry, University of Utrecht, P.O. Box 80083, 3508 TB Utrecht, The Netherlands. Telefax: (+31-30) 518219 (all other countries).

0003-2670/94/$07.00

This issue is printed on acid-free paper.

PRINTED IN THE NETHERLANDS

Chromatography of Mycotoxins

Techniques and Applications

edited by **V. Betina**

Journal of Chromatography Library Volume 54

This work comprises two parts, Part A: Techniques and Part B: Applications. In Part A the most important principles of sample preparation, extraction, clean-up, and of established and prospective chromatographic techniques are discussed in relation to mycotoxins. In Part B the most important data, scattered in the literature, on thin-layer, liquid, and gas chromatography of mycotoxins have been compiled. Mycotoxins are mostly arranged according to families, such as aflatoxins, trichothecenes, lactones etc. Chromatography of individual important mycotoxins and multi-mycotoxin chromatographic analyses are also included. Applications are presented in three chapters devoted to thin-layer, liquid, and gas chromatography of mycotoxins.

Contents: **PART A. TECHNIQUES.**

1. Sampling, Sample Preparation, Extraction and Clean-up *(V. Betina).* Introduction. Sampling and Sample Preparation. Sample Extraction and Clean-up. Illustrative Example. Conclusions.

2. Techniques of Thin Layer Chromatography *(R.D. Coker, A.E. John, J.A. Gibbs).* Introduction. Clean-up Methods. Normal Phase TLC. Reverse-phase TLC (RPTLC). High Performance Thin Layer Chromatography (HPTLC). Preparative TLC. Detection. Quantitative and Semi-Quantitative Evaluation. Illustrative Examples. Conclusions.

3. Techniques of Liquid Column Chromatography. *(P. Kuronen).* Introduction. Sample Pretreatment. Column Chromatography. Mini-Column Chromatography. High-Performance Liquid Chromatography. Conclusions.

4. Techniques of Gas Chromatography *(R.W. Beaver).* Introduction. Resolution in Gas Chromatography. Extracolumn Resolution. Conclusions.

5. Emerging Techniques: Immunoaffinity Chromatography *(A.A.G. Candlish, W.H. Stimson).* Introduction. Immunoaffinity Chromatography Theory. Practical Aspects and Instrumentation. Sample Preparation. Illustrative Examples.

6. Emerging Techniques: Enzyme-Linked Immunosorbent Assay (ELISA) as Alternatives to Chromatographic Methods *(C.M. Ward, A.P. Wilkinson, M.R.A. Morgan).* Introduction. Principles of ELISA. Sample Preparation. Instrumentation and Practice. Illustrative Examples. Conclusions.

PART B, APPLICATIONS.

7. Thin-Layer Chromatography of Mycotoxins *(V. Betina).* Introduction. Aflatoxins. Sterigmatocystin and Related Compounds. Trichothecenes. Small Lactones. Macrocyclic Lactones. Ochratoxins. Rubratoxins. Hydroxyanthraquinones. Epipolythiopiperazine-3,6-diones. Tremorgenic Mycotoxins. Alternaria Toxins. Citrinin. α-Cyclopiazonic Acid. PR Toxin and Roquefortine. Xanthomegnin, Viomellein and Vioxanthin. Naphtho-γ-pyrones. Secalonic Acids. TLC of Miscellaneous Toxins. Multi-Mycotoxin TLC. TLC in Chemotaxonomic Studies of Toxigenic Fungi. Conclusions.

8. Liquid Column Chromatography of Mycotoxins *(J.C. Frisvad, U. Thrane).* Introduction. Column Chromatography. Mini-Column Chromatography. High Performance Liquid Chromatography. Informative On-line Detection Methods. Conclusions.

9. Gas Chromatography of Mycotoxins *(P.M. Scott).* Introduction. Trichothecenes. Zearalenone. Moniliformin. Alternaria Toxins. Slaframine and Swainsonine. Patulin. Penicillic Acid. Sterigmatocystin. Aflatoxins. Ergot Alkaloids. Miscellaneous Mycotoxins. Conclusions.

Subject Index.

1993 xiv + 440 pages
Price: US $ 180.00 / Dfl. 315.00
ISBN 0-444-81521-X

ORDER INFORMATION

For USA and Canada
ELSEVIER SCIENCE INC.
P.O. Box 945
Madison Square Station
New York, NY 10160-0757
Fax: (212) 633 3880

In all other countries
ELSEVIER SCIENCE B.V.
P.O. Box 330
1000 AH Amsterdam
The Netherlands
Fax: (+31-20) 5862 845

US$ prices are valid only for the USA & Canada and are subject to exchange rate fluctuations; in all other countries the Dutch guilder price (Dfl.) is definitive. Customers in the European Union should add the appropriate VAT rate applicable in their country to the price(s). Books are sent postfree if prepaid.

ELSEVIER SCIENCE B.V.

0003-2670(19940310)287:1/2;1-E